The Dissertation Committee for Ashley Darius Biria
certifies that this is the approved version of the following dissertation:

Revisiting Vinti Theory: Generalized Equinoctial Elements and Applications to Spacecraft Relative Motion

Committee:

Ryan P. Russell, Supervisor

Maruthi R. Akella

Srinivas V. Bettadpur

Brandon A. Jones

Chris A. Sabol

Revisiting Vinti Theory: Generalized Equinoctial Elements and Applications to Spacecraft Relative Motion

by

Ashley Darius Biria

DISSERTATION

Presented to the Faculty of the Graduate School of

The University of Texas at Austin

in Partial Fulfillment

of the Requirements

for the Degree of

DOCTOR OF PHILOSOPHY

The University of Texas at Austin

August 2017

To my family.

Be like the sun for grace and mercy

Be like the night to cover others' faults

Be like running water for generosity

Be like death for rage and anger

Be like the Earth for modesty

Appear as you are

Be as you appear

— Rumi

Acknowledgments

This experience has been made richer and more rewarding by the advice, mentorship, encouragement, and support of many, many people. The opposing views I've encountered along the way have been equally valuable.

First and foremost, I thank my family. I cannot thank my parents enough for their overwhelming support during my tenure at UT Austin. They have been there for me through the best and worst of times, and for that I am grateful. And to my grandmother, may you someday rest in peace, you have been and continue to be a guide and an inspiration, even in your absence. I know you would be proud.

I am grateful to my Ph.D. advisor of five years, Dr. Ryan P. Russell. All good things must one day come to an end. Through all this time, his mentorship and guidance have been indispensable. Perhaps more than anything, the freedom he gave me to pursue my own ideas has made this journey one worth having and an unparalleled learning experience.

I also extend my gratitude to each of the remaining members of my dissertation committee: Drs. Maruthi Akella, Srinivas Bettadpur, Brandon Jones, and Chris Sabol. They have selflessly invested their time to review this document and serve on my committee. Looking back, I can recall many conversations and interactions over the years with each member that have ultimately shaped this body of work. Even the smallest of conversations,

which at the time seemed isolated, have had surprisingly profound impacts that I could not have foreseen.

I couldn't have asked for a better support group of friends, whether from Austin or from earlier chapters of my life, and I've learned a lot from them. The fourth floor crew has been a reliable sounding board during my time here. There are too many people to name, but I think you know who you are.

Finally, a large subset of this body of work developed equinoctial elements for Vinti theory. I had been developing the idea for more than a year off and on when I met Dr. Paul Schumacher, when progress on the concept was slow or very slow, often made in the background while I was focused on using Vinti theory for something else. In a brief conversation, he rekindled my motivation. His encouragement to continue pursuing their development convinced me I should prioritize it and marked an inflexion point in my research. Sometimes a little encouragement goes a long way. Thanks for the kick.

Revisiting Vinti Theory: Generalized Equinoctial Elements and Applications to Spacecraft Relative Motion

by

Ashley Darius Biria, Ph.D.

The University of Texas at Austin, 2017

SUPERVISOR: Ryan P. Russell

Early phases of complex astrodynamics applications often require broad searches of large solution spaces. For these studies, mission complexity generally motivates the use of the coarsest dynamical models with analytical solutions because of the implied lightening of the computational load. In this context, two-body dynamics are typically employed in practice, but higher-fidelity models with analytical solutions exist, an attractive prospect for modern applications that may require or benefit from greater accuracy.

Vinti theory, which prescribes one of the many alternative described models known as intermediaries, is revisited because it leads to a direct generalization of two-body dynamics, naturally incorporating the dominant effect of oblateness and optionally the top/bottom-heavy characteristic of a celestial body without recourse to perturbation methods. Prior to the innovations introduced in this dissertation, Vinti theory and associated solutions possessed many singularities in popular orbital regimes. The theory has received limited

use. The goals of this dissertation are to assess Vinti theory's effectiveness in a modern application and remove its long-standing disincentives. These objectives inform the two main contributions, respectively: 1) Vinti theory is applied to the relative motion problem through the development of a state transition matrix (STM), enabled by improvements to the existing theory; 2) a new nonsingular element set is introduced.

The relative motion application leverages Vinti's approximate analytical solution with J_3. An analytical relative motion model is derived and subsequently reformulated so that Vinti's solution is piecewise differentiable, developed alongside boosts in accuracy and removal of singularities in polar and nearly circular or equatorial orbits. Some of these singularities reside in the solution, others in the partials. Solving the problem in oblate spheroidal elements leads to large linear regions of validity. The new STM is compared with side-by-side simulations of a benchmark STM obtained from perturbation methods and is shown to offer improved accuracy over a broad design space. To defray the costs of software development, robust code is provided online.

The second major thrust area is the introduction of a nonsingular element set that is at once novel and familiar. Vinti theory suffers from other well-known singularities, strictly artifacts of classical elements that are detrimental to many applications. To mitigate these singularities, the standard (spherical) equinoctial elements are chosen to inform in a natural way their generalization to a new nonsingular element set: the oblate spheroidal equinoctial orbital elements. The new elements are derived without J_3 and concise algorithms presented for common coordinate transformations. The transfor-

mations are valid away from the nearly rectilinear orbital regime and are exact except near the poles. When near the poles, the transformations match the accuracy of the approximate analytical solution. As a result, the singularity on the poles is completely eliminated for the first time. Analytical state propagation of the new elements in time for bounded orbits completes their formal introduction. Benefits of the new elements are identified.

The dissertation is organized as follows. To convey Vinti theory's broader context, extensive background on intermediaries and related topics is provided in Chapter 1. General enhancements that grew out of the main efforts, including the removal of some singularities, are consolidated in Chapter 2 along with mathematical preliminaries. Relative motion is explored as the selected application in Chapter 3 and the major deficiencies of Vinti theory are removed in Chapter 4 with the introduction of the new element set. Analytical orbit propagation in the new set is developed in Chapter 5.

Table of Contents

List of Tables

List of Figures

Chapter 1

Introduction

A seemingly boundless capability surrounds the modern world of computer simulation and numerical methods. With such extensive resources, it is perhaps a wonder, looking in from outside, that analytical methods persist in the field of astrodynamics. The landscape now is certainly different from that of the 1960s during the space race, when researchers aggressively pursued analytical models for describing satellite motion. The trend toward numerical methods is clear. And yet analytical methods persist. They persist largely because numerical methods have some shortcomings in certain applications. In these instances, analytical methods may be sufficient or the marriage of the two approaches may perform better than either could do alone. Some of their benefits are innate while others are synergetic. Consider the following possible uses for analytical methods:

1. they can offer geometrical and physical insight to broad solution spaces;

2. they can deliver inputs to numerical methods, such as those that require good initial guesses;

3. they enable a variety of analytical and numerical perturbation methods, which require an analytical reference solution;

4. they are faster than numerical integration for long flight times in the context of orbit prediction;

5. they enable attractive numerical techniques for computation of various-order partial derivatives, which are required or useful in numerous applications, including spacecraft guidance, navigation, and relative motion modeling;

6. they can act as components of hybrid, semi-analytical theories;

7. they can validate numerical methods and vice versa.

At the AAS/AIAA Spaceflight Mechanics Meeting on February 6, 2017, Felix Hoots presented some compelling, sobering arguments for how analytical methods in astrodynamics continue to shape modern research and the state of the art. An analytical method is not always the right method, and there is a fundamental question to ask to assess its use for any application. To this end, Hoots quoted Garfinkel, who summarized this problem quite eloquently with the following question:

> Do you want an exact solution to an approximate problem? Or an approximate solution to an exact problem?

Analytical solutions often correspond to these so-called approximate problems, like the Vinti problem. They may be indispensable for obtaining a good initial guess needed as part of a more accurate technique and can serve as excellent guidelines for numerical work [140]. In the context of orbit propagation, if maximum accuracy is desired, then an analytical solution would be

insufficient where numerical integration of a high-fidelity dynamical model (an approximate solution to an exact problem) would meet the objective. Even for numerical integration, though, analytical solutions can be exploited for performance gains.

It is with these ideas in mind that the nature and nuances of Vinti theory are explored in this dissertation. Alongside a nearly exhaustive exposition of the history and evolution of Vinti theory, the following sections expound broadly on topics pertaining to Vinti theory, focusing initially on intermediaries and how Vinti's intermediary fits into the category. A more rigorous definition is given later, but intermediaries are essentially intermediate force models with analytical solutions, specifically surpassing the accuracy of the Kepler problem without recourse to perturbation methods. Vinti's intermediary is then related to various orbit prediction techniques, including analytical (general perturbations), numerical (special perturbations), and semianalytical methods for context. By association, other intermediaries are compared as well. A discussion of motivational problems follows, with an emphasis on the spacecraft relative motion problem, the main application of Vinti theory demonstrated in this dissertation. To facilitate making connections and associations, Vinti theory is not confined to one section. Instead, sections address more general concepts. If a facet of Vinti theory is relevant to one of those concepts then that facet is included in the relevant section and discussed in that context. This approach has the effect of introducing various aspects of Vinti theory at a slow pace, hopefully making the material not only digestible, but also clearer. The chapter concludes with an explanation of the organization of

3

the dissertation and a summary of the main contributions.

1.1 Integrable Problems

The context here primarily concerns mathematical modeling of dynamical systems. The number of known problems with analytical solutions in astrodynamics is limited. These integrable problems can be treated as unperturbed problems in the context of high-level goals seeking realism in dynamics models, where these goals are often accomplished through perturbation methods. For spacecraft orbit prediction, the subset of complete problems, referring to those that consider all three spatial degrees of freedom of a spacecraft, is even more limited[1]. For example, the equatorial problem with oblateness included is still integrable, but the model's validity does not extend to motion outside the equatorial plane. The goal of this section is to touch on two primary unperturbed problems of interest in addition to a few others in the literature, at a high level, and to elaborate on their potential uses. Mathematical details are reserved for later chapters.

1.1.1 Terminology

Some stricter-than-usual terminology is adopted in this dissertation. Most of the choices will be explained in Section 2.1.2, but it is helpful to discuss terminology associated with perturbations up front. To describe the motion of

---

[1] An integrable problem also exists in rigid-body attitude dynamics called the Euler-Poinsot problem, but attitude dynamics are outside the scope of this dissertation. The problem specifically describes the torque-free motion of a triaxial rigid body.

an Earth-orbiting satellite, for example, traditional, physics-based techniques would regard all but one of the acting physical forces as perturbations. The one exception is associated with a gravitational field generated by a point mass, in which a satellite's motion is described exactly by a conic section. Since all other forces are small relative to this force and an exact solution exists when all other forces are neglected, it is useful to consider the true satellite motion as following a path that deviates slightly from a conic section. Visualizing the orbit is easier with this perspective, and having this reference solution enables a variety of mathematical tools for modeling the perturbative forces. This reference solution corresponds to the unperturbed problem and can equivalently be called the unperturbed solution.

The confusion in terminology arises when discussing other unperturbed problems, because the above described perspective is so pervasive and universal. For example, consider the problem of including the dominant force due to a planet's oblateness, denoted by the J_2 coefficient. The J_2-perturbed problem, often called the main problem, has received tremendous attention over the years. It turns out that an exact solution exists to this problem when the spacecraft resides in the equatorial plane. Jezewski referred to this problem as the J_2-perturbed equatorial problem, but from a different viewpoint, what he found is a new unperturbed problem. His solution could be used as a reference trajectory, different from but analogous to the conic section, and the effects of other forces on the orbit can be viewed as perturbations to this more accurate reference orbit.

Seeing as the contributions of this dissertation are entirely focused on

alternative unperturbed problems, it behooves the reader to keep the above ideas in mind at all times. Different unperturbed problems incorporating different dynamics may be directly compared and discussed simultaneously. Additionally, perturbations may be discussed with respect to various unperturbed problems, but note that, as in the above example, perturbations to one unperturbed problem may be entirely folded into the dynamics of a different unperturbed problem. Effort is made throughout the dissertation to be abundantly clear about what reference orbits are associated with various analytical solutions, which may or may not include perturbations.

1.1.2 The Kepler Problem

While a strong understanding of the Kepler problem is assumed, a brief review is offered for the purposes of drawing analogies and facilitating comparison to other unperturbed problems. The Kepler problem is the initial value problem associated with the simplest dynamical model for propagating an orbit, specifically the relative two-body problem or one-center problem [13, 50]. A spherically symmetric primary body generates a central force field that is equivalent to that generated by a point mass. For a spacecraft traveling through such a field, its motion is completely described by a conic section. The conic is constrained to an invariant plane, which is oriented orthogonal to the spacecraft's angular momentum vector. The mathematical representation can be viewed as a constant three-dimensional rotation with respect to the equatorial plane plus the evolution in time governed by the equation for a conic in polar coordinates.

Another property of Keplerian dynamics is that all of the various descriptions of the motion are directly tied to spherical geometry. While the solution can be derived in multiple ways, when representing the dynamics in spherical coordinates, the above result can be derived blind to any geometrical insight [50]. In this way, there is an implicit choice of coordinates associated with the Kepler problem. The classical angular orbital elements describe arcs on the celestial sphere, and they can be directly related to longitude and latitude through spherical trigonometry. While perhaps less obvious, the semimajor axis and eccentricity are also tied to spherical geometry. To see how, consider the conic equation, which describes the radial distance from the origin, r, of a spacecraft as a function of its true anomaly. The level surfaces of r are concentric spheres. At an instant in time, the sphere $r = r_k$ associated with the time $t = t_k$ is tangent to the spacecraft, so that, for an elliptical orbit, this tangent sphere expands and contracts over time as it follows the spacecraft around the orbit. But the expansions and contractions are in sync with the orbit, expanding monotonically from periapsis to apoapsis and contracting monotonically from apoapsis to periapsis. At the extrema of the orbit, corresponding to periapsis and apoapsis, the tangent sphere is at its minimum and maximum size, respectively. The semimajor axis is simply the arithmetic average of these minimum and maximum radial distances. Eccentricity is similarly tied to spherical geometry.

There are several takeaways from this discussion. Certainly the choice of spherical coordinates leads to a connection between the dynamical description and spherical geometry, and the connection is retained under perturba-

tions. It follows that the connection to spherical geometry is not a necessity because other coordinate systems may have been used instead. A valid gravitational potential must satisfy Laplace's equation outside the body, and there are 11 coordinate systems, 10 of which are degenerate forms of ellipsoidal coordinates, that may lead to separability [119, 50]. Among these 10 degenerate coordinate systems are rectangular coordinates, spherical coordinates, oblate spheroidal coordinates, and parabolic coordinates. The Kepler problem is a consequence of separability using spherical coordinates. The next integrable problem also results from separability, but instead made possible by the use of oblate spheroidal coordinates.

1.1.3 The Vinti Problem: Vinti's Intermediary

Vinti theory constructs orbits on an oblate spheroidal geometry. The Vinti problem is the simplest initial value problem associated with Vinti theory. Inspired by the oblate spheroidal shape of the Earth, Vinti sought a solution in oblate spheroidal (OS) coordinates to capture the gravitational effects of the Earth's oblateness in addition to the spherical contribution. Saving the details for later, suffice it to say, that the gravitational potential he derived in OS coordinates has a simple form, similar to that for a central force field, and, just as in the Kepler problem, this potential simultaneously solves Laplace's equation (as expected from the earlier discussion) and leads to separability of the Hamilton-Jacobi equation [152]. Such is an intermediary: an intermediate force model that should capture, in a qualitative sense, at least the first-order secular and periodic effects in the main problem of artificial satellite theory [59]

(nuances are discussed in the next section). By this definition, Vinti's potential qualifies as an intermediary, but those of the Kepler problem and J_2-perturbed equatorial problem do not. Other intermediaries are discussed in the next section.

Limiting the discussion to coordinates for the time being, it should be apparent that transitioning from spherical to OS coordinates introduces a free parameter into the coordinate system. In OS coordinates, two of the three axes of the ellipsoid are equal and larger than the other axis, which is the semiminor axis. But how much larger? Indeed, the free parameter is associated with the flattening of the coordinate system, and there are apparently many options and possibilities as to what can be done with it. Details are given later for the particular path Vinti decided to take, but he essentially tuned the free parameter of the OS coordinate system to capture the J_2 contribution for the Earth application. Clearly, the approach generalizes to oblate bodies other than Earth.

Without discussing the dynamical model, one can already anticipate the existence of some sort of analogous set of orbital elements associated with the Vinti problem. Consider again the expanding and contracting sphere of radius r described for the Kepler problem. Transitioning to OS coordinates, this sphere flattens into an expanding and contracting oblate spheroid of semiminor axis ρ, still tangent to the spacecraft at each instant in time. The level surfaces of ρ are confocal oblate spheroids. Considering J_2 as a perturbation to the two-body problem, it is not surprising that behavior similar to that described earlier for the Kepler problem would occur under the Vinti potential. Defining

periapsis and apoapsis respectively as the minimum and maximum semiminor axis of the tangent oblate spheroid (ρ_1 and ρ_2), analogous to the sphere in the Kepler problem, then the expansions and contractions of the spheroid are in sync with the orbit, expanding monotonically from periapsis to apoapsis and contracting monotonically from apoapsis to periapsis. At the extrema of the orbit, the tangent spheroid is at its minimum and maximum size. The arithmetic average of these minimum and maximum semiminor axes is exactly analogous to the semimajor axis of the Kepler problem. Be careful not to confuse the semimajor axes of the tangent spheroid with the "semimajor axis" of the trajectory. An analogous eccentricity can also be defined that is similarly tied to the underlying oblate spheroidal geometry, in addition to four others associated with the usual angles. Perhaps not surprisingly, the evolution of ρ is also governed by the equation for a conic, except in terms of these alternative elements, so that the actual trajectory generally looks nothing like a conic. While a Vinti trajectory applied at the Earth would look like a perturbed conic, the trajectory would look less and less like a conic as the magnitude of J_2 increases.

Due to these striking analogies, it is convenient, if not incredibly helpful and logical, to call these alternative elements oblate spheroidal orbital elements, as coined by Lang [104] in 1968. In the text, they may also be referred to as spheroidal elements for short or just OS elements, or if there is no ambiguity the qualifier may be dropped all together. The word "oblate" is considered safe to omit for readability because prolate spheroids are not investigated. It is worth pointing out that the spheroidal semimajor axis does not

possess some of the geometrical interpretations of its spherical counterpart. For example, consider an elliptical orbit. The spherical semimajor axis is the distance from the center of the ellipse to the location of spherical periapsis or apoapsis on the ellipse. However, under the Vinti potential, a bounded spacecraft trajectory is not necessarily (usually not) a closed curve. In general, there is no single spheroidal periapsis or apoapsis location in space, even though the notion of minimum and maximum ρ still holds and the trajectory oscillates between the "periapse spheroid" and "apoapse spheroid".

These concepts are illustrated in animations included as supplementary files in the MP4 video format. Each example considers polar orbits so that all motion is constrained to one plane, the same plane that is viewed head-on in the animations. The `sphere_KeplerTraj_2D.mp4` file corresponds to the Keplerian case described in Section 1.1.2, where the trajectory is drawn in green, the current spacecraft location is drawn as a large red dot, and the tangent sphere is drawn in magenta. The analogy to oblate spheroidal geometry is conveyed through three other files that can be viewed sequentially. Each of these three files shows the same Vinti trajectory represented side by side in the two different coordinate systems, assuming a large J_2 on the order of 0.1 to exaggerate the effects. The color schemes used are the same as in the Keplerian example, except that a yellow dashed osculating ellipse is also drawn for the representation in spherical coordinates on the left and the tangent spheroid is drawn in red on the right. In the graph on the bottom, a spheroidal classical element is plotted in red and the osculating spherical counterpart is plotted in magenta. The `compare_coords_VintiTraj_2D_a_J2....mp4` file shows the effect on

11

the semimajor axis and the `compare_coords_VintiTraj_2D_e_J2....mp4` file shows the effect on eccentricity for an unperturbed Vinti problem. While the osculating spherical eccentricity varies between 0 and nearly 0.9, the spheroidal eccentricity is constant and just under 0.2. The trajectory is not even close to being unbounded, and this important qualitative characteristic is reflected clearly in the spheroidal eccentricity. The spherical eccentricity is not as easily interpreted in this sense. The `compare_coords_VintiTrajP_2D_a_J2....mp4` file shows the effect on the semimajor axis for a perturbed Vinti problem, so that both spherical and spheroidal elements are now osculating. As expected, the osculating spheroidal semimajor axis is no longer constant, but its variations in this example are notably an order of magnitude smaller than the variations in the spherical semimajor axis.

With an emphasis on visualizing coordinates, the Vinti problem in a way has been framed as a natural generalization of the Kepler problem to motion around an oblate body. Given the connection to spherical geometry, the appearance of trigonometric functions in the solution may be expected in the Kepler problem. The appearance of (Jacobi or Weierstrass) elliptic functions in the solution of the Vinti problem may be anticipated from the analogy that connects trigonometric functions to the unit circle similarly to how elliptic functions are connected to the unit ellipse. The unit circle is connected to spherical geometry as the unit ellipse is connected to oblate spheroidal geometry.

Note also that Vinti theory is not the only instance of uncommon coordinate systems finding their way into astrodynamics. Drawing on analogies

between atoms and planets, the Stark problem, which concerns two-body motion plus a constant inertial force, is separable in parabolic coordinates with an analytical solution in terms of Jacobi [105] or Weierstrass [19] elliptic functions. It is also separable in Kustaanheimo-Stiefel (KS) variables [99], which regularize the two-body problem[2]. The Stark problem is named after Johannes Stark, a Physics Nobel Prize laureate (and outspoken antisemite) who discovered the Stark effect [138]. The Stark problem has been the focus of several recent studies [105, 124, 71, 19] and has applications to modeling forces like solar radiation pressure (SRP), third body effects, and low thrust [126]. Incidentally, Vinti himself obtained an approximate solution to the Stark problem using parabolic Delaunay variables [157].

1.1.4   Other Intermediaries

Astronomer Johan August Hugo Gyldén coined the term "intermediary" in 1885 for a lunar theory, originally in German as "intermediäre" [70]. But he did not invent the idea. The notion of an intermediary may be traced back to Peter Hansen's work in lunar theory [58]. English mathematician and astronomer Ernest Brown writes that Gyldén's definition of an intermediary, where he superposed the dominant secular motions of the Moon on a Keplerian ellipse, differs slightly from that adopted by later authors [30]. In 1896, Brown developed his own intermediary. Beginning with a secularly precessing ellipse, Brown's intermediary also aimed to approximate the true path

---

[2]KS variables are comprised of eight, not six, fully nonsingular elements that emulate a quaternion and transform the two-body problem to a harmonic oscillator. One tradeoff is that they lack a clear physical interpretation.

of the Moon [30] (pp. 45–47). In 1957[3], Sterne devised what appears to be the first intermediary to tackle the main problem [139]. (The concept was previously used for natural satellites, not artificial ones.) He used spherical coordinates and, similar to Izsak [85] and eventually Vinti [154], expressed the solution in terms of some orbital elements he identified as analogous to the Keplerian ones. Sterne [139] ultimately reduced the problem to four elliptic integrals. Many intermediaries followed, and the following list is not exhaustive. For the present discussion, a background in Hamiltonian mechanics and Hamilton-Jacobi theory [50], perturbation methods [120] as applied to astrodynamics [50], and the use of spherical harmonics to represent a gravitational potential [149] is assumed, although some of these concepts are given greater attention in later sections.

Garfinkel proposed his first intermediary in 1958 [56] and continued to modify it over the following years [57, 58]. In 1964, Garfinkel [58] identified a four-parameter family of intermediaries that include his earlier intermediary and Sterne's. By choosing to zero a different parameter compared to Sterne's choice, Garfinkel minimized the number of elliptic integrals. While a first-order theory for the family of intermediaries is manageable, a second-order theory was considered prohibitively complex, or at least it was considered as much by 1970 standards [59]. Nevertheless, Aksnes found a way through, opening a path to a second-order theory in 1965 by carefully choosing one of the parameters to fold in first-order secular perturbations [4]. Aksnes' result

---

[3]Sterne's work was published in 1958, but the work was presented well before then.

is remarkable because it enabled a second-order theory via a Hori-Lie perturbation method [82] in Hill variables [74] that includes J_3 and J_4 [5, 6]. His result is free of singularities except at the critical inclination [6], as typically seen when invoking series expansions in powers of J_2.

While all intermediaries discussed thus far make use of elliptic functions in their solutions, they are not unavoidable. In 1969, Cid and Lahulla deviated from most of the earlier approaches, not just by developing their intermediary in polar-nodal variables instead of spherical coordinates, but by reimagining how an intermediary could be obtained [35]. An intermediary in earlier research was defined as a separable Hamiltonian, where the perturbation is simply the remainder, obtained by subtracting the separable part from the main problem's Hamiltonian. Cid and Lahulla, on the other hand, applied a canonical transformation to the main problem to obtain an intermediary [46]. Deprit formalized this new notion of "natural intermediaries" roughly 11 years later [45] and observed that each of the existing intermediaries in the sense of Garfinkel or Sterne could be considered a natural intermediary because each is the result of a particular contact transformation[4]. It turns out that Cid and Lahulla's intermediary is part of a family of what Deprit termed the "radial intermediaries", which are a family of natural intermediaries in polar coordinates [45]. While the original intermediary was developed by Cid and Lahulla, it is typically referred to as Cid's intermediary in the literature for some reason. Cid's intermediary does invoke elliptic functions,

---

[4]The term "contact transformation" is an older term synonymous with "canonical transformation".

but Deprit's radial intermediary does not. Deprit and Richardson [47] actually revisited Aksnes' intermediary in 1982, offering some improvements and drawing connections to the radial intermediary.

The topic of intermediaries is seen to represent a rich branch of literature that departs from traditional perturbation techniques based on averaging, to be discussed in later sections. Intermediaries of any kind did not garner sustained interest. Vinti theory was steadily developed until around 1970, with some literary staccatos in the 1970s and 1980s. Of the other intermediaries, the radial intermediaries have received the most sustained interest. Progressively simpler intermediaries were devised by successive canonical transformations. The work of Alfriend and Coffey begins with Deprit's elimination of the parallax [45] and then introduces elimination of the perigee [7] as the next canonical transformation in the sequence. Cid's intermediary employs elimination of the latitude [35, 36]. More recently, in 2014, Gurfil and Lara investigated the utility of Deprit's radial intermediary for onboard orbit propagation [69]. When juxtaposed with tradition, it is a spirit of mapping favored over one of averaging that sets the philosophies apart, or, put more precisely, the former philosophy advocates that mapping should be thoroughly explored before averaging. It is the author's belief that the notion of natural intermediaries should exist in spheroidal-type coordinates as well, though the merging of Vinti theory with the natural intermediary toolbox has never been investigated in any way.

16

1.1.5 Possible Uses

Applications discussed here generally refer to any of the above unperturbed problems. The most obvious use for these analytical solutions is orbit prediction. For some application, one of these analytical solutions may meet the desired model fidelity, and a satellite's orbit may be predicted to some arbitrary time, past or future, without numerical integration. For sufficiently long times of flight, the analytical solution is faster. Analytical or numerical partial derivatives may also be obtained for a variety of applications, including orbit determination and trajectory optimization. There are, however, other implications.

The previous applications are subject to limitations on the model fidelity, but techniques based on analytical solutions exist that generalize the dynamics to arbitrary force models. One popular and powerful technique is variation of parameters (VOP) [149, 50], which lends itself to analytical or numerical analyses. Equations of motion (EOMs) can be derived in terms of any set of orbital elements, and these equations can be numerically integrated. The power of this method originates in the choice of coordinates. The most basic numerical integration scheme would act on Cartesian or rectangular coordinates, but the dynamics are highly nonlinear and rapidly changing in these coordinates, implying that a numerical integrator must take small time steps to achieve some desired accuracy. In contrast, the dynamics are generally better behaved in orbital elements. Five of the six elements change slowly over time and only one changes rapidly. As a result, to achieve some desired accuracy, a numerical integrator may be able to take much larger time

steps if the dynamics or EOMs are represented in orbital elements instead of Cartesian coordinates. More importantly, the fast variable can alternatively be removed. Larger time steps mean faster compute times.

The VOP approach, in this context, utilizes the conic reference solution of the Kepler problem by design, but suppose that Vinti's intermediary is adopted instead as the reference solution and new EOMs are accordingly derived. Because Vinti theory embeds oblateness in the coordinates, the dynamics should be better behaved in these alternative orbital elements, lacking short-periodic variations, and an integrator should be able to take even larger time steps relative to a basic application of VOP.

Detail has been given in this section on applications of Vinti theory in general, but the focus of this body of work is on Vinti's analytical solution. The next section focuses and elaborates on two particularly relevant analytical orbit propagators in detail. More motivational problems are given in later sections.

1.2 Analytical Orbit Propagators

With the advent of not only computers, but the power and widespread availability of modern computing, analytical orbit propagators may be considered less popular as they often take a back seat. The growth in computing power stemmed not just from increases in processor speed, but also from the use of sophisticated parallel architectures found in high-performance computing (HPC) facilities. Nonetheless, analytical solutions have seen a resurgence

in the field of formation flying, typically in the form of linear models that are desirable for onboard guidance, navigation, and control algorithms [143]. A new relative motion model based on Vinti theory is a main contribution of this dissertation. One of the existing perturbed models, a state transition matrix (STM) developed by Gim and Alfriend [64], relies heavily on Brouwer's work [27], warranting a brief juxtaposition of the two theories.

1.2.1 Vinti and Brouwer Theories

In 1959, the same time that Brouwer [27] published his seminal and celebrated work, Vinti [152] was pioneering a different theory, also referred to as the spheroidal method, that he and others continued to develop over more than a decade [85, 154, 155, 156, 158, 160, 104, 62]. Both approaches rest on Hamilton-Jacobi theory and lend themselves to canonical perturbation methods. However, the choice of coordinates makes them fundamentally different. Brouwer began with spherical coordinates, for which the Hamilton-Jacobi equation is separable under Keplerian dynamics. A perturbation method is then required to model small effects not included in the reference solution, and he chose to develop his solution in Delaunay variables using the von Zeipel method of averaging [120]. In sharp contrast, Vinti used oblate spheroidal coordinates [119], for which the Hamilton-Jacobi equation is separable for a general form of the potential. Remarkably, such a potential can simultaneously satisfy Laplace's equation outside the planet, leading to a special form of the potential valid for a gravitational theory that naturally accounts for a planet's oblateness. To put his result in terms of traditional potential theory,

Vinti expands the potential in spherical harmonics and fits it exactly to the zeroth and second zonal harmonics of the traditional expansion. The solution of his original theory [85, 154] to higher order would effectively be exact for a perfect oblate spheroid where $J_4 = -J_2^2$, $J_6 = +J_2^3$, etc., but, in the case of the Earth and other bodies, an exact Vinti reference solution notionally includes the contributions of $J_2 + \epsilon J_4 + \epsilon^2 J_6 + \cdots$, where ϵ represents a small error. At this juncture, it is clear that solving Vinti's Hamilton-Jacobi equation would produce a more accurate reference solution than Brouwer's: Brouwer's reference solution models spacecraft motion around a spherical planet, while Vinti's reference solution models that around a spheroidal planet.

A number of improvements were made to Vinti's theory over the following years. The first advancement extended the solution to model equatorial orbits by removing the singularity there [155]. Vinti [156] then applied von Zeipel's method to incorporate J_3 and correct J_4 effects. However, in his later work, Vinti [159, 158] devised a way to include the third zonal harmonic in the potential by shifting the origin of the oblate spheroidal frame by the correct distance and direction along the polar axis of the body. This idea makes sense, as J_3 is associated with the top-heavy or bottom-heavy characteristic of the central body. The newer potential fits the J_3 harmonic exactly and, in that sense, is an improvement over invoking von Zeipel's method to model J_3. Vinti [160] also removed the singularities in his solution[5] that are associated

_____

[5]The "solution" is traditionally distinguished from the initialization process of converting position and velocity vectors to orbital elements. With this publication, Vinti [160] did not address singularities remaining in the initial conversion process. Methods for completely removing these singularities are a main contribution of this dissertation.

with polar orbits, rendering his solution nonsingular for bounded orbits in all inclinations. The same cannot be said of Brouwer's solution and its variants, which fail near the critical inclinations of approximately $63.4°$ and $116.6°$. It is emphasized that this special angle is still a critical inclination in Vinti's solution in the sense that there is still zero drift of periapsis to first order. Lang [104] subsequently extended the solution to include unbounded orbits, and Getchell [62] unified the solutions for bounded and unbounded orbits via universal variables. Note that Lang [104] solved the "parabolic" and "hyperbolic" cases separately and also developed explicit equations for the asymptotes and hyperbolic excess velocity vectors. This collection of work arguably establishes the fundamentals of the theory and associated solutions, and a good exposition and resource on these ideas is offered by Der and Bonavito [50], editors for Vinti's book, which is compiled from his lecture notes. Note that Izsak's report of 1960 [85] was formally published in 1963 [87], and one reference may be easier to find than the other. Further notes and commentary on Vinti theory appear in other books as well, including in Chapter 8 of Geyling and Westerman [63].

Assuming the symmetric form of the Vinti potential, notable alternative representations include a recent numerical solution by Wiesel [166] in the Earth-centered rotating frame in terms of action-angle variables and two analytical solutions: the extended phase space formulation of Alfriend et al. [8] and the Lagrangian solution of Mathúna [115] utilizing Jacobi elliptic func-

tions[6]. The work of Alfriend et al. [8] is the only instance in the Vinti theory literature of an attempt made to alleviate usual concerns associated with angle ambiguities in classical elements when eccentricities and inclinations are small. Their approach is unique to the extended phase space. It does not involve equinoctial-type elements and does not address singularities in polar orbits. With respect to Vinti theory, Mathúna's book seems to elaborate on two of his earlier works [113, 114] (his book is also notable for reasons discussed in Section 1.2.2.1).

In the pursuit of analytical solutions, both Vinti and Brouwer theories had to make extensive use of series expansions in various orders of J_2, but for different reasons. The expansions show up in Brouwer's solution because von Zeipel's method expresses the perturbed Hamiltonian and generating function as power series in a small parameter; higher order solutions, such as Kozai's (1962), are difficult to obtain because the terms of the generating function are determined recursively by solving a sequence of partial differential equations. In contrast, Vinti invokes series expansions for two main purposes: factoring a quartic and solving elliptic and other integrals. He also solves a generalized form of Kepler's equation by successive approximation to obtain periodic terms. Including higher order terms in Vinti's solution would arguably not be as difficult. Both methods address the main problem to differing degrees of accuracy as well as higher order geopotential terms. Specifically, Brouwer's solution considered secular terms through $O(J_2^2)$ and periodic terms through

---

[6]Mathúna transliterates his name in different ways, using the spelling "O'Mathuna" in his earlier work.

22

$O(J_2)$ (both short- and long-period terms), followed by secular and long-period contributions of J_3, J_4, and J_5 (assuming they are $O(J_2^2)$ as for the Earth); Vinti's later solution, which is employed in this paper, considered secular terms through $O(J_2^3)$ and periodic terms through $O(J_2^2)$, in addition to J_3 and approximately 72% of J_4 [158]. The portion of J_4 included can be larger or smaller depending on the central body, i.e. $-J_2^2/J_4 \approx 72\%$ for the Earth. While the higher-order geopotential terms of Brouwer's solution are noted, they will be ignored in comparisons in Chapter 3 because the Brouwer-based STM used in this dissertation neglects them [64]. Since the appearance of the original Gim-Alfriend (GA) STM, however, some higher order terms have been added via Brouwer theory [171, 174].

1.2.2 Advancements in Vinti Theory

With a brief history of Vinti theory fresh in the reader's mind, it is convenient to next explore some of the advancements and inspired directions of research, in addition to some important parallel studies. First, as a quick anecdote, the reader may be interested to know that the use of a J to denote the zonal harmonic coefficients can actually be traced back to Vinti, noted at the end of Brouwer's paper [27].

1.2.2.1 Equivalence between Vinti Theory and the Problem of Two Fixed Centers

Euler established the integrability of the problem of two fixed centers in the 1760s [115, 28]. Legendre, Lagrange, and Jacobi subsequently observed

that the solution could be expressed in terms of elliptic functions [20]. The equivalence between the Vinti potential and the problem of two fixed centers (PTFC) has been known since 1961 [2, 28]. As Brouwer and Clemence point out on pages 573–574, the potential function of the PTFC is appropriate for a special type of prolate spheroid, in which case the respective gravitational fields are equivalent assuming equal masses. To make the PTFC valid for a special type of oblate spheroid, the masses need only be separated by an imaginary distance instead of a real distance. For this reason, the PTFC is often said to be useful for modeling motion around rotationally symmetric bodies. The problem is also known as Euler's three-body problem, the Euler-Jacobi problem, and the two-center Kepler problem [20]. Note that Aksenov et al. [2] also discussed the equivalence in 1961 in a USSR publication, Beletsky [15] claiming that the Russians did it first. However, based on a thorough search, it appears that Aksenov et al. first published the Russian version of their work in the third quarter of 1961. Evidence suggests that Brouwer and Clemence published their book in January 1961.

Mathúna [115] offers a very detailed history and exposition on the PTFC, which he calls the Euler problem. He limits his analysis to bounded orbits, remarking that the results generalize to unbounded orbits by following the same techniques customary in the Kepler problem. Biscani and Izzo [20] explicitly generalize the solution to encompass with the same equations bounded and unbounded orbits as well as repulsive forces. Notably, in 1901, Darboux [43] was the first to generalize the PTFC in a way that has clear connections to the Vinti problem. Darboux's generalization showed that the

24

problem is still integrable with complex masses and complex distances. Aksenov et al. [1] used this fact to enable the exact fitting of a gravitational potential to J_2 and J_3. This result should sound similar to the 1966 potential of Vinti, who was influenced by this very paper. A key difference is that Vinti [158] shifted the origin of the OS reference frame while Aksenov et al. [1] did not, an important detail referenced again in Chapter 4.

1.2.2.2   Russian Literature on the Vinti Problem

Referring to a paper by Kislik [100], a Russian book by Beletsky [15], which has been translated to English, claims that the Russians were the first to model satellite motion around an oblate Earth using an integrable problem. Kislik's work was published in 1960 in Russian and translated to English in 1961. Vinti's seminal work was published in October 1959 [152], with a generous preview given in July 1959 in the *Physical Review Letters* [151]. Beletsky believes that Kislik's work began in 1958, citing only Kislik's 1960 paper, but arguably Vinti's work may well have begun in 1958. Which author conceived of the idea first may be up for debate, but the literature shows that Vinti published his work first, and therefore the problem is still called the Vinti problem. In any case, the work of the two authors appears to be independent. Subsequent Russian authors, Aksenov et al.[7], cited both Vinti and Kislik in their work [2, 3] and found Kislik's potential to be a special case of the Vinti potential [1]. Lavrik [107] later investigated the boundary value problem under

---

[7]Note that in these publications, Aksenov and Grebenikov transliterate their first names with the initial "Ye.", though they also transliterate the initial as "E." in other work [1, 67], possibly making it difficult to find.

the Vinti potential.

1.2.2.3   Other Studies Based on Vinti's Work

While Vinti's intermediary has remained relatively lesser-known, a number of researchers have developed his theory further over the years. Spies [137] presented a solution to the Vinti problem for polar orbits in 1961 (printed in 1963), and connected the work to the PTFC using prolate spheroidal coordinates. Vinti theory with atmospheric drag has also been investigated on occasion, first in Sherrill's doctoral work [133] in 1966 and then almost 10 years later by Watson et al. [165]. Both approaches are analytical, but the latter method uses a heuristic to properly combine a drag-free Vinti solution with a drag-perturbed Kepler solution. In 2016, Wright [168] also proposed an analytical solution to account for drag in action-angle variables, though he did not cite or compare his solution to those of earlier authors mentioned above. Once the perturbative effects are obtained, he proposed to apply a linear coordinate transformation from action-angle variables to Cartesian coordinates before adding the perturbations to Vinti's solution. It is not clear why this is preferred over adding the effects in the action-angle space and then performing a nonlinear coordinate transformation. Note that Wright's ultimate goal was to perform orbit determination with Vinti theory in some follow-on work to Wiesel's approach. To work in an inertial frame, he set the Earth rotation rate to zero, since Wiesel's solution includes the rotation. The study of perturbations under the Vinti potential were not limited to drag, however. A follow-on paper to the extended phase space study of Alfriend et al. [8] incorporated

26

luni-solar perturbations [96].

A quick search will reveal that Izsak's second-order solution initiated its own branch of literature, often referred to as the Izsak-Borcher's solution after the appearance of Borcher's technical report [23] in 1963, which offered a complete computational procedure for Izsak's solution. Note that this potential corresponds to Vinti's symmetric potential from 1959. Subsequent papers developed a differential corrections procedure [10] and used it to model perturbative effects of J_3 and J_{22} [11], where $J_{22} = \sqrt{C_{22}^2 + S_{22}^2}$ is the amplitude as used in the gravity phase angle representation of the sectoral and tesseral terms. Allen [9] later developed the earlier work of Allen and Knolle [11] for application to some different problems. Interestingly, in the latter reference, Allen [9] was apparently affiliated with the U.S. Department of Agriculture in 1969, citing a burgeoning interest in remote sensing for assessing the footprint and health of crops and detecting diseases.

Other authors investigated separability in other coordinate systems. In an exhaustive survey in 1966, Cook [39] explored all 11 coordinate systems for which the Hamilton-Jacobi equation and Laplace's equation are separable, deriving valid gravitational potentials if they were proven to exist. Cook apparently made an error in the last coordinate system he investigated, the triaxially ellipsoidal coordinates, claiming that no such potential exists. Madden [92] seems to have subsequently disproved this detail of Cook's work, demonstrating that such a potential does in fact exist in ellipsoidal coordinates. Together these papers represent an exhaustive survey of the possible gravitational potentials permitted by the 11 coordinate systems.

A body of Chinese literature also emerged in the early 1980s, containing a number of notable contributions. A consistent feature of the Chinese literature is the use of Vinti's 1966 potential and the adoption of sets of secular orbital elements, for which the angular variables are canonical (Izsak and Vinti derived these elements, where three are constants of the motion [85] and the other three vary linearly with time [154, 156, 158, 160]). In 1980, Wu and Tong [169] developed Vinti's 1966 solution to the third order and also obtained the Poisson brackets. Note that Getchell [62] had already advanced the solution to the third order a decade earlier, his work having the profound distinction of removing the singularities at zero energy. Later that year, Tong and Wu [145] derived explicit forms of the Gaussian variational equations (GVEs) based on Vinti's work [162], exact for the momenta variables and accurate to second order for the angular variables. In 1981, based on the preceding two contributions, Tong and Wu [146] showed how to combine their earlier results into a semi-analytical third-order perturbation theory. In the same year, Tong and Chen [144] related Vinti's 1966 solution to that of Mathúna [114], using Mathúna's regularizing change of independent variable to reduce the problem to two Lindstedt's equations with constant coefficients. They first demonstrate a solution technique using a Lie transform and then apply it to the Vinti problem, thus obtaining a second-order solution to the Vinti problem using an alternative method.

1.2.3 General Perturbations, Brouwer and Kozai Theories, and SGP4

General perturbations (GP) techniques encompass all strictly analytical approaches to solving a set of differential equations of motion that aim to describe a satellite's state. GP generally refers to the orbit propagation problem, including translational and rotational dynamics. The scope of this dissertation is limited to the translational dynamics. With respect to idealized, true/exact EOMs, which do not admit analytical solutions, the EOMs are simplified, hopefully allowing for exact or approximate solutions to the simplified, approximate problem that are obtained in closed form. A brief discussion of general perturbations for the translational dynamics is offered in the rest of this section.

The theories of Brouwer [27] and Kozai [101] are examples of general perturbations approaches, Kozai's article immediately preceding Brouwer's in the November 1959 issue of *The Astronomical Journal*. Their seminal work together formed the basis of the two operational analytical orbit propagators operated by the U.S. Navy and U.S. Air Force. These operational models are currently known respectively as Position and Partials as functions of Time (PPT3) and Simplified General Perturbations (SGP4) [81]. While averaging is the cornerstone of both theories, the theories use very different averaging techniques. Recall from Section 1.2.1 that Brouwer theory uses von Zeipel's method of averaging, a canonical approach. Kozai, on the other hand, invoked the Lagrange planetary equations (LPEs) [149] and then applied an ad hoc method of averaging. Like Brouwer, he accounted for J_2 through J_5 zonal

harmonics and neglected drag, considering J_2 as the perturbation and other zonals as $O(J_2^2)$. He retained secular terms through $O(J_2^2)$ and periodic terms through $O(J_2)$, identical to Brouwer theory.

Brouwer's original theory underwent many modifications and improvements over the years. Brouwer and Hori [29] added drag via a simple spherical exponential model atmosphere. Lyddane [112] removed the singularities at zero eccentricity and zero inclination by employing what are essentially Poincaré variables [76, 136]. The incorporation of the more accurate 1969 drag model of Lane and Cranford [103] led to the first operational implementation of SGP4 in 1970 (an upgrade from SGP), although the implementation of their drag model was simplified to alleviate computational load [81]. Nearly a decade later, Hujsak [83, 84] added luni-solar perturbations along with resonance effects. Greater historical detail and mathematical documentation is offered by Hoots et al. [81] and other sources [80, 91]. The documentation includes a numerical spline to work around issues near the singularity at the critical inclination, where Brouwer's theory breaks down when the (double-primed) inclination is within 1.5 degrees of the critical value. Vallado et al. [150] developed the most up-to-date non-proprietary version of SGP4 in 2006 (revised in 2007).

Another notable analytical propagator[8] is the Hoots Analytic Dynamic Ephemeris (HANDE) theory, which uses a Jacchia [88] 1970 dynamic at-

---

[8]Presumably, HANDE is considered analytical because the propagation is analytical, congruent with the terminology for analytical propagators. While Gauss-Legendre quadrature is employed to perform the averaging for the drag terms, it is only required for initialization. Perhaps this is the reason Vallado [149] considers HANDE to be semianalytical.

mosphere to account for the average solar flux and geomagnetic index [79]. HANDE also boasts an improved implementation of Brouwer-Lyddane theory that requires significantly fewer algebraic and trigonometric computations [77, 78]. Based on the preceding discussion of Section 1.2, it should be evident that Vinti theory can also form the basis of a general perturbations method.

1.3   Hybrid Satellite Theories

Hybrid or semianalytical theories aim to harness the best of analytical and numerical methods while overcoming the drawbacks of each, GP nominally lacking in accuracy and SP nominally lacking in speed. A primary example of such a hybrid theory is the Semianalytic Satellite Theory (SST) [42] conceived by Cefola et al. As a product of the Charles Stark Draper Laboratory, the theory was originally called the Draper Semi-analytical Satellite Theory (DSST), developed in the mid-1970s and early 1980s. The works of Cefola [32], McClain [116, 117], and Danielson et al. [41, 42] comprise thorough expositions of the mathematical details. The performance gains of SST are seen in the numerical integration stage, specifically its ability to take large time steps, typically a half day for Earth-orbiting satellites. SST develops a solution in spherical equinoctial orbital elements, employing both the Lagrange and Gauss forms of the variational equations (VOP) [14]. The EOMs are separated into a singly-averaged part and a short-periodic part. The averaging is performed analytically or numerically, depending on the type of perturbing acceleration [33], in the process producing Fourier coefficients and mean element rates. In par-

31

ticular, SST employs a Gaussian quadrature weighting to numerically average contributions from atmospheric drag and SRP with eclipsing [42]. Another important detail is the use of truncation algorithms in eccentricity that can limit the accuracy of SST for highly eccentric orbits. Techniques that alleviate this limitation are discussed in the next section. For applications to state estimation problems, SST can also simultaneously numerically integrate a mean element STM while maintaining the capability to take the same large step sizes for the variational equations. Analytical partials associated with some of the perturbations have been obtained [42] and the STM capability continues to be developed [34]. Another notable semianalytical theory is the Semianalytical Liu Theory (SALT) [109].

Recall from Section 1.1.5 that Vinti theory prescribes its own variational equations through an application of VOP. As VOP plays a central role in SST, one can extrapolate the above concepts to the oblate spheroidal geometry of Vinti theory. Whether a semianalytical theory referenced to the Vinti problem would be fruitful is an entirely separate question, but the fact remains that such a theory could be developed.

1.4 Numerical Techniques for Orbit Propagation

A vast number of numerical techniques exist for orbit propagation. A small selection is discussed here, specifically special perturbations (SP) and numerical averaging. Neta [121] gives an extensive though not exhaustive list of GP, SP, and semianalytical orbit propagators.

1.4.1 Special Perturbations

The methods of special perturbations involve numerical integration of the EOMs, which can incorporate all desired perturbations. Because perturbing accelerations are added linearly to the EOMs, it is easy in theory for these mathematical models to attain very high accuracy. Due to the complexity of the EOMs, they are not amenable to analytical solutions, but the practical necessity for high levels of accuracy spurred the development of techniques for solving the EOMs numerically. There are a vast number of numerical integration methods and it is outside the scope of the dissertation to review them here. The main takeaways are that they offer approximate solutions to the EOMs and they are often distinguished by their efficiency and accuracy. A method suitable to one problem or application may not be suitable to another. Consult Vallado [149] and the references therein for additional details.

Separate from numerical integration techniques are SP problem formulations. The two main ones are reviewed here. Encke's method is historically significant, enabling increased computational precision in numerical integrators at a time when computing power was limited, i.e. before the invention of modern computers. Generally speaking, Encke's method first requires the definition of an osculating orbit, which is customarily Keplerian. Instead of directly integrating the EOMs, only the perturbation away from the osculating reference is integrated [149]. The increased precision stems from the implied small magnitudes of the perturbing accelerations. When the perturbation in position becomes too large relative to the true path, the osculating orbit is rectified, meaning that it is re-initialized to be tangent to the most

recent position on the true trajectory. In contrast, Cowell's formulation and its variations directly integrate the EOMs [149]. While generally less popular, Encke's method continues to find use in certain applications [167].

The generality of these formulations does not free them from limitations. These methods are always limited by the accurate modeling of the underlying physical processes. For example, the modeling of atmospheric drag, in all its complexity, still falls short of capturing certain details, including the Sun's internal processes and the interaction of solar radiation with the atmosphere [149].

Encke and Cowell formulations may both be referenced to the Vinti problem instead of the Kepler problem. In other words, the osculating orbit in Encke's method could be Vinti's intermediary instead of a Keplerian ellipse. The claim is not that this choice will lead to countless benefits, but it is instructive to consider. One possible deduction and benefit is that rectification will need to be performed less frequently relative to a Keplerian reference. Another important detail is that the use of Vinti theory does not bind all analysis to oblate spheroidal techniques. For example, spherical harmonics are not rendered useless and the use of Vinti theory does not demand the use of oblate spheroidal harmonics. In fact, Vinti showed in 1971 how spherical harmonics could be constructed with respect to the Vinti potential [161]. From a geophysical perspective, this representation is arguably a more natural way to view the geopotential. Since the essential shape of the Earth is an oblate spheroid, such a spherical harmonic expansion would capture asymmetries.

1.4.2 Numerical Averaging

Numerical methods in orbit propagation often imply the use of strictly numerical integration, but this is not necessarily the case. Recent work has gone in the direction of some hybrid theories that average out the short-periodic dynamics before integrating. In the hybrid approach, much of this averaging is analytical, but the entirety of the averaging can alternatively be done numerically. This idea is the focus of recent work by Ely [54, 55], who applies fast Fourier transforms (FFTs) to determine the Fourier coefficients. The strength of this approach is its broader utility and application to many bodies in the solar system. It obviates the need for deriving expansions for each type of perturbing acceleration, and the absence of series truncation in eccentricity means the method is valid for highly eccentric orbits.

1.5 Motivational Problems

Vinti theory has now been set in context relative to a non-exhaustive yet broad array of astrodynamics tools. This dissertation is focused on analytical methods, and so the present discussion now homes in on some motivational problems. The advantages of analytical solutions may be leveraged in certain scenarios. A couple applications are highlighted in this section as examples of where Vinti's analytical solution may prove useful. As a main contribution of this dissertation involves the application of Vinti theory to the relative motion problem, emphasis is placed on this topic with an extensive literature review.

1.5.1 Spacecraft Trajectory Optimization

Spacecraft trajectory optimization represents another area that may benefit from the Vinti problem. When visiting bodies like Saturn with large J_2 perturbations, performing preliminary mission design with two-body dynamics may not be adequate. Specifically, solutions may disappear when adding perturbations through continuation methods. For capture or orbit insertion scenarios, it is possible that the issue may be traced to a strongly perturbed threshold between bounded and unbounded orbits. While the Vinti potential does not exactly capture Saturn's gravitational environment, it does capture the dominant effect of J_2 in addition to the point mass contribution. Recall that Vinti's solution can be cast in universal variables, just like the Kepler problem, and so it may be advantageous for other analyses as well near such bodies.

1.5.2 Space Object Catalog

This topic is largely included because researchers at the Air Force Institute of Technology (AFIT) have recently expressed strong interest in applying Vinti theory to the problem [168][9]. While the GP catalog is slated to transition to an SP catalog, current practice employs both. The current number of cataloged objects larger than a softball now exceeds 22,000 and only 5% are active satellites. The SP catalog is used for conjunction analysis, but SGP4 screens for close approaches. For this reason, the more accurate the tool used for

---

[9]The views expressed in Wright's dissertation do not represent the opinion of the U.S. Air Force, Department of Defense, or U.S. Government.

screening the better, since less time may be wasted on false alarms. Wright's thesis claims that Vinti theory can fill this role. Since it is not clear when the GP catalog will be discontinued, it is possible Vinti theory may be beneficial in this area, even if its use is temporary. Wright [168] assessed the utility of Wiesel's solution to the Vinti problem in an orbit determination (OD) framework, also incorporating drag through his own method (see Section 1.2.2.3). He made extensive comparisons to SGP4, noting several singularities in the particular solution employed based on the Vinti potential. These singularities exist for equatorial orbits, nearly circular orbits, and polar orbits. Wright also cites a strong interest in replacing his numerical STM with an analytical one for performing OD. The generalized equinoctial elements developed in this dissertation remove each mentioned singularity. An analytical STM and many enhancements are also contained herein, and so the contributions of this dissertation should aid significantly in their work.

1.5.3 The Spacecraft Relative Motion Problem

Missions involving on-orbit inspection of spacecraft and formation flying are both of great interest and are well-posed as relative motion problems. The nature of either application may be such that perturbations cannot be neglected, whether due to long time spans or large separations between constituent spacecraft [128]. In the literature on the relative motion problem, the reference orbit is generally a Keplerian orbit, where improvements in accuracy are obtained through perturbation methods. The approach in this dissertation leverages the theory of Vinti [152, 159] that analytically folds the first

37

few zonal harmonics into the reference orbit. A major goal of this dissertation is to demonstrate how Vinti's intermediary can be used to obtain an analytical solution to the relative motion problem and to ultimately assess its accuracy. Therefore, establishing a context requires a review of the relative motion problem.

The relative motion problem is concerned with characterizing the dynamics of one or more spacecraft with respect to a reference trajectory. The chief refers to a spacecraft or point in a reference trajectory. The deputy refers to a spacecraft or object flying in a neighboring trajectory, whose motion relative to the chief is portrayed in the rotating local-vertical, local-horizontal (LVLH) reference frame, or Hill's frame, centered on the chief. For a task of short duration, such as rendezvous, the popular Hill-Clohessy-Wiltshire (HCW) equations [73, 37] may suffice for nearly circular orbits and the Lawden [108], de Vries [44, 94][10], or Tschauner-Hempel [147] equations may serve well for other orbit regimes. These equations admit exact analytical solutions for circular [149, 110], elliptical [170, 25], or non-degenerate [31] reference orbits, but they are linearizations of the dynamics under spherical gravity. Thus, in addition to the stated assumptions on the reference orbit's eccentricity, the models are limited by two other major assumptions: 1) the deputy is sufficiently close to the chief such that nonlinear terms and perturbing forces are negligible; 2) the Earth is a point mass. These assumptions are violated for

---

[10]Karrenberg [94] noted some corrections to de Vries' *solution* (his EOMs are for arbitrary eccentricity but his solution is limited to small eccentricity) and also generalized his solution, removing the limitation that the initial position must coincide with the chief's periapsis.

the applications of interest in this dissertation.

Consideration of Earth's gravity perturbations in the relative motion problem began relatively recently, many neglecting the effects of eccentricity by utilizing circular reference orbits. Schweighart and Sedwick [131] obtained a solution including J_2 derived from equations of motion that possess a similar form to the HCW equations in Cartesian coordinates. Kasdin et al. [95] approached the HCW equations from the perspective of Hamiltonian mechanics, establishing the so-called epicyclic orbital elements through application of Hamilton-Jacobi theory. They then applied variation of parameters to obtain solutions for J_2-perturbed circular equatorial orbits as well as for circular inclined orbits. More recently, Omran and Newman [123] proposed a nonlinear Cartesian formulation that applies Volterra series theory to the case of a circular reference orbit subjected to the J_2 perturbation. This approach, for both perturbed and unperturbed models, has seen continued developments [141, 142, 122], though has still only been applied to a circular reference orbit.

Some models have considered eccentricity in addition to the J_2 perturbation. Kechichian's exact representation uses a frame also subjected to drag, but it requires numerical integration to propagate the orbit [97]. In the process, Kechichian also derived a transformation from Earth-centered inertial (ECI) to LVLH Cartesian coordinates in an arbitrarily perturbed environment. An approach by D'Amico and Montenbruck [40] adapts the eccentricity/inclination vector separation concept, initially designed and customarily used for colocated geostationary spacecraft, to describe relative motion of satellites in low

Earth orbit. Their linearized model assumes small eccentricities, or nearly circular orbits, for each spacecraft and accounts for certain effects of J_2 and differential drag. Schaub and Alfriend [130] used Brouwer's mean orbital elements to establish J_2-invariant relative orbits, essentially by matching the spacecraft drift rates. Resulting spacecraft formations appear fixed in an averaged sense for a variety of geometries. The Cid intermediary [35, 46] has also been applied to the relative motion problem [106], approximating the effects of J_2 and establishing periodicity conditions.

The use of analytical STMs to model relative motion has a long history and includes the solution to the HCW equations. As stated, the incorporation of perturbations into relative motion models, including eccentricity, started relatively recently, but STMs have broader applications. The earliest such STM known to the author is one developed in 1970. Specifically, the first analytical STM to consider J_2 and eccentricity together was apparently developed by Born and Kirkpatrick [24] and has been overlooked in the relative motion literature. While they omitted analytical expressions for the STM, they did provide explicit methods and numerical results. Using classical orbital elements, they define one STM that propagates the relative Brouwer mean elements to $O(J_2^2)$ and a second that propagates the relative osculating elements to $O(J_2^2)$ for the secular terms and $O(J_2)$ for the periodic terms. The method uses the Jacobian of the Brouwer transformation and optionally another to convert the STM to ECI coordinates. The underlying approach bears a strong resemblance to Gim and Alfriend's development [64], but with some notable differences. In Gim and Alfriend's work, the fundamental STM

propagates the relative state in Brouwer's mean element space to $O(J_2)$ using quasi-nonsingular elements. Depending on the desired inputs, the STM can be transformed to the Keplerian osculating element space to $O(J_2)$ using the Jacobian of the Brouwer transformation, or, through an additional Jacobian, further transformed to a type of spherical curvilinear coordinates in the LVLH frame, following closely the geometric method of Garrison et al. [61]. This linear model has seen continued developments. The quasi-nonsingular elements are defined for circular orbits but not for equatorial orbits, a problem remedied in a later study that re-expresses the STM in equinoctial elements [65]. Sengupta et al. [132] supplemented the original STM with a second-order state transition tensor, enlarging the region of validity via a nonlinear (quadratic) propagation theory. However, the model still suffers from the singularity at the critical inclination. Another quadratic relative model was proposed by Russell and Lantoine [127] that instead requires a single numerical propagation for the chief while allowing for arbitrary perturbations. This CURVE model was applied at Deimos, where gravity and third-body perturbations are extremely large.

Considerable attention has additionally been given to alternative coordinates in the rotating reference frame and even in the choice of rotating frame. In at least one instance, the adopted rotating reference frame is nonorthogonal, decomposing the in-plane motion into the chief position and velocity directions while the out-of-plane motion is still referenced to the angular momentum direction [98]. The cluster orbits with perturbations of Keplerian elements (COWPOKE) equations [129] and the unit sphere model [148] both

relate classical orbital elements to curvilinear LVLH coordinates, the former based on the direct application of spherical trigonometry and the latter derived from direction cosine matrices. This component is purely kinematic, where the unit sphere technique is exact and the COWPOKE equations propose to approximate the exact spherical trigonometry relations to first order in the element differences (the radial component is still exact). Using mean elements, the idea is that perturbations can be added to either model. True anomaly is related to time through expansions in eccentricity. The COWPOKE equations have found use in relative orbit determination for satellite clusters [75], in this case borrowing the along-track equation from the unit sphere approach for increased accuracy. Yan et al. [172] later developed an STM based on the unit sphere method.

Gleaning physical and geometrical insight is a priority as well when possible. To that end, the relative orbit element parameterization proposed by Lovell et al. [111] and advanced by Lovell and Spencer [110] converts the Cartesian representation of the HCW equations to six new parameters, each having unique geometrical insight into the linearized relative motion. Five of the six parameters describe the constant shape of the relative orbit and the sixth describes the orbit's linear drift, making the relative trajectory easy to visualize. The relative elements are directly related to the epicyclic elements [95] described earlier. Healy and Henshaw [72] tweaked the definitions to be exact geometric analogues to the classical Keplerian elements for relative motion,

calling them "geometric relative orbital elements"[11]. The preceding element sets of this paragraph are only valid for circular reference orbits. The eccentricity/inclination vector formulation mentioned earlier is also quite useful, having the distinct advantage of being valid for eccentric reference orbits.

1.6   Road Map

This dissertation is structured to set off distinct contributions as opposed to adhering to the structure of published content. Each major thrust of the research entailed a number of important but ancillary enhancements to Vinti theory itself that were essential to that particular topic or application. At the conclusion of this work, the number of enhancements had accumulated to a point where they could comprise an entire chapter. These miscellaneous improvements are contained in Chapter 2, which begins with some mathematical preliminaries for Vinti theory. The application to relative motion modeling may logically fit better toward the end of the dissertation, but the remaining chapters are instead organized chronologically, with good reason. The relative motion model presented in Chapter 3 is developed in terms of the classical spheroidal orbital elements, which are closely tied to Vinti's original work and the vast majority of enhancements. At this juncture, the research could have gone in many different directions. One could argue that there is no point in developing Vinti theory unless it is proven to be viable and competitive for

---

[11]Healy and Henshaw [72] also define so-called "apocentral" coordinates, the analogue of perifocal coordinates. They describe guidance schemes leveraging periodic relative orbits with respect to these parameterizations.

one or more important applications. On the other hand, one could argue that Vinti theory will never be taken seriously unless convenient, wholly nonsingular formulations are proven to exist for all orbit types. Of particular interest is validity for circular equatorial orbits, which are the "bread and butter" of astrodynamics in practice. Ideally, the contributions would rebut both arguments. As it stands, the relative motion model addresses the first argument, but greater effort is concentrated on developing a nonsingular theory. To that end, Chapters 4 and 5 focus on OS equinoctial orbital elements. Chapter 4 develops the coordinate transformations and Chapter 5 addresses analytical orbit propagation. The interfacing of equinoctial elements with universal variables is discussed in Chapter 2. Chapter 6 offers reflections on the main conclusions of the dissertation and identifies directions for future work.

1.7   Summary of Contributions

- A large number of enhancements to Vinti's analytical solution to the Vinti problem are introduced, all generally increasing the accuracy and precision, but in different ways. All enhancements are developed for the 1966 potential that includes J_3, which means that they also apply to the case when $J_3 = 0$ (Chapter 2).

  - New equations are developed that avoid catastrophic loss of precision.

  - Algorithms are identified to handle multiple revolution scenarios.

  - Singularities and indeterminate computations are removed for nearly

equatorial orbits.

- – A new equation is established for the element that Vinti introduced to resolve the polar orbit problem, enabling its computation in the initialization phase when converting from ECI coordinates to elements.

- – Several singularities associated with the zero-energy regime are removed, specifically associated with the anomalistic angles. The original equations were indeterminate in this regime, even though the quantities are physically well-defined.

- – An equation for the third fundamental frequency is derived for the first time. Subsequently, a new expression is derived for the secular motion of the ascending node that does not become indeterminate for polar orbits.

- – Several issues associated with universal variable implementations are resolved, generally encountered near the zero-energy threshold. Some solutions are proposed.

- – Practical issues in orbit design using classical OS elements are discussed and algorithms are presented that mitigate those issues.

- Vinti theory is successfully applied to the spacecraft relative motion problem. An analytical STM is derived in the orbital element space, and the linear transformations to rectangular coordinates are also included for both the inertial and rotating frames. New partial derivatives are obtained, some tied to the element that resolves some polar orbit

singularities, while other partials remove singularities contained in the original partials (Chapter 3).

- Casting the solution in a piecewise differentiable form enables the complete removal of the remaining singularities in the partial derivatives associated with polar and nearly equatorial orbits (Chapter 3).

- The Vinti-based STM is evaluated by comparison against a benchmark Brouwer-based STM and a numerically integrated solution. Over a range of eccentricity, inclination, and spacecraft separation distance, including the critical inclination, the Vinti-based model is shown to be more accurate than the other model (Chapter 3).

- A robust implementation of state propagation with STM computation (Chapters 2 and 3) has been released online as an open-source tool for Vinti-based relative motion modeling.

- Oblate spheroidal equinoctial orbital elements are introduced for the first time and derived. They are the generalization of the traditional, spherical equinoctial elements to an oblate spheroidal geometry. Concise algorithms for converting between inertial rectangular coordinates and the generalized equinoctial elements are presented. The transformations are exact except near the poles, where it is as accurate as the analytical solution (Chapter 4).

- As presented, the OS equinoctial elements completely remove all singularities except the nearly rectilinear orbit case. The singularities on the

poles are resolved for the first time in a robust fashion. Limitations on the maximum magnitude of J_2 are also relaxed with the development of an exact expression for the time derivative of the right ascension of the ascending node (Chapter 4).

- Analytical state propagation in Vinti's solution is recast and derived in OS equinoctial orbital elements. New elements are introduced and the equinoctial form of the generalized Kepler's equation is solved. Properties of OS equinoctial elements are established by comparison to their spherical counterparts (Chapter 5).

- With a view to universal analytical state propagation, an alternative quasi-nonsingular element set is proposed that is a very slight modification of the OS equinoctial set derived in Chapter 4. When properly coupled with the OS equinoctial set, the resulting piecewise element set forms the basis of a wholly nonsingular Vinti theory (Chapter 2).

Chapter 2

Enhancements to Vinti Theory: Relaxing Assumptions, Increasing Accuracy and Precision, and Removing Singularities

The overarching contribution of this chapter is a broadened applicability of Vinti theory achieved by better handling if not complete removal of known and newly discovered deficiencies. Accuracy and precision is improved and certain singularities are removed. Methods for dealing with some practical issues of orbit design are also presented. Each section and sub-section of this chapter represents or contains a new contribution to Vinti theory.

2.1 Revisiting Vinti's Solution

Vinti's analytical solution can be expressed as a nonlinear function $\mathbf{f}$ of the initial state $\mathbf{x}_i$:

$$\mathbf{x}^{\mathcal{J}} = \mathbf{f}(t, \mathbf{x}_i^{\mathcal{J}}) \tag{2.1}$$

where the superscript denotes the coordinates used to represent the state and the state vector is defined as

$$\mathbf{x}^{\top} = \begin{bmatrix} \mathbf{r}^{\top} & \mathbf{v}^{\top} \end{bmatrix} \tag{2.2}$$

so that in ECI coordinates, $\mathbf{x}^{\mathcal{J}} = [X, Y, Z, \dot{X}, \dot{Y}, \dot{Z}]^{\top} = [X, Y, Z, v_x, v_y, v_z]^{\top}$. Because the model in Chapter 3 is largely derived from Bonavito's computa-

tional procedure [21], the discussion of modifications and issues is often with respect to that particular reference. First, some nuances of factoring the quartics are discussed and improvements are suggested. Also to be addressed are some of the singularities punctuating the basic initialization process, defined as the steps required to convert initial ECI coordinates to a set of constant osculating spheroidal orbital elements or Vinti orbital elements (VOEs). The entire algorithm for the modified Vinti orbit propagator is depicted in the flow chart in Fig. 2.1. The main differences are the use of Ω' in the algorithm.

Initialization:
Transformation from ECI coordinates to spheroidal orbital elements

Orbit propagation in spheroidal orbital element space and transformation from spheroidal orbital elements to ECI coordinates
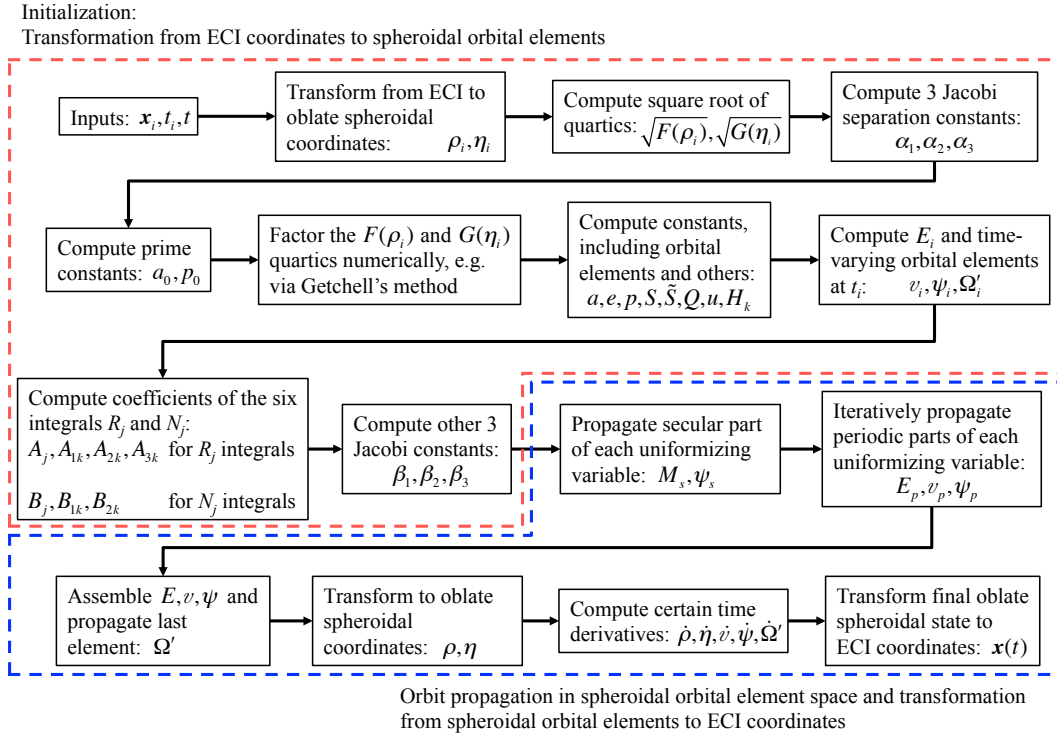
Figure 2.1: Flow chart for the modified bounded Vinti orbit propagator using the element Ω'.

While Vinti [160] formally defined the element Ω', its definition in terms of ini-

tial conditions given in ECI coordinates had remained elusive until now. The identification of appropriate methods of factoring the quartics for the bounded case, including those intended for universal formulations, is also new.

2.1.1 Oblate Spheroidal Coordinates

Vinti's method uses oblate spheroidal coordinates of the hybrid variety. Assuming that the ECI and OS frames share an origin at the Earth's center of mass, as in Vinti's original potential, ECI coordinates can be expressed in terms of OS coordinates as

$$X = \sqrt{(\rho^2 + c^2)(1 - \eta^2)} \cos \phi$$
$$Y = \sqrt{(\rho^2 + c^2)(1 - \eta^2)} \sin \phi \qquad (2.3)$$
$$Z = \rho\eta$$

where ρ is the semiminor axis of the oblate spheroid tangent to the spacecraft, η is the sine of a latitude-like angle, ϕ is the right ascension, and c is the radius of the spheroid's focal circle in the spheroidal equatorial plane (the focal separation is $2c$). The geometry of the coordinate system is depicted in Fig. 2.2. The notion of hybrid OS coordinates refers to the fact that the set retains one angle and eliminates the other. Notably, constant values of ρ specify confocal oblate spheroids, those of η specify confocal hyperboloids of one sheet [1], and those of ϕ specify meridional planes. The spheroids and hyperboloids share the same foci. In orbital mechanics applications, i.e. because the motion occurs

---

[1]There are two types of hyperboloids: one-sheet and two-sheet. Two-sheet hyperboloids of revolution are revolved around the axis passing through the foci, forming two separate surfaces. One-sheet hyperboloids of revolution are revolved around an axis perpendicular to the other that passes through the origin, forming one single surface.
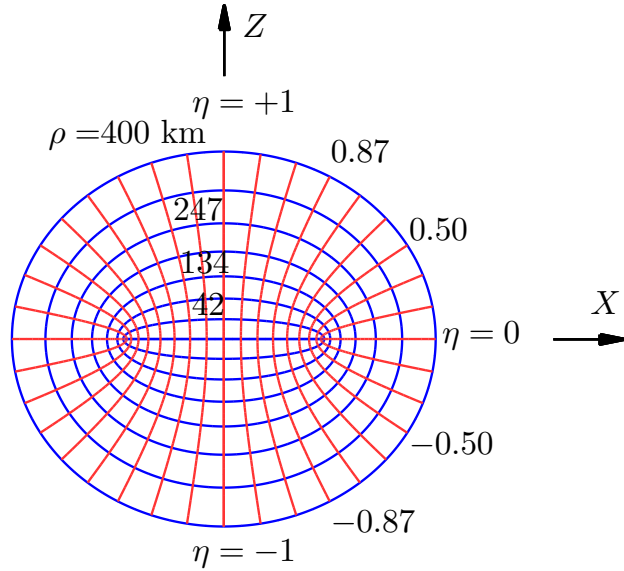
Figure 2.2: Geometry of oblate spheroidal coordinates: cross-section of the XZ-plane (the $\eta = 0$ line marks the equatorial plane) zoomed in to an equatorial radius of approximately 451 km.

outside the Earth, ρ is approximately the magnitude of the position vector and the latitude-like angle can be regarded approximately as the declination θ, where $\eta \approx \sin\theta$. The ranges on the coordinates are $\rho > 0$, $-1 \le \eta \le 1$, and $0 \le \phi < 2\pi$, where $\rho = 0$ defines the focal circle and the surface $\eta = 0$ is the portion of the equatorial plane outside the focal circle. The focal circle is actually a forbidden zone [104, 50]. Trajectories hypothetically passing through the forbidden zone are rare but still physically realizable, as for rockets or meteors having a near-unity eccentricity, representing a special case for which an analytical Vinti trajectory does not exist. Such trajectories must be handled numerically.

Sherrill [133] points out that the oblate spheroids of the coordinate

51

system as fitted above are not confocal with the oblate spheroid that approximates the shape of the Earth's figure. For the Earth, while $c \approx 210$ km for the fitted coordinate system, Sherrill finds the semi-focal separation of the approximating spheroid to be roughly 2.5 times greater at 520 km.

The present study uses the 1966 Vinti potential [158] given by

$$V = -\mu \frac{\rho + \eta z_\delta}{\rho^2 + c^2 \eta^2} \tag{2.4}$$

where μ is the gravitational parameter and z_δ is a parameter for capturing J_3 by shifting the origin of the OS frame along the Z axis. Thus, c and z_δ are parameters to be fitted to the primary body, chosen as

$$c^2 = R_e^2 J_2 \left(1 - \frac{J_3^2}{4 J_2^3} \right) ; \qquad z_\delta = -\frac{R_e J_3}{2 J_2}$$

where R_e is the primary body's equatorial radius. For the Earth, $c \approx 210$ km and $z_\delta \approx 7$ km. If the magnitude of J_3 approaches or exceeds J_2, then it is possible to find $c^2 < 0$ and an analytical Vinti trajectory does not exist in this case either. The specific condition for model validity is

$$J_3^2 < 4 J_2^3 \tag{2.5}$$

Also notice that these parameters reduce to the expected values if J_3 is to be neglected.

2.1.2 Orbital Element Sets

The proposed relative motion model makes use of multiple spheroidal orbital element sets. The VOEs, denoted as $\boldsymbol{\text{œ}}^V$, are obtained from initial

conditions mostly following Bonavito's mechanization [21]. This procedure can furnish the element set $[a, e, S, \beta_1, \beta_2, \beta_3]$, where a is the semimajor axis, e is the eccentricity, notionally $S \approx \sin^2 I$, I is the inclination, and the β_j are Jacobi constants derived from the kinematic equations. An alternative interpretation of the same set is given by $[a, e, S, -\tau, \omega, \Omega]$, where the β_j are replaced with the familiar symbols of τ for time of periapsis passage, ω for argument of periapsis, and Ω for right ascension of the ascending node (RAAN). While not mentioned in the literature, the theory appears to be valid if the equality $S = \sin^2 I$ is enforced and I is adopted as an element instead of S, but only if the inclination is allowed to extend into the complex plane. Alternatively, a different inclination could be defined from $Q = \sin I'$, as suggested by Getchell [62], where I' remains real (the connection between S and Q is discussed later in Eq. (2.11)). Of the elements $[a, e, S, -\tau, \omega, \Omega]$, those written without subscripts refer to the Vinti or spheroidal orbital elements. Lang [104], who apparently coined the term spheroidal elements, uses the phrase to distinguish between Vinti elements and Keplerian elements, which are spherical. As motivation for coining the term, consider that an orbit having $e = 0$ is circular for spherical elements (constrained to the surface of a sphere), while for spheroidal elements, the orbit could be circular or elliptical [159], or otherwise constrained to the surface of a spheroid. These spheroidal orbital elements are constants of the motion. They are analogous to, but different from, the osculating Keplerian elements (and are completely different from Brouwer's mean elements).

The spheroidal element set just described is useful for drawing connec-

tions to the Kepler problem, but it is less favorable for a perturbation theory. A better element set is what Vinti calls the new Delaunay set [156]. Garfinkel et al. [60] refer to these as "natural" Delaunay elements. In this chapter, the VOEs are based on this Delaunay set such that $\mathbf{œ}^V = [a, e, S, l_0, g_0, \beta_3]^\top$, which results from several canonical transformations that Vinti partly attributes to Izsak [86]. Vinti used the subscript "0" to denote that these quantities are initial conditions, but they actually reference the time of spheroidal periapsis passage. The subscript "i" will be used instead to denote actual initial conditions to be consistent with the notation in this dissertation and Vinti's notation. The notation adopted for these alternative elements is $\lambda_1 = l_0$ and $\lambda_2 = g_0$. From another canonical transformation, Vinti also derived a relation for the third spheroidal Delaunay element, $\lambda_3 = h_0$, but suggested that $\lambda_3 = \beta_3$ is a better choice. The quantity h_0 will become necessary in Chapter 5. To summarize, the notation adopted here is related to Vinti's notation as

$$
\mathbf{œ}^V =
\begin{bmatrix}
a \\
e \\
S \\
\lambda_1 \\
\lambda_2 \\
\lambda_3
\end{bmatrix}
=
\begin{bmatrix}
a \\
e \\
S \\
l_0 \\
g_0 \\
\beta_3
\end{bmatrix}
\tag{2.6}
$$

except that to remove singularities in the partials, which is discussed later, S is replaced with other related quantities. The element l_0 is analogous to M_0 in the Kepler problem, except that l_0 is the initial value of only the secular part of $M(t)$. The mean anomaly in the Kepler problem is purely secular, but in the Vinti problem, the analogue has a periodic part. The element g_0 does not have an analogue in the Kepler problem, where g would be equivalent

to the original Jacobi constant, but its mathematical form follows that of l_0. One could consider the secular evolution of the argument of periapsis in the equivalently perturbed Kepler problem as being related to the variable g in the Vinti problem.

The particular element set in Eq. (2.6) leads to some simplifications in the partial derivatives (see Appendix C.3). However, VOEs are actually not the primary set used in the current work. Instead, they serve more as an intermediate set. As Tong and Wu [145] did in their perturbation work, the λ_j are replaced with time-varying angles for the application to relative state propagation. A distinct difference is that the present study adopts an element set that includes the secular and periodic contributions to the angular variations, whereas Tong and Wu only considered secular effects. An appealing state representation is also one for which all the time-varying quantities in the nonlinear transformation to ECI coordinates appear in the state. Thus, the chosen spheroidal element set is $\text{œ}^S = [a, e, S, f, \psi, \Omega']^\top$, where f is the true anomaly, ψ is the true argument of latitude, and Ω' is a slowly varying angle similar to RAAN, originally suggested by Izsak [85]. Vinti [160] developed the last element to remove singularities for polar orbits, which are discussed in detail in later sections. It is convenient at this time to also establish the other orbital element sets used in the GA STM. In particular, the quasi-nonsingular Keplerian osculating element set is defined as $\text{œ}^K = [a_K, \psi_K, I_K, q_{K_1}, q_{K_2}, \Omega_K]^\top$ and the associated Brouwer mean element set is defined as $\overline{\text{œ}}^K = [\bar{a}_K, \bar{\psi}_K, \bar{I}_K, \bar{q}_{K_1}, \bar{q}_{K_2}, \bar{\Omega}_K]^\top$. In these sets, $\psi_K = f_K + \omega_K$ is the Keplerian true argument of latitude, $q_{K_1} = e_K \cos \omega_K$

and $q_{K_2} = e_K \sin \omega_K$ are components of the Keplerian eccentricity vector, and ω_K is the Keplerian argument of periapsis. Interestingly, Kozai's justification for not using Vinti's solution as an intermediary orbit is that the VOEs are too different in value from the mean values of standard elements [102]. He was reluctant to adopt a new definition of orbital elements.

2.2   General Enhancements in Accuracy and Precision

General improvements to Vinti theory are associated with factoring the quartics, handling multiple-revolution scenarios for bounded orbits, and avoiding catastrophic cancellation in computations. Note that the section on the quartics includes a discussion relevant to a singularity-free factorization for bounded orbits, in addition to unbounded orbits and trajectories having nearly zero specific energy.

2.2.1   Factoring the Quartics

Factoring the quartics $F(\rho)$ and $G(\eta)$ is an important step in Vinti's solution because the first three orbital elements are expressed in terms of their roots. In notable integrable problems in celestial mechanics, periapsis and apoapsis distances can be obtained from the roots of a characteristic polynomial. This polynomial is a quadratic in r in the Kepler problem [50], a cubic (degenerate quartic) in r in the J_2-perturbed equatorial problem [90], and a general quartic $F(\rho)$ in the Vinti problem[2,3]. In the last two cases, the

---

[2]The $F(\rho)$ quartic is also degenerate in the equatorial Vinti problem.
[3]The polynomial in the Stark problem is also a quartic.

corresponding roots can be thought of as perturbed periapsis and apoapsis distances. Using these distances with Keplerian relations, it is easy to obtain quantities analogous to semi-major axis and eccentricity from the Jacobi separation constants. In the spirit of maintaining an analytical form of solution, Vinti [154] proposed a method of successive approximations to analytically factor $F(\rho)$ into the form

$$F(\rho) = -2\alpha_1(\rho - \rho_1)(\rho_2 - \rho)(\rho^2 + A\rho + B) \tag{2.7}$$

and, for the other quartic [158], an iterative procedure based on analytical relations truncated to certain orders when necessary, factoring $G(\eta)$ into the form

$$G(\eta) = \frac{\alpha_2^2 - \alpha_3^2}{S}(S + 2P\eta - \eta^2)(1 + C_1\eta - C_2\eta^2) \tag{2.8}$$

In Eqs. (2.7) and (2.8), α_j are the separation constants for $j = 1, 2, 3$. The a and e elements are related to two roots of $F(\rho)$ as

$$a = \frac{1}{2}(\rho_1 + \rho_2) \tag{2.9}$$

$$e = \frac{\rho_2 - \rho_1}{\rho_2 + \rho_1} = 1 - \frac{\rho_1}{a} \tag{2.10}$$

where $\rho_1 \leq \rho \leq \rho_2$, and the S element is related to two roots of $G(\eta)$ as

$$S = -\eta_0\eta_1 = Q^2 - P^2 \tag{2.11}$$

where $-1 \leq \eta_1 \leq \eta_i \leq \eta_0 \leq 1$ and

$$P = \frac{1}{2}(\eta_0 + \eta_1) \tag{2.12}$$

$$Q = \frac{1}{2}(\eta_0 - \eta_1) \tag{2.13}$$

57

Equation (2.13) is not explicitly given in the literature. Notice that P and Q are defined in terms of the roots of $G(\eta)$ in a way analogous to how a and ae are defined in terms of the roots of $F(\rho)$. In turn, the way P and Q are used in the equation $\eta(\psi) = P + Q \sin \psi$ to propagate η is analogous to how a and e are used in the equation $\rho(E) = a - ae \cos E$ to propagate ρ.

2.2.1.1 Discussion of Methods

A number of researchers have since addressed the question of how to factor the quartics, but the methods have not been compared systematically in terms of advantages and disadvantages. For computing S and related quantities, Bonavito [21] closely follows Vinti's suggestion and lays out an iterative procedure that converges rapidly. In practice, however, precision suffers significantly in some cases, and a more robust solution is to use a different numerical approach. One option, which Wiesel [166] chose for the 1961 potential, is to obtain the roots as the eigenvalues of the companion matrices [53], but the approach is prone to precision issues and raises questions on root identification. A better option is Getchell's technique [62], which enjoys excellent numerical properties and a significant speedup. Note that these results assume a small J_2 value like the Earth's. If J_2 is large, e.g. greater than 10^{-1}, then Getchell's method will require more iterations to converge, and the eigenvalue approach may be preferable.

Getchell's method of factorization iteratively factors both quartics using four simple equations per quartic [62], typically converging to double precision in no more than five iterations each. More iterations may be required in some

cases, such as for nearly parabolic orbits or for large J_2. His method does not appear to suffer from losses in precision that can arise in the eigenvalue approach, and it is also robust, except as Getchell notes in the case where the trajectory is characterized by a very small p_0, which is similar to semilatus rectum [62]. Orbits exhibiting such small p_0 values are not relevant for the present study because periapsis for this class of orbits is near the forbidden zone. While valid for bounded and unbounded orbits, it is straightforward to adapt Getchell's algorithm to an overall formulation that avoids universal variables, as needed in the present study.

In terms of speed, tests in MATLAB for a representative case with $J_2 = 1.08 \times 10^{-3}$ revealed that Getchell's algorithm, as compared to the eigenvalue-based approach, is roughly 18 times faster for factoring $F(\rho)$ and 14 times faster for factoring $G(\eta)$. The chosen example required 7 iterations for Getchell's algorithm to factor $F(\rho)$, which is toward the high end for typical Earth scenarios, and 4 iterations to factor $G(\eta)$, which is on the low end. These timings neglect overhead in the eigenvalue-based approach that may be devoted to handling numerical issues. They also specify a convergence tolerance in Getchell's algorithm that leads to a double precision factorization, so that the maximum number of iterations is executed. As such, actual speedups attained with Getchell's method may be higher in practice. Note that the implementation of Getchell's method uses Getchell and Monuki's technique for factoring $F(\rho)$, initializing the algorithm at the second iteration by analytically determining the values output after the first iteration [50]. In the current study, the author applied a similar technique to factor $G(\eta)$. If forced

to execute 7 iterations, factoring $G(\eta)$ is still roughly 10 times faster than the eigenvalue method.

2.2.1.2 Connecting Getchell's Method to Vinti's Solution for Bounded Orbits

To adapt Getchell's method to the present formulation for bounded orbits, there are a number of notational differences to keep track of and a few additional quantities to compute after factoring. Der and Bonavito [50] give some of these relations, not all, and of those that they give, several contain typographical errors, which are corrected here. For $F(\rho)$, the relations between Getchell's notation and Vinti's, giving Getchell's first, are $A_1 = b_1 = -A/2$, $B_1 = B$, $\gamma_0/\gamma_1 = \gamma$, and $\gamma_0 = 2\alpha_1/\mu = -1/a_0$, where $\gamma = -p/(\rho_1\rho_2) = -2/(\rho_1 + \rho_2) = -1/a$. Note that a_0 and p_0 are among the so-called "prime constants" [21]. These two constants are analogues of semimajor axis and semilatus rectum, having the usual relationships to the separation constants. The quantities related to semimajor axis are used in Vinti's solution, but would never be computed in the universal variables approach. For $G(\eta)$, the equivalent quantities in Getchell's notation are $\sigma = \eta$, $P_1 = C_1$, $Q_1 = C_2$, $S_0/S_1 = S$, $S_0 = 1 - \alpha_3^2/\alpha_2^2$; the notation for S, P, and Q is unchanged. After obtaining C_2, Vinti's derived constant u must also be computed and can be obtained from

$$u = \frac{a_0 p_0}{c^2} C_2 \tag{2.14}$$

which avoids Vinti's treatment that approximates u as a root of a cubic equation in $1/u$ [158]. One obvious issue with Eq. (2.14) is that as $c \to 0$, i.e. as the

dynamics become more Keplerian, the computation of u becomes inaccurate due to the division by zero. This property is undesirable, as the Vinti solution should smoothly approach the Kepler solution as oblateness decreases to zero. A better equation for computing u is to use Getchell's equation for S_1 noting that $u = 1/S_1$. Getchell computes S_1 as

$$S_1 = \frac{p_0 - c^2\gamma_0 - S_0 p_0 Q_1}{(1 - 2PP_1)p_0} \tag{2.15}$$

2.2.1.3 Connection to Fundamental Frequencies

Factorization of the quartics is also essential to computing accurate fundamental frequencies. Getchell's factorization algorithm can enable the calculation of the mean frequencies to very high accuracy. Effectively, the only limit on the accuracy of the mean frequencies is imposed by the secular coefficients B_1', B_2, and B_3, which are respectively correct to $O(J_2^3)$, $O(J_2^4)$, and $O(J_2^4)$ (Walden and Watson [164] corrected Vinti's expressions for these coefficients). To increase accuracy, these expressions need only be carried to higher order. Section 2.4 gives a new expression for the third mean frequency and relates the fundamental frequencies to Wiesel's [166] equations for the frequencies.

2.2.2 Avoiding Catastrophic Cancellation

One important caveat to using any of the mentioned procedures to factor the quartics is that α_2 and the difference $\alpha_2^2 - \alpha_3^2$ must not be computed blindly. Some formulas for α_2 have singularities at the poles and $\alpha_2^2 - \alpha_3^2$ is prone to catastrophic cancellation for nearly equatorial orbits, which is not

61

mentioned in the literature. These Jacobi constants are close in value in this case because α_3 is the polar component of angular momentum and α_2 is closely related to the total angular momentum. In general, it is better to use the singularity-free equation [62]

$$\alpha_2^2 = 2\mu\rho_i + 2\alpha_1\rho_i^2 + \frac{c^2\alpha_3^2 - F(\rho_i)}{\rho_i^2 + c^2} \tag{2.16}$$

to compute α_2, but the alternative equation [62]

$$\alpha_2^2 = -2\mu\eta_i z_\delta - 2\alpha_1 c^2\eta_i^2 + \frac{\alpha_3^2 + G(\eta_i)}{1 - \eta_i^2} \tag{2.17}$$

is useful for nearly equatorial orbits, far from the singularity at $\eta_i = 1$, when trying to compute the difference $\alpha_2^2 - \alpha_3^2$. To retain significant digits in the difference, this quantity should be computed as

$$\alpha_2^2 - \alpha_3^2 = -2\mu\eta_i z_\delta - 2\alpha_1 c^2\eta_i^2 + \frac{\alpha_3^2\eta_i^2 + G(\eta_i)}{1 - \eta_i^2} \tag{2.18}$$

for orbits sufficiently close to equatorial. Using Eqs. (2.16) and (2.18) has shown to help prevent violations of the various bounds on η_i, η_0, and η_1 in the eigenvalue method and generally improves precision in Getchell's method, directly affecting the number of correct digits in S_0. Obtaining the most precise estimates of a, e, S, P, and Q is important because these constants are used directly in equations toward the end of the propagator without further modification to propagate ρ and η. Errors in the final OS coordinates perceived to be small can grow substantially under the nonlinear transformation back to ECI coordinates. Without the enhancements of this sub-section, it is impossible to obtain a reliable analytical solution for nearly equatorial orbits.

2.2.3 Error Growth under the Nonlinear Coordinate Transformation

This sub-section explores and expands on the above statement regarding the potential for large error growth under the nonlinear transformation from OS coordinates back to ECI coordinates. The point is most easily illustrated with the Z coordinate, where $Z = \rho\eta - z_\delta$. The shift of z_δ is dropped in the following discussion without loss of generality.

Suppose the final, propagated OS coordinates ρ and η are modeled as having some error ϵ:

$$\rho = \bar{\rho} + \epsilon_\rho \tag{2.19}$$

$$\eta = \bar{\eta} + \epsilon_\eta \tag{2.20}$$

The Z coordinate can then be expressed as

$$Z = \rho\eta = (\bar{\rho} + \epsilon_\rho)(\bar{\eta} + \epsilon_\eta) = \bar{\rho}\bar{\eta} + \bar{\rho}\epsilon_\eta + \bar{\eta}\epsilon_\rho + \epsilon_\rho\epsilon_\eta \tag{2.21}$$

The $\bar{\rho}\bar{\eta}$ term represents the exact value of Z. The quadratic error term $\epsilon_\rho\epsilon_\eta$ may be neglected because it is $O(J_2^6)$, assuming a solution correct to $O(J_2^2)$. The $\bar{\eta}\epsilon_\rho$ term does not worsen the accuracy of Z beyond the error already in ρ because $-1 \leq \eta \leq 1$. However, the $\bar{\rho}\epsilon_\eta$ term could be a real problem that potentially adds orders of magnitude of error because $\bar{\rho}$ may be around 10^4 km and ϵ_η may be around 10^{-6}. If catastrophic cancellation has entered into the ϵ_η error for an equatorial case, then the error in Z could be several meters, for example.

2.2.4 Handling Multiple Revolutions

Recall from Vinti [158] that the propagation step is solved in three stages to successively higher order, concluding with second order periodic terms. If the spacecraft is near spheroidal periapsis, then it is possible during the propagation step for the anomaly to bounce around the boundary in the range $-\epsilon \leq v \leq \epsilon$ for some small ϵ. At each stage, the various anomalistic angles must be consistent. In the Kepler problem, the angles must locate the spacecraft in the same half of the ellipse, on one side of the apse line, which when restricted to near periapsis amounts to the angles being in the same quadrant. In the Vinti problem, then, an equivalent requirement is that $\{v, E, M\} \in [0, \pi)$ or $\{v, E, M\} \in [\pi, 2\pi)$ in general and at each stage of state propagation.

Let n_{p_j} be the number of times the spacecraft passes through periapsis determined as

$$n_{p_j} = \left\lfloor \frac{M_j}{2\pi} \right\rfloor \tag{2.22}$$

for each stage j, where M_j is the effective mean anomaly and the brackets denote the floor function, rounding the argument to the nearest integer toward negative infinity. Note that by this definition, n_p can be negative, which has the advantage of allowing the use of the same formulas for forward and backward propagation. Note also that precision loss would become an issue after millions of revolutions, but it does not represent a practical issue because a Vinti trajectory would need to be rectified to improve accuracy well before such a precision problem arises.

The following discussion walks through the necessary steps for an algorithm. It begins with stage $j = 0$, which considers only the incorporation of zeroth order periodic terms. For stage $j = 0$, the effective mean anomaly is $M_0 = M_s$. In other words, the periodic contribution in stage 0, which is the zeroth order periodic term, is $M_{p_0} = 0$. If $n_{p_0} = 0$, then the mean anomaly for the stage is $M_0 = M_s$ with no adjustment for periapsis passes. Otherwise, or more generally, M_0 is determined as

$$M_{\text{mod}_0} = M_s - 2\pi n_{p_0} \tag{2.23}$$

The stage ends with the determination of E_0, f_0, and ψ_0. Note that the notation in this section for these angles indicates the effective or total angle, whereas Vinti used this notation to denote periodic components of order equal to the number in the subscript. For clarity in this section, the periodic components are instead indicated with an additional subscript "p" as in E_{p_0}. The anomalies E_{mod_0} and f_{mod_0} are obtained from solving Kepler's equation and applying the anomaly relations. The effective argument of latitude is determined as $\psi_0 = \psi_s + \psi_{p_0}$, where ψ_{p_0} is computed once f_{p_0} is known. These equations are all available in Vinti [158], although due to typographical errors it is better to reference Bonavito [21].

Incrementing j, stage $j = 1$ begins with computing M_{p_1} from Eq. (5.6) in Bonavito [21]. Now, the effective mean anomaly is

$$M_1 = M_s + M_{p_1} \tag{2.24}$$

Equation (2.22) can be applied to obtain a corrected count n_{p_1} for the number

of passes through periapsis.

$$M_{\text{mod}_1} = M_s + M_1 - 2\pi n_{p_1} \tag{2.25}$$

Equations in Bonavito [21] relevant to stage $j = 1$ are applicable for determining E_1, f_1, and ψ_1, and the algorithm continues in this fashion to arbitrary stage/order j. The emerging pattern can be generalized to an arbitrary number of stages as

$$M_{\text{mod}_j} = \left(M_s + \sum_{k=1}^{j} M_{p_k} \right) - 2\pi n_{p_j} \tag{2.26}$$

or

$$M_{\text{mod}_j} = M_j - 2\pi n_{p_j} \tag{2.27}$$

where n_{p_j} is properly corrected at each stage j in the event that successive higher order corrections push the satellite location alternately beyond and behind periapsis.

2.3   Removing Singularities

This section discusses how to remove the troublesome singularities that appear in Vinti's original work, referring to either of his solutions. Recall that his 1961 solution [154] is based on the separable problem defined by the 1959 potential [152] ($J_3 = 0$) and his 1966 solution [158] is based on the separable problem defined by the 1966 potential [159] ($J_3 \neq 0$). He summarized these solutions in 1969 with a modification that introduced spheroidal RAAN as an orbital element [160] to extend his solution to polar orbits. The singularities mitigated here are strong singularities, meaning that they are at some point

associated with a division by zero, whether in theory or implementation. Singularities associated with nearly zero energy are ignored because neither Vinti's nor Lang's solution was designed to be valid in that orbit regime. Nonetheless, nonsingular expressions are derived for the time derivatives of several key angular elements because of their subsequent use in the equinoctial elements solution in Chapter 4. Existing expressions for those quantities are singular or indeterminate when the energy is near zero. The singularities associated with angle ambiguities in the orbital elements are treated separately in Chapter 4 with the introduction of oblate spheroidal equinoctial orbital elements ($J_3 = 0$ case).

2.3.1 Singularities Associated with Polar Orbits

As for spherical coordinates, the azimuthal angle in oblate spheroidal coordinates becomes undefined for polar orbits. This problem can be remedied by replacing right ascension with the slowly varying angle Ω', which was mentioned previously. After incorporating the z_δ offset and this alternative element of Vinti [160], the ECI coordinates satisfy:

$$X = \sqrt{\rho^2 + c^2} \left[H_1 \cos \Omega' \cos \psi - \operatorname{sgn} \alpha_3 \frac{\sqrt{1-S}}{H_1} \sin \Omega' (H_2 + H_3 \sin \psi) \right]$$

$$Y = \sqrt{\rho^2 + c^2} \left[H_1 \sin \Omega' \cos \psi + \operatorname{sgn} \alpha_3 \frac{\sqrt{1-S}}{H_1} \cos \Omega' (H_2 + H_3 \sin \psi) \right]$$

$$Z = \rho \eta - z_\delta$$

$$(2.28)$$

where H_k are constants for $k = 1, 2, 3$. The signum function $\operatorname{sgn}(\cdot)$ is used throughout this dissertation and should be interpreted without the zero condition so that $\operatorname{sgn}(0) = 1$. While Vinti's equations address the singularity

67

associated with propagation, without the inverse transformation from ECI coordinates to Ω', Vinti orbit initialization is still poorly defined for nearly polar orbits and for the pathological case of initializing when a spacecraft is on a pole. The element β_3 must be computed using the nonsingular equation given by Vinti [160]:

$$
\begin{aligned}
\beta_3 = \Omega'_i &+ \frac{\alpha_3 c^2}{(-2\alpha_1)^{\frac{1}{2}}} \left(A_3 v_i + \sum_{k=1}^{4} A_{3k} \sin k v_i \right) \\
&- \frac{\alpha_3 u^{\frac{1}{2}}}{\alpha_2} \left(B_3 \psi_i - \frac{3}{4} C_1 C_2 Q \cos \psi_i + \frac{3}{32} C_2 Q^2 \sin 2\psi_i \right)
\end{aligned}
\tag{2.29}
$$

which requires that Ω' be computed directly from initial conditions (the singularity at zero energy is still present). Expressions for the constants A_j A_{3j}, B_3, and C_j are given by Vinti [154, 158]. Such a relationship for Ω' was never given, however. In addition to the singularity, the original equation for β_3 also requires evaluating the initial right ascension as $\phi = \text{atan2}\,(Y, X)$, so that near a pole, whether the orbit is exactly or nearly polar, ϕ is highly sensitive to variations in X and Y. After some manipulation of the X and Y equations in Eq. (2.28), it can be shown that

$$
\begin{aligned}
\Omega' = \text{atan2} \Big[& Y H_1 \cos \psi - \text{sgn}\,\alpha_3 X H_1^{-1} \sqrt{1-S}(H_2 + H_3 \sin \psi), \\
& X H_1 \cos \psi + \text{sgn}\,\alpha_3 Y H_1^{-1} \sqrt{1-S}(H_2 + H_3 \sin \psi) \Big]
\end{aligned}
\tag{2.30}
$$

Eq. (2.30) is valid for any time, exhibiting improved behavior near the poles for nearly polar orbits. While not defined exactly at the pole, this situation can only occur for exactly polar orbits, when Ω' is equal to the easily computed Keplerian RAAN. When sufficiently far from the $e = 0$ singularity, an alternative way to handle the pathological case that would guarantee smooth

behavior near the poles is to use a differential correction procedure [163], which generally converges to the VOEs in two to four iterations. Note that this procedure uses a different element set discussed in a later section, where S is replaced with $\tilde{S}$. A similar procedure is used in the present study to transform Keplerian osculating elements to Brouwer mean elements. To obtain mean elements, an iterative procedure is always required, whereas to obtain classical Vinti elements, it may only be required in rare, pathological cases.

2.3.2 Singularities Associated with Equatorial Orbits: b_2

Vinti has an elegant way of expressing the secular coefficients A_1, A_2, and A_3 with Legendre polynomials. The expressions for these coefficients contain terms of the form $(b_2/p)^n P_n(b_1/b_2)$, where $b_1 = -A/2$, $b_2 = \sqrt{B}$, and $p = a(1 - e^2)$. These terms clearly become indeterminate when $b_2 = 0$, occurring for equatorial orbits under Vinti's 1959 potential (reminiscent of the degenerate quartic in the J_2-perturbed equatorial problem). For the 1966 potential, when the origin of the OS frame is shifted z_δ below the ECI frame, b_2 transitions from real and positive to zero to purely imaginary at a small inclination greater than equatorial when $\alpha_2 = \alpha_3$. This statement is equivalent to saying that B transitions from positive to negative at the same inclination because $b_2 = \sqrt{B}$. Vinti [155] pointed out this singularity and devised a way to remove the indeterminacy by using $(b_1/p)^n R_n(b_2/b_1)$ instead near the singularity, where $R_n(x) \equiv x^n \cdot P_n(1/x)$. Note that this alternative form is not always valid either because b_1 approaches zero for nearly polar orbits.

In this study, in which partial derivatives are also required, the b_2 singu-

larity appears in new places such that a new approach to handle the singularity is necessary. The Walden and Watson [164] equations for partial derivatives are useful away from the singularity and can leverage the recursive definition of Legendre polynomials and their first derivative. However, these equations suffer from the same singularity, originating from the equation for the partial of b_2:

$$\frac{\partial b_2}{\partial \sigma_j} = \frac{1}{2ab_2} \left[(ap - c^2) \left(\frac{b_1}{a} \delta_{1j} - \frac{\partial b_1}{\partial \sigma_j} \right) - b_1 \left(p\delta_{1j} + a \frac{\partial p}{\partial \sigma_j} \right) \right] \qquad (2.31)$$

A convenient notation similar to Walden and Watson's is adopted here, where $\sigma_1 = a$, $\sigma_2 = e$, and $\sigma_3 = S$, and δ_{jk} is the Kronecker delta [164]. Expanding and simplifying all relevant equations of Vinti's theory [154] and Walden and Watson's partials reveals that b_2 never appears in the denominator and $\partial b_2 / \partial \sigma_j$ is always multiplied by b_2 or higher powers of b_2. In other words, the singularity at $b_2 = 0$ is artificial, a product of how the equations are expressed or computed.

In most cases, the singularity in the partials is easily avoided by directly computing $b_2 \cdot \partial b_2 / \partial \sigma_j$ from Eq. (2.31) without dividing by b_2. However, the partials of the A_i coefficients are problematic as presented by Walden and Watson [164]. First, they imply computing Legendre polynomials separately, which means Vinti's remedy must be used near the singularity. But regardless of whether Vinti's technique for removing the indeterminacy is used, there are terms containing $\partial b_2 / \partial \sigma_j$ that are not multiplied by b_2. For example, in the equation for $\partial A_1 / \partial \sigma_j$, the term containing $\partial/\partial \sigma_j (b_1/b_2)$ can at best be multiplied by b_2^2, so that the $\partial b_2 / \partial \sigma_j$ term within $\partial/\partial \sigma_j (b_1/b_2)$ still contains

the singularity. As long as the condition $J_2 < 0.17$ is satisfied, the Legendre expansion for the A_i coefficients is valid over all inclinations [50]. Instead of treating the Legendre polynomials as isolated recursive computations within the summed terms, the product $(b_2/p)^n P_n(b_1/b_2)$ should be multiplied out before computation to avoid dividing by zero. Because $(b_2/p)^n P_n(b_1/b_2)$ and $(b_1/p)^n R_n(b_2/b_1)$ are interchangeable with overlapping regions of validity, it is justified to expand the expressions in this manner as Vinti did for the analogous periodic coefficients A_{ij}. The cost is the extra compute effort associated with explicit (as opposed to recursive) Legendre polynomials. The modified partial derivatives of these secular coefficients are included in Appendix C.1.

2.3.3 Some Singularities Associated with Zero Energy

Vinti writes $\dot{f}$ as

$$
\begin{aligned}
\dot{f} &= \frac{a}{\rho} \left[-2\alpha_1(1-e^2) \right]^{1/2} \frac{(\rho^2 - 2b_1\rho + b_2^2)^{1/2}}{\rho^2 + c^2\eta^2} \\
&= \frac{a}{\rho} \left[\frac{\mu(1-e^2)}{a_0} \right]^{1/2} \frac{(\rho^2 - 2b_1\rho + b_2^2)^{1/2}}{\rho^2 + c^2\eta^2}
\end{aligned}
\tag{2.32}
$$

which is indeterminate when $e = 1$ due to $0 \cdot \infty$ computations. Noting $a = \sqrt{a^2}$, the equation can be rewritten as

$$
\begin{aligned}
\dot{f} &= \frac{1}{\rho} \left[\mu \left(\frac{a}{a_0} \right) a(1-e^2) \right]^{1/2} \frac{(\rho^2 - 2b_1\rho + b_2^2)^{1/2}}{\rho^2 + c^2\eta^2} \\
&= \frac{(\mu\gamma_1 p)^{1/2}}{\rho} \frac{(\rho^2 - 2b_1\rho + b_2^2)^{1/2}}{\rho^2 + c^2\eta^2}
\end{aligned}
\tag{2.33}
$$

which is always defined for all non-degenerate orbits. Similar manipulations can be made to expressions for $e \sin f$ and $e \sin E$ to remove indeterminacies. Bonavito [21] arrives at the following expression for the elliptical case for

71

$e \sin f$:

$$e \sin f = \frac{\sqrt{F} \left(1 - e^2\right)^{1/2}}{\rho \sqrt{(-2\alpha_1)(\rho^2 - 2b_1\rho + b_2^2)}} \tag{2.34}$$

A 0/0 computation is observed in Eq. (2.34) for zero-energy orbits, where $\left(1 - e^2\right)^{1/2}$ goes to zero in the numerator and α_1 goes to zero in the denominator. With more care, the indeterminacy can be removed with a generalization to unbounded orbits by multiplying the expression by $\sqrt{a}/\sqrt{a}$ and performing manipulations similar to those done to arrive at Eq. (2.33):

$$e \sin f = \frac{\sqrt{F} p^{1/2}}{\rho \left[\mu\gamma_1(\rho^2 - 2b_1\rho + b_2^2)\right]^{1/2}} = \text{sgn} \sqrt{F} \frac{[p(\gamma\rho^2 + 2\rho - p)]^{1/2}}{\rho} \tag{2.35}$$

The second equation in Eq. (2.35) can be obtained by comparison to Eq. (8) in Getchell [62]. Its counterpart, $e \cos f$, is determined as

$$e \cos f = \frac{p}{\rho} - 1 \tag{2.36}$$

Similarly for $e \sin E$, Bonavito [21] arrives at the following expression:

$$e \sin E = \frac{\sqrt{F}}{a \sqrt{(-2\alpha_1)(\rho^2 - 2b_1\rho + b_2^2)}} \tag{2.37}$$

which has a $0 \cdot \infty$ computation in the denominator for zero-energy orbits. By again absorbing a factor of $\sqrt{a}$ into the radical, this time in the denominator, the equation can be rewritten as

$$e \sin E = \frac{\sqrt{F}|\gamma|^{1/2}}{\left[\mu\gamma_1(\rho^2 - 2b_1\rho + b_2^2)\right]^{1/2}} = \text{sgn} \sqrt{F} \, |\gamma|^{1/2}(\gamma\rho^2 + 2\rho - p)^{1/2} \tag{2.38}$$

2.4   Fundamental Frequencies

There are three fundamental frequencies, denoted as either anomalistic, draconitic, or sidereal. They are defined from a dynamical systems perspective,

where each is fast and, in general, distinct, having similar values to first order. The anomalistic frequency is associated with the rate at which a spacecraft passes through periapsis, tied to anomalistic angles like mean anomaly. The draconitic frequency is associated with the rate at which a spacecraft passes through the equatorial plane or ascending node, tied to the argument of latitude. The sidereal frequency is associated with the rate at which a spacecraft makes a complete orbit relative to the stars, tied to angles like mean longitude and right ascension. In astrodynamics, practitioners are typically concerned with three different but related frequencies, one fast and two slow. The fast one is the same anomalistic frequency described above. The first slow frequency is tied to the motion of periapsis, associated with the rate at which periapsis passes through the equatorial plane. The second slow frequency is tied to the motion of the ascending node, associated with the rate at which the ascending node makes a complete revolution relative to the stars. Equations (2.47–2.49) define these last three frequencies in terms of the fast ones. Note that the orbital period can be defined by the sidereal frequency, i.e. the time derivative of the secular mean longitude, and that a frozen orbit results when the anomalistic frequency is commensurate with the draconitic frequency.

With respect to these frequencies, dynamical systems are generally not degenerate. The Kepler problem is degenerate because the three fast frequencies are not distinct and collapse into one. The Vinti problem is non-degenerate, wherein all three frequencies take on distinct values that are similar to each other for an Earth application. Vinti [153] presents a general mathematical proof that connects the mean frequencies to the energy and ac-

tion variables for a special class of separable system of which Vinti theory is a member. Specifically, each frequency is equal to the partial derivative of the energy with respect to one of the three action variables. The proof is applicable to any nonpolar orbit in an artificial satellite context. The case of a nearly or exactly polar orbit is addressed for the first time in this section and actually utilized to derive a new expression for the secular motion of spheroidal RAAN.

Vinti [158] developed analytical expressions for the first two mean frequencies (anomalistic and draconitic) assuming the 1966 potential ($J_3 \neq 0$). These frequencies are determined as

$$2\pi\nu_1 = \frac{(-2\alpha_1)^{1/2}}{a + b_1 + A_1 + c^2 A_2 B_1' B_2^{-1}} \tag{2.39}$$

$$2\pi\nu_2 = \frac{\alpha_2 u^{-1/2}}{a + b_1 + A_1 + c^2 A_2 B_1' B_2^{-1}} \tag{2.40}$$

but a similar analytical expression for the third (sidereal) has not been previously published and will be derived in the next section.

2.4.1 The Third Fundamental Frequency: $2\pi\nu_3$

For comparison to the results of Wiesel [166], it is useful to have an analytical expression for the third mean frequency. From Eq. (7.14) in Vinti [154], the third mean frequency can be expressed as

$$2\pi\nu_3 = -\nu_1 j_{13} - \nu_2 j_{23} \tag{2.41}$$

where ν_m for $m = 1, 2, 3$ are the mean frequencies associated with ρ, η, and ϕ, respectively, and j_{mn} are the partials of the action variable j_m with respect

to α_n for $n = 1, 2, 3$. The expression for j_{13} is unchanged from Eq. (7.18) in Vinti [154], given as

$$j_{13} = 2\pi c^2 \alpha_3 (-2\alpha_1)^{-\frac{1}{2}} A_3 \tag{2.42}$$

but j_{23} under the 1966 Vinti potential is not the same. First, it can be shown that the generic form for j_{23} becomes

$$j_{23} = -2\alpha_3 N_3(\eta_0) = -2\alpha_3 N_3(\psi = \pi/2) \tag{2.43}$$

After much algebra, the expression for j_{23} reduces to

$$j_{23} = -\frac{2\pi\alpha_3\sqrt{u}}{\alpha_2} \left[B_3 + \frac{1}{\sqrt{1-S}} \left(\frac{h_1}{\sqrt{1-2\zeta}} + \frac{h_2}{\sqrt{1+2\zeta}} \right) \right] \tag{2.44}$$

The mean frequency ν_3 is finally obtained by substituting Eqs. (2.42) and (2.44), along with Eq. (122) from Vinti [158] for ν_1 and ν_2, into Eq. (2.41). After simplifying the result into a form similar to the expressions for ν_1 and ν_2, ν_3 can be determined as

$$2\pi\nu_3 = \frac{\alpha_3}{a_0 + A_1 + c^2 A_2 B_1' B_2^{-1}} \\ \times \left\{ -c^2 A_3 + \frac{A_2}{B_2} \left[B_3 + \frac{1}{\tilde{S}} \left(\frac{h_1}{\sqrt{1-2\zeta}} + \frac{h_2}{\sqrt{1+2\zeta}} \right) \right] \right\} \tag{2.45}$$

The expression for ν_3 in Eq. (2.45) is exact. Note that the singularity for polar orbits is expected here because the right ascension, ϕ, is discontinuous for polar orbits. Neglecting the rotation of the Earth, the notational relationship between the frequencies derived by Wiesel [166], which he denoted as Ω_m, and those of Vinti is

$$\Omega_m = 2\pi\nu_m \tag{2.46}$$

2.4.2 Secular Motion

Recalling the coordinates and conjugate momenta of Hamiltonian mechanics, the source of secular growth can be traced to the time derivatives of the coordinates l, g, and h, using Delaunay's notation. These variables correspond to mean anomaly, argument of periapsis, and right ascension of the ascending node, respectively. Vinti [156] derived expressions for analogous variables that describe the secular drift rates of three analogous spheroidal elements. Their time derivatives are determined as

$$\dot{l} = 2\pi\nu_1 \tag{2.47}$$

$$\dot{g} = 2\pi(\nu_2 - \nu_1) \tag{2.48}$$

$$\dot{h} = 2\pi(\nu_3 - \nu_2 \mathrm{sgn}\,\alpha_3) \tag{2.49}$$

where the ν_j are the fundamental frequencies

$$\dot{M}_s = 2\pi\nu_1 = \frac{(-2\alpha_1)^{1/2}}{a_0 + A_1 + c^2 A_2 B_1' B_2^{-1}} \tag{2.50}$$

$$\dot{\psi}_s = 2\pi\nu_2 = \frac{\alpha_2 u^{-1/2} A_2 B_2^{-1}}{a_0 + A_1 + c^2 A_2 B_1' B_2^{-1}} \tag{2.51}$$

$$\dot{\phi}_s = 2\pi\nu_3 = \frac{-\alpha_3}{a_0 + A_1 + c^2 A_2 B_1' B_2^{-1}}$$
$$\times \left\{ c^2 A_3 - \frac{A_2}{B_2} \left[B_3 + \frac{1}{\tilde{S}} \left(\frac{h_1}{\sqrt{1 - 2\zeta}} + \frac{h_2}{\sqrt{1 + 2\zeta}} \right) \right] \right\} \tag{2.52}$$

M is the spheroidal mean anomaly, ψ is the spheroidal argument of latitude, ϕ is the right ascension, and the "s" subscript indicates that the quantity only contains the secular part. Equations (2.50) and (2.51) are derived by Vinti [158] and Eq. (2.52) is derived in Section 2.4.1. Note that ν_3 is composed of a linear combination of ν_1 and ν_2, and is directly related to the secular

76

motion of right ascension. Since right ascension is discontinuous for polar orbits and poorly defined for nearly polar orbits, observable in the division by $\tilde{S}$, an alternative variable or expression is required to make the theory uniformly valid. One option is to directly replace h by Ω'_s, the secular part of a slowly-changing variable Ω' similar to RAAN that tracks a slowly rotating reference plane [160], obtained by removing the part of ϕ_s that varies rapidly near a pole. Equation (2.49) can be replaced by

$$\dot{\Omega}'_s = -\frac{\alpha_3}{a_0 + A_1 + c^2 A_2 B'_1 B_2^{-1}} \left(c^2 A_3 - \frac{A_2}{B_2} B_3 \right) \tag{2.53}$$

This expression agrees with the derivative of Wu and Tong's formula [169] for Ω'_s. Further justification for removing the fast part is that the ECI coordinates can be expressed in terms of the elements in such a way that they do not depend on the fast part, only on Ω'. An alternative approach leading to the same result begins with an observation: since the present goal is to derive a formula for $\dot{h}$, an alternative expression for $\dot{\phi}_s$ can be used that does not contain the singularity. By substituting Eqs. (27), (147), (149.1), and (154) from Vinti [158] into Eq. (2.45) of this dissertation and manipulating the equations, it is possible to show that

$$\frac{\alpha_3}{\sqrt{1-S}} \left(\frac{h_1}{\sqrt{1-2\zeta}} + \frac{h_2}{\sqrt{1+2\zeta}} \right) = \frac{\alpha_2}{\sqrt{u}} \mathrm{sgn}\, \alpha_3 \tag{2.54}$$

where the $\sqrt{1-S}$ in the denominator cancels with the term in α_3. Making this substitution in Eq. (2.45), Eq. (2.49) can be readily applied to arrive at the expression in Eq. (2.53) for $\dot{h} = \dot{\Omega}'_s$.

2.4.3 Returning to the Third Fundamental Frequency

By substituting Eq. (2.53) into Eq. (2.49) and moving $\dot{\phi}_s = 2\pi\nu_3$ to the left-hand side, a nonsingular expression for $2\pi\nu_3$ is obtained as

$$2\pi\nu_3 = \frac{1}{a_0 + A_1 + c^2 A_2 B_1' B_2^{-1}} \left[\operatorname{sgn}\alpha_3\alpha_2 u^{-1/2} A_2 B_2^{-1} \right.$$
$$\left. - \alpha_3 \left(c^2 A_3 - \frac{A_2}{B_2} B_3 \right) \right] \qquad (2.55)$$

2.5 Spheroidal Universal Variables

Neither Vinti's solutions [154, 158] (bounded) nor Lang's solution [104] (unbounded) is valid when the spacecraft's specific energy, α_1, is near zero. Getchell [62] went to great lengths to express a solution to the Vinti problem in universal variables, unifying the existing solutions for bounded and unbounded orbits. An important neglected detail of his work is the presentation of a method of computing the universal variable $\hat{X}$ at the initial time when the trajectory is near the zero-energy threshold or nearly "parabolic". The word "parabolic" is used in quotes because, while many of the orbit parameters signify what is considered a parabola in the Kepler problem ($e = 1$ and $\alpha_1 = 0$), trajectories in the Vinti problem are generally not conic sections, and so the Vinti "parabola" is not a parabola in a geometric sense. That being said, a "parabola" still represents the boundary between bounded and unbounded motion in the Vinti problem. From this point forward, quotes will only be used on the word "parabola" if necessary, and it should generally be clear from context whether the word refers to the zero-energy case in the Vinti problem or the Kepler problem.

2.5.1 Definition for the Vinti Problem

There are some key differences between the Vinti and Kepler problems that lead to differences in the definition of the universal variables. In the Kepler problem, the spacecraft is constrained to move in an invariant plane. The solution can be expressed in terms of the f and g functions to directly propagate the position and velocity vectors, without computation of most of the orbital elements. The problem is solved iteratively with a good initial guess of the variable $\hat{X}_K$ at the *final* time. There is no need to ever compute $\hat{X}_K$ at the initial time. Consequently, in the Kepler problem, $\hat{X}_K$ is associated with a *change* in the eccentric-anomaly-like variable, which in the elliptical case is expressed as

$$\hat{X}_K = \sqrt{a_K} \left(E_K - E_{K_i} \right) \tag{2.56}$$

In the Vinti problem, there are a number of complications. The solution cannot be expressed only in terms of eccentric anomaly as the fast variable because an invariant plane no longer exists. True anomaly is also required, as is the true argument of latitude. Additionally, determination of the orbital elements cannot be avoided. Extra steps are required to obtain the Jacobi constants, and these constants must be known before propagating the orbit. As a result, it seems that $\hat{X}$ must be computed first at the *initial* time from known quantities. The familiar process of guessing $\hat{X}$ at the final time is still essential but it is done at a later stage, after obtaining the Jacobi constants. These requirements inform a different definition of the universal variable, which

is essentially defined by a different form of the spheroidal conic equation [62]:

$$\rho = \rho_1 + e\hat{C} \tag{2.57}$$

where $\hat{C}$ is another universal variable. Equation (2.57) is equivalent to $\rho = a(1 - e\cos E)$. The universal variables $\hat{X}$, $\hat{C}$, $\hat{S}$, $\hat{U}$ are defined in Table 2.1 for the different regimes in terms of the classical orbital elements [125]. Note that D is the parabolic eccentric anomaly and E_h is the hyperbolic eccentric anomaly. As a word of caution, these equations should not be used to convert between the representations when e is near unity, but they are nonetheless very helpful for understanding what the universal variables represent physically. The equations in Table 2.1 are also critical for computing $\hat{X}$ and $\hat{U}$ given $\hat{C}$ and $\hat{S}$, as will be seen shortly.

Table 2.1: Spheroidal universal variables in terms of classical spheroidal elements

Variable	Ellipse $e < 1$	Parabola $e = 1$	Hyperbola $e > 1$
γ	$-1/a$	0	$1/a$
$\hat{X}$	$(a)^{1/2}E$	D	$(-a)^{1/2}E_h$
$\hat{S}$	$(a)^{1/2}\sin E$	D	$(-a)^{1/2}\sinh E_h$
$\hat{C}$	$a(1 - \cos E)$	$\frac{1}{2}D^2$	$a(1 - \cosh E_h)$
$\hat{U}$	$(a)^{3/2}(E - \sin E)$	$\frac{1}{6}D^3$	$(-a)^{3/2}(\sinh E_h - E_h)$

2.5.2 Computing Universal Variables at the Initial Time

By defining the auxiliary variable

$$z = \gamma \hat{X}^2 \tag{2.58}$$

it is possible to define the Stumpff functions [13] in terms of z as

$$C(z) \equiv \frac{1 - \cos \sqrt{z}}{z} = \frac{1 - \cosh \sqrt{-z}}{z} = \frac{1}{2!} - \frac{z}{4!} + \frac{z^2}{6!} - \frac{z^3}{8!} + \cdots \tag{2.59}$$

$$U(z) \equiv \frac{\sqrt{z} - \sin \sqrt{z}}{\sqrt{z^3}} = \frac{\sinh \sqrt{-z} - \sqrt{-z}}{\sqrt{-z}} = \frac{1}{3!} - \frac{z}{5!} + \frac{z^2}{7!} - \frac{z^3}{9!} + \cdots \tag{2.60}$$

The series representations of $C(z)$ and $U(z)$ are equivalent to the respective expressions in terms of circular and hyperbolic trigonometric functions. For each function, all three representations are equivalent, but the value of z should dictate which form to use. Any of the expressions involving trigonometric functions have a potential for catastrophic cancellation due to the subtraction in the numerators. The loss in precision approximately begins when z is less than ≈ 0.1 in magnitude, which serves as a good threshold for switching between each representation of a Stumpff function. In other words, let $\epsilon = 0.1$ and compute $C(z)$ and $U(z)$ according to the conditions in Table 2.2, retaining terms up to and including z^5. The value of z generally indicates the type of orbit, where $z > 0$ signifies an elliptical orbit, $z < 0$ signifies a hyperbolic orbit, and $z = 0$ signifies either a parabolic orbit or that the spacecraft is at periapsis. The last interpretation here differs from the Kepler problem, where $z_K = 0$ would indicate a parabolic orbit or that the change in eccentric anomaly is zero. Note that the function $U(z)$ is traditionally denoted as $S(z)$,

81

Table 2.2: Conditions on z for Stumpff function computation

Condition	$C(z)$	$U(z)$
$z > \epsilon$	$\dfrac{1 - \cos\sqrt{z}}{z}$	$\dfrac{\sqrt{z} - \sin\sqrt{z}}{\sqrt{z^3}}$
$\lvert z \rvert < \epsilon$	$\dfrac{1}{2!} - \dfrac{z}{4!} + \dfrac{z^2}{6!} - \dfrac{z^3}{8!} + \cdots$	$\dfrac{1}{3!} - \dfrac{z}{5!} + \dfrac{z^2}{7!} - \dfrac{z^3}{9!} + \cdots$
$z < -\epsilon$	$\dfrac{1 - \cosh\sqrt{-z}}{z}$	$\dfrac{\sinh\sqrt{-z} - \sqrt{-z}}{\sqrt{-z}}$

but the author has changed the notation to avoid confusion with $\hat{S}$ and to stress its connection to $\hat{U}$.

It remains to connect the universal variables to the Stumpff functions in addition to establishing several relations between the universal variables themselves. Two of the universal variables can be defined as functions of $\hat{X}$ and γ, or equivalently as functions of $\hat{X}$ and z [62]:

$$\hat{C}(\hat{X}, \gamma) = \hat{X}^2 C(\gamma \hat{X}^2) = \hat{X}^2 C(z) \tag{2.61}$$

$$\hat{U}(\hat{X}, \gamma) = \hat{X}^3 U(\gamma \hat{X}^2) = \hat{X}^3 U(z) \tag{2.62}$$

where $\hat{X}$ is the independent variable. The universal variables also obey the

82

following relations [125, 62]:

$$\hat{S}(\hat{X}, \gamma) = \hat{X} + \gamma \hat{U}(\hat{X}, \gamma) \tag{2.63}$$

$$\hat{S}^2 = 2\hat{C} + \gamma \hat{C}^2 \tag{2.64}$$

$$\hat{U}' = \hat{C} \tag{2.65}$$

$$\hat{C}' = \hat{S} \tag{2.66}$$

$$\hat{S}' = 1 + \gamma \hat{C} \tag{2.67}$$

The prime symbol as used here indicates differentiation with respect to $\hat{X}$.

Two of the universal variables, $\hat{C}$ and $\hat{S}$, can be computed from initial conditions given in ECI coordinates. Since $\hat{X}$ is one of the sought unknowns and $\hat{C}$ is given, Eq. (2.61) suggests a possible path to computing $\hat{X}$ without loss of precision as long as an alternative to Eq. (2.58) exists for computing z. The following shows how to compute z from initial conditions. Since it is not necessary to divide by e, the quantities are left as $e\hat{C}$ and $e\hat{S}$. By manipulating Eq. (2.57), $e\hat{C}$ is determined at the initial time as

$$e\hat{C}_i = \rho_i - \rho_1 \tag{2.68}$$

where

$$\rho_1 = \frac{p}{1+e} \tag{2.69}$$

It can also be shown that

$$\sqrt{F} = e\hat{S}\sqrt{\mu \gamma_1 (\rho^2 - 2\rho b_1 + B)} \tag{2.70}$$

which by rearranging gives $e\hat{S}$ at the initial time as

$$e\hat{S}_i = \frac{\sqrt{F_i}}{\sqrt{\mu \gamma_1 (\rho_i^2 - 2\rho_i b_1 + B)}} \tag{2.71}$$

83

Equation (2.71) is equivalent to the alternative expression:

$$e\hat{S}_i = \operatorname{sgn}\left(\sqrt{F_i}\right)\sqrt{\gamma\rho_i^2 + 2\rho_i - p} \qquad (2.72)$$

It is also straightforward to compute $e\hat{S}_i'$ as

$$e\hat{S}_i' = e + \gamma e\hat{C}_i \qquad (2.73)$$

The rest of the derivation is based on the elliptical case, where $\sqrt{z} = E$. From Table 2.1, $\hat{S}'$ can be written in terms of elements as

$$\begin{aligned}
\hat{S}' &= 1 + \gamma\frac{(1 - \cos E)}{-\gamma}\\
&= 1 - 1 + \cos E\\
&= \cos E \qquad (2.74)
\end{aligned}$$

which means that $e\hat{S}' = e\cos E$. If an equation for $e\sin E$ is also available, then it may be possible to compute E_i. Pointing again to Table 2.1, it is immediately evident that $\hat{S} = \sqrt{a}\sin E$ may fill this role, but it must be multiplied by a scaling factor $|\gamma|^{1/2}$ to cancel the $\sqrt{a}$ coefficient. As a result of the scaling, however, the (elliptical, parabolic, or hyperbolic) eccentric anomaly is not actually computed in general because in the equation

$$\sqrt{z} = \operatorname{atan2}\left(\frac{|\gamma|^{1/2}\hat{S}}{\hat{S}'}\right) \qquad (2.75)$$

the numerator $|\gamma|^{1/2}\hat{S}$ is always zero for a parabola even though $\sin D$ is clearly not always zero for a parabola. This behavior is not an issue, though, because it agrees with the definition of z, behaving as z is supposed to behave. The derivation would be similar for parabolic and hyperbolic orbits, but Eq. (2.75)

would not be applicable for the hyperbolic case. The latter case would require an inverse hyperbolic trigonometric function, such as the inverse hyperbolic tangent function. Der and Monuki [50] used Eq. (2.75) to compute $\sqrt{z}$.

What is new up to this point in this section is the documentation, explanations, comparisons to the Kepler problem, filling in important details of Getchell's derivation [62], and the emphasis on taking full advantage of the Taylor series representation when applying universal variables to Vinti theory. The next two equations represent the main contribution of this section with the observation that they retain precision in $\hat{X}$ and $\hat{U}$. These computations are required in both the initialization and propagation steps.

Once z is obtained, then $\hat{X}$ can be computed from

$$\hat{X} = \sqrt{\frac{\hat{C}(\hat{X}, \gamma)}{C(z)}} \qquad (2.76)$$

without any loss of precision when z is near zero. Note from Eq. (2.59) that the denominator is never zero. With $\hat{X}$ determined, $\hat{U}$ can be obtained from

$$\hat{U}(\hat{X}, \gamma) = \hat{X}^3 U(z) \qquad (2.77)$$

It is emphasized that the identification and subsequent use of Eqs. (2.76) and (2.77) to avoid precision loss in this manner is new. They are not used in the universal formulation of the Kepler problem and have not been used in the Vinti problem until now. Without this technique, precision loss can be severe, tending to one correct digit not just for nearly "parabolic" orbits, but near periapsis as well ($z = 0$ in both cases), and so this very practical issue of precision loss can arise for the full range of eccentricity. Recall that in the

85

Kepler problem, $z_K = 0$ corresponds to parabolic orbits or a zero change in anomalistic angle, and as a result generally does not correspond to periapsis. Therefore, it would be common to encounter $z = 0$ in the Vinti problem because the vicinity of periapsis is often targeted for certain maneuvers and one may often wish to propagate exactly to periapsis or initialize a simulation in the vicinity of periapsis.

2.5.3   Orbit Propagation with Universal Variables

There is essentially one existing proposed method of Vinti orbit propagation with universal variables. While Getchell [62] regularized the Vinti problem, a significant accomplishment, he stopped short of recommending a procedure for obtaining a good initial guess to the universal anomaly $\hat{X}$ at a desired time t, where the initial guess feeds into a root-solve routine. Der's approach, in the `vinti6` computer routine [50], is to use $\hat{X}_j = \hat{X}_i + \hat{X}_K$ for $j = 1$, adding the initial value of the spheroidal $\hat{X}$ to the value obtained from a universal Kepler propagator [50]. This equation may seem strange, but recall that $\hat{X}_K$ is the *change* in universal anomaly for the Kepler problem. Viewing J_2 as a perturbation to the Kepler problem, the change in $\hat{X}$ for the Vinti problem should be comparable to its change in value for the Kepler problem.

While the idea of exploiting the Kepler problem is attractive and should work in general, some pitfalls can be anticipated, discussed presently for the first time. In particular, the cases of nearly parabolic orbits can cause trouble. Near the zero-energy boundary, a hyperbolic Keplerian trajectory can translate to a bounded Vinti trajectory. The actual differences in eccentricity depend

strongly on the magnitude of J_2 and the geometry, but it is entirely feasible to have $e_K = 1.001$ and $e = 0.9$ or less. The implication for multi-revolution scenarios in the Vinti problem is that the Kepler-based initial guess can be very poor, leading to slow convergence or a failure of the algorithm. The algorithm only makes sense if the Keplerian and Vinti trajectories are in the same orbital regime, either both bounded or both unbounded.

An approach proposed here is to directly adapt the initial guess formulas for the Kepler problem to the Vinti problem. For example, in the Kepler problem, if dealing with elliptical orbits, the change in universal anomaly is proportional to the orbital period. Using instead the period for the Vinti problem associated with the universal anomaly, the same formula will give a good initial guess for a bounded Vinti trajectory, including the case where the Keplerian trajectory is unbounded. The approach that leverages a universal Kepler solution should still be appropriate for low to medium eccentricities, and similarly for very hyperbolic orbits. However, the technique should be used with caution within a very wide margin of the zero-energy threshold, since the syncing of the qualitative behavior of the Kepler and Vinti solutions depends strongly on the magnitude of J_2 and is not known a priori. If a simulated trajectory lies within that margin, an implementation should verify the syncing of the two solutions before accepting direct assistance from a Kepler propagator.

2.5.4   Mitigating Singularities with Universal Variables

While the use of universal variables for Vinti theory removes the singularity at $e = 1$, contrary to their use in the Kepler problem, angle ambiguities still exist for small eccentricities and small inclinations, though they are not discussed in the literature. Even in the universal formulation, Vinti theory still requires computation of true anomaly, argument of latitude, and, in theory, RAAN. Note that Getchell [62] used right ascension instead of Ω' in his solution, and so his solution still has singularities associated with polar orbits. The polar singularities would be easy to remove because, arising strictly from the N integrals, they are decoupled from those associated with small eccentricities and inclinations.

It would seem a merging of the universal variables formulation with the equinoctial formulation presented in Chapter 4 is in order, but a unified solution seems inaccessible. Recall that the equinoctial elements require adding the anomaly to other angles, but the anomaly is imaginary for hyperbolic orbits, i.e. the hyperbolic anomaly is associated with an area, not an angle. As such, it cannot generally be added to other angles. Alternatively, a piecewise solution is quite feasible. The equinoctial formulation may be used for $e < 0.9$, for example, and the universal variables formulation can be used for other eccentricities. However, small inclinations may still lead to inaccurate calculations in the universal formulation, and the representation will lead to singularities in a variety of applications. For example, linear coordinate transformations (Jacobians) will be singular. Singularities will also appear in the EOMs resulting from a VOP application. The issue can be remedied with the

adoption of an element set inspired by the equinoctial set but without using the eccentricity vector components. The set would include semilatus rectum, eccentricity, vector components of the ascending node, longitude of periapsis, and true anomaly. Note that $J_3 = 0$ is required for this approach to work, as with the equinoctial elements. The results of Chapter 4 would still apply, but the propagation stage layed out in Chapter 5 would have to be adjusted.

2.6   Practical Considerations

Up to this point, solving the Vinti problem has been viewed as the combination of converting ECI coordinates to spheroidal elements, propagating the orbit in element space, and then converting the elements back to ECI coordinates. In other words, the initial state is assumed to be given as ECI position and velocity vectors. But orbit design is often performed in the orbital element space. A natural question to ask, then, is why not design orbits using spheroidal orbital elements or VOEs? A variety of momenta elements can theoretically be used to describe the same geometrical properties, and the aim in this section is to make clear the implications and consequences of those choices. Without proper care, a number of practical issues may arise when using VOEs to design orbits subject to the asymmetric Vinti potential ($J_3 \neq 0$).

2.6.1   Initializing an Orbit with Vinti Elements

As evident from Vinti [158], the elements S and Q are both associated with spheroidal inclination. More importantly, as will be made clear in this

section, they are not identical and one is more intuitive and useful than the other as a starting point for orbit design. The quantity Q behaves as $\sin I$ and its range is well defined as $0 \leq Q \leq 1$. The quantity S, which was Vinti's choice, can be defined as $\sin^2 I'$, where $I \neq I'$ in general, but its range is not well defined for nearly equatorial orbits when $S < 0$. There is no obvious lower bound on S other than knowing that its magnitude must be small. From the perspective of preliminary orbit design, the element S, with the implicit extension of inclination into the complex plane, leaves the designer ruminating on the inscrutability of one imaginary degree. If Q is chosen as an element instead of S to represent inclination, then this issue associated with S is avoided entirely.

Using Q as an element, a designer can appeal to most of the usual notions of orbit inclination. The exception to this statement is for nearly equatorial orbits. When J_3 is included in Vinti theory, equatorial orbits do not strictly exist because gravitational forces from that assymetry would drive a spacecraft out of the equatorial plane [159]. Choosing $I = Q = 0$ would give an orbit parallel to the equatorial plane, but the orbital plane would not pass through the center of mass of the primary. When J_3 is not included in Vinti theory, then in fact $Q = S = \sin I$ and $I = I'$, and a zero spheroidal inclination would prescribe an equatorial orbit.

The remaining question of how to determine S and other quantities given a, e, and Q is resolved through a procedure similar to the iterative method summarized in Eqs. (10–17) of Getchell [62]. The idea is to essentially reverse the process by manipulating the equations, something that Getchell

90

vaguely describes. The initial guesses suggested by Getchell are still good initial guesses in the reverse process. The major difference is that, when going from VOEs to the prime constants, all eight of those equations are coupled and the equation for Q must be added to the process. When going from prime constants to VOEs, however, the eight equations can be decoupled into two parts so that the iterative processes are carried out separately for each group of four equations.

The new form of Getchell's equations are as follows for the iterative process that computes the prime constants from the VOEs.

$$S = Q^2 - P^2 \tag{2.78}$$

$$\frac{1}{\gamma_1} = 1 - \gamma A_1 \tag{2.79}$$

$$\frac{p_0}{\gamma_1} = p + c^2 \gamma - B_1 \gamma + 4A_1 \tag{2.80}$$

$$B_1 = \frac{c^2 S S_1}{p} \frac{p_0}{\gamma_1} \tag{2.81}$$

$$A_1 = \frac{c^2/\gamma_1 - B_1}{p} \tag{2.82}$$

$$Q_1 = -\frac{c^2 \gamma}{(p_0/\gamma_1) S_1} \tag{2.83}$$

$$P_1 = \frac{2z_\delta/\gamma_1}{(p_0/\gamma_1) S_1} - 2PQ_1 \tag{2.84}$$

$$2P = \frac{2z_\delta/\gamma_1}{(p_0/\gamma_1) S_1} - P_1 S \tag{2.85}$$

$$S_1 = \frac{p_0/\gamma_1 - c^2 \gamma - (p_0/\gamma_1) S S_1 Q_1}{(1 - 2PP_1)(p_0/\gamma_1)} \tag{2.86}$$

To use Eqs. (2.78–2.86), first compute $p = a(1 - e^2)$ and $\gamma = -1/a$. Then begin the iterative process with $A_1 = B_1 = P = 0$ and $S_1 = 1$. Note that since $S = Q^2 - P^2$, the initial estimate of S is Q^2, which would be exact if $z_\delta = 0$.

Terminate the process when S_1 is correct to within some desired tolerance. Arbitrarily accurate values for p_0, γ_0, A_1, B_1, Q_1, P_1 P, S, and S_1 can be obtained after a few iterations. In Vinti's notation, $\gamma_0 = -1/a_0$, $A_1 = b_1$, $B_1 = B$, $Q_1 = C_2$, $P_1 = C_1$, and $S_1 = 1/u$. Note that, to compute I or $\cos I$, only the absolute value of $\cos I$ is available from Q, i.e. $|\cos I| = \sqrt{1 - Q^2}$. To obtain the inclination, compute I as

$$I = \operatorname{sgn} \alpha_3 \sqrt{1 - Q^2} \tag{2.87}$$

2.7 Final Remarks

Many enhancements to Vinti's original solutions have been derived and presented in this chapter. The improvements are derived for the 1966 potential that includes J_3, but they apply equally well to the 1959 potential for which $J_3 = 0$. The net result of these enhancements is to enable greater accuracy and precision for more applications over the full range of practical orbit regimes. Some of the improvements to Vinti theory offer a substantial increase in accuracy for nearly circular equatorial orbits (Sections 2.2.2 and 2.3.2), while others address issues encountered in polar orbits (Sections 2.3.1 and 2.4) and near the zero-energy boundary (Sections 2.3.3 and 2.5). Algorithms are also presented to handle multiple revolutions (Section 2.2.4) and to alleviate practical issues that arise when designing orbits with spheroidal elements, enabling broader use (Section 2.6).

All methods presented in this chapter have been implemented, except for the contents of Section 2.5.3. As stated in Chapter 1, the open-source code

contains topics relevant to the relative motion model presented in Chapter 3, drawing from Sections 2.2.1.2, 2.2.2, 2.3, and 2.2.4. The eigenvalue-based method for factoring the quartics is separately implemented with heuristics for root identification. The remedies for zero-energy issues discussed in Section 2.3.3 are implemented for the equinoctial formulation, in addition to the frequencies introduced in Section 2.4. Some of the universal variable methods are implemented, specifically the remedy for precision loss described in Section 2.5.2 and the coordinate transformation described in Section 2.5.4. The algorithm in Section 2.6 for orbit design is implemented but is not needed in the orbit propagators and stands alone as a separate tool.

Chapter 3

A Satellite Relative Motion Model Including J_2 and J_3 via Vinti's Intermediary

The present chapter focuses first on developing a new relative motion model that leverages Vinti theory and second on evaluating its performance. The core model consists of an analytical state transition matrix that propagates the relative orbit in the oblate spheroidal orbital element space, where the elements of the STM are the partial derivatives of Vinti's solution for state propagation. The partials are verified against complex-step derivatives and central differences. Der and Danchick [51] devised an algorithm for obtaining a numerical Vinti-based STM, which Der [48] subsequently used in a study that introduces a universal, analytical Keplerian STM, with comparisons to several other STMs in ECI and LVLH Cartesian coordinates. However, an analytical Vinti-based STM has not previously appeared in the literature. Further details of the Vinti problem are given as they pertain to the development of the relative motion model and references are given to the partial derivatives that are not derived in this dissertation. The Vinti-based STM and a Brouwer-based STM are then simultaneously compared for accuracy to a higher fidelity Earth gravity model. The original Brouwer-based STM of Gim and Alfriend in quasi-nonsingular elements is chosen for this preliminary evaluation because

it has served as a benchmark in multiple studies. Recall from Chapter 1 that the Brouwer-based STM is often referred to as the GA STM in the literature. Each model's accuracy is assessed over a range of eccentricity, inclination, and separation distance.

From these two STMs, it is generally not straightforward to draw conclusions on the accuracy of Vinti versus Brouwer theories. To do so should require both STMs to model the same perturbations to the same order of approximation. Bonavito et al. [22][1] and Gordon et al. [66][2] made good efforts toward that goal for the main problem. Their conclusions that Vinti's model performs better served to motivate the application of Vinti theory to the relative motion problem in the present study, though similar studies are yet to be done in a relative motion context. Further motivation to apply Vinti theory to the relative motion problem stems from the idea that the Vinti STM should possess a larger linear region of validity because spheroidal, as opposed to spherical, orbital elements naturally fit the shape of the Earth. As demonstrated by Junkins et al. [93], the accuracy of linear propagation theory is poorest in Cartesian coordinates, significantly improved in cylindrical coordinates, and further improved in spherical orbital elements. It stands to reason, then, that accuracy would be further improved in spheroidal orbital elements. Nonetheless, the Brouwer-based STM is certainly a good benchmark, and advantages of the Vinti-based STM are still discussed as appropriate.

---

[1]Bonavito et al. [22] compared two theories: the original Brouwer theory and Vinti theory.
[2]Gordon et al. [66] compared three theories: Brouwer, Brouwer-Lyddane, and Vinti.

3.1 Development of the Relative Motion Model

The proposed dynamical model utilizes an STM to describe the relative motion. It takes into consideration how the choice of coordinates affects the linear region of validity as well as the distinction between static and dynamic nonlinearity [93]. A useful vocabulary and analysis of various types of static bookend transformations is given by Sinclair et al., distinguishing between linearized, calibrated [134], and decalibrated [135] solutions. These transformations arise from the desire to propagate a relative state in some preferred, likely more accurate, coordinates, followed by the need to transform the inputs and outputs to coordinates that are different and likely driven by measurements or constraints. An attractive and common means of state propagation in the vicinity of a reference solution is the STM. The linear bookend transformation is the familiar similarity transformation applied to the STM, the decalibrated solution utilizes the exact nonlinear bookend transformations, and the calibrated solution uses a hybrid of the two transformations. Though the vocabulary did not exist at the time, the results of Junkins et al. [93] are the consequence of a decalibrated solution; they also used a linear transformation to initialize the states.

Note that typical nonlinear transformations suffer from precision loss due to a subtraction of the chief's state from the deputy's. Therefore, nonlinear bookend transformations should always be used with caution. In fact, a main purpose of using relative motion models is to avoid the precision loss associated with subtracting the absolute state simulations of two objects in close vicinity. The relative motion model proposed here would employ the decalibrated or

linearized solution, depending on the application. After presenting the STM, methods of removing singularities in the partial derivatives are discussed. New partial derivatives are included in Appendix C.

3.1.1 The Vinti-Based Analytical State Transition Matrix

The 6×6 STM can be obtained from the first-order Taylor series expansion of the analytical solution to the Vinti problem as

$$\Phi^{\jmath}(t, t_i) = \frac{\partial \mathbf{x}^{\jmath}}{\partial \mathbf{x}_i^{\jmath}} \tag{3.1}$$

evaluated at the chief's state, where Φ denotes an STM. The STM $\Phi^{\jmath}(t, t_i)$ propagates the deputy's relative state from time t_i to time t in ECI coordinates, but propagation can also be done in other coordinates. Using the chain rule, the partial derivatives can be rewritten in different forms, for example:

$$\frac{\partial \mathbf{x}^{\jmath}}{\partial \mathbf{x}_i^{\jmath}} = \frac{\partial \mathbf{x}^{\jmath}}{\partial \mathbf{œ}^S} \frac{\partial \mathbf{œ}^S}{\partial \mathbf{œ}^V} \frac{\partial \mathbf{œ}^V}{\partial \mathbf{œ}_i^V} \frac{\partial \mathbf{œ}_i^V}{\partial \mathbf{œ}_i^S} \frac{\partial \mathbf{œ}_i^S}{\partial \mathbf{x}_i^{\jmath}} \tag{3.2}$$

Observe that the middle partial, $\partial \mathbf{œ}^V / \partial \mathbf{œ}_i^V$, is the identity matrix because the VOEs are constants of the motion. To simplify the notation, define the 6×6 transformation matrix ${}^B T^A$ as the Jacobian that linearly maps coordinate set A to coordinate set B at time t, with the shorthand ${}^B T_i^A = {}^B T^A(t_i)$. The propagation could then be effectively captured in the Jacobian that maps VOEs to the time-varying spheroidal elements:

$$\Phi^S(t, t_i) = {}^S T^V {}^V T_i^S = {}^S T^V ({}^S T_i^V)^{-1} \tag{3.3}$$

where

$$^S T^V \equiv \frac{\partial \mathbf{œ}^S}{\partial \mathbf{œ}^V} \tag{3.4}$$

97

The STM $\Phi^S(t, t_i)$ propagates the relative state in the spheroidal element space according to the variational equations

$$\delta \text{œ}^S = \Phi^S(t, t_i) \delta \text{œ}_i^S \tag{3.5}$$

Many of the partial derivatives comprising $\partial \text{œ}^S / \partial \text{œ}^V$ in Eq. (3.4) were established in Walden and Watson's technical report for use in a different application where the partials of the inverse transformation are not explicitly required [164]. Although these partials are required in the current study, there is an easier way to obtain the inverse transformation. Other than directly obtaining the inverse transformation via partial derivatives, alternative general techniques require computing a matrix inverse numerically or solving a linear system of equations. By virtue of the chosen element set, however, a relatively simple expression for the analytical inverse exists due to the sparsity of $^S T^V$:

$$^S T^V = \begin{bmatrix} 1 & 0 & 0 & 0 & 0 & 0 \\ 0 & 1 & 0 & 0 & 0 & 0 \\ 0 & 0 & 1 & 0 & 0 & 0 \\ T_{41} & T_{42} & T_{43} & T_{44} & T_{45} & 0 \\ T_{51} & T_{52} & T_{53} & T_{54} & T_{55} & 0 \\ T_{61} & T_{62} & T_{63} & T_{64} & T_{65} & 1 \end{bmatrix} \tag{3.6}$$

The inverse maintains the exact same structure and only requires approximately 70 operations, which is small considering there are 19 nonzero elements of the matrix. The inverse is simple in the sense of fast computation and the explicit form is given in Appendix A. A readily accessible companion code is also provided as an Online Resource[3]. It is important to note that

---

[3]Code updates will be available from this website: `http://russell.ae.utexas.edu/index_files/vinti.html`

the analytical inverse need only be computed once because its value is only required at the initial time. The process of obtaining $\Phi^S(t, t_i)$ is depicted in Fig. 3.1, which shows how the procedure interfaces with the initialization and
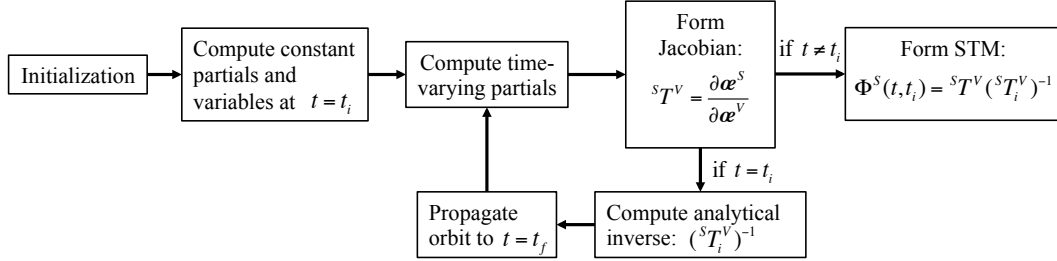
Figure 3.1: Flow chart for computing the Vinti-based STM.

propagation steps depicted in Fig. 2.1.

Once the STM $\Phi^S(t, t_i)$ is obtained, a number of options are available for the transformation to desired coordinates. Desired coordinates could be ECI coordinates or the standard LVLH Cartesian coordinates common to the relative motion problem. In principle, the most accurate and straightforward transformation is the nonlinear one corresponding to a decalibrated solution. As mentioned earlier, it should be used in practice with caution for applications to relative motion, specifically for small separation distances, when differencing two nearly identical state vectors leads to a loss of precision. That being said, the decalibrated solution presents no such problems for sufficiently large relative orbits. At the other end of the spectrum, a linearized solution will be valid for sufficiently small relative orbits and will avoid the precision loss problem. It is up to the user, then, to ascertain the validity of either solution and the trade-offs in accuracy and precision for a particular application.

Due to the complexity of the partial derivatives, the partials are given in the form of companion code. In the interest of greater versatility, the code contains the partials for three STMs most likely to be used: $\Phi^S(t, t_i)$ in the spheroidal orbital element space, $\Phi^{\mathfrak{I}}(t, t_i)$ in ECI coordinates, and $\Phi^{\mathcal{L}}(t, t_i)$ in LVLH Cartesian coordinates. Note that a great loss in accuracy may be incurred under a linear map from curvilinear to rectangular coordinates, for which the linear region of validity is smallest. For the relative motion problem, presumably LVLH Cartesian coordinates are ultimately desired, and of course both these and ECI coordinates are rectangular. In fact, the transformation from ECI coordinates to LVLH Cartesian coordinates is linear by nature, i.e. the transformation is just a rotation. Therefore, the STMs most relevant to the relative motion problem are $\Phi^S(t, t_i)$ and $\Phi^{\mathcal{L}}(t, t_i)$. The STM $\Phi^{\mathfrak{I}}(t, t_i)$ is mainly provided for other applications, such as estimation or optimization, and also because its components could be used in a differential correction procedure.

To obtain $\Phi^{\mathcal{L}}(t, t_i)$, the 6×6 Jacobians mapping between LVLH Cartesian coordinates and ECI coordinates are required. The matrices are given here for convenience. The transformation matrix that maps LVLH Cartesian coordinates to ECI coordinates is determined as

$$
{}^{\mathfrak{I}}T^{\mathcal{L}} = \begin{bmatrix} {}^{\mathfrak{I}}Q^{\mathcal{L}} & \mathbf{0} \\ {}^{\mathfrak{I}}Q^{\mathcal{L}}\boldsymbol{\omega}_{\times} & {}^{\mathfrak{I}}Q^{\mathcal{L}} \end{bmatrix} \tag{3.7}
$$

and the inverse transformation matrix is given by

$$
{}^{\mathcal{L}}T^{\mathfrak{I}} = \begin{bmatrix} ({}^{\mathfrak{I}}Q^{\mathcal{L}})^{\top} & \mathbf{0} \\ -\boldsymbol{\omega}_{\times}({}^{\mathfrak{I}}Q^{\mathcal{L}})^{\top} & ({}^{\mathfrak{I}}Q^{\mathcal{L}})^{\top} \end{bmatrix} \tag{3.8}
$$

where $\boldsymbol{\omega}$ is the angular velocity of the LVLH frame with respect to the ECI frame, $\boldsymbol{\omega}_{\times}$ is the skew-symmetric matrix representation of the cross product

applied to $\boldsymbol{\omega}$ so that

$$\boldsymbol{\omega}_\times = \begin{bmatrix} 0 & -\omega_z & \omega_y \\ \omega_z & 0 & -\omega_x \\ -\omega_y & \omega_x & 0 \end{bmatrix} \tag{3.9}$$

and

$$^{\mathcal{I}}Q^{\mathcal{L}} = \begin{bmatrix} \hat{\mathbf{r}} & \hat{\mathbf{s}}_K & \hat{\mathbf{w}}_K \end{bmatrix} \tag{3.10}$$

is a 3×3 rotation matrix. The unit vectors $\{\hat{\mathbf{r}}, \hat{\mathbf{s}}_K, \hat{\mathbf{w}}_K\}$ form the basis of the LVLH frame, where $\hat{\mathbf{r}}$ points along the chief's position vector, $\hat{\mathbf{w}}_K$ points along the chief's angular momentum vector, and $\hat{\mathbf{s}}_K = \hat{\mathbf{w}}_K \times \hat{\mathbf{r}}$. The vectors can be obtained from ECI coordinates using equations given by Vallado [149]. The angular velocity can be obtained via the approach of Kechichian [97] or others, which all require knowledge of the Vinti inertial acceleration vector in ECI coordinates. Monuki [118] derived this acceleration in an unpublished report, and Der and Danchick [52] have briefly explained the method, but the equation is repeated here for convenience:

$$\ddot{\mathbf{r}}^{\mathcal{I}} = -\frac{\mu}{r_v^3} \begin{bmatrix} X & Y & Z + z_v \end{bmatrix}^\top \tag{3.11}$$

where

$$r_v^3 = \frac{(\rho^2 + c^2\eta^2)^3}{\rho^3 + 3z_\delta\eta\rho^2 - 3c^2\eta^2\rho - z_\delta c^2\eta^3} \tag{3.12}$$

and

$$z_v = \frac{\eta(3\rho^2 - c^2\eta^2)(c^2 + z_\delta^2)}{\rho^3 + 3z_\delta\eta\rho^2 - 3c^2\eta^2\rho - z_\delta c^2\eta^3} \tag{3.13}$$

For Kechichian's approach, the spherical gravity term should be subtracted from the Vinti acceleration to obtain the "perturbing" acceleration.

While extensive use is made of the partials derived by Walden and Watson [164], the underlying Vinti theory that they used becomes singular for polar orbits and nearly circular equatorial orbits, and also when a spacecraft is at either of the poles. Distinctions are made between nearly polar orbits and vicinity to a pole because those issues arise from different terms in the equations. Some terms in the denominators approach zero when the spacecraft is anywhere in a nearly polar orbit, and other terms approach zero when the spacecraft nears a pole. In an effort to circumvent these issues, partial derivatives were rederived as necessary in this study to be consistent with Vinti's nonsingular orbit propagation theory. These partials are given in Appendices C.3–C.4. However, some singularities persist in the partials, necessitating the use of two different element sets whose validity depends on the spheroidal inclination I. These singularities are now addressed in the following sections.

3.1.2 Singularities Associated with Polar Orbits: $S = 1$

As alluded to in an earlier section, the partial derivatives with respect to S are discontinuous for polar orbits, when $S = 1$. The discontinuity occurs because of the appearance of $\sqrt{1 - S}$ or $\sqrt{1 - S/u}$ terms in a few equations of the solution, where u also tends to unity for polar orbits. This problem is alleviated with a change of variables by defining $\tilde{S} \equiv \sqrt{1 - S}$ and then choosing to use $\tilde{S}$ instead of S as an element or independent variable. The new functional dependency should be thought of as $S = S(\tilde{S}) = 1 - \tilde{S}^2$. Most partials, specifically those that do not possess the singularity, can be adjusted

with a simple application of the chain rule:

$$\frac{\partial(\cdot)}{\partial \tilde{S}} = \frac{\partial(\cdot)}{\partial S}\frac{\partial S}{\partial \tilde{S}} = -2\tilde{S}\frac{\partial(\cdot)}{\partial S} \tag{3.14}$$

Only five partials with respect to S contain the singularity: that of α_3 has $\sqrt{1 - S/u}$ in the denominator and those of X, Y, $\dot{X}$, and $\dot{Y}$ all have $\sqrt{1 - S}$ in the denominator. The partial of α_3 is given by Walden and Watson [164] while the other four were developed in the current work. Of course, the last four partials are only required if seeking the STM in ECI or LVLH Cartesian coordinates.

The trivial case is for the ECI coordinates, where the $\sqrt{1 - S}$ terms in Eq. (2.28) and its time derivatives are readily replaced with $\tilde{S}$. In contrast, the Jacobi constant α_3 is expressed in terms of elements as

$$\alpha_3 = \text{sgn}\,\alpha_3\alpha_2\left(1 - \frac{S}{u}\right)^{\frac{1}{2}} \tag{3.15}$$

which in the present form is not amenable to the same substitution and subsequent removal of the square root. However, substituting $1/u$ in Eq. (3.15) with Vinti's third order approximation and collecting terms will recover Eq. (148) in Vinti [158]:

$$\alpha_3 = \text{sgn}\,\alpha_3\alpha_2\sqrt{1 - S}\left\{1 - \frac{c^2}{a_0 p_0}S - \frac{\left(\frac{2z_\delta}{p_0}\right)^2\left(1 - \frac{c^2}{a_0 p_0}S\right)}{\left[1 + \frac{c^2}{a_0 p_0}(1 - 2S)\right]^2}S\right\}^{\frac{1}{2}} \tag{3.16}$$

Having now isolated the problematic $\sqrt{1 - S}$ term, it can be replaced with $\tilde{S}$ as done for the ECI coordinates. The other square root term is not an issue because it never approaches zero. The partials of $\mathbf{x}^{\text{J}}$ with respect to $\tilde{S}$ are now

103

readily obtained. The results of this section suggest that $\tilde{S}$ is a more natural element compared to S because the solution $\mathbf{x}^{\jmath}$ is differentiable with respect to $\tilde{S}$ over a larger domain.

3.1.3 Singularities Associated with Nearly Equatorial Orbits: $Q = 0$

Vinti [158] introduces the derived quantity

$$Q = Q(a, e, S) \equiv \sqrt{P^2 + S} \tag{3.17}$$

as an intermediate parameter of his solution, and its partial derivatives, as given in Walden and Watson [164], are

$$\frac{\partial Q}{\partial \sigma_j} = Q^{-1} \left(P \frac{\partial P}{\partial \sigma_j} + \frac{1}{2} \delta_{3j} \right) \tag{3.18}$$

A singularity clearly exists in the partial derivative of Q if Q can vanish. It turns out that Q tends to zero for nearly equatorial orbits, so that the singularity does indeed exist. Quotes are used on "equatorial" because true equatorial Vinti orbits do not exist; equatorial, in this context, should be interpreted in the Keplerian sense, when $S < 0$. The case $Q = 0$ is specifically when the orbit remains at a constant latitude close to the equatorial plane. This singularity is not mentioned in Walden and Watson [164]. Although Tong and Wu [145] mention singularities involving $Q = 0$ in the context of perturbation equations, their removal is left to future work.

One viable option for removing the singularity in Eq. (3.18) is proposed here. The basic idea is to replace S with Q in the state vector. This action is reasonable because both S and Q are constants closely related to inclination

104

and are otherwise seemingly arbitrary quantities to select as an element or independent variable. The choice of S was certainly motivated by the functional dependencies of the equations that make up Vinti's solution. It would not be straightforward to use a direct approach like that of Walden and Watson [164] to obtain the partials when Q is used instead of S. But an alternative approach can be used to circumvent the issue: redefine the functional dependencies, adjust the chain rule accordingly, and isolate the desired new partials in terms of the old partials through algebraic manipulation. The partials of Q, which contain the singularity at $Q = 0$, are rendered unnecessary.

The first step is to manipulate Eq. (3.17), which relates S, Q, and P in a simple way, to redefine S as a function of Q and P:

$$S = S(Q, P) \equiv Q^2 - P^2 \tag{3.19}$$

This relationship was also pointed out in Eq. (2.11). In terms of partial derivatives, the redefinition of S results in a circular functional dependence captured in Table 3.1, which is adapted from Walden and Watson [164]. Note that Table 3.1 contains a very small subset of the partial derivatives that comprise the solution. In the original formulation, the partials of b_1 only depend on those of p, so that the explicit expressions for the partials of P flow directly from those of b_1. In the new formulation, the expressions for the partials of P are now implicit: 1) partials of b_1 depend on those of S; 2) partials of S depend on those of P; 3) and partials of P depend directly on those of S and on the chain of partials that flow from b_1 to P.

The key is to observe that the last two lines of Table 3.1 are unique

105

Table 3.1: Functional dependence of a subset of the time-independent partial derivatives

Partial Derivative	Functional Dependence on Other Partials
p	none
b_1	p, S
b_2	p, b_1
p_0	p, b_1, b_2
$(a_0 p_0)^{-1}$	b_1, p_0
u	p_0, $(a_0 p_0)^{-1}$, S
C_2	$(a_0 p_0)^{-1}$, u
C_1	p_0, u, C_2, S
P	p_0, u, C_2, S
S	P

in that they contain or point to three isolated systems of two equations in two unknowns. First, let $q_1 = a$, $q_2 = e$, and $q_3 = Q$. Then, each system of equations is associated with q_j for $j = 1, 2, 3$. In each of the three systems, one of the unknowns is $\partial S / \partial q_j$ and the other unknown is $\partial P / \partial q_j$. In other words, the partials of S are obtained from Eq. (3.19) as

$$\frac{\partial S}{\partial q_j} = 2Q\delta_{3j} - 2P\frac{\partial P}{\partial q_j} \tag{3.20}$$

and the chain rule is used to express the partials of P with respect to q_j, in general, as

$$\frac{\partial P}{\partial q_j} = f_j\left(\left(\frac{\partial P}{\partial q_j}\right)_{\text{old}}, \frac{\partial P}{\partial S}, \frac{\partial S}{\partial q_j}\right) \tag{3.21}$$

where f_j is some function to be defined shortly. For each value of j, the pair of equations represented by Eqs. (3.20) and (3.21) constitute one of the three systems of equations, which are to be solved for $\partial S / \partial q_j$ and $\partial P / \partial q_j$. As a

first step, express the partial of P with respect to Q as

$$\frac{\partial P}{\partial Q} = f_3\left(\frac{\partial P}{\partial S}, \frac{\partial S}{\partial Q}\right) = \frac{\partial P}{\partial S}\frac{\partial S}{\partial Q} \qquad (3.22)$$

Substituting Eq. (3.20) with $j = 3$ into Eq. (3.22) gives

$$\frac{\partial P}{\partial Q} = \frac{\partial P}{\partial S}\left(2Q - 2P\frac{\partial P}{\partial Q}\right)$$

and isolating $\partial P/\partial Q$ leads to

$$\frac{\partial P}{\partial Q} = \frac{2Q\frac{\partial P}{\partial S}}{1 + 2P\frac{\partial P}{\partial S}} \qquad (3.23)$$

The steps to obtain the partials of P with respect to a and e are slightly different. The old partials are correct assuming S is an independent variable, which means that the new partial derivatives are simply the old ones plus a term accounting for the new functional dependence of S via the chain rule:

$$\frac{\partial P}{\partial q_{1,2}} = f_{1,2}\left(\left(\frac{\partial P}{\partial q_{1,2}}\right)_{old}, \frac{\partial P}{\partial S}, \frac{\partial S}{\partial q_{1,2}}\right) = \left(\frac{\partial P}{\partial q_{1,2}}\right)_{old} + \frac{\partial P}{\partial S}\frac{\partial S}{\partial q_{1,2}} \qquad (3.24)$$

Substituting Eq. (3.20) with $j = 1, 2$ into Eq. (3.24) gives

$$\frac{\partial P}{\partial q_{1,2}} = \left(\frac{\partial P}{\partial q_{1,2}}\right)_{old} + \frac{\partial P}{\partial S}\left(-2P\frac{\partial P}{\partial q_{1,2}}\right)$$

and isolating $\partial P/\partial q_{1,2}$ leads to

$$\frac{\partial P}{\partial q_{1,2}} = \frac{\left(\frac{\partial P}{\partial q_{1,2}}\right)_{old}}{1 + 2P\frac{\partial P}{\partial S}} \qquad (3.25)$$

The denominator in Eqs. (3.23) and (3.25) may raise concern, but it does not approach zero because the magnitudes of P and $\partial P/\partial S$ are $O(J_2^{1/2})$.

107

After obtaining expressions for $\partial P/\partial q_j$, the partials $\partial S/\partial q_j$ are subsequently determined from Eq. (3.20) and, although tedious, it is straightforward to modify the remaining partials. The modification process mostly follows a simple rule. If the quantity does not depend on S explicitly, then

$$\frac{\partial(\cdot)}{\partial q_{1,2}} = \left(\frac{\partial(\cdot)}{\partial q_{1,2}}\right)_{\text{old}} \tag{3.26}$$

Otherwise,

$$\frac{\partial(\cdot)}{\partial q_{1,2}} = \left(\frac{\partial(\cdot)}{\partial q_{1,2}}\right)_{\text{old}} + \frac{\partial(\cdot)}{\partial S}\frac{\partial S}{\partial q_{1,2}} \tag{3.27}$$

In either case, for the partials with respect to Q,

$$\frac{\partial(\cdot)}{\partial Q} = \frac{\partial(\cdot)}{\partial S}\frac{\partial S}{\partial Q} \tag{3.28}$$

However, further adjustments are required if there is explicit dependence on Q. In this case, the partials given in Walden and Watson [164] can still be used, but with the following modification:

$$\frac{\partial Q}{\partial q_j} = \delta_{3j} \tag{3.29}$$

where only the terms without explicit dependence on Q are multiplied by $\partial S/\partial Q$. None of the intermediate quantities depends on both S and Q explicitly.

3.2 Model Evaluation

This section contains a quick assessment of the Vinti-based model and side-by-side comparisons with the GA STM. The Vinti and GA relative motion models are compared against a more realistic numerically integrated solution

to assess their accuracy by way of simple absolute position errors. Portions of the GA model include code provided by Alfriend. The "truth" equations of motion are represented in ECI coordinates using a gravity field that includes J_2 through J_5 zonal harmonics, which is the same fidelity used by Gim and Alfriend [64]. Both spacecraft states are initially obtained in the ECI frame in quad precision and then independently propagated with a fourth order, variable step size Runge-Kutta integrator in double precision over 15 orbits using an accuracy tolerance of 2.3×10^{-14}. The quad precision is necessary for the initial states because they will ultimately have to be differenced for use with either of the STMs, and it is desired to isolate as much as possible the errors in the model evaluations from artifacts of finite precision arithmetic. This way, errors in the results will reflect the accuracy of the underlying theory. Note that the publicly available High Precision Floating-point (HPF) tool[4] for MATLAB will work when the quartics are factored with Getchell's method [62], but not with the eigenvalue method. The Multiprecision Computing Toolbox[5] is a third-party MATLAB software package that can compute eigenvalues in quad precision.

Interest in a precision-preserving error metric guided the analysis toward a set of decalibrated solutions. The need to make the fairest comparison between the two models further guided the choice of coordinates toward a direct comparison of the deputy's ECI state because those are the most acces-

---

[4]D'Errico, J., "HPF - A Big Decimal Class," `https://www.mathworks.com/matlabcentral/fileexchange/36534-hpf-a-big-decimal-class`.

[5]Advanpix, Multiprecision Computing Toolbox, `http://www.advanpix.com`.

sible coordinates that the two models share and, for both models, the deputy's ECI state can be obtained without differencing. A comparison in the LVLH Cartesian coordinates would present challenges because the transformation from LVLH curvilinear to Cartesian coordinates in the GA model requires differencing of potentially similar values, and the Vinti-based model would require differencing of the two ECI states. Modeling errors cannot be compared in the orbital element space either because it is spheroidal in the Vinti model and spherical in the GA model. The best option, then, is to propagate the Vinti-based model in the spheroidal element space according to Eq. (3.5) and the GA model in the Keplerian (spherical) element space. Next, add the resulting deputy relative state to the corresponding chief state, and finally apply the appropriate nonlinear transformations to recover the deputy's ECI state. This transformation is given by Eq. (2.28) for the Vinti-based model and a straightforward spherical elements to ECI transformation for the GA model. The fact that both models are propagated in some type of osculating element space is further indication that the comparison is fair, in terms of the ability to assess how accurate one model is relative to the other.

Note that each model requires a unique input. For the Vinti-based STM, the relative state is needed in time-varying, osculating spheroidal orbital elements, and so those elements are computed for the chief and deputy in quad precision and then differenced. For the GA STM, the relative state is needed in quasi-nonsingular, osculating spherical orbital elements, also requiring the corresponding states of the chief and deputy in quad precision. All remaining computations are done in double precision. The Vinti-based model

110

also requires an analytical Vinti solution for the chief, while the GA model additionally requires an initial state for the chief in Brouwer mean elements. A differential correction procedure is implemented using the Jacobian of the Brouwer transformation that converges from osculating to Brouwer mean elements in several iterations. The Brouwer transformation is defined as the following nonlinear function $\mathbf{f}_B$ that transforms Brouwer's mean elements to osculating spherical elements as

$$\text{œ}^K = \mathbf{f}_B\left(\overline{\text{œ}}^K\right) \tag{3.30}$$

The Jacobian of the Brouwer transformation is defined as

$$D = \mathbf{g}_B\left(\overline{\text{œ}}^K\right) = \frac{\partial \text{œ}^K}{\partial \overline{\text{œ}}^K} \tag{3.31}$$

The following algorithm can be used to convert from osculating spherical elements to Brouwer mean elements:

1. Set $j = 1$, $\epsilon = 10^{-12}$, and $\overline{\text{œ}}_j^K = \text{œ}_0^K$ as an initial guess for the Brouwer mean elements.

2. Compute $\text{œ}_j^K = \mathbf{f}_B\left(\overline{\text{œ}}_j^K\right)$ and $D_j = \mathbf{g}_B\left(\overline{\text{œ}}_j^K\right)$.

3. Compute $\delta\text{œ}_j^K = \text{œ}_0^K - \text{œ}_j^K$.

4. Compute $\delta\overline{\text{œ}}_j^K = D_j^{-1}\delta\text{œ}_j^K$.

5. Compute $\overline{\text{œ}}_{j+1}^K = \overline{\text{œ}}_j^K + \delta\overline{\text{œ}}_j^K$.

6. If $\|\delta\text{œ}_j^K\| > \epsilon$, then increment $j \to j+1$ and return to Step 2. Otherwise, stop.

Note, however, that the algorithm fails near the critical inclination and near equatorial orbits due to known singularities. As stated previously, the equinoctial element version of the GA model solves the equatorial problem, but not the critical inclination problem [65].

Figures 3.2 and 3.3 present modeling errors on a wide swath of a three-dimensional parameter space that considers variations in Keplerian eccentricity e_K, inclination I_K, and initial separation distance δr_i. Orbits are initialized with the parameterization of Biria and Russell [16], which in the absence of perturbations would lead to relative periodic orbits. The quantities associated with position are defined in Fig. 3.4(a) while those associated with the deputy's velocity vector are defined in Fig. 3.4(b). When applied to a perturbed model, those initial conditions can lead to similar relative orbits with small drift rates. Results in Figs. 3.2 and 3.3 are generated from the initial conditions in Table 3.2, which are chosen to result in relatively simple drift rate behavior. Both models completely account for eccentricity, and since

Table 3.2: Parameter sets [16] for error trends in Figs. 3.2–3.3, where the chief has initial Keplerian elements $a_K = 12{,}000$ km, $I_K = 30°$, 63.4°, or 90°, $\Omega_K = 10°$, and $\omega_K = 20°$

Figure	e_K	f_{K_i} (°)	ϕ_v (°)	$\delta\lambda_v$ (°)	δr_i (km)	α (°)	β (°)
3.2	[0, 0.4]	0	0	0	0.01	30	30
3.3	0.4	0	0	0	[0.01, 100]	30	30

spacecraft in highly eccentric orbits spend most of their time far away from the effects of the perturbations considered, it is not as instructive to show the
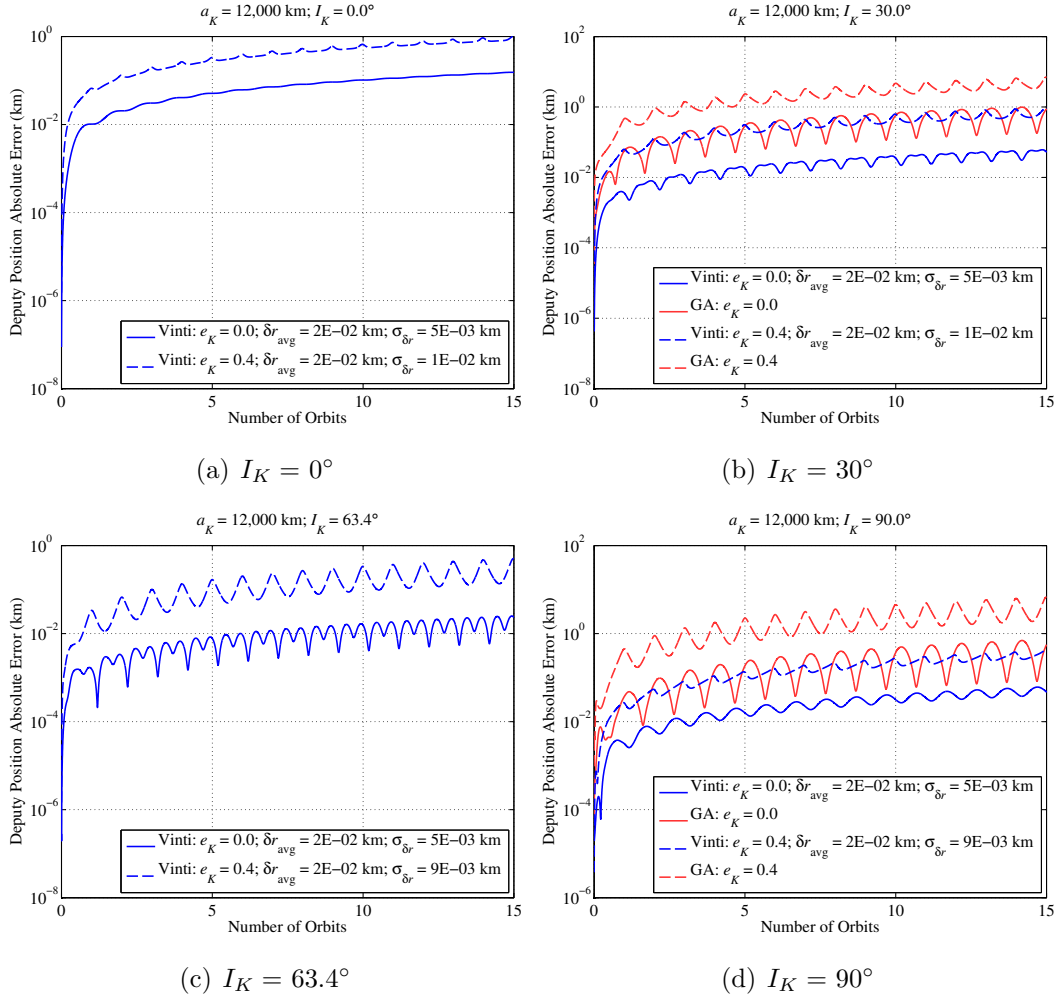
Figure 3.2: Comparison of relative motion models characterized by deputy position absolute error: varying eccentricity and inclination with $a_K = 12{,}000$ km and $\delta r_{\mathrm{avg}} \approx 20$ m. The original GA STM is invalid for the I_K of Figs. 3.2(a) and 3.2(c).
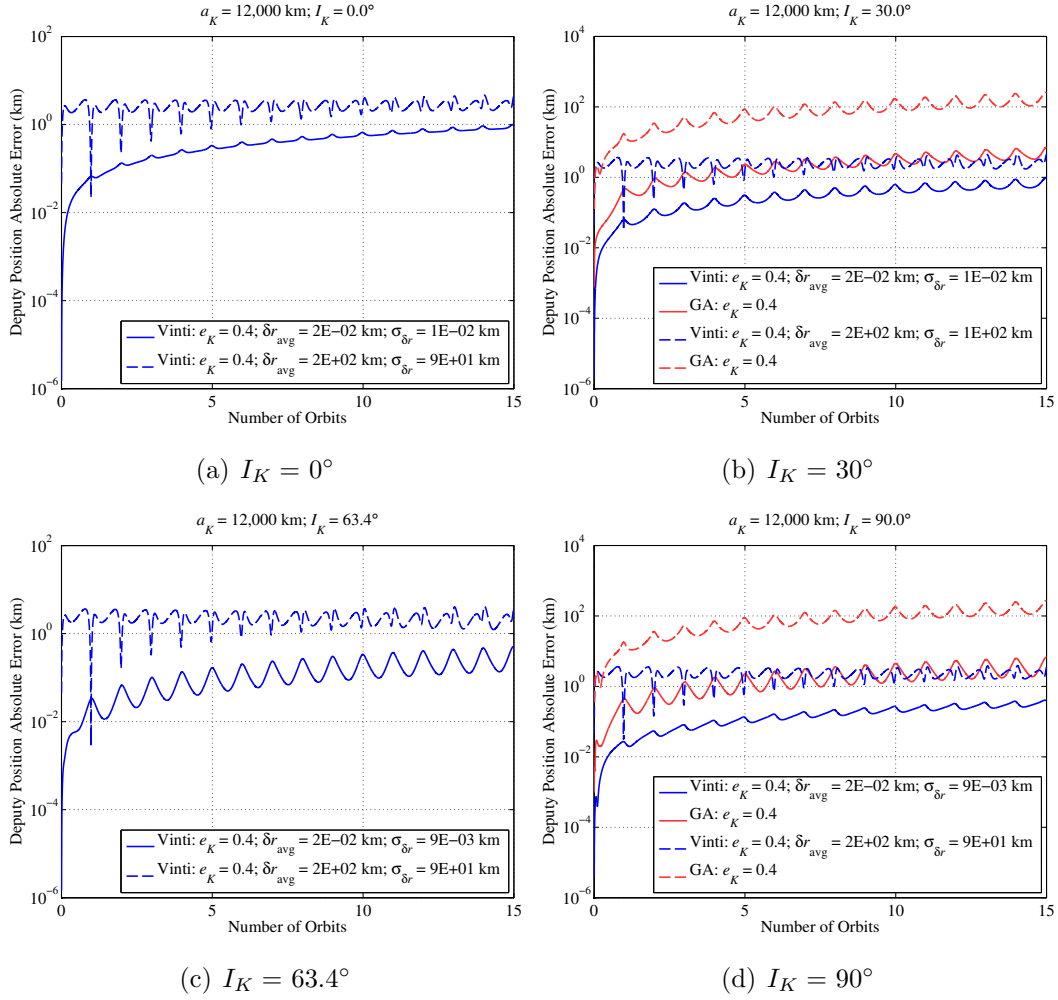
Figure 3.3: Comparison of relative motion models characterized by deputy position absolute error: varying relative position and inclination with $a_K = 12,000$ km and $e_K = 0.4$. The original GA STM is invalid for the I_K of Figs. 3.3(a) and 3.3(c).
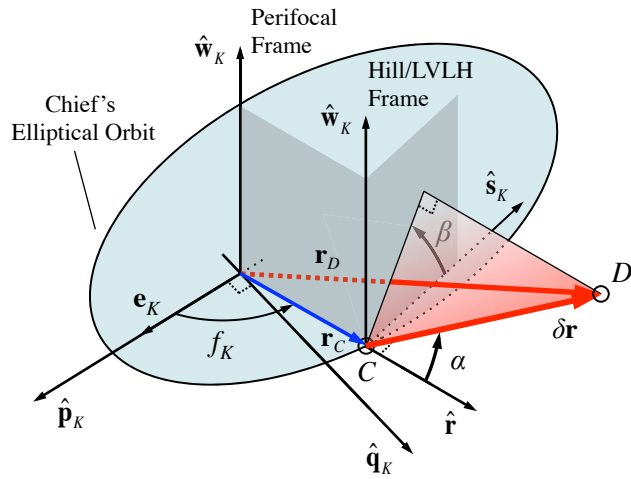
(a) Parameterization of chief position with e_K and f_K and deputy position with δr, α, and β
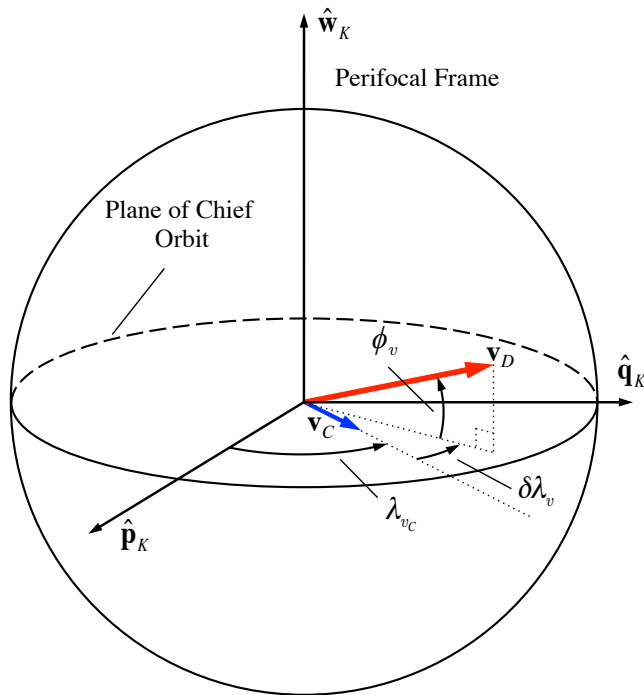
(b) Parameterization of deputy velocity (direction): ϕ_v and $\delta\lambda_v$

Figure 3.4: Schematic illustrating the nonlinear parameterization in the perifocal frame.

error trends for higher eccentricities. The legends in Figs. 3.2 and 3.3 contain useful statistics on the average and standard deviation of the deputy's relative position, denoted as δr_{avg} and $\sigma_{\delta r}$, respectively. These statistics help to ascertain the size of the relative orbit over time, which is directly related to the validity of the linear approximations.

Granted that the Vinti STM models more perturbations than the GA STM, the general trends in the errors are not surprising, with oscillations superimposed on secular growth. Figures 3.2–3.3 show that the accuracy of the Vinti model can be one to two orders of magnitude higher than that of the GA model. Notice in Figs. 3.2(c) and 3.3(c) that the proposed Vinti model has no trouble near the critical inclination. Figure 3.2(a) confirms that the Vinti model can also handle circular equatorial orbits, and Figs. 3.2(d) and 3.3(d) confirm the same for polar orbits. After 15 orbits, the $a_K = 12,000$ km, $I_K = 63.4°$, $e_K = 0.4$, $\delta r_i = 200$ km case leads to errors on the order of 1 km. The speed of Vinti versus Brouwer theories has not been documented in the literature since the work of Bonavito et al. [22] and it has not been benchmarked in the present investigation. The fairest test would require both models to include the same perturbations to the same order of approximation and also implementation in a compiled language such as Fortran. Bonavito et al. revealed the speeds to be comparable when Brouwer theory was not extended to include $O(J_2^3)$ secular terms, and they reasoned that based on the large number of additional terms required in the higher order solution of Kozai [102], Vinti's solution should be faster.

It is worthwhile to explore further the errors observed in Figs. 3.2–3.3

116

to try to better assess the root causes. There are at least three error sources. First, the perturbations included in the two models are different from each other and from the truth model. The Vinti-based model includes J_2, J_3, and 72% of J_4, the GA model includes J_2 only, and the truth model includes J_2 through J_5. Relative to this truth model, the neglected perturbations lead to $O(J_2^2)$ errors. Second, the order of the solutions are different. The Vinti-based model includes $O(J_2^4)$ secular and $O(J_2^2)$ periodic terms, while the GA model includes $O(J_2)$ secular and periodic terms. In other words, the STMs are not exact with respect to their force models. Third, the solution itself is truncated to first order, i.e. higher order STMs (state transition tensors) are not used. If the linearity assumption is violated, then the truncation to a linear theory would also contribute to the error.

An effort is made in the following to isolate errors. First, a relative orbit is chosen, as in some of the preceding scenarios, with an average size of 20 meters, which keeps linear truncation errors small. The first-order GA STM is compared in Fig. 3.5 to a two-body plus J_2 only truth model. Notice that secular error growth is still present in the GA model. All forces of the truth model are modeled in the STM, the linear approximation is expected to be valid, and so the error can be attributed mainly to the approximate nature of the perturbation theory, lacking second-order and higher terms. The Vinti-based STM is performing slightly worse because its errors are now $O(J_2^2)$. A physical interpretation is that the secular rates are poorly matched between the truth model and STMs, i.e. only to first-order. One can imagine different ways of better matching the secular rates. One option is to simply use a
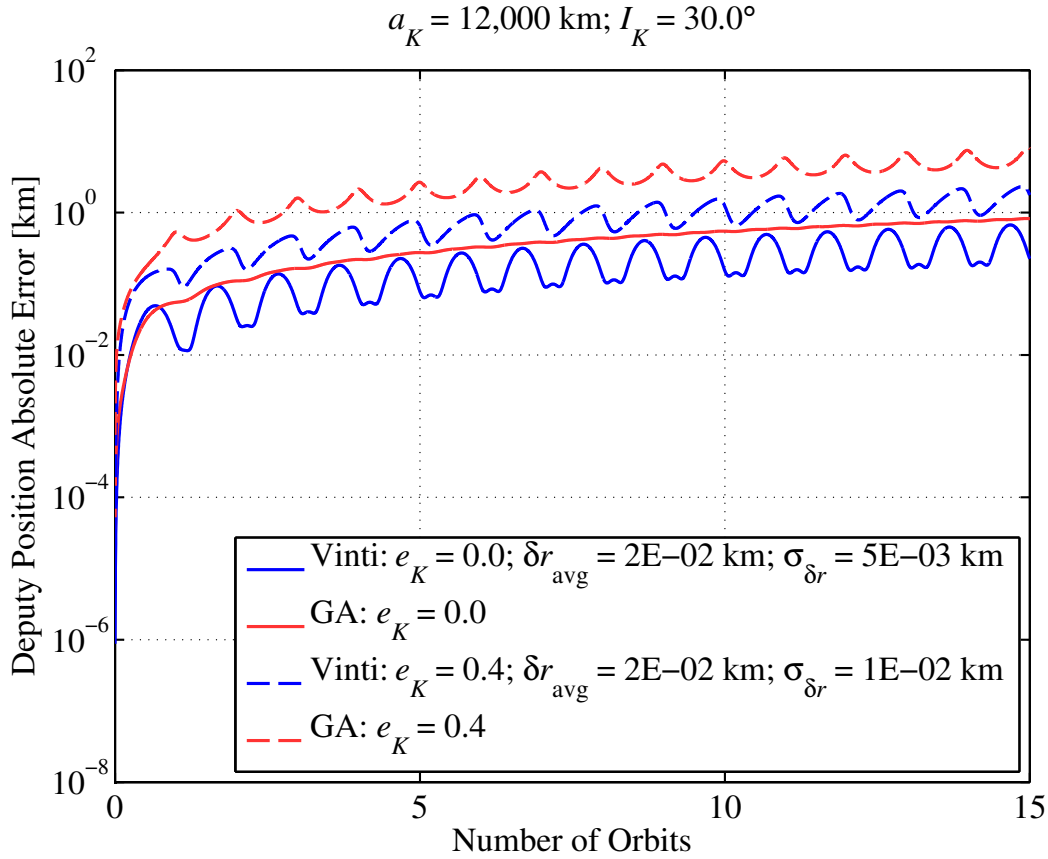
Figure 3.5: Errors relative to a J_2 truth model.

higher order perturbation theory with the same truth model, such as the extended GA STM with second-order effects. Comparing the Vinti-based STM to a Vinti numerically integrated truth is expected to have a similar effect. Figure 3.6 shows these latter errors, wherein the secular error growth appears to be substantially mitigated. An alternative option to using a higher order perturbation theory is to generate an ephemeris from the truth model and determine initial conditions for the approximate model that lead to a best
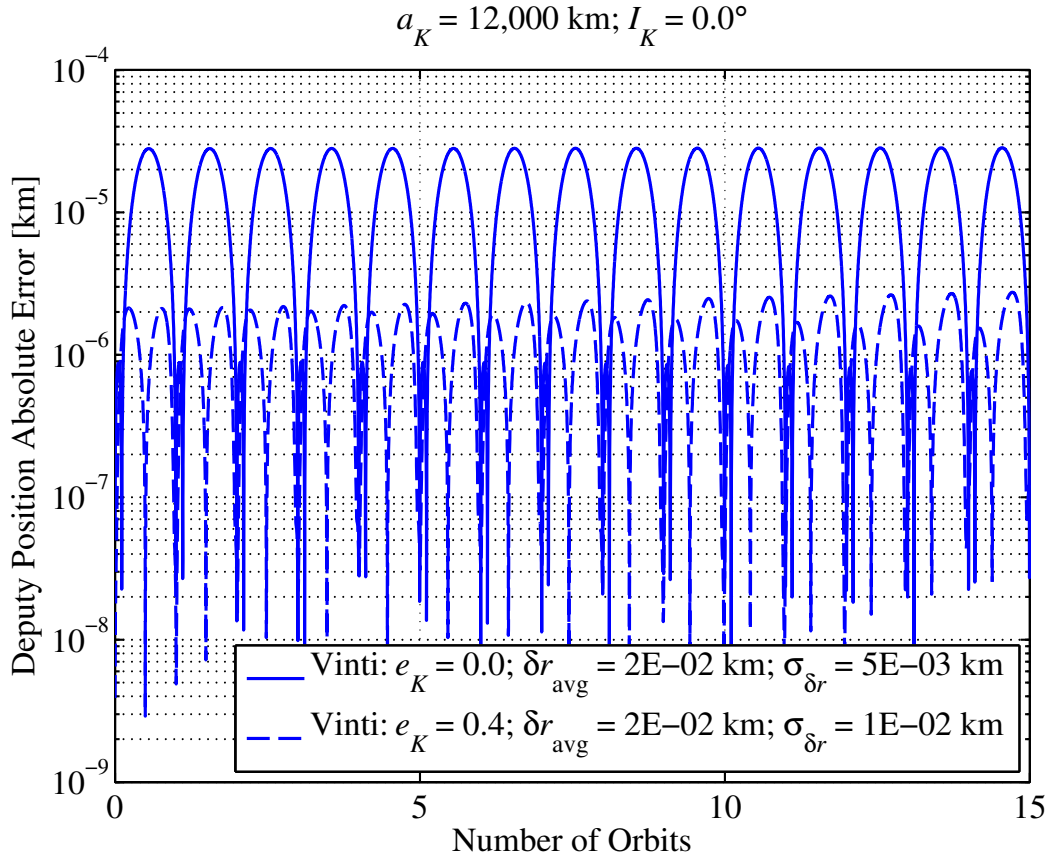
Figure 3.6: Errors of the Vinti-based STM relative to a Vinti truth model.

fit of the ephemeris data. Getchell [62] suggested this idea for his universal Vinti propagator. More recently, Yan et al. [173] have suggested least squares algorithms that could be adopted for this purpose.

3.3 Final Remarks

Vinti theory is successfully applied to the relative motion problem, naturally incorporating J_2, J_3, and a partial J_4 into the dynamics. An analytical

approach is employed that leverages the state transition matrix (STM), which is derived in the oblate spheroidal orbital element space. The scope of work includes fixes to singularities in some partials, reformulations to avoid singularities in the partials, and in general the development of a complete analytical STM. While the STM is singularity-free, not all singularities associated with the linear transformation from rectangular coordinates to spheroidal elements are handled, leaving the door open to new ideas addressed in Chapters 4 and 5. The solution is recast in a piecewise differentiable form comprised of two parts. Companion code is provided online for the Vinti orbit propagator and associated STM.

The analytical STM derived from Vinti theory is also compared to Gim and Alfriend's benchmark STM derived from Brouwer theory. Over the range of eccentricity, inclination, and spacecraft separation distance considered, the Vinti-based STM is shown to have greater accuracy, including near the critical inclination and for circular equatorial orbits, where the underlying Brouwer solution either loses accuracy or does not exist. Note that the version of the GA STM implemented only models J_2, and improved or extended versions include other perturbations. The Vinti-based STM is an attractive candidate for modeling relative motion of widely-distributed spacecraft formations or for rendezvous in environments strongly perturbed by a central body. The STM can also be useful in optimization, guidance and control, and other applications.

Chapter 4

Equinoctial Elements for Vinti Theory: Generalizations to an Oblate Spheroidal Geometry

To remove the linear dependence for all combinations of spheroidal eccentricity and inclination, the effort continues presently with the development of a nonsingular element set. Two choices must be made upfront regarding the various flavors of nonsingular elements and the two different flavors of Vinti theory. The equinoctial element variety [12, 26] is chosen over its canonical counterpart, the Poincaré elements [76], because of their popularity over the last few decades, particularly with respect to their role in the development of the Draper Semianalytic Satellite Theory (DSST) [42] and also the Gim-Alfriend STM [65]. Their geometrical interpretation is also straightforward. The selected flavor of Vinti theory utilizes the symmetric potential wherein $J_3 = 0$ so that the origins of the oblate spheroidal (OS) and ECI reference frames coincide. The reasoning here requires a deeper understanding of the implications of each potential. When the origins coincide, a single spheroidal inclination governs a spacecraft's maximum latitude. If the OS frame is shifted along the polar axis to capture J_3, then the inclination splinters into two inclinations that are similar in value and not independent. Due to the dual nature of the spheroidal inclination, the latter theory presents complications for the

definition of nonsingular orbital elements. For this reason, the new orbital elements are developed for the original Vinti potential that prescribes an OS reference frame whose origin is coincident with that of the inertial frame. That being said, it may be worth exploring in future work the inclusion of J_3 using the method of Aksenov et al. [1], for which the origin is not shifted, possibly mitigating the described issues in the definition of equinoctial elements for Vinti's 1966 potential. But it is considered a reasonable stepping stone of sufficient complexity to study the original Vinti potential first and leave to future work the study of Vinti's latter potential or that of Aksenov et al. [1] in the same vein.

The nuances of Vinti theory and customary use of equinoctial elements have thus brought into focus a starting point for linking familiar notions of nonsingular element sets to a largely unfamiliar theory of orbits. The introduction of oblate spheroidal equinoctial orbital elements begins by imposing the standard definition in terms of classical elements and unfolds from there. Their complete, formal introduction is divided between two chapters. The theory developed in this chapter enables analytical state propagation with equinoctial elements, and this latter topic is introduced in Chapter 5. Presently, the point transformations between ECI coordinates and the elements are derived. The transformations are completely separate and independent from any solution method, analytical or numerical, generally representing all the steps required prior to evaluating the integrals in the kinematic equations. Strong emphasis is placed on eliminating indeterminate forms and ensuring the transformation is valid and exact for all orbit regimes. Naturally, the transformations are not

122

valid for nearly rectilinear orbits passing through the forbidden zone, when the spheroidal semi-latus rectum is very small [62]. Otherwise, the transformations are valid for all orbits. With the exception of performing a transformation near a pole, where it is as accurate as the analytical solution, the transformations are also exact.

4.1 Definition of the Oblate Spheroidal Equinoctial Elements

The spheroidal equinoctial elements are tied to the Vinti problem in the same way that the spherical equinoctial elements are tied to the Kepler problem. Those dynamical problems define the respective element sets and they cannot be separated from each other. It is therefore understood that any mention of spherical elements concerns a perturbed or unperturbed Kepler problem, and any mention of spheroidal elements concerns a perturbed or unperturbed Vinti problem. Notions of osculating elements can be adopted if the dynamical problems are perturbed.

The six modified spheroidal equinoctial elements are described as follows using the notation of Gim and Alfriend [65] for the vector components:

$$
\begin{array}{lll}
\text{œ}_1 = p & \text{spheroidal semi-latus rectum} \\
\left.\begin{array}{l} \text{œ}_2 = q_1 \\ \text{œ}_3 = q_2 \end{array}\right\} & \text{components of the spheroidal eccentricity vector} \\
\left.\begin{array}{l} \text{œ}_4 = p_1 \\ \text{œ}_5 = p_2 \end{array}\right\} & \text{components of the spheroidal ascending node vector} \\
\text{œ}_6 = L & \text{spheroidal true longitude}
\end{array}
\tag{4.1}
$$

The standard equinoctial elements use semimajor axis a instead of p and the

mean longitude λ instead of L. The modified set is chosen because it is non-singular for the full range of eccentricity and inclination. The spherical and spheroidal equinoctial reference frames differ from each other in several key ways. First, notice the repeated use of the word "spheroidal" to emphasize, for example, that the spheroidal eccentricity vector is not the same as the one in Keplerian dynamics, which is the spherical eccentricity vector. These notions of spheroidal vectors are new concepts that have not been discussed before with respect to Vinti theory. Geometrically, the discrepancy is the result of stretching the coordinates in the equatorial plane and contracting them along the polar axis. These notions will be further elaborated later in the derivation. Another major difference is that the frame rotates in the spheroidal case, while it is fixed in the spherical case. The rotating trait is a natural result of transforming from the original Jacobi constants to natural Delaunay variables, which define the secular motion of the spheroidal frame; its rotation rate is such that it approximately tracks the averaged motion of the osculating spherical frame in the equivalently perturbed Kepler problem. The true rate of the spheroidal frame is the rate of change of the spheroidal ascending node vector. Note that the angular elements (not the momenta) that define the spherical equinoctial elements are also Delaunay variables, i.e. the two equinoctial frames are consistent in that respect.

The representation of the dynamics in terms of fast and slow variables is also different. First consider the unperturbed problems. In the spherical case, the first five elements are dynamical constants and the sixth varies rapidly in time. In the spheroidal case, the first element is a dynamical con-

stant (no averaging involved), the next four vary slowly in time, and the sixth varies rapidly (still no explicit averaging). Now consider the perturbed problems. In both the spherical and spheroidal cases, the first five elements vary slowly in time and the sixth varies rapidly. The new spheroidal element set then arguably represents an improvement over the final set recommended by Vinti [160], who effectively parameterized the solution with three dynamically constant elements, one slow variable, and two fast variables.

Before proceeding, it is important to review the major contributions to the formulation of Vinti theory in classical spheroidal orbital elements. Izsak [85] is credited with the observation that the solution under the original Vinti potential can be expressed in terms of classical spheroidal elements, especially with regard to identifying the spheroidal semimajor axis, eccentricity, and inclination. Recall from Chapter 1 that Izsak's solution sprouted a few follow-on studies and explicit computational procedures that branch off from the track of Vinti's solutions; Izsak even foresaw the usefulness of a RAAN-like variable that tracks a slowly rotating reference plane. However, this last variable was not formally introduced until nearly a decade later in Vinti's 1968 technical report, which is very difficult to find. Lang subsequently used it in his thesis [104] and Vinti thoroughly archived the new element in 1969 for both potentials [160]. It is the author's opinion that Vinti's formulation is easier to implement. The present work develops the spheroidal equinoctial elements by building on these early contributions in classical elements.

It follows from the preceding discussion that, when spherical equinoctial elements are generalized to spheroidal elements, the familiar relationships

125

between classical and equinoctial elements still apply both to the elements' secular components and to the complete elements, which are formed by adding in the periodic parts. The symbols used to define the spherical equinoctial elements in terms of classical spherical elements are essentially used to define the oblate spheroidal equinoctial elements, with the understanding that the classical elements are now spheroidal. In other words, it is possible to convert the classical spheroidal elements to spheroidal equinoctial elements using the following formulas:

$$p = p$$

$$q_1 = e \cos \left(\omega' + K\Omega' \right)$$

$$q_2 = e \sin \left(\omega' + K\Omega' \right)$$

$$p_1 = \left[\tan \left(\frac{I}{2} \right) \right]^K \cos \Omega'$$

$$p_2 = \left[\tan \left(\frac{I}{2} \right) \right]^K \sin \Omega'$$

$$L = f + \omega' + K\Omega'$$

(4.2)

where e is the spheroidal eccentricity, ω' is the argument of spheroidal periapsis, Ω' is the right ascension of the spheroidal ascending node (RASAN, but better understood when shortened to spheroidal RAAN), and f is the spheroidal true anomaly. The notion of complete elements is associated with the angular variables, Ω', ω', and f (and combinations thereof), which are viewed as the composition of secular and periodic parts, expressed mathemat-

ically as

$$\Omega' = \Omega'_s + \Omega'_p \tag{4.3}$$

$$\omega' = \omega'_s + \omega'_p \tag{4.4}$$

$$f = M_s + f_p \tag{4.5}$$

The subscript "s" denotes a secular component of the angular variable and the subscript "p" a periodic component. The $'$ symbol serves to distinguish the Ω' and ω' elements from the Jacobi constants, i.e. $\beta_2 = \omega$ and $\beta_3 = \Omega$. In this way, the notation for the complete spheroidal RAAN is consistent with Vinti's notation [160]. If only the secular components of the elements are considered, then the equation for spheroidal true longitude is replaced with one for the secular part of the spheroidal mean longitude, which is determined as

$$\lambda_s = M_s + \omega'_s + K\Omega'_s \tag{4.6}$$

where M is the spheroidal mean anomaly. Usually, I is used to denote the retrograde factor, but here I denotes the spheroidal inclination. Thus, K is used instead to refer to the retrograde factor, defined as follows:

$$K = \begin{cases} +1 & \text{direct spheroidal equinoctial elements} \\ -1 & \text{retrograde spheroidal equinoctial elements} \end{cases} \tag{4.7}$$

There is one more important longitudinal angle to define, specifically the spheroidal eccentric longitude, F. It should be clear from context whether F refers to the spheroidal eccentric longitude or to the $F(\rho)$ quartic. The spheroidal eccentric longitude has the following relationship to the spheroidal eccentric anomaly, E:

$$F = E + \omega' + K\Omega' \tag{4.8}$$

127

4.2 Anomalistic and Draconitic Motion

Vinti theory distinctly prescribes the propagation of the anomalistic and draconitic components of the motion. Two of the oblate spheroidal coordinates are tied to these motions by way of the spheroidal conic equation and the spheroidal latitude equation, respectively.

4.2.1 The Spheroidal Conic Equation

The familiar conic equation prescribes a conic section in spherical geometry. It can be thought of as governing the radial distance r of a spacecraft or the point where a spacecraft is tangent to a sphere of that radius. When described in oblate spheroidal geometry, the spheroidal conic equation governs the point where a spacecraft is tangent to a spheroid of semiminor axis ρ. The spheroidal conic equation is expressed as

$$\rho = \frac{p}{1 + e\cos f} \tag{4.9}$$

and is identical in form to the spherical conic equation. As such, the equation generalizes in the familiar way when written in terms of spheroidal equinoctial elements:

$$\rho = \frac{p}{1 + q_1 \cos L + q_2 \sin L} \tag{4.10}$$

4.2.2 The Spheroidal Latitude Equation

The spheroidal latitude equation is the analogue of the familiar spherical trigonometry equation that relates latitude to orbital elements. The spher-

ical form is given by

$$\sin \theta = \sin I_K \sin(\omega_K + f_K) \tag{4.11}$$

In oblate spheroidal geometry, the equation becomes

$$\eta = \sin I \sin (\omega' + f) = \sin I \sin \psi \tag{4.12}$$

when $J_3 = 0$ or

$$\eta = P + Q \sin (\omega' + f) = P + Q \sin \psi \tag{4.13}$$

when $J_3 \neq 0$. Note that ψ is the argument of spheroidal latitude. Some of the notation is very different between the solutions of the 1961 and 1966 Vinti potentials. The notation of the $J_3 \neq 0$ theory is used to facilitate referencing of recent work [17]. The $J_3 = 0$ assumption is then applied, and simplifications follow, such as $P = 0$ and $Q = \sin I$. With these assumptions, the form of the spheroidal latitude equation in spheroidal equinoctial elements becomes

$$\eta = (p_1 \sin L - K p_2 \cos L)(1 + K \cos I) \tag{4.14}$$

if the inclination associated with Q is tied to the one in Eq. (4.2). Using the identity $2 \cos^2 I/2 = 1 + \cos I$, Eq. (4.14) can be expressed strictly in equinoctial elements as

$$\eta = \frac{2}{1 + p_1^2 + p_2^2} (p_1 \sin L - K p_2 \cos L) \tag{4.15}$$

but Eq. (4.14) is useful for converting between coordinates.

129

4.3 ECI Coordinates in Terms of Spheroidal Equinoctial Elements

The ECI coordinates are expressed in terms of oblate spheroidal elements as

$$X = \sqrt{\rho^2 + c^2}\,(\cos\Omega'\cos\psi - \sin\Omega'\cos I\sin\psi) \tag{4.16}$$

$$Y = \sqrt{\rho^2 + c^2}\,(\sin\Omega'\cos\psi + \cos\Omega'\cos I\sin\psi) \tag{4.17}$$

$$Z = \rho\eta \tag{4.18}$$

After extensive manipulation of Eqs. (4.16–4.18), these equations can be written in terms of oblate spheroidal equinoctial elements as

$$X = \frac{\sqrt{\rho^2 + c^2}}{1 + p_1^2 + p_2^2}\left[\left(1 + p_1^2 - p_2^2\right)\cos L + 2Kp_1p_2\sin L\right] \tag{4.19}$$

$$Y = \frac{\sqrt{\rho^2 + c^2}}{1 + p_1^2 + p_2^2}\left[2p_1p_2\cos L + \left(1 - p_1^2 + p_2^2\right)K\sin L\right] \tag{4.20}$$

$$Z = \frac{2\rho}{1 + p_1^2 + p_2^2}\left(-Kp_2\cos L + p_1\sin L\right) \tag{4.21}$$

Equations (4.19–4.21) can be arranged into matrix form as

$$
\begin{bmatrix} X \\ Y \\ Z \end{bmatrix} = \frac{1}{1 + p_1^2 + p_2^2} \times
$$
$$
\begin{bmatrix} \sqrt{\rho^2 + c^2}\,(1 + p_1^2 - p_2^2) & \sqrt{\rho^2 + c^2}\,2Kp_1p_2 \\ \sqrt{\rho^2 + c^2}\,2p_1p_2 & \sqrt{\rho^2 + c^2}\,(1 - p_1^2 + p_2^2)\,K \\ -2K\rho p_2 & 2\rho p_1 \end{bmatrix}
\begin{bmatrix} \cos L \\ \sin L \end{bmatrix} \tag{4.22}
$$

but they can also be arranged into the form

$$
\begin{bmatrix} X' \\ Y' \\ Z' \end{bmatrix} = \frac{1}{1 + p_1^2 + p_2^2} \underbrace{\begin{bmatrix} 1 + p_1^2 - p_2^2 & 2Kp_1p_2 \\ 2p_1p_2 & (1 - p_1^2 + p_2^2)\,K \\ -2Kp_2 & 2p_1 \end{bmatrix}}_{\mathbf{f} \qquad\qquad \mathbf{g}}
\begin{bmatrix} \cos L \\ \sin L \end{bmatrix} \tag{4.23}
$$

where

$$X' = \frac{X}{\sqrt{\rho^2 + c^2}} \tag{4.24}$$

$$Y' = \frac{Y}{\sqrt{\rho^2 + c^2}} \tag{4.25}$$

$$Z' = \frac{Z}{\rho} \tag{4.26}$$

Two columns in Eq. (4.23) are identified as very similar to the familiar $\mathbf{f}_K$ and $\mathbf{g}_K$ vectors that define the spherical equinoctial reference frame and are therefore labeled accordingly. It is emphasized that their directions generally are not identical to their spherical counterparts because the spheroidal p_1 and p_2 are generally different in value from the spherical ones. Similarly, the $\mathbf{w}$ vector, which is aligned with the angular momentum in the Kepler problem, has a slightly different direction in the Vinti problem. For completeness, the equation for $\mathbf{w}$ is determined as

$$\mathbf{w} = \begin{bmatrix} 2p_2 \\ -2p_1 \\ \left(1 - p_1^2 - p_2^2\right) K \end{bmatrix} \tag{4.27}$$

The $\mathbf{f}$, $\mathbf{g}$, and $\mathbf{w}$ vectors become unit vectors when divided by the factor $1 + p_1^2 + p_2^2$. The direct equinoctial reference frames associated with spherical and spheroidal geometry are respectively illustrated side by side in Figs. 4.1(a) and 4.1(b). Notice that the equinoctial frames result after a particular 3-1-3 sequence of rotations from the ECI frame. Specifically, the first rotation is a counterclockwise rotation by Ω about the $\hat{\mathbf{Z}}$ axis, the second is a counterclock-wise rotation by I about the node vector, and the third is a clockwise rotation by Ω about the $\hat{\mathbf{w}}$ vector or axis. In contrast, the analogous rotations to the
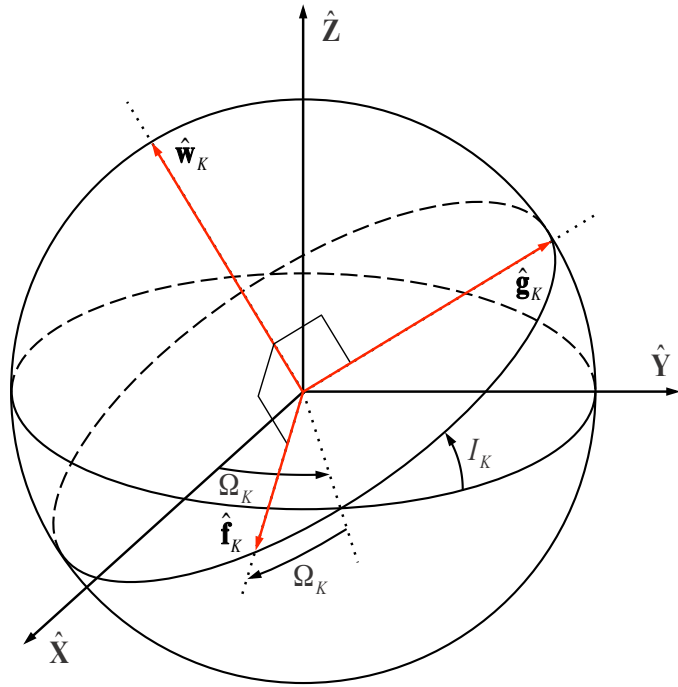
(a) Spherical geometry (Keplerian elements)
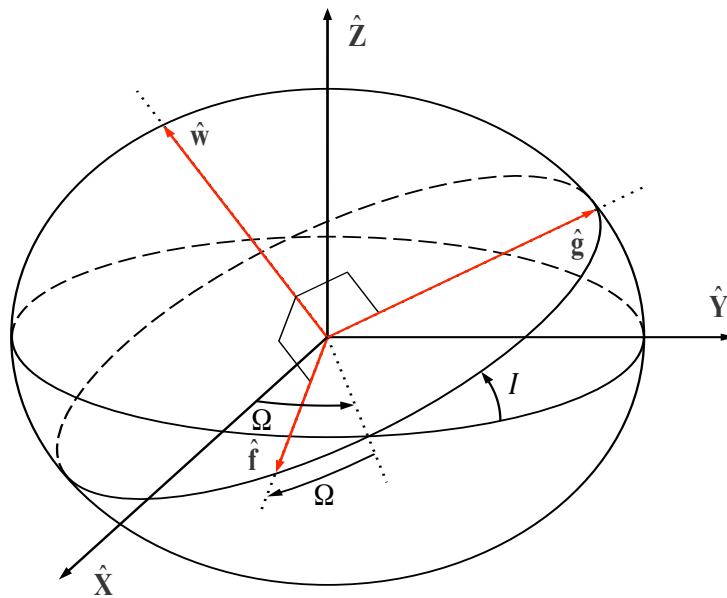
(b) Oblate spheroidal geometry (non-Keplerian elements)

Figure 4.1: Direct equinoctial reference frames for different geometries.

perifocal frame differ in the third rotation, which instead involves a counter-clockwise rotation by ω about the $\hat{\mathbf{w}}$ axis. Notice also that the left-hand side in Eq. (4.23) now contains *scaled* inertial position coordinates. This detail is crucial for reasons explored in the next paragraph.

Before moving on, let us spend some time on Eq. (4.22). In the limit as $c \rightarrow 0$, several things happen: 1) the Vinti problem "approaches" or reduces to the Kepler problem; 2) the oblate spheroidal coordinates reduce to spherical coordinates, i.e. $\rho \rightarrow r$. As evidenced by an earlier discussion, it is not a coincidence that these changes happen in concert. The quantity r can be factored out in this limit, and Eq. (4.22) becomes

$$\begin{bmatrix} X \\ Y \\ Z \end{bmatrix} = \frac{1}{1 + p_1^2 + p_2^2} \begin{bmatrix} 1 + p_1^2 - p_2^2 & 2Kp_1p_2 \\ 2p_1p_2 & (1 - p_1^2 + p_2^2)K \\ -2Kp_2 & 2p_1 \end{bmatrix} \begin{bmatrix} r\cos L \\ r\sin L \end{bmatrix} \quad (4.28)$$

where L and the p_j are now spherical equinoctial elements, and it is clear that Eq. (4.22) is a generalization of Eq. (4.28) to an oblate spheroidal geometry. The reduction of symmetry is manifested as an asymmetric scaling by the factor $\sqrt{\rho^2 + c^2}$ in the equatorial plane and the factor ρ along the polar axis. The scaling agrees with intuition. For example, consider that $\sqrt{\rho^2 + c^2} > r > \rho$, so that relative to a sphere of radius r, the coordinates are stretched in the equatorial plane and contracted along the polar axis.

4.4 The Spheroidal Eccentricity and Ascending Node Vectors

The notion of an oblate spheroidal equinoctial reference frame has now been established, but there are still certain physical quantities that lack a clear

equivalent in the Vinti problem. For example, the eccentricity vector is a well defined constant in the Kepler problem easily computed from inertial position and velocity vectors. While it does not point in a constant direction in the Vinti problem, the spheroidal eccentricity vector is still defined mathematically. However, so far, the computation of the vector seems inaccessible. Its magnitude is easily obtained from factoring the $F(\rho)$ quartic, but its direction is not obvious. There is a similar issue understanding the direction of the spheroidal ascending node vector. To answer these questions, equations are derived connecting the components of these vectors to the initial conditions in ECI coordinates using only the true longitude as a fast variable.

It is important to note that angles associated with the eccentric anomaly will not always be well defined over the range of orbit inclinations and eccentricities (the variable itself changes definition to parabolic or hyperbolic eccentric anomaly depending on the respective orbit type). The angles associated with the true anomaly, in contrast, will always be defined and their computation will be free of singularities. The same holds for time derivatives. These facts were also discussed in Section 2.3.3 with derivations of relevant equations for the classical spheroidal elements. To access the spheroidal eccentricity vector, it must be connected to the spheroidal true longitude since that is calculable directly from initial conditions, and the expressions for true anomaly enable this connection.

4.4.1 Computing the Spheroidal Eccentricity Vector When True Longitude Is Known

In spherical elements, the eccentricity vector is calculable from a simple vector equation. A similar statement does not hold in the Vinti problem, and an alternative approach must be found to obtain the spheroidal eccentricity vector. Recall Eqs. (2.36) and (2.35) for $e \cos f$ and $e \sin f$. Using the definitions in Eq. (4.2), these quantities can be put in terms of true longitude by applying the angle sum and difference identities of trigonometry:

$$e \cos f = e \cos \left(L - \omega' - K\Omega' \right)$$

$$= e \cos L \cos \left(\omega' + K\Omega' \right) + e \sin L \sin \left(\omega' + K\Omega' \right)$$

$$e \sin f = e \sin \left(L - \omega' - K\Omega' \right)$$

$$= e \sin L \cos \left(\omega' + K\Omega' \right) - e \cos L \sin \left(\omega' + K\Omega' \right)$$

Applying the definitions of q_j leads to the relations:

$$e \cos f = q_1 \cos L + q_2 \sin L \tag{4.29}$$

$$e \sin f = q_1 \sin L - q_2 \cos L \tag{4.30}$$

and substituting into the left-hand side of Eqs. (4.29) and (4.30) and rearranging gives

$$q_1 \cos L + q_2 \sin L = \frac{p}{\rho} - 1 \tag{4.31}$$

$$q_1 \sin L - q_2 \cos L = \frac{\sqrt{F} p^{1/2}}{\rho \left[\mu \gamma_1 (\rho^2 - 2b_1 \rho + b_2^2) \right]^{1/2}} \tag{4.32}$$

Equations (4.31) and (4.32) can be combined into a compact matrix form as

$$
\begin{bmatrix} \cos L & \sin L \\ \sin L & -\cos L \end{bmatrix} \begin{bmatrix} q_1 \\ q_2 \end{bmatrix} = \begin{bmatrix} \dfrac{p}{\rho} - 1 \\[2ex] \dfrac{\sqrt{F} p^{1/2}}{\rho \left(\mu\gamma_1\right)^{1/2} \left(\rho^2 - 2b_1\rho + b_2^2\right)^{1/2}} \end{bmatrix}
$$

If L is known, then q_1 and q_2 can be determined as

$$
\begin{bmatrix} q_1 \\ q_2 \end{bmatrix} = \begin{bmatrix} \cos L & \sin L \\ \sin L & -\cos L \end{bmatrix} \begin{bmatrix} \dfrac{p}{\rho} - 1 \\[2ex] \dfrac{\sqrt{F} p^{1/2}}{\rho \left(\mu\gamma_1\right)^{1/2} \left(\rho^2 - 2b_1\rho + b_2^2\right)^{1/2}} \end{bmatrix} \tag{4.33}
$$

Equation (4.33) is exact and accurately gives q_1 and q_2 for any orbit. The implication is that the spheroidal eccentricity vector is now mathematically well defined because its components in the spheroidal equinoctial frame are calculable.

4.4.2 Computing the Spheroidal Ascending Node Vector When True Longitude Is Known

A similar procedure is necessary for the spheroidal ascending node vector. When obtaining spherical equinoctial elements from ECI coordinates, the angular momentum vector is one of the three vectors that define the equinoctial reference frame. Its normalized components, $\mathbf{w}_K = (w_{K_x}, w_{K_y}, w_{K_z})$, readily define the components of the spherical ascending node vector as

$$
p_{1_K} = -\frac{w_{K_y}}{1 + K w_{K_z}} \tag{4.34}
$$

$$
p_{2_K} = +\frac{w_{K_x}}{1 + K w_{K_z}} \tag{4.35}
$$

However, in the Vinti problem, the angular momentum vector does not define the spheroidal equinoctial reference frame, and an alternative approach is nec-

essary for computing p_1 and p_2, the components of the spheroidal ascending node vector.

This time the focus is on $Q\cos\psi$ and $Q\sin\psi$, and the first step is to express these quantities in terms of initial conditions. A formula for $Q\sin\psi$ is already available from the spheroidal latitude equation. Rearranging Eq. (4.13), which is for the general case when $J_3 \neq 0$, the quantity $Q\sin\psi$ is simply given by

$$Q\sin\psi = \eta - P \tag{4.36}$$

The time derivative of Eq. (4.36) gives

$$Q\dot{\psi}\cos\psi = \dot{\eta} \tag{4.37}$$

where

$$\dot{\eta} = \frac{\sqrt{G}}{\rho^2 + c^2\eta^2} \tag{4.38}$$

and

$$\dot{\psi} = \frac{\alpha_2\left(1 + C_1\eta - C_2\eta^2\right)^{1/2}}{u^{1/2}\left(\rho^2 + c^2\eta^2\right)} \tag{4.39}$$

as given in the literature [50, 160]. Substituting Eqs. (4.38) and (4.39) into Eq. (4.37) and rearranging gives

$$Q\cos\psi = \frac{\sqrt{G}u^{1/2}}{\alpha_2\left(1 + C_1\eta - C_2\eta^2\right)^{1/2}} \tag{4.40}$$

Now, assume $J_3 = 0$ so that $P = C_1 = 0$, consistent with the 1959 Vinti potential. Again using the definitions in Eq. (4.2), the quantities $Q\cos\psi$ and

$Q \sin \psi$ can be put in terms of true longitude by applying the same trigonometric identities as before:

$$Q \cos \psi = Q \cos (L - K\Omega')$$

$$= Q \cos L \cos (K\Omega') + Q \sin L \sin (K\Omega')$$

$$= Q \cos L \cos \Omega' + KQ \sin L \sin \Omega' \tag{4.41}$$

$$Q \sin \psi = Q \sin (L - K\Omega')$$

$$= Q \sin L \cos (K\Omega') - Q \cos L \sin (K\Omega')$$

$$= Q \sin L \cos \Omega' - KQ \cos L \sin \Omega' \tag{4.42}$$

Now, recall that $Q = \sin I$. To apply the definitions of p_j in Eq. (4.2), one additional step is required that makes use of the following identities:

$$\tan \left(\frac{I}{2}\right) = \frac{\sin I}{1 + \cos I} \tag{4.43}$$

$$\cot \left(\frac{I}{2}\right) = \frac{\sin I}{1 - \cos I} \tag{4.44}$$

which can be combined into one equation using the retrograde factor K:

$$\left[\tan \left(\frac{I}{2}\right)\right]^{K} = \frac{\sin I}{1 + K \cos I} \tag{4.45}$$

After dividing Eqs. (4.41) and (4.42) by $1 + K \cos I$, their right-hand sides can be simplified to the following forms by applying Eq. (4.45) and the definitions of p_1 and p_2 in Eq. (4.2):

$$\frac{Q \cos \psi}{1 + K \cos I} = p_1 \cos L + Kp_2 \sin L \tag{4.46}$$

$$\frac{Q \sin \psi}{1 + K \cos I} = p_1 \sin L - Kp_2 \cos L \tag{4.47}$$

Using Eqs. (4.40) and (4.36) to substitute respectively into the left-hand side of Eqs. (4.46) and (4.47) for $Q \cos \psi$ and $Q \sin \psi$ gives

$$p_1 \cos L + K p_2 \sin L = \frac{\sqrt{G} u^{1/2}}{\alpha_2 \left(1 - C_2 \eta^2\right)^{1/2} \left(1 + K \cos I\right)} \tag{4.48}$$

$$p_1 \sin L - K p_2 \cos L = \frac{\eta}{1 + K \cos I} \tag{4.49}$$

It is emphasized that the assumption $J_3 = 0$ was imposed to arrive at these equations. While not useful for obtaining p_1 and p_2 from ECI coordinates, it is still interesting to arrange Eqs. (4.48) and (4.49) in matrix form as

$$\begin{bmatrix} \cos L & K \sin L \\ \sin L & -K \cos L \end{bmatrix} \begin{bmatrix} p_1 \\ p_2 \end{bmatrix} = \begin{bmatrix} \dfrac{\sqrt{G} u^{1/2}}{\alpha_2 \left(1 - C_2 \eta^2\right)^{1/2} \left(1 + K \cos I\right)} \\ \dfrac{\eta}{1 + K \cos I} \end{bmatrix}$$

Then, as in the derivation of Eq. (4.33), if L is known, p_1 and p_2 can be determined as

$$\begin{bmatrix} p_1 \\ p_2 \end{bmatrix} = \begin{bmatrix} \cos L & \sin L \\ K \sin L & -K \cos L \end{bmatrix}$$
$$\times \begin{bmatrix} \dfrac{\sqrt{G} u^{1/2}}{\alpha_2 \left(1 - C_2 \eta^2\right)^{1/2} \left(1 + K \cos I\right)} \\ \dfrac{\eta}{1 + K \cos I} \end{bmatrix} \tag{4.50}$$

Solving these equations for p_1 and p_2 implies that L is known. However, L is not known before the determination of p_1 and p_2. The following explains how to obtain p_1 and p_2 without knowledge of L, and Eqs. (4.48) and (4.49) are essential to this process.

4.4.3 Computing the Spheroidal Ascending Node Vector When True Longitude Is Unknown

The goal in this section is to derive expressions for p_1 and p_2 that depend directly on initial conditions and not on L. The derivation begins with the equations for X and Y given by Eqs. (4.16) and (4.17):

$$X = \sqrt{\rho^2 + c^2}\left(\cos\Omega'\cos\psi - \sin\Omega'\cos I\sin\psi\right)$$

$$Y = \sqrt{\rho^2 + c^2}\left(\sin\Omega'\cos\psi + \cos\Omega'\cos I\sin\psi\right)$$

To obtain the first relationship, multiply the X equation by $\cos\Omega'$ and the Y equation by $\sin\Omega'$, which gives

$$X\cos\Omega' = \sqrt{\rho^2 + c^2}\left(\cos^2\Omega'\cos\psi - \cos\Omega'\sin\Omega'\cos I\sin\psi\right) \qquad (4.51)$$

$$Y\sin\Omega' = \sqrt{\rho^2 + c^2}\left(\sin^2\Omega'\cos\psi + \cos\Omega'\sin\Omega'\cos I\sin\psi\right) \qquad (4.52)$$

Adding Eqs. (4.51) and (4.52) leads to

$$X\cos\Omega' + Y\sin\Omega' = \sqrt{\rho^2 + c^2}\left(\cos^2\Omega' + \sin^2\Omega'\right)\cos\psi$$

$$= \sqrt{\rho^2 + c^2}\cos\psi \qquad (4.53)$$

where the second term in each equation cancels out. Equation (4.53) can be written in terms of p_1 and p_2 through several steps. First, note $\cos\psi = \cos(L - K\Omega')$ and employ the usual identities:

$$X\cos\Omega' + Y\sin\Omega' = \sqrt{\rho^2 + c^2}\cos\left(L - K\Omega'\right)$$

$$= \sqrt{\rho^2 + c^2}\left(\cos L\cos\Omega' + K\sin L\sin\Omega'\right) \qquad (4.54)$$

Then multiply both sides of Eq. (4.54) by $[\tan(I/2)]^K$:

$$\left[\tan\left(\frac{I}{2}\right)\right]^K \cdot \left[\frac{X\cos\Omega' + Y\sin\Omega'}{\sqrt{\rho^2 + c^2}} = \left(\cos L\cos\Omega' + K\sin L\sin\Omega'\right)\right] \qquad (4.55)$$

140

From the definition of p_1 and p_2 in Eq. (4.2), Eq. (4.55) above simplifies to

$$X p_1 + Y p_2 = \sqrt{\rho^2 + c^2} \left(p_1 \cos L + K p_2 \sin L \right) \tag{4.56}$$

Notice that the right-hand side contains the term found in Eq. (4.48).

A similar process is performed to obtain a relationship connecting X and Y to Eq. (4.49). To obtain this second relationship, multiply the X equation by $\sin \Omega'$ and the Y equation by $\cos \Omega'$, which gives

$$X \sin \Omega' = \sqrt{\rho^2 + c^2} \left(\cos \Omega' \sin \Omega' \cos \psi - \sin^2 \Omega' \cos I \sin \psi \right) \tag{4.57}$$

$$Y \cos \Omega' = \sqrt{\rho^2 + c^2} \left(\cos \Omega' \sin \Omega' \cos \psi + \cos^2 \Omega' \cos I \sin \psi \right) \tag{4.58}$$

Subtracting Eq. (4.57) from Eq. (4.58) leads to

$$Y \cos \Omega' - X \sin \Omega' = \sqrt{\rho^2 + c^2} \left(\cos^2 \Omega' + \sin^2 \Omega' \right) \cos I \sin \psi$$

$$= \sqrt{\rho^2 + c^2} \cos I \sin \psi \tag{4.59}$$

where the second term in each equation cancels out. Equation (4.59) can then be written in terms of p_1 and p_2 through several steps, similar to the steps just carried out to arrive at Eq. (4.56). First, note that $\sin \psi = \sin(L - K\Omega')$ and employ the usual identities:

$$Y \cos \Omega' - X \sin \Omega' = \sqrt{\rho^2 + c^2} \cos I \sin \left(L - K\Omega' \right)$$

$$= \sqrt{\rho^2 + c^2} \cos I \left(\sin L \cos \Omega' - K \cos L \sin \Omega' \right) \tag{4.60}$$

Then multiply both sides of Eq. (4.60) by $[\tan(I/2)]^K$:

$$\left[\tan \left(\frac{I}{2} \right) \right]^K \cdot \left[\frac{Y \cos \Omega' - X \sin \Omega'}{\sqrt{\rho^2 + c^2}} \right.$$

$$\left. = \cos I \left(\sin L \cos \Omega' - K \cos L \sin \Omega' \right) \right] \tag{4.61}$$

From the definition of p_1 and p_2 in Eq. (4.2), Eq. (4.61) above simplifies to

$$Yp_1 - Xp_2 = \sqrt{\rho^2 + c^2}\,(p_1 \sin L - Kp_2 \cos L) \cos I \qquad (4.62)$$

Notice that the right-hand side contains the term found in Eq. (4.49).

Equations (4.56) and (4.62) are in a form in which it is easy to substitute Eqs. (4.48) and (4.49), respectively. Making these substitutions leads to two equations:

$$Xp_1 + Yp_2 = \sqrt{\rho^2 + c^2}\left[\frac{\sqrt{G}u^{1/2}}{\alpha_2\left(1 - C_2\eta^2\right)^{1/2}\left(1 + K \cos I\right)}\right] \qquad (4.63)$$

$$Yp_1 - Xp_2 = \sqrt{\rho^2 + c^2}\left(\frac{\eta \cos I}{1 + K \cos I}\right) \qquad (4.64)$$

In matrix form, Eqs. (4.63) and (4.64) become

$$\begin{bmatrix} X & Y \\ Y & -X \end{bmatrix} \begin{bmatrix} p_1 \\ p_2 \end{bmatrix} = \begin{bmatrix} \dfrac{\sqrt{\rho^2 + c^2}\sqrt{G}u^{1/2}}{\alpha_2\left(1 - C_2\eta^2\right)^{1/2}\left(1 + K \cos I\right)} \\[1.5em] \dfrac{\sqrt{\rho^2 + c^2}\,\eta \cos I}{1 + K \cos I} \end{bmatrix} \qquad (4.65)$$

Inverting the matrix equation gives

$$\begin{bmatrix} p_1 \\ p_2 \end{bmatrix} = \frac{1}{X^2 + Y^2}\begin{bmatrix} X & Y \\ Y & -X \end{bmatrix}\begin{bmatrix} \dfrac{\sqrt{\rho^2 + c^2}\sqrt{G}u^{1/2}}{\alpha_2\left(1 - C_2\eta^2\right)^{1/2}\left(1 + K \cos I\right)} \\[1.5em] \dfrac{\sqrt{\rho^2 + c^2}\,\eta \cos I}{1 + K \cos I} \end{bmatrix} \qquad (4.66)$$

which expresses p_1 and p_2 in terms of ECI coordinates instead of the true longitude L as in Eq. (4.50). The quantities in the column vector on the right-hand side are well defined for all orbits and can be obtained directly from ECI coordinates. Note that $K = \pm 1$. One obvious issue with Eq. (4.66) is the singularity associated with computing $0/0$ when the spacecraft is on a pole, and the next section discusses options for handling it.

4.4.4 Mitigating the Singularity Associated with a Spacecraft Located on a Pole

Finally, at the conclusion of the previous section, an equation defining the spheroidal ascending node vector in terms of ECI coordinates has been obtained. The only issue with Eq. (4.66) is the division by $X^2 + Y^2$, which goes to zero when the spacecraft is on a pole. This singularity is only an issue if converting from ECI coordinates to spheroidal equinoctial elements when the spacecraft is on a pole, which, as pointed out in Section 2.3.1, is a pathological case in practice because this conversion may only be done once for initialization. Nevertheless, if this situation is encountered, it should not present any real trouble, as there are two options that avoid the singularity.

One option for mitigating the singularity is to appeal to Keplerian definitions of orbital elements. The spacecraft can only be near a pole when the orbit is nearly polar. When the orbit is exactly polar, the spheroidal RAAN is identical to the spherical or Keplerian RAAN, and there is readily available an equation free of polar-orbit singularities for the Keplerian RAAN.

First, compute the angular momentum from

$$\mathbf{h} = \mathbf{r} \times \mathbf{v} \tag{4.67}$$

and obtain the unit vector as

$$\hat{\mathbf{w}}_K = \frac{\mathbf{h}}{|\mathbf{h}|} = \begin{bmatrix} w_{K_x} \\ w_{K_y} \\ w_{K_z} \end{bmatrix} \tag{4.68}$$

Then, the spherical ascending node vector is

$$\mathbf{n}_K = \begin{bmatrix} -w_{K_y} \\ w_{K_x} \\ 0 \end{bmatrix} \tag{4.69}$$

Finally, the Keplerian RAAN can be computed unambiguously for nearly or exactly polar orbits as

$$\Omega_K = \arctan\left(\frac{n_{K_y}}{n_{K_x}}\right) = \arctan\left(\frac{w_{K_x}}{-w_{K_y}}\right) \tag{4.70}$$

Note that `atan2` should be used in implementation to unambiguously compute the arctangent of Ω_K. The components of the spheroidal ascending node vector are then approximated well by using the definition of p_1 and p_2 with the spheroidal inclination and the spherical RAAN

$$p_1 = \left[\tan\left(\frac{I}{2}\right)\right]^K \cos\Omega_K \tag{4.71}$$

$$p_2 = \left[\tan\left(\frac{I}{2}\right)\right]^K \sin\Omega_K \tag{4.72}$$

These equations would only be used for nearly or exactly polar orbits, and in particular only when a spacecraft is sufficiently close to a pole and a conversion from ECI coordinates to spheroidal equinoctial elements is required. However, in practice, an actual implementation would require a weighting function in the vicinity of a pole. Due to this inconvenience, this approach is not very appealing except when the orbit is exactly polar.

A second and arguably much better option is to take the time derivative of Eq. (4.65). Beginning with the left-hand side,

$$\frac{d}{dt}(Xp_1 + Yp_2) = \dot{X}p_1 + X\dot{p}_1 + \dot{Y}p_2 + Y\dot{p}_2 \tag{4.73}$$

$$\frac{d}{dt}(Yp_1 - Xp_2) = \dot{Y}p_1 + Y\dot{p}_1 - \dot{X}p_2 - X\dot{p}_2 \tag{4.74}$$

144

Next, observe that the time derivatives of p_1 and p_2 are determined simply as

$$\dot{p}_1 = \left[\tan\left(\frac{I}{2}\right)\right]^K \left(-\dot{\Omega}'\sin\Omega'\right) = -p_2\dot{\Omega}' \tag{4.75}$$

$$\dot{p}_2 = \left[\tan\left(\frac{I}{2}\right)\right]^K \left(+\dot{\Omega}'\cos\Omega'\right) = +p_1\dot{\Omega}' \tag{4.76}$$

Substituting Eqs. (4.75) and (4.76) into the right-hand side of Eqs. (4.73) and (4.74) gives

$$\frac{d}{dt}\left(Xp_1 + Yp_2\right) = \dot{X}p_1 + X\left(-X\dot{\Omega}'\right) + \dot{Y}p_2 + Y\left(Y\dot{\Omega}'\right)$$

$$= \left(\dot{X} + Y\dot{\Omega}'\right)p_1 + \left(\dot{Y} - X\dot{\Omega}'\right)p_2 \tag{4.77}$$

$$\frac{d}{dt}\left(Yp_1 - Xp_2\right) = \dot{Y}p_1 + Y\left(-X\dot{\Omega}'\right) - \dot{X}p_2 - X\left(Y\dot{\Omega}'\right)$$

$$= \left(\dot{Y} - X\dot{\Omega}'\right)p_1 - \left(\dot{X} + Y\dot{\Omega}'\right)p_2 \tag{4.78}$$

Writing Eqs. (4.77) and (4.78) in matrix form gives the time derivative of the left-hand side of Eq. (4.65) as

$$\frac{d}{dt}\left\{\begin{bmatrix} X & Y \\ Y & -X \end{bmatrix}\begin{bmatrix} p_1 \\ p_2 \end{bmatrix}\right\} = \begin{bmatrix} \dot{X} + Y\dot{\Omega}' & \dot{Y} - X\dot{\Omega}' \\ \dot{Y} - X\dot{\Omega}' & -\dot{X} - Y\dot{\Omega}' \end{bmatrix}\begin{bmatrix} p_1 \\ p_2 \end{bmatrix} \tag{4.79}$$

Equating Eq. (4.79) with the time derivative of the right-hand side of Eq. (4.65) (equating the left- and right-hand sides) gives

$$\begin{bmatrix} \dot{X} + Y\dot{\Omega}' & \dot{Y} - X\dot{\Omega}' \\ \dot{Y} - X\dot{\Omega}' & -\dot{X} - Y\dot{\Omega}' \end{bmatrix}\begin{bmatrix} p_1 \\ p_2 \end{bmatrix} = \frac{1}{1 + K\cos I}$$

$$\times \begin{bmatrix} \left(\dfrac{\rho\dot{\rho}Q\cos\psi}{\sqrt{\rho^2 + c^2}} - \eta\dot{\psi}\sqrt{\rho^2 + c^2}\right) \\ \cos I\left(\dfrac{Z\dot{\rho}}{\sqrt{\rho^2 + c^2}} + \dot{\eta}\sqrt{\rho^2 + c^2}\right) \end{bmatrix} \tag{4.80}$$

As Eq. (4.80) will need to be inverted, note that its determinant is given by

$$\det = -\left(\dot{X} + Y\dot{\Omega}'\right)^2 - \left(\dot{Y} - X\dot{\Omega}'\right)^2 \tag{4.81}$$

Inverting Eq. (4.80) determines p_1 and p_2 as

$$
\begin{bmatrix} p_1 \\ p_2 \end{bmatrix} = \frac{1}{\left(\dot{X} + Y\dot{\Omega}' \right)^2 + \left(\dot{Y} - X\dot{\Omega}' \right)^2} \begin{bmatrix} \dot{X} + Y\dot{\Omega}' & \dot{Y} - X\dot{\Omega}' \\ \dot{Y} - X\dot{\Omega}' & -\dot{X} - Y\dot{\Omega}' \end{bmatrix}
$$
$$
\times \frac{1}{1 + K \cos I} \begin{bmatrix} \left(\dfrac{\rho\dot{\rho}Q \cos \psi}{\sqrt{\rho^2 + c^2}} - \eta\dot{\psi}\sqrt{\rho^2 + c^2} \right) \\ \cos I \left(\dfrac{Z\dot{\rho}}{\sqrt{\rho^2 + c^2}} + \dot{\eta}\sqrt{\rho^2 + c^2} \right) \end{bmatrix}
$$

(4.82)

This equation can lead to computations of $0/0$ if the spacecraft is located on the equator in an exactly polar orbit, but this equation was derived with the intent of applying it only when the spacecraft is near a pole, not near the equator. Therefore, the equation is valid in the region of interest.

There are several trade-offs to be aware of between the methods of determining p_1 and p_2 that are based on Vinti theory. Equation (4.66) is based on the inertial position vector and is exact inasmuch as the factoring of the quartics can be arbitrarily accurate. Equation (4.82) is based on the inertial position and velocity vectors, but while the equation is exact in form, its accuracy is actually limited by the accuracy of $\dot{\Omega}'$. Vinti carried the accuracy of $\dot{\Omega}'$ out to $O(J_2^3)$ in secular terms and $O(J_2^2)$ in periodic terms, but it can in theory be made arbitrarily accurate. As implemented here, the secular terms are accurate to $O(J_2^4)$. Note that $\dot{\Omega}'$ is determined to second order as [160]

$$
\dot{\Omega}' = -\frac{c^2\alpha_3}{(-2\alpha_1)^{1/2}} \left(A_3 + \sum_{k=1}^{4} k A_{3k} \cos kf \right) \dot{f}
$$
$$
+ \frac{\alpha_3 u^{1/2}}{\alpha_2} \left(B_3 + \sum_{k=1}^{2} k B_{3k} \genfrac{}{}{0pt}{}{\sin}{\cos} k\psi \right) \dot{\psi}
$$

(4.83)

and to third order as

$$\dot{\Omega}' = -\frac{c^2\alpha_3}{(-2\alpha_1)^{1/2}} \left(A_3 + \sum_{k=1}^{6} kA_{3k}\cos kf \right) \dot{f}$$
$$+ \frac{\alpha_3 u^{1/2}}{\alpha_2} \left(B_3 + \sum_{k=1}^{4} kB_{3k} \begin{smallmatrix} \sin \\ \cos \end{smallmatrix} k\psi \right) \dot{\psi} \qquad (4.84)$$

The first term in Eqs. (4.83) and (4.84) indicates that $\dot{\Omega}'$ becomes infinite as the orbit energy approaches zero, which violates the physics. For nearly parabolic, parabolic, or hyperbolic orbits, Eqs. (4.83) and (4.84) are invalid. Getchell's equations [62] readily handle orbits of arbitrary eccentricity and they can be used here to compute the first term of $\dot{\Omega}'$ to third order as

$$\dot{\Omega}' = -\frac{c^2\alpha_3}{(\mu p\gamma_1)^{1/2}} \left[W_2 + A_1 W_3 + \left(A_2 - c^2 \right) W_4 \right.$$
$$+ \left(A_3 - A_1 c^2 \right) W_5 + \left(A_4 - A_2 c^2 + c^4 \right) W_6 \right] \dot{f} \qquad (4.85)$$
$$+ \frac{\alpha_3 u^{1/2}}{\alpha_2} \left(B_3 + \sum_{k=1}^{4} kB_{3k} \begin{smallmatrix} \sin \\ \cos \end{smallmatrix} k\psi \right) \dot{\psi}$$

where $W = f$ in Getchell's notation and the W_j and A_j refer to different quantities from Vinti's notation. Note that Getchell's solution does not use Ω'. Equation (4.85) is new, obtained by combining part of the R_3 integral of Getchell's solution with the N_3 integral of Vinti's solution.

This approach to mitigating the singularity that invokes pieces of the analytical solution may seem like a lot of extra computational effort, but almost all of the quantities in Eqs. (4.83)–(4.85) would have to be computed anyway if the ultimate goal is analytical state propagation ($\dot{\rho}$, $\dot{\eta}$, $\dot{f}$, $\dot{\psi}$, A_3, B_3, A_{3k} for $k = 1, \ldots, 4$, and B_{32} for Eq. (4.83) and $\dot{\rho}$, $\dot{\eta}$, $\dot{f}$, $\dot{\psi}$, W_j for $j = 1, \ldots, 6$, B_3, A_j for $j = 1, \ldots, 4$, B_{32} for Eq. (4.85)). The exceptions, i.e. the steps

147

not required in the analytical solution, are the determination of $\dot{\rho}$ and $\dot{\eta}$, which are very simple to calculate [160, 62]. The appearance of f and ψ in Eqs. (4.83) and (4.85) implies that f and ψ must be calculable to compute $\dot{\Omega}'$, but this inference can be refuted. Careful examination of the periodic coefficients reveals that each A_{jk} contains a factor of e^k and each B_{jk} contains a factor of Q^k. Consequently, the requirement is not knowledge of f and ψ, but rather knowledge of $e \cos f$, $Q \sin \psi$, and $Q \cos \psi$, which are obtained from Eqs. (2.36), (4.36), and (4.40), respectively. Of course, when $J_3 = 0$, the equations simplify because $B_{jk} = 0$ for odd k, and $Q \cos \psi$ is not required in this case. Nevertheless, the three quantities can always be determined exactly from initial conditions, even if f and/or ψ are undefined.

Figure 4.2 assesses how the accuracy of the approximation that patches the poles affects the precision of the coordinate transformation near the poles. To carry out such an analysis, a successive forward-backward sequence of transformations is performed, from ECI coordinates to OS equinoctial elements and back to ECI coordinates. The initial ECI state is therefore known to double precision and perfect coordinate transformations would give an exactly zero error between the final and initial ECI states. Exactly zero error is possible and is represented in Fig. 4.2 as 17 correct digits (even though there are only 16). Otherwise, the number of correct digits plotted corresponds to the true number of correct digits. If the digits of a quantity are correct to 5 digits and the 6th digit rounds to the correct digit, then the number of preserved digits is considered to be 6 and not 5. The co-latitude is plotted in degrees on the horizontal axis using a log scale, while the number of preserved digits is

148
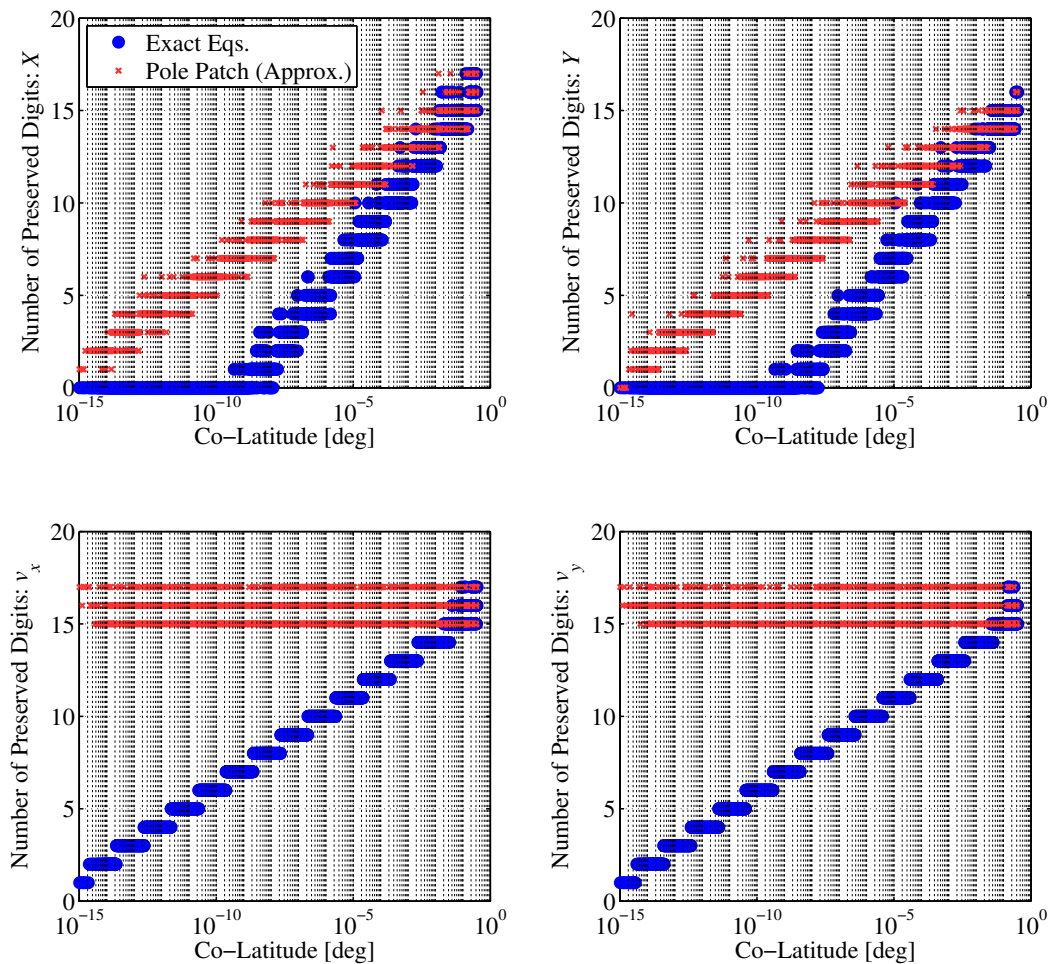
Figure 4.2: The second-order pole patch for an Earth application effectively removes any precision loss near the poles due to singularities, supported by recording the number of digits preserved near the poles for each of the four ECI coordinates affected by the singularity on the poles: X, Y, v_x, and v_y.

plotted on the vertical axis. The precision of the exact equations, which are singular on the poles, is shown in blue filled circles and the precision using the second-order approximating pole patch is shown in red x's. As the Z direction is agnostic to this singularity issue, only the other four ECI states, X, Y, v_x, and v_y, are analyzed.

Notice that, due to the singularity, the precision of the exact equations in X and Y reaches zero for co-latitudes as large as 10^{-8} degrees for an Earth application. The precision appears to tend to zero in X and Y for the pole patch as well, albeit at a much slower rate that diverges from the exact case around co-latitudes of 10^{-2} degrees, but this trend is somewhat misleading. As far as doing what it is designed to do (mitigating singularities on the poles), the pole patch is in fact retaining double precision for essentially the entire range of co-latitudes, which is clearly observable in the v_x and v_y plots. Recall that these trends in Fig. 4.2 result when applying the second-order patch at the Earth. The diminishing of precision in X and Y for the pole patch is actually an artifact of the equinoctial elements themselves. Consider that the final equation (given later as Eq. (4.108)) that transforms to X and Y coordinates involves a subtraction of nearly equal numbers when applied near a pole and precision is preserved up to this point. Essentially the same equation (see Eq. (B.33) in Appendix B.2.2) is used for the spherical equinoctial elements, which means that the same trend exists in the spherical case, where precision is lost on the poles, reaching 1 correct digit for co-latitudes around 10^{-15} degrees. In this sense, the precision of the coordinate transformations for the OS equinoctial elements is shown to be, at best, as high as that of the

150

analogous spherical coordinate transformations. Note that even though the equations that transform to v_x and v_y use the corrupted X and Y values, the precision in the velocities is still around 16 digits near the poles.

In general, the Keplerian definition of RAAN is never required, but in some circumstances, it may be preferable to use it. In exactly polar orbits, computing the spherical RAAN certainly consists of fewer computations and is greatly simplified relative to the equations of Vinti theory. For this reason, a programmer may wish to simply compute the spherical RAAN for an arbitrary polar orbit. However, away from the exactly polar case, the rate of divergence of the spherical RAAN from the spheroidal RAAN is not clear and certainly depends on the magnitude of J_2. For nearly polar orbits, one of the approximate approaches based on Vinti theory should be preferred. Alternatively, in practice, there is also the option of simply not performing the coordinate transformation in the vicinity of the poles, e.g. when the spacecraft's co-latitude is less than 10^{-2} degrees.

Note that a similar singularity has always existed in Vinti theory for scenarios in which a spacecraft flies over a pole, whether the quantity sought is right ascension, spheroidal RAAN, or the spheroidal node vector components p_1 and p_2. Using right ascension is arguably the worst option because there is no recourse to Keplerian elements to mitigate the singularity. Using spheroidal RAAN is an improvement because one can appeal to the Keplerian RAAN near the singularity. Similarly, the use of spheroidal equinoctial elements allows for a simple adoption of Keplerian RAAN if necessary, but the new elements also completely mitigate the singularity, which has until now never been resolved.

The use of spheroidal equinoctial elements marks a major improvement in handling a singularity that has persisted in Vinti theory for decades.

4.5 Computing True Longitude from ECI Coordinates When the Spheroidal Ascending Node Vector Is Known

The only remaining question regarding how to obtain the spheroidal equinoctial elements from ECI coordinates is how to determine the true longitude. Recall Eq. (4.23) derived in Section 4.3 that determines the scaled position vector in terms of the true longitude and the spheroidal ascending node vector as

$$
\begin{bmatrix} X' \\ Y' \\ Z' \end{bmatrix} = \frac{1}{1 + p_1^2 + p_2^2} \underbrace{\begin{bmatrix} 1 + p_1^2 - p_2^2 & 2K p_1 p_2 \\ 2 p_1 p_2 & \left(1 - p_1^2 + p_2^2\right) K \\ -2K p_2 & 2 p_1 \end{bmatrix}}_{\mathbf{f} \qquad \mathbf{g}} \begin{bmatrix} \cos L \\ \sin L \end{bmatrix}
$$

The unit vectors $\hat{\mathbf{f}}$, $\hat{\mathbf{g}}$, and $\hat{\mathbf{w}}$ associated with $\mathbf{f}$, $\mathbf{g}$, and $\mathbf{w}$ are defined as

$$
\hat{\mathbf{f}} = \frac{\mathbf{f}}{1 + p_1^2 + p_2^2} \tag{4.86}
$$

$$
\hat{\mathbf{g}} = \frac{\mathbf{g}}{1 + p_1^2 + p_2^2} \tag{4.87}
$$

$$
\hat{\mathbf{w}} = \frac{\mathbf{w}}{1 + p_1^2 + p_2^2} \tag{4.88}
$$

and so the equation can be written alternatively as

$$
\mathbf{r}' = \begin{bmatrix} \hat{\mathbf{f}} & \hat{\mathbf{g}} \end{bmatrix} \begin{bmatrix} \cos L \\ \sin L \end{bmatrix}
$$

or

$$
\mathbf{r}' = \begin{bmatrix} \hat{\mathbf{f}} & \hat{\mathbf{g}} & \hat{\mathbf{w}} \end{bmatrix} \begin{bmatrix} \cos L \\ \sin L \\ 0 \end{bmatrix} \tag{4.89}
$$

152

where

$$\mathbf{r}' \equiv \begin{bmatrix} X' \\ Y' \\ Z' \end{bmatrix} \tag{4.90}$$

It follows that

$$\cos L = \mathbf{r}' \cdot \hat{\mathbf{f}} \tag{4.91}$$

$$\sin L = \mathbf{r}' \cdot \hat{\mathbf{g}} \tag{4.92}$$

because inverting Eq. (4.89) gives

$$\begin{bmatrix} \hat{\mathbf{f}} & \hat{\mathbf{g}} & \hat{\mathbf{w}} \end{bmatrix}^{-1} \mathbf{r}' = \begin{bmatrix} \hat{\mathbf{f}} & \hat{\mathbf{g}} & \hat{\mathbf{w}} \end{bmatrix}^{\top} \mathbf{r}' = \begin{bmatrix} \cos L \\ \sin L \\ 0 \end{bmatrix}$$

Finally, an unambiguous equation for L is available after dividing Eq. (4.92) by Eq. (4.91) and taking the arctangent, so that L is determined as

$$L = \arctan\left(\frac{\sin L}{\cos L}\right) = \arctan\left(\frac{\mathbf{r}' \cdot \hat{\mathbf{g}}}{\mathbf{r}' \cdot \hat{\mathbf{f}}}\right) \tag{4.93}$$

Note that `atan2` should be used in implementation to unambiguously compute the arctangent of L. Its range should be shifted to $0 \leq L < 2\pi$ for an elliptical orbit.

4.6 Computing ECI Coordinates When Equinoctial Elements Are Known

Up to this point, most of the discussion has been in the spirit of how to convert ECI coordinates to spheroidal equinoctial elements, but the inverse transformation is also required. With a few exceptions, most of the required equations have already been stated or derived, some in other chapters. The

exceptions will be discussed in this section, covering an exact equation for the spheroidal RAAN, the time derivatives of the spheroidal equinoctial reference frame basis vectors, and the final transformation to ECI coordinates. The summary in Section 4.8 ties the seemingly disparate equations together into a single algorithm for converting spheroidal equinoctial elements to ECI coordinates.

4.6.1 An Exact Equation for the Time Derivative of Spheroidal RAAN

An exact expression for $\dot{\Omega}'$ does not exist in the literature. Such an equation can be found by directly taking the time derivative of the third kinematic equation

$$\beta_3 = \phi + c^2\alpha_3 R_3 - \alpha_3 N_3 \tag{4.94}$$

where

$$R_3 = \int_{\rho_1}^{\rho} \pm \frac{1}{(\rho^2 + c^2)\sqrt{F}} d\rho \tag{4.95}$$

$$N_3 = \int_{0}^{\eta} \pm \frac{1}{(1 - \eta^2)\sqrt{G}} d\eta \tag{4.96}$$

and subtracting out the part that varies quickly when a spacecraft is near a pole. This fast part is contained in the N_3 integral, as evident by the division by zero in that scenario where $1 - \eta^2 \to 0$ in the denominator. The time derivative of Eq. (4.94) after re-arranging is

$$\dot{\phi} = -c^2\alpha_3\dot{R}_3 + \alpha_3\dot{N}_3 \tag{4.97}$$

Several substitutions later, an expression is obtained for $\dot{\Omega}'$ as

$$
\dot{\Omega}' = \alpha_3 \left[-\frac{c^2}{(\rho^2 + c^2)(\rho^2 + c^2\eta^2)} \right.
$$
$$
\left. + \frac{1}{(1 - \eta^2)(\rho^2 + c^2\eta^2)} - \frac{u^{1/2}\dot{\psi}}{\alpha_2(1 - \eta^2)(1 - C_2)^{1/2}} \right] \tag{4.98}
$$

Substituting for $\dot{\psi}$ and u into Eq. (4.98), $\dot{\Omega}'$ is determined from

$$
\dot{\Omega}' = \frac{1}{\rho^2 + c^2\eta^2} \left\{ -\frac{c^2\alpha_3}{\rho^2 + c^2} + \frac{\alpha_3}{1 - \eta^2} \left[1 - \frac{(1 - C_2\eta^2)^{1/2}}{(1 - C_2)^{1/2}} \right] \right\} \tag{4.99}
$$

as long as a spacecraft is not nearly on a pole ($\eta \neq 1$). On a pole, the expression

$$
\frac{\alpha_3}{1 - \eta^2} \left[1 - \frac{(1 - C_2\eta^2)^{1/2}}{(1 - C_2)^{1/2}} \right]
$$

evaluates to

$$
\frac{0}{0} \cdot [0]
$$

when it is known that $\dot{\Omega}' = 0$ for polar orbits. The approximations for $\dot{\Omega}'$ and corresponding discussion in Section 4.4.4 apply when a spacecraft is near a pole.

4.6.2 Time Derivatives of the Spheroidal Equinoctial Reference Frame Basis Vectors

Recall Eqs. (4.86) and (4.87) for the basis vectors $\hat{\mathbf{f}}$ and $\hat{\mathbf{g}}$ in terms of p_1 and p_2:

$$
\hat{\mathbf{f}} = \frac{1}{1 + p_1^2 + p_2^2} \begin{bmatrix} 1 + p_1^2 - p_2^2 \\ 2p_1 p_2 \\ -2Kp_2 \end{bmatrix}
$$

$$
\hat{\mathbf{g}} = \frac{1}{1 + p_1^2 + p_2^2} \begin{bmatrix} 2Kp_1 p_2 \\ (1 - p_1^2 + p_2^2) K \\ 2p_1 \end{bmatrix}
$$

Taking the derivative of $\hat{\mathbf{f}}$ and $\hat{\mathbf{g}}$ with respect to time gives

$$\dot{\hat{\mathbf{f}}} = \frac{2}{1 + p_1^2 + p_2^2} \begin{bmatrix} p_1\dot{p}_1 - p_2\dot{p}_2 \\ p_1\dot{p}_2 + p_2\dot{p}_1 \\ -K\dot{p}_2 \end{bmatrix} \tag{4.100}$$

$$\dot{\hat{\mathbf{g}}} = \frac{2}{1 + p_1^2 + p_2^2} \begin{bmatrix} (p_1\dot{p}_2 + p_2\dot{p}_1)\, K \\ (p_2\dot{p}_2 - p_1\dot{p}_1)\, K \\ \dot{p}_1 \end{bmatrix} \tag{4.101}$$

Recall from Eqs. (4.75) and (4.76) that $\dot{p}_1 = -p_2\dot{\Omega}'$ and $\dot{p}_2 = p_1\dot{\Omega}'$, so that substituting them into Eq. (4.100) and (4.101) gives the simplified form

$$\dot{\hat{\mathbf{f}}} = \frac{2\dot{\Omega}'}{1 + p_1^2 + p_2^2} \begin{bmatrix} -2p_1p_2 \\ p_1^2 - p_2^2 \\ -Kp_1 \end{bmatrix} \tag{4.102}$$

$$\dot{\hat{\mathbf{g}}} = \frac{2\dot{\Omega}'}{1 + p_1^2 + p_2^2} \begin{bmatrix} (p_1^2 - p_2^2)\, K \\ 2Kp_1p_2 \\ -p_2 \end{bmatrix} \tag{4.103}$$

The time derivatives of the basis vectors are functions only of the spheroidal ascending node vector and the time derivative of spheroidal RAAN, $\dot{\Omega}'$, which agrees with intuition.

4.6.3   ECI Coordinates

Expressions for X', Y', and Z' can be written in a compact form as

$$\mathbf{r}' = \cos L\, \hat{\mathbf{f}} + \sin L\, \hat{\mathbf{g}} \tag{4.104}$$

From here, a simple rearrangement of Eqs. (4.24–4.26) gives X, Y, and Z as

$$X = \sqrt{\rho^2 + c^2}\, X' \tag{4.105}$$

$$Y = \sqrt{\rho^2 + c^2}\, Y' \tag{4.106}$$

$$Z = \rho Z' \tag{4.107}$$

An alternative way to write these equations is to separate the determination of Z by obtaining its value without using the basis vectors as follows:

$$\mathbf{r}_{1:2} = \sqrt{\rho^2 + c^2} \left(\cos L \, \hat{\mathbf{f}}_{1:2} + \sin L \, \hat{\mathbf{g}}_{1:2} \right) \tag{4.108}$$

and Z from

$$Z = \rho \eta$$

Taking the derivative of X, Y, and Z with respect to time leads to the following equations for $\dot{X}$ and $\dot{Y}$

$$
\begin{aligned}
\dot{X} = {}& \frac{\rho \dot{\rho}}{\rho^2 + c^2} X + \frac{\sqrt{\rho^2 + c^2}}{1 + p_1^2 + p_2^2} \Big[-4 p_1 p_2 \dot{\Omega}' \cos L + 2 \left(p_1^2 - p_2^2 \right) K \dot{\Omega}' \sin L \\
& - \left(1 + p_1^2 - p_2^2 \right) \dot{L} \sin L + 2 K p_1 p_2 \dot{L} \cos L \Big]
\end{aligned}
\tag{4.109}
$$

$$
\begin{aligned}
\dot{Y} = {}& \frac{\rho \dot{\rho}}{\rho^2 + c^2} Y + \frac{\sqrt{\rho^2 + c^2}}{1 + p_1^2 + p_2^2} \Big[2 \left(p_1^2 - p_2^2 \right) \dot{\Omega}' \cos L + 4 K p_1 p_2 \dot{\Omega}' \sin L \\
& - 2 p_1 p_2 \dot{L} \sin L + \left(1 - p_1^2 + p_2^2 \right) K \dot{L} \cos L \Big]
\end{aligned}
\tag{4.110}
$$

and a simple equation for $\dot{Z}$:

$$\dot{Z} = \dot{\rho} \eta + \rho \dot{\eta} \tag{4.111}$$

These equations for $\dot{X}$ and $\dot{Y}$ are more compactly written as

$$
\begin{aligned}
\mathbf{v}_{1:2} = {}& \frac{\rho \dot{\rho}}{\rho^2 + c^2} \mathbf{r}_{1:2} + \sqrt{\rho^2 + c^2} \\
& \times \left[\cos L \, \dot{\hat{\mathbf{f}}}_{1:2} + \sin L \, \dot{\hat{\mathbf{g}}}_{1:2} + \dot{L} \left(-\sin L \, \hat{\mathbf{f}}_{1:2} + \cos L \, \hat{\mathbf{g}}_{1:2} \right) \right]
\end{aligned}
\tag{4.112}
$$

4.7 Summary: Converting Position and Velocity Vectors to Spheroidal Equinoctial Elements

The process of converting inertial position and velocity vectors to oblate spheroidal equinoctial orbital elements $\boldsymbol{\alpha} = \{ p, q_1, q_2, p_1, p_2, L \}$ is summarized

in the following algorithm:

1. Compute $c^2 = R_e^2 J_2$ and then ρ, η, $\sqrt{F}$, and $\sqrt{G}$ from

$$d = r^2 - c^2;$$

$$\rho = \left[\frac{1}{2}d + \frac{1}{2}\left(d^2 + 4c^2 Z^2\right)^{1/2} \right]^{1/2}; \quad \eta = \frac{Z}{\rho};$$

$$r\dot{r} = X\dot{X} + Y\dot{Y} + Z\dot{Z};$$

$$\sqrt{F} = \rho r\dot{r} + c^2 \eta \dot{Z}; \quad \sqrt{G} = -\eta r\dot{r} + \rho\dot{Z}$$

2. Compute α_1, α_2, α_3, and K from

$$\alpha_1 = \frac{1}{2}v^2 - \frac{\mu\rho}{\rho^2 + c^2\eta^2}$$

$$\alpha_3 = X\dot{Y} - Y\dot{X}$$

$$\alpha_2^2 = 2\mu\rho + 2\alpha_1\rho^2 + \frac{c^2\alpha_3^2 - F(\rho)}{\rho^2 + c^2}$$

$$K = \begin{cases} +1 & \alpha_3 \geq 0 \\ -1 & \alpha_3 < 0 \end{cases}$$

If the orbit is nearly or exactly equatorial (for example, $|\eta| < 0.1$), compute $\alpha_2^2 - \alpha_3^2$ from

$$\alpha_2^2 - \alpha_3^2 = -2\alpha_1 c^2 \eta^2 + \frac{\alpha_3^2 \eta^2 + G(\eta)}{1 - \eta^2}$$

instead of directly differencing the two quantities

3. Factor the $F(\rho)$ and $G(\eta)$ quartics numerically with $z_\delta = 0$ to obtain p, γ_1, e, I, C_2, and u using Getchell's method [62] or an eigenvalue approach [18], whichever is appropriate. Note that this step is also required anyway for state propagation.

4. If a spacecraft is not nearly on a pole (for example, $1 - |\eta| \geq 10^{-8}$), then compute p_1 and p_2 from

$$
\begin{bmatrix} p_1 \\ p_2 \end{bmatrix} = \frac{1}{X^2 + Y^2} \begin{bmatrix} X & Y \\ Y & -X \end{bmatrix} \begin{bmatrix} \dfrac{\sqrt{\rho^2 + c^2}\sqrt{G}u^{1/2}}{\alpha_2 \left(1 - C_2\eta^2\right)^{1/2}\left(1 + K\cos I\right)} \\ \dfrac{\sqrt{\rho^2 + c^2}\,\eta\cos I}{1 + K\cos I} \end{bmatrix}
$$

If a spacecraft is nearly or exactly on a pole (for example, $1 - |\eta| < 10^{-8}$), compute $\dot{\rho}$, $\dot{\eta}$, $\dot{f}$, $\dot{\psi}$, A_3, B_3, A_{3k} for $k = 1, \ldots, 4$, B_{32}, and $\dot{\Omega}'$ first (see Eq. (4.83) or Eq. (4.85)), and then compute p_1 and p_2 from

$$
\begin{bmatrix} p_1 \\ p_2 \end{bmatrix} = \frac{1}{\left(\dot{X} + Y\dot{\Omega}'\right)^2 + \left(\dot{Y} - X\dot{\Omega}'\right)^2} \begin{bmatrix} \dot{X} + Y\dot{\Omega}' & \dot{Y} - X\dot{\Omega}' \\ \dot{Y} - X\dot{\Omega}' & -\dot{X} - Y\dot{\Omega}' \end{bmatrix}
$$

$$
\times \frac{1}{1 + K\cos I} \begin{bmatrix} \left(\dfrac{\rho\dot{\rho}\dot{\eta}}{\dot{\psi}\sqrt{\rho^2 + c^2}} - \eta\dot{\psi}\sqrt{\rho^2 + c^2}\right) \\ \cos I\left(\dfrac{Z\dot{\rho}}{\sqrt{\rho^2 + c^2}} + \dot{\eta}\sqrt{\rho^2 + c^2}\right) \end{bmatrix}
$$

5. Compute $\mathbf{r}'$ from

$$
\mathbf{r}' = \begin{bmatrix} \dfrac{X}{\sqrt{\rho^2 + c^2}} \\ \dfrac{Y}{\sqrt{\rho^2 + c^2}} \\ \dfrac{Z}{\rho} \end{bmatrix}
$$

and then compute $\hat{\mathbf{f}}$ and $\hat{\mathbf{g}}$ from

$$
\hat{\mathbf{f}} = \begin{bmatrix} 1 + p_1^2 - p_2^2 \\ 2p_1 p_2 \\ -2Kp_2 \end{bmatrix} ; \quad \hat{\mathbf{g}} = \begin{bmatrix} 2Kp_1 p_2 \\ \left(1 - p_1^2 + p_2^2\right)K \\ 2p_1 \end{bmatrix}
$$

159

6. Compute L from

$$L = \text{atan2}\left(\sin L, \cos L\right) = \text{atan2}\left(\mathbf{r}' \cdot \hat{\mathbf{g}}, \mathbf{r}' \cdot \hat{\mathbf{f}}\right)$$

7. Compute q_1 and q_2 from

$$\begin{bmatrix} q_1 \\ q_2 \end{bmatrix} = \begin{bmatrix} \cos L & \sin L \\ \sin L & -\cos L \end{bmatrix} \begin{bmatrix} \dfrac{p}{\rho} - 1 \\[2ex] \dfrac{\sqrt{F}p^{1/2}}{\rho \left(\mu\gamma_1\right)^{1/2} \left(\rho^2 - 2b_1\rho + b_2^2\right)^{1/2}} \end{bmatrix}$$

The preceding algorithm completes the point transformation from inertial position and velocity vectors such as ECI coordinates to the oblate spheroidal equinoctial element set $\text{œ} = \{p, q_1, q_2, p_1, p_2, L\}$.

4.8 Summary: Converting Spheroidal Equinoctial Elements to Position and Velocity Vectors

The process of converting oblate spheroidal equinoctial orbital elements $\text{œ} = \{p, q_1, q_2, p_1, p_2, L\}$ to inertial position and velocity vectors is summarized in the following algorithm, assuming the only quantities given are the elements and the retrograde factor, K:

1. Compute $c^2 = R_e^2 J_2$ and then the basis vectors $\hat{\mathbf{f}}$ and $\hat{\mathbf{g}}$ of the oblate spheroidal equinoctial reference frame from

$$\hat{\mathbf{f}} = \begin{bmatrix} 1 + p_1^2 - p_2^2 \\ 2p_1p_2 \\ -2Kp_2 \end{bmatrix}; \quad \hat{\mathbf{g}} = \begin{bmatrix} 2Kp_1p_2 \\ \left(1 - p_1^2 + p_2^2\right)K \\ 2p_1 \end{bmatrix}$$

2. Compute e, γ, and I from

$$e = \sqrt{q_1^2 + q_2^2}; \quad \gamma = \frac{e^2 - 1}{p}; \quad I = \pi\left(\frac{1 - K}{2}\right) + 2K \arctan\sqrt{p_1^2 + p_2^2}$$

3. Compute $Q = \sin I$, then use Eqs. (2.78–2.86) with $z_\delta = 0$ (not iterative) to compute the prime constants p_0, γ_0, γ_1, b_1, b_2^2, C_2, u (when $e < 1$, $a = -1/\gamma$ and $a_0 = -1/\gamma_0$).

   Note, this step is unnecessary if a particular application already required the conversion process summarized in Section 4.7, because all these quantities will have already been computed.

4. Compute the Jacobi constants α_1, α_2, and α_3 from

$$\alpha_1 = \frac{\mu\gamma_0}{2}; \quad \alpha_2 = \sqrt{\mu p_0}; \quad \alpha_3 = \alpha_2 \left(1 - \frac{C_2 Q^2}{u}\right)^{1/2} \cos I$$

   Note that α_1 need only be computed if a spacecraft is near a pole and Eq. (4.83) is used instead of Eq. (4.85) to compute $\dot{\Omega}'$.

5. Compute ρ and η from

$$\rho = \frac{p}{1 + q_1 \cos L + q_2 \sin L}; \quad \eta = \frac{2}{1 + p_1^2 + p_2^2}\left(p_1 \sin L - K p_2 \cos L\right)$$

6. Compute $\dot{f}$ and $\dot{\psi}$ from

$$\dot{f} = \frac{(\mu\gamma_1 p)^{1/2}\left(\rho^2 - 2b_1\rho + b_2^2\right)^{1/2}}{\rho\left(\rho^2 + c^2\eta^2\right)}; \quad \dot{\psi} = \frac{\alpha_2\left(1 - C_2\eta^2\right)^{1/2}}{u^{1/2}\left(\rho^2 + c^2\eta^2\right)}$$

7. Compute $\dot{\rho}$ and $\dot{\eta}$ from

$$\dot{\rho} = \frac{\dot{f}\rho^2}{p}\left(q_1 \sin L - q_2 \cos L\right); \quad \dot{\eta} = \frac{2\dot{\psi}}{1 + p_1^2 + p_2^2}\left(p_1 \cos L + K p_2 \sin L\right)$$

8. If a spacecraft is not nearly on a pole $(1 - |\eta| \geq 10^{-8})$, then compute $\dot{\Omega}'$ from

$$\dot{\Omega}' = \frac{1}{\rho^2 + c^2\eta^2}\left\{-\frac{c^2\alpha_3}{\rho^2 + c^2} + \frac{\alpha_3}{1 - \eta^2}\left[1 - \frac{\left(1 - C_2\eta^2\right)^{1/2}}{\left(1 - C_2\right)^{1/2}}\right]\right\}$$

161

If a spacecraft is nearly or exactly on a pole $(1 - |\eta| < 10^{-8})$, compute A_3, B_3, A_{3k} for $k = 1, \ldots, 4$, B_{32}, and $\dot{\Omega}'$ from Eq. (4.83) or (4.85).

9. Compute $\dot{L}$ from

$$\dot{L} = \dot{\psi} + K\dot{\Omega}'$$

10. Compute $\dot{\hat{\mathbf{f}}}$ and $\dot{\hat{\mathbf{g}}}$ from

$$\dot{\hat{\mathbf{f}}} = \frac{2\dot{\Omega}'}{1 + p_1^2 + p_2^2} \begin{bmatrix} -2p_1 p_2 \\ p_1^2 - p_2^2 \\ -Kp_1 \end{bmatrix} ; \quad \dot{\hat{\mathbf{g}}} = \frac{2\dot{\Omega}'}{1 + p_1^2 + p_2^2} \begin{bmatrix} (p_1^2 - p_2^2) K \\ 2Kp_1 p_2 \\ -p_2 \end{bmatrix}$$

11. Compute X and Y from

$$\mathbf{r}_{1:2} = \sqrt{\rho^2 + c^2} \left(\cos L \, \hat{\mathbf{f}}_{1:2} + \sin L \, \hat{\mathbf{g}}_{1:2} \right)$$

and Z from

$$Z = \rho\eta$$

12. Compute $\dot{X}$ and $\dot{Y}$ from

$$\mathbf{v}_{1:2} = \frac{\rho\dot{\rho}}{\rho^2 + c^2} \mathbf{r}_{1:2}$$
$$+ \sqrt{\rho^2 + c^2} \left[\cos L \, \dot{\hat{\mathbf{f}}}_{1:2} + \sin L \, \dot{\hat{\mathbf{g}}}_{1:2} + \dot{L} \left(- \sin L \, \hat{\mathbf{f}}_{1:2} + \cos L \, \hat{\mathbf{g}}_{1:2} \right) \right]$$

and $\dot{Z}$ from

$$\dot{Z} = \dot{\rho}\eta + \rho\dot{\eta}$$

The preceding algorithm completes the point transformation from the oblate spheroidal equinoctial element set $\boldsymbol{\alpha} = \{p, q_1, q_2, p_1, p_2, L\}$ to inertial position and velocity vectors such as ECI coordinates.

4.9 Final Remarks

The coordinate transformations of Vinti theory are generally separated from any solution to Vinti's dynamical problem. However, until now, a set of orbital elements of the Vinti problem has never been presented as independent from and invariant to any particular solution method, let alone presented as separate from a particular approach. As such, the new oblate spheroidal equinoctial orbital elements lead to a more natural view to the Vinti problem. Moreover, with their introduction, the symmetric Vinti theory can now benefit from all the desirable properties that equinoctial elements hold over the classical ones in the two-body problem. These properties include straightforward geometrical interpretation in addition to the complete removal of non-physical singularities associated with small eccentricities and inclinations. Consequently, the Jacobian of the transformation will not present singularities for those orbit regimes.

The particular approach presented leads to a number of other advantages as well. With careful attention to avoiding indeterminate forms, the transformations are valid for nearly or exactly zero-energy orbits, while generally maintaining validity for other bounded or unbounded orbit regimes. The range of valid orbit regimes is limited only by Vinti theory itself, which prescribes a forbidden zone associated with nearly or exactly rectilinear orbits for which an analytical solution does not exist. When combined with certain techniques, the spheroidal equinoctial elements also completely remove the singularity on the poles, a persistent problem in Vinti theory that has evaded resolution for decades. Specifically, looking to the analytical solution,

the approximate expression for the time derivative of spheroidal RAAN can be used when a spacecraft is near a pole. The approximation is accurate to $O(J_2^n)$ for an arbitrary order n, but analytical solutions in the literature do not exceed the third order. An exact expression for spheroidal RAAN is also derived for the first time so that the coordinate transformations are otherwise exact. Having developed the mathematical framework of equinoctial elements for Vinti theory in this chapter, the stage is set for exploring state propagation in the new element set in the next chapter.

Chapter 5

Analytical State Propagation in Time Using Oblate Spheroidal Equinoctial Elements

The complete introduction of the spheroidal equinoctial orbital elements is divided into two parts. Chapter 4 generalized the standard, spherical equinoctial orbital elements to an oblate spheroidal geometry congruent with Vinti theory. The effort focused on developing the point transformations that map between the equinoctial elements and the inertial position and velocity vectors, including derivations and algorithms. Their function, as such, is akin to that of the transformations established for spherical elements, wherein notions of osculating elements can be adopted for a perturbed Vinti problem. State propagation in time is viewed as a wholly separate problem, and the analytical treatment is the subject of the present chapter.

The approach to analytical state propagation proceeds in the spirit of Vinti [154, 160], reducing the inversion of the kinematic equations to successive solutions of Kepler's equation but modified for equinoctial elements. Other techniques have been suggested for the inversion expressed in classical elements [169], but the approach here can exploit iterative root-solve algorithms typical for solving Kepler's equation. The author recommends Laguerre's method modified from Conway's form [38] because of the robustness

it affords in the form of a free parameter that controls the order of the root-solve. Der employs this method for the same reason [49]. Other aspects of the solution include the definition of the spheroidal equinoctial constants of the motion and their derivation, re-expressing the kinematic equations in equinoctial elements, and extracting the periodic components of the equinoctial elements. The investigation concludes with a number of examples to test the analytical Vinti orbit propagator.

5.1 Problem Statement

Recall that Vinti's analytical solution can be expressed as a nonlinear function $\mathbf{f}$ of the initial state $\mathbf{x}_i$:

$$\mathbf{x}^{\jmath} = \mathbf{f}(t, \mathbf{x}_i^{\jmath})$$

The dynamical problem considered in this chapter concerns a spacecraft traveling under the influence of the 1959 Vinti potential [152]

$$V = -\frac{\mu\rho}{\rho^2 + c^2\eta^2} \tag{5.1}$$

Now, the ECI and OS reference frames share the same origin. It still holds that constant values of ρ specify confocal oblate spheroids, those of η specify confocal hyperboloids of one sheet, and those of ϕ specify meridional planes. The focal separation is fit to the dominant term of the traditional spherical harmonic potential as

$$c^2 = R_e^2 J_2 \tag{5.2}$$

where R_e is the equatorial radius, but $z_\delta = 0$. With this fit, the Vinti potential is exact for a symmetric oblate spheroid, where $J_4 = -J_2^2$, $J_6 = +J_2^3$, ..., but

166

relative to the Earth's potential, for example, the fit is approximate, notionally modeling $J_2 + \epsilon J_4 + \epsilon^2 J_6 + \cdots$ for some small ϵ. In the case of the Earth, the Vinti potential includes about 72% of J_4.

Using the gravitational potential V of Eq. (5.1) and OS coordinates, Vinti derived the Hamiltonian, $\mathcal{H}$, as

$$\mathcal{H} = \frac{1}{2}\left[\frac{\rho^2 + c^2}{\rho^2 + c^2\eta^2}p_\rho^2 + \frac{1-\eta^2}{\rho^2 + c^2\eta^2}p_\eta^2 + \frac{1}{(\rho^2+c^2)(1-\eta^2)}p_\phi^2\right] - \frac{\mu\rho}{\rho^2 + c^2\eta^2} \quad (5.3)$$

where

$$p_\rho^2 = \frac{\rho^2 + c^2\eta^2}{\rho^2 + c^2}\dot\rho \quad (5.4)$$

$$p_\eta^2 = \frac{\rho^2 + c^2\eta^2}{1 - \eta^2}\dot\eta \quad (5.5)$$

$$p_\phi^2 = \left(\rho^2 + c^2\right)\left(1 - \eta^2\right)\dot\phi \quad (5.6)$$

are the conjugate momenta. He then solved the dynamical problem by obtaining the Hamilton-Jacobi equation and applying separation of variables [152].

Details on the notation and computation of certain constants and intermediate quantities are available in a number of references [154, 158, 160] and are not covered in this thesis. Corrections to certain quantities, such as the B_j and B_{jk} coefficients, are given in Walden and Watson [164]. The notation in this chapter continues to follow the notation of Vinti's 1966 theory [158] except that J_3 is set to zero. Also note the use of the RAAN-like variable Ω' that Vinti developed in 1969 [160].

5.2   Kinematic Equations

Following the methods of Hamilton-Jacobi theory, the problem is reduced to a set of kinematic equations that define three of the six constants of the motion. The kinematic equations are generally expressed as

$$t + \beta_1 = R_1 + c^2 N_1 \tag{5.7}$$

$$\beta_2 = -\alpha_2 R_2 + \alpha_2 N_2 \tag{5.8}$$

$$\beta_3 = \phi + c^2 \alpha_3 R_3 - \alpha_3 N_3 \tag{5.9}$$

where t denotes the time, R_j denotes the ρ-integrals for $j = 1, 2, 3$ defined as

$$R_1 = \int_{\rho_1}^{\rho} \pm \rho^2 F(\rho)^{-1/2} \, d\rho \tag{5.10}$$

$$R_2 = \int_{\rho_1}^{\rho} \pm F(\rho)^{-1/2} \, d\rho \tag{5.11}$$

$$R_3 = \int_{\rho_1}^{\rho} \pm (\rho^2 + c^2)^{-1} F(\rho)^{-1/2} \, d\rho \tag{5.12}$$

N_j denotes the η-integrals for $j = 1, 2, 3$ defined as

$$N_1 = \int_0^{\eta} \pm \eta^2 G(\eta)^{-1/2} \, d\eta \tag{5.13}$$

$$N_2 = \int_0^{\eta} \pm G(\eta)^{-1/2} \, d\eta \tag{5.14}$$

$$N_3 = \int_0^{\eta} \pm (1 - \eta^2)^{-1} G(\eta)^{-1/2} \, d\eta \tag{5.15}$$

and α_j and β_j are the Jacobi constants for $j = 1, 2, 3$. Specifically, α_1 is the total energy or Hamiltonian, α_2 is closely related to the total angular momentum, α_3 is the polar component of the angular momentum, $\tau = -\beta_1$ is the time of spheroidal periapsis passage, $\beta_2 = \omega$ is the argument of spheroidal periapsis,

and $\beta_3 = \Omega$ is the right ascension of the spheroidal ascending node (spheroidal RAAN). These six quantities are canonical constants of the motion analogous to the Jacobi constants obtained for the two-body problem. The quantities $F(\rho)$ and $G(\eta)$ correspond to the quartics that must be factored to obtain a, e, and I, which are respectively the spheroidal semimajor axis, eccentricity, and inclination. For readability, the "spheroidal" qualifier is often omitted and elements should be understood as spheroidal unless noted otherwise.

The derivation of the approximate analytical solution in OS equinoctial elements begins with Vinti's solution in classical elements. His classical element solution expresses Eqs. (5.7–5.9) correct to $O(J_2^3)$ in secular terms and $O(J_2^2)$ in periodic terms using truncated series as

$$t + \beta_1 = (-2\alpha_1)^{-1/2} \left[b_1 E + a\,(E - e \sin E) + A_1 f + \sum_{k=1}^{2} A_{1k} \sin kf \right]$$
$$+ c^2 \alpha_2^{-1} u^{1/2} \left(B_1' \psi + B_{12} \sin 2\psi + B_{14} \sin 4\psi \right) \tag{5.16}$$

$$\beta_2 = -\alpha_2 (-2\alpha_1)^{-1/2} \left[A_2 f + \sum_{k=1}^{4} A_{2k} \sin kf \right]$$
$$+ u^{1/2} \left(B_2 \psi + B_{22} \sin 2\psi + B_{24} \sin 4\psi \right) \tag{5.17}$$

$$\beta_3 = \Omega' + c^2 \alpha_3 (-2\alpha_1)^{-1/2} \left[A_3 f + \sum_{k=1}^{4} A_{3k} \sin kf \right]$$
$$- \alpha_3 \alpha_2^{-1} u^{1/2} \left(B_3 \psi + + B_{32} \sin 2\psi \right) \tag{5.18}$$

Readers can identify the familiar $E - e \sin E$ term of the Kepler problem in Eq. (5.16) and view its appearance here as part of a generalized Kepler's equation. The variable f is the spheroidal true anomaly, E is the spheroidal eccentric anomaly, and ψ is the true argument of spheroidal latitude equal to $f + \omega'$. The quantities b_1, A_j, A_{jk}, B_j, B_{jk}, and u are constants.

169

5.2.1 Converting to Equinoctial Elements: Secular Terms

Writing the secular components in terms of equinoctial elements requires the definition for eccentric spheroidal longitude, $F = E + \omega' + K\Omega'$ [Eq. (4.8)]. It is also convenient at this time to similarly define the mean spheroidal longitude as

$$\lambda = M + \omega' + K\Omega' \tag{5.19}$$

which differs from Eq. (4.6) in that it includes the periodic contributions to λ, whereas Eq. (4.6) only defined the secular component λ_s. Recall that the $'$ symbol distinguishes these variables from the constants of the motion β_2 and β_3 and also indicates a closer connection to the spheroidal Delaunay variables obtained after various canonical transformations. The connection will be made clear in subsequent sections.

From Eqs. (4.2) and (4.8), observe that certain combinations of angles must be added to both sides of Eqs.(5.16–5.18) to obtain L and F on the right-hand side (RHS). First, focus on Eq. (5.16) and consider the term $(a + b_1)E$. Adding $(-2\alpha_1)^{-1/2}(a + b_1)(\omega' + K\Omega')$ to both sides will result in a $(a + b_1)F$ term on the RHS and the left-hand side (LHS) can simply absorb the unknown quantity into the unknown constant β_1. The new constants on the LHS are denoted as $\tilde{\beta}_j$ for $j = 1, 2, 3$. This procedure is generally applied to the remaining secular terms in Eqs.(5.16–5.18), resulting in the following

transformed equations:

$$t + \tilde{\beta}_1 = (-2\alpha_1)^{-1/2} \left[b_1 F + a \left(F - e \sin E \right) + A_1 L + \sum_{k=1}^{2} A_{1k} \sin kf \right]$$
$$+ c^2 \alpha_2^{-1} u^{1/2} \left(B_1' L + B_{12} \sin 2\psi + B_{14} \sin 4\psi \right) \tag{5.20}$$

$$\tilde{\beta}_2 \alpha_2^{-1} = - (-2\alpha_1)^{-1/2} \left[A_2 L + \sum_{k=1}^{4} A_{2k} \sin kf \right]$$
$$+ \alpha_2^{-1} u^{1/2} \left(B_2 L + B_{22} \sin 2\psi + B_{24} \sin 4\psi \right) \tag{5.21}$$

$$\tilde{\beta}_3 = c^2 \alpha_3 (-2\alpha_1)^{-1/2} \left[A_3 L + \sum_{k=1}^{4} A_{3k} \sin kf \right]$$
$$- \alpha_3 \alpha_2^{-1} u^{1/2} \left(B_3 L + B_{32} \sin 2\psi \right) \tag{5.22}$$

where

$$\tilde{\beta}_1 = \beta_1 + (-2\alpha_1)^{-1/2} (a + b_1 + A_1)(\omega' + K\Omega') + c^2 \alpha_2^{-1} u^{1/2} B_1' K\Omega' \tag{5.23}$$

$$\tilde{\beta}_2 \alpha_2^{-1} = \beta_2 \alpha_2^{-1} - (-2\alpha_1)^{-1/2} A_2(\omega' + K\Omega') + \alpha_2^{-1} u^{1/2} B_2 K\Omega' \tag{5.24}$$

$$\tilde{\beta}_3 = \beta_3 + c^2 (-2\alpha_1)^{-1/2} A_3(\omega' + K\Omega') - \alpha_2^{-1} u^{1/2} B_3 K\Omega' - \Omega' \tag{5.25}$$

Naturally, the transformation is not yet complete because the periodic terms have not been addressed and still contain f and ψ.

5.2.2 Converting to Equinoctial Elements: Periodic Terms

There are multiple ways to proceed, but the approach here aims to maintain the form of the periodic terms where the sines contain multiple-angle arguments of kf or $k\psi$ for $k = 1, \ldots, 4$. These trigonometric terms can be written in terms of equinoctial elements by applying Chebyshev's recursive formula and observing that the periodic coefficients A_{jk} contain a factor e^k and B_{jk} contain a factor Q^k, where $j = 1, 2, 3$ denotes the kinematic equation

171

and $k = 1, \ldots, 4$. Define new periodic coefficients in terms of the old as

$$\tilde{A}_{jk} \equiv \frac{A_{jk}}{e^k} \tag{5.26}$$

$$\tilde{B}_{jk} \equiv \frac{B_{jk}}{Q^k} \tag{5.27}$$

Of course, the new coefficients should not be computed this way since e and/or Q can go to zero. To compute $\tilde{A}_{jk}$ or $\tilde{B}_{jk}$, simply use the original formulas with omission of e^k and Q^k. Now, e^k and Q^k are instead grouped with the sine functions, such as $e \sin f$ or $Q^4 \sin 4\psi$.

The basic conversion process is demonstrated for the $e \sin E$ term. It is straightforward to show from angle sum and difference identities that

$$e \sin E = e \sin \left(F - \omega' - K\Omega' \right)$$

$$= e \sin F \cos \left(\omega' + K\Omega' \right) - e \cos F \sin \left(\omega' + K\Omega' \right) \tag{5.28}$$

Therefore,

$$e \sin E = q_1 \sin F - q_2 \cos F \tag{5.29}$$

Applying similar identities for $e \cos E$ gives

$$e \cos E = q_1 \cos F + q_2 \sin F \tag{5.30}$$

This process can be applied recursively for any argument x and for all terms of higher frequency using Chebyshev's formula:

$$\sin nx = 2 \cos x \sin \left(n - 1 \right) x - \sin \left(n - 2 \right) x \tag{5.31}$$

for a positive integer $n \geq 2$. For example, with $n = 2$, $e^2 \sin 2f = 2e^2 \cos f \sin f$ can be grouped in terms of lower-frequency quantities as $2 \left(e \cos f \right) \left(e \sin f \right)$.

172

Carrying out the process to the fourth term gives the following relations for periodic functions of kf in terms of periodic functions of kL:

$$\tilde{q}_1\left(q_1, q_2, L\right) \equiv e \sin f = q_1 \sin L - q_2 \cos L \tag{5.32}$$

$$\tilde{q}_2\left(q_1, q_2, L\right) \equiv e^2 \sin 2f = \left(q_1^2 - q_2^2\right) \sin 2L - 2q_1 q_2 \cos 2L \tag{5.33}$$

$$\tilde{q}_3\left(q_1, q_2, L\right) \equiv e^3 \sin 3f = \left(q_1^3 - q_1 q_2^2\right) \sin 3L + \left(q_2^3 - q_1^2 q_2\right) \cos 3L \tag{5.34}$$

$$\tilde{q}_4\left(q_1, q_2, L\right) \equiv e^4 \sin 4f = \left(q_1^4 - 6q_1^2 q_2^2 + q_2^4\right) \sin 4L$$
$$+ 4\left(q_1 q_2^3 - q_1^3 q_2\right) \cos 4L \tag{5.35}$$

The periodic functions of $k\psi$ in terms of periodic functions of kL are slightly more complicated to derive. The form of these relations is identical to that of the relations for kf except that there is now a coefficient $(1 + K \cos I)^k$. The relations are stated as

$$\tilde{p}_2\left(p_1, p_2, L\right) \equiv Q^2 \sin 2\psi = (1 + K \cos I)^2$$
$$\times \left[\left(p_1^2 - p_2^2\right) \sin 2L - 2p_1 p_2 \cos 2L\right] \tag{5.36}$$

$$\tilde{p}_4\left(p_1, p_2, L\right) \equiv Q^4 \sin 4\psi = (1 + K \cos I)^4 \left[\left(p_1^4 - 6p_1^2 p_2^2 + p_2^4\right) \sin 4L\right.$$
$$+ 4\left(p_1 p_2^3 - p_1^3 p_2\right) \cos 4L\bigg] \tag{5.37}$$

These equations can be written strictly in terms of p_1 and p_2 by observing that

$$\begin{aligned}
(1 + K \cos I)^2 &= \frac{4}{4}(1 + K \cos I)^2 \\
&= 4\left(\frac{1 + K \cos I}{2}\right)^2 \\
&= \begin{cases} 4 \cos^4\left(\frac{I}{2}\right), & \text{if } K = +1 \\ 4 \sin^4\left(\frac{I}{2}\right), & \text{if } K = -1 \end{cases}
\end{aligned} \tag{5.38}$$

It follows that

$$(1 + K \cos I)^2 = \frac{4}{(1 + p_1^2 + p_2^2)^2} \tag{5.39}$$

for either value of K. Equation (5.39) can be substituted into Eq. (5.36). Squaring Eq. (5.39) gives

$$(1 + K \cos I)^4 = \frac{16}{(1 + p_1^2 + p_2^2)^4} \tag{5.40}$$

which can be substituted into Eq. (5.37). After the substitutions, Eqs. (5.36) and (5.37) become

$$Q^2 \sin 2\psi = \frac{4}{(1 + p_1^2 + p_2^2)^2}$$
$$\times \left[\left(p_1^2 - p_2^2 \right) \sin 2L - 2p_1 p_2 \cos 2L \right] \tag{5.41}$$

$$Q^4 \sin 4\psi = \frac{16}{(1 + p_1^2 + p_2^2)^4}$$
$$\times \left[\left(p_1^4 - 6p_1^2 p_2^2 + p_2^4 \right) \sin 4L + 4 \left(p_1 p_2^3 - p_1^3 p_2 \right) \cos 4L \right] \tag{5.42}$$

5.2.3 Converting to Equinoctial Elements: Final Kinematic Equations

Finally, having represented the secular and periodic terms with equinoctial elements, the kinematic equations can be expressed strictly in terms of

these nonsingular orbital elements to second order as

$$
t + \tilde{\beta}_1 = (-2\alpha_1)^{-1/2} \left[b_1 F + a \left(F - q_1 \sin F + q_2 \cos F \right) \right.
$$

$$
\left. + A_1 L + \sum_{k=1}^{2} \tilde{A}_{1k} \tilde{q}_k \left(q_{1_j}, q_{2_j}, L_j \right) \right]
$$

$$
+ c^2 \alpha_2^{-1} u^{1/2} \left[B_1' L + \sum_{k=1}^{2} \tilde{B}_{1(2k)} \tilde{p}_{2k} \left(p_{1_j}, p_{2_j}, L_j \right) \right] \tag{5.43}
$$

$$
\tilde{\beta}_2 \alpha_2^{-1} = - (-2\alpha_1)^{-1/2} \left[A_2 L + \sum_{k=1}^{4} \tilde{A}_{2k} \tilde{q}_k \left(q_{1_j}, q_{2_j}, L_j \right) \right]
$$

$$
+ \alpha_2^{-1} u^{1/2} \left[B_2 L + \sum_{k=1}^{2} \tilde{B}_{2(2k)} \tilde{p}_{2k} \left(p_{1_j}, p_{2_j}, L_j \right) \right] \tag{5.44}
$$

$$
\tilde{\beta}_3 = c^2 \alpha_3 \left(-2\alpha_1 \right)^{-1/2} \left[A_3 L + \sum_{k=1}^{4} \tilde{A}_{3k} \tilde{q}_k \left(q_{1_j}, q_{2_j}, L_j \right) \right]
$$

$$
- \alpha_3 \alpha_2^{-1} u^{1/2} \left[B_3 L + \sum_{k=1}^{1} \tilde{B}_{3(2k)} \tilde{p}_{2k} \left(p_{1_j}, p_{2_j}, L_j \right) \right] \tag{5.45}
$$

Note that Eqs. (5.32–5.35) and (5.41–5.42) need not be substituted for the periodic terms in $e^k \sin kf$ and $Q^k \sin k\psi$ depending on the intended use. For

example, if the equations are left in the form

$$t + \tilde{\beta}_1 = (-2\alpha_1)^{-1/2} \left[b_1 F + a \left(F - q_1 \sin F + q_2 \cos F \right) \right.$$

$$\left. + A_1 L + \sum_{k=1}^{2} \tilde{A}_{1k} e^k \sin kf \right]$$

$$+ c^2 \alpha_2^{-1} u^{1/2} \left(B_1' L + \sum_{k=1}^{2} \tilde{B}_{1(2k)} Q^{2k} \sin 2k\psi \right) \tag{5.46}$$

$$\tilde{\beta}_2 \alpha_2^{-1} = - (-2\alpha_1)^{-1/2} \left[A_2 L + \sum_{k=1}^{4} \tilde{A}_{2k} e^k \sin kf \right]$$

$$+ \alpha_2^{-1} u^{1/2} \left(B_2 L + \sum_{k=1}^{2} \tilde{B}_{2(2k)} Q^{2k} \sin 2k\psi \right) \tag{5.47}$$

$$\tilde{\beta}_3 = c^2 \alpha_3 (-2\alpha_1)^{-1/2} \left[A_3 L + \sum_{k=1}^{4} \tilde{A}_{3k} e^k \sin kf \right]$$

$$- \alpha_3 \alpha_2^{-1} u^{1/2} \left(B_3 L + \sum_{k=1}^{1} \tilde{B}_{3(2k)} Q^{2k} \sin 2k\psi \right) \tag{5.48}$$

then these equations are still useful for initialization. The substitution is essential for the propagation step, but not for the present coordinate transformation. The reason is that, while $\sin f$ and $\sin \psi$ are undefined for the singular cases, nonsingular expressions do exist for $e \sin f$ and $Q \sin \psi$. For this particular coordinate transformation, it is more computationally efficient to combine these latter expressions with Chebyshev's formula in Eq. (5.31) than to use the more complicated equinoctial form. When computing the elements from initial conditions in ECI coordinates at an initial time t_i, the right-hand sides of Eqs. (5.43–5.45) are calculable.

176

For arbitrary order $O(J_2^n)$, the kinematic equations can be written as

$$t + \tilde{\beta}_1 = (-2\alpha_1)^{-1/2} \left[b_1 F + a\left(F - q_1 \sin F + q_2 \cos F \right) \right.$$

$$\left. + A_1 L + \sum_{k=1}^{2(n-1)} \tilde{A}_{1k} \tilde{q}_k \left(q_{1_j}, q_{2_j}, L_j \right) \right]$$

$$+ c^2 \alpha_2^{-1} u^{1/2} \left[B_1' L + \sum_{k=1}^{n} \tilde{B}_{1(2k)} \tilde{p}_{2k} \left(p_{1_j}, p_{2_j}, L_j \right) \right] \tag{5.49}$$

$$\tilde{\beta}_2 \alpha_2^{-1} = -(-2\alpha_1)^{-1/2} \left[A_2 L + \sum_{k=1}^{2n} \tilde{A}_{2k} \tilde{q}_k \left(q_{1_j}, q_{2_j}, L_j \right) \right]$$

$$+ \alpha_2^{-1} u^{1/2} \left[B_2 L + \sum_{k=1}^{n} \tilde{B}_{2(2k)} \tilde{p}_{2k} \left(p_{1_j}, p_{2_j}, L_j \right) \right] \tag{5.50}$$

$$\tilde{\beta}_3 = c^2 \alpha_3 (-2\alpha_1)^{-1/2} \left[A_3 L + \sum_{k=1}^{2n} \tilde{A}_{3k} \tilde{q}_k \left(q_{1_j}, q_{2_j}, L_j \right) \right]$$

$$- \alpha_3 \alpha_2^{-1} u^{1/2} \left[B_3 L + \sum_{k=1}^{n-1} \tilde{B}_{3(2k)} \tilde{p}_{2k} \left(p_{1_j}, p_{2_j}, L_j \right) \right] \tag{5.51}$$

where the secular coefficients A_j and B_j are correspondingly carried out to $O(J_2^n)$.

5.3 Constants of the Motion and Spheroidal Delaunay Variables

It is instructive to first give a motivation of why oblate spheroidal equinoctial constants of the motion are desired and a road map of how to obtain them. As emphasized in Chapter 4, there is a notion of complete elements associated with the angular variables, Ω', ω', and f (and combinations thereof), which are viewed as the composition of secular and periodic parts,

expressed mathematically as

$$\Omega' = \Omega'_s + \Omega'_p$$

$$\omega' = \omega'_s + \omega'_p$$

$$f = M_s + f_p$$

If the initial values of the secular parts of the spheroidal equinoctial elements are available, then their linear dependence on time facilitates their propagation. The periodic parts can be added later in concert with solving the generalized Kepler's equation. These initial values may be given somehow, but if they must be obtained from initial ECI coordinates, then the following discussion and derivations apply.

The analysis of Chapter 4 demonstrated how to obtain the complete equinoctial elements $\{p, q_1, q_2, p_1, p_2, L\}$ from ECI coordinates. Applying angle sum identities to the definitions of q_1 and q_2 in Eq. (4.2) after separating the angles into secular and periodic parts as

$$q_1 = e\cos\left(\omega' + K\Omega'\right) = e\cos\left(\omega'_s + K\Omega'_s + \omega'_p + K\Omega'_p\right) \tag{5.52}$$

$$q_2 = e\sin\left(\omega' + K\Omega'\right) = e\sin\left(\omega'_s + K\Omega'_s + \omega'_p + K\Omega'_p\right) \tag{5.53}$$

gives

$$q_1 = q_{1_s}\cos\left(\omega'_p + K\Omega'_p\right) - q_{2_s}\sin\left(\omega'_p + K\Omega'_p\right) \tag{5.54}$$

$$q_2 = q_{1_s}\sin\left(\omega'_p + K\Omega'_p\right) + q_{2_s}\cos\left(\omega'_p + K\Omega'_p\right) \tag{5.55}$$

and inverting the equations to solve for q_{j_s} gives

$$\begin{bmatrix} q_{1_s} \\ q_{2_s} \end{bmatrix} = \begin{bmatrix} \cos\left(\omega'_p + K\Omega'_p\right) & \sin\left(\omega'_p + K\Omega'_p\right) \\ -\sin\left(\omega'_p + K\Omega'_p\right) & \cos\left(\omega'_p + K\Omega'_p\right) \end{bmatrix} \begin{bmatrix} q_1 \\ q_2 \end{bmatrix} \tag{5.56}$$

Equation (5.56) indicates that the secular parts of q_1 and q_2 are calculable as long as the periodic parts of ω' and Ω' are known. Similarly, the elements p_{j_s} are determined as

$$\begin{bmatrix} p_{1_s} \\ p_{2_s} \end{bmatrix} = \begin{bmatrix} \cos \Omega'_p & \sin \Omega'_p \\ -\sin \Omega'_p & \cos \Omega'_p \end{bmatrix} \begin{bmatrix} p_1 \\ p_2 \end{bmatrix} \tag{5.57}$$

Lastly, the secular part of the true longitude, $L_s = M_s + \omega'_s + K\Omega'_s$, is also desired. Note that L_s is equivalent to the secular part of the mean longitude, λ_s. As shown in the following, it turns out that λ_s can be obtained directly. Therefore, the unknowns to be solved for in the following derivation are ω'_p, Ω'_p, and λ_s.

The oblate spheroidal equinoctial constants of the motion are obtained from the spheroidal Delaunay elements that Vinti employed for his perturbation work [156]. This particular set of natural Delaunay elements may be contrasted to the familiar spherical Delaunay elements reviewed in Appendix B.2.3. Vinti partly attributes these elements to Izsak [86]. The oblate spheroidal Delaunay elements describe the secular evolution of a Vinti trajectory and are the result of several canonical transformations. They are given in terms of the original canonical elements as

$$l_0 = 2\pi\nu_1 \left(\beta_1 - c^2 \beta_2 \alpha_2^{-1} B'_1 B_2^{-1} \right) \tag{5.58}$$

$$l_0 + g_0 = 2\pi\nu_2 \left[\beta_1 + \beta_2 \alpha_2^{-1} \left(a + b_1 + A_1 \right) A_2^{-1} \right] \tag{5.59}$$

$$h_0 = \beta_3 - c^2 \alpha_3 \left(-2\alpha_1 \right)^{-1/2} A_3 l_0 + \alpha_3 \alpha_2^{-1} u^{1/2} B_3 \left(l_0 + g_0 \right) \tag{5.60}$$

Naturally, these relations still hold, as the dynamical problem is unchanged. These Delaunay elements are not calculable when seeking nonsingular elements

179

because the β_j are unknown, but Eqs. (5.58–5.60) will still be of great use. To see how, notice that the $\tilde{\beta}_j$ are known and Eqs. (5.23–5.25) can be used to substitute for β_j in Eqs. (5.58–5.60). Note that while Vinti preferred to maintain β_3 as an element in his classical element solution, this luxury is no longer available because the third kinematic equation is no longer decoupled from the others in an equinoctial element solution. The spheroidal Delaunay element h_0 must then be used instead of β_3, as will be seen shortly.

Substituting Eqs. (5.23–5.25) for β_j in Eqs. (5.58–5.60) and simplifying leads to the following simple equations

$$l_0 + \omega_i' + K\Omega_i' = 2\pi\nu_1 \left(\tilde{\beta}_1 - c^2\tilde{\beta}_2\alpha_2^{-1}B_1'B_2^{-1} \right) \tag{5.61}$$

$$l_0 + g_0 + K\Omega_i' = 2\pi\nu_2 \left[\tilde{\beta}_1 + \tilde{\beta}_2\alpha_2^{-1} (a + b_1 + A_1) A_2^{-1} \right] \tag{5.62}$$

$$h_0 - \Omega_i' = \tilde{\beta}_3 - c^2\alpha_3 (-2\alpha_1)^{-1/2} A_3 (l_0 + \omega_i' + K\Omega_i')$$
$$+ \alpha_3\alpha_2^{-1}u^{1/2}B_3 (l_0 + g_0 + K\Omega_i') \tag{5.63}$$

The right-hand sides of Eqs. (5.61–5.63) are identical in form to Eqs. (5.58–5.60), but β_j is replaced by $\tilde{\beta}_j$, making the right-hand sides calculable. Notice on the left-hand sides of Eqs. (5.61–5.63) that the elements are referenced to different epochs. The spheroidal Delaunay elements reference the time of spheroidal periapsis passage, denoted by subscript "0", while the classical spheroidal elements reference some given initial time, denoted by subscript "i".

To reconcile these differences in epoch, the Delaunay elements are adjusted to reference the same given initial time. Vinti wrote the secular evolution of these elements referenced to the time of spheroidal periapsis passage

180

as

$$l = l_0 + 2\pi\nu_1 t \tag{5.64}$$

$$l + g = l_0 + g_0 + 2\pi\nu_2 t \tag{5.65}$$

$$h = h_0 + 2\pi \left(\nu_3 - \nu_2 \text{sgn}\, \alpha_3\right) t \tag{5.66}$$

but these dynamics can be equivalently referenced to a given initial time (or arbitrary time) as

$$l = l_i + 2\pi\nu_1 \left(t - t_i\right) \tag{5.67}$$

$$l + g = l_i + g_i + 2\pi\nu_2 \left(t - t_i\right) \tag{5.68}$$

$$h = h_i + 2\pi \left(\nu_3 - \nu_2 \text{sgn}\, \alpha_3\right) \left(t - t_i\right) \tag{5.69}$$

where

$$l_i = l_0 + 2\pi\nu_1 t_i \tag{5.70}$$

$$l_i + g_i = l_0 + g_0 + 2\pi\nu_2 t_i \tag{5.71}$$

$$h_i = h_0 + 2\pi \left(\nu_3 - \nu_2 \text{sgn}\, \alpha_3\right) t_i \tag{5.72}$$

Note that the secular components of certain spheroidal orbital elements are equivalent to the Delaunay elements. Using the subscript "s" to indicate that the quantity only contains the secular part, the relations are given by

$$M_s = l \tag{5.73}$$

$$\psi_s = l + g \tag{5.74}$$

$$\Omega'_s = h \tag{5.75}$$

Adopting Delaunay's notation serves as a helpful reminder that these are canonical elements. However, it is emphasized that the elements M, ψ, and Ω' are not canonical when the periodic components are included. This feature is distinctly different from the two-body problem, wherein the mean anomaly is canonical and simply varies linearly with time. Interestingly, the relation $\Omega'_s = h$ was not pointed out until 1980 [169]. The ν_j are the constant fundamental frequencies discussed in Chapter 2 and their definitions in Eqs. (2.39), (2.40), and (2.45) are repeated here for convenience:

$$\dot{M}_s = 2\pi\nu_1 = \frac{(-2\alpha_1)^{1/2}}{a_0 + A_1 + c^2 A_2 B_1' B_2^{-1}}$$

$$\dot{\psi}_s = 2\pi\nu_2 = \frac{\alpha_2 u^{-1/2} A_2 B_2^{-1}}{a_0 + A_1 + c^2 A_2 B_1' B_2^{-1}}$$

$$\dot{\phi}_s = 2\pi\nu_3 = \frac{-\alpha_3}{a_0 + A_1 + c^2 A_2 B_1' B_2^{-1}}$$

$$\times \left\{ c^2 A_3 - \frac{A_2}{B_2} \left[B_3 + \frac{1}{\tilde{S}} \left(\frac{h_1}{\sqrt{1 - 2\zeta}} + \frac{h_2}{\sqrt{1 + 2\zeta}} \right) \right] \right\}$$

where $\tilde{S} = \sqrt{1 - S}$, and $S = \sin^2 I$, h_1, h_2, and ζ are constants from Vinti's 1966 solution [158]. Also recall from Eq. (2.53) that

$$\dot{h} = \dot{\Omega}'_s = -\frac{\alpha_3}{a_0 + A_1 + c^2 A_2 B_1' B_2^{-1}} \left(c^2 A_3 - \frac{A_2}{B_2} B_3 \right)$$

is available and presents no singularities. It is essential for the present analysis to have this uniformly valid equation.

Finally, Eqs. (5.61–5.63) can be referenced to a consistent epoch (the given initial time) and the singularity associated with polar orbits can be

removed. The final result is

$$l_i + \omega'_i + K\Omega'_i = 2\pi\nu_1 \left(t_i + \tilde{\beta}_1 - c^2\tilde{\beta}_2\alpha_2^{-1}B'_1 B_2^{-1} \right) \tag{5.76}$$

$$l_i + g_i + K\Omega'_i = 2\pi\nu_2 \left[t_i + \tilde{\beta}_1 + \tilde{\beta}_2\alpha_2^{-1} \left(a + b_1 + A_1 \right) A_2^{-1} \right] \tag{5.77}$$

$$h_i - \Omega'_i = \tilde{\beta}_3 + \dot{h}t_i$$
$$- c^2\alpha_3 \left(-2\alpha_1 \right)^{-1/2} A_3 \left(2\pi\nu_1 \right) \left(\tilde{\beta}_1 - c^2\tilde{\beta}_2\alpha_2^{-1}B'_1 B_2^{-1} \right)$$
$$+ \alpha_3\alpha_2^{-1}u^{1/2}B_3 \left(2\pi\nu_2 \right) \left[\tilde{\beta}_1 + \tilde{\beta}_2\alpha_2^{-1} \left(a + b_1 + A_1 \right) A_2^{-1} \right] \tag{5.78}$$

Equations (5.76–5.78) may now be used to obtain expressions for the three unknowns: ω'_p, Ω'_p, and λ_s. From the definitions in Eq. (4.3–4.4), it is seen that subtracting Eq. (5.77) from Eq. (5.76) gives ω'_{p_i} as

$$\omega'_{p_i} = 2\pi\nu_1 \left(t_i + \tilde{\beta}_1 - c^2\tilde{\beta}_2\alpha_2^{-1}B'_1 B_2^{-1} \right)$$
$$- 2\pi\nu_2 \left[t_i + \tilde{\beta}_1 + \tilde{\beta}_2\alpha_2^{-1} \left(a + b_1 + A_1 \right) A_2^{-1} \right] \tag{5.79}$$

Equation (5.78) already gives the negative of Ω'_p so that Ω'_{p_i} is determined as

$$\Omega'_{p_i} = - \left(\tilde{\beta}_3 + \dot{h}t_i \right)$$
$$+ c^2\alpha_3 \left(-2\alpha_1 \right)^{-1/2} A_3 \left(2\pi\nu_1 \right) \left(\tilde{\beta}_1 - c^2\tilde{\beta}_2\alpha_2^{-1}B'_1 B_2^{-1} \right) \tag{5.80}$$
$$- \alpha_3\alpha_2^{-1}u^{1/2}B_3 \left(2\pi\nu_2 \right) \left[\tilde{\beta}_1 + \tilde{\beta}_2\alpha_2^{-1} \left(a + b_1 + A_1 \right) A_2^{-1} \right]$$

Lastly, adding Eq. (5.77) to K times Eq. (5.78) gives λ_{s_i} as

$$\lambda_{s_i} = K\tilde{\beta}_3 + \left(2\pi\nu_2 + K\dot{h} \right) t_i$$
$$- Kc^2\frac{\alpha_3}{(-2\alpha_1)^{1/2}} A_3 \left(2\pi\nu_1 \right) \left(\tilde{\beta}_1 - c^2\tilde{\beta}_2\alpha_2^{-1}B'_1 B_2^{-1} \right) \tag{5.81}$$
$$+ \left(1 + K\alpha_3\alpha_2^{-1}u^{1/2}B_3 \right) \left(2\pi\nu_2 \right) \left[\tilde{\beta}_1 + \tilde{\beta}_2\alpha_2^{-1} \left(a + b_1 + A_1 \right) A_2^{-1} \right]$$

Equations (5.79) and (5.80) enable the computation of q_{1_s}, q_{2_s}, p_{1_s}, and p_{2_s} at time t_i through Eqs. (5.56) and (5.57) and λ_{s_i} is determined by Eq. (5.81).

183

The spheroidal semi-latus rectum p is already known because it is a constant of the motion in both classical and equinoctial elements; it is obtained from factoring the $F(\rho)$ quartic.

5.4 Propagating the Secular Parts of the Spheroidal Equinoctial Elements

It is now assumed that the secular oblate spheroidal equinoctial element set, which is defined as $\mathbf{œ}_s = \{p, q_{1_s}, q_{2_s}, p_{1_s}, p_{2_s}, L_s\}$, has been obtained somehow, either as given quantities or as a result of a transformation from ECI coordinates as described in the preceding sections. These secular elements are either constant or evolve with time according to the following formulas:

$$p(t) = p \tag{5.82}$$

$$\begin{bmatrix} q_{1_s}(t) \\ q_{2_s}(t) \end{bmatrix} = \begin{bmatrix} \cos\left[\left(\dot{g} + K\dot{h}\right)(t - t_i)\right] & -\sin\left[\left(\dot{g} + K\dot{h}\right)(t - t_i)\right] \\ \sin\left[\left(\dot{g} + K\dot{h}\right)(t - t_i)\right] & \cos\left[\left(\dot{g} + K\dot{h}\right)(t - t_i)\right] \end{bmatrix}$$
$$\times \begin{bmatrix} q_{1_s}(t_i) \\ q_{2_s}(t_i) \end{bmatrix} \tag{5.83}$$

$$\begin{bmatrix} p_{1_s}(t) \\ p_{2_s}(t) \end{bmatrix} = \begin{bmatrix} \cos\left[\dot{h}(t - t_i)\right] & -\sin\left[\dot{h}(t - t_i)\right] \\ \sin\left[\dot{h}(t - t_i)\right] & \cos\left[\dot{h}(t - t_i)\right] \end{bmatrix} \begin{bmatrix} p_{1_s}(t_i) \\ p_{2_s}(t_i) \end{bmatrix} \tag{5.84}$$

$$\lambda_s(t) = \lambda_s(t_i) + \left(\dot{l} + \dot{g} + K\dot{h}\right)(t - t_i) \tag{5.85}$$

5.5 Solving the Generalized Kepler's Equation

The selected approach to solving the generalized Kepler's equation follows that of other authors, such as Getchell [62], where periodic terms are

neglected in the first iteration. The complication is that the use of equinoctial elements means that all three kinematic equations are coupled.

For iteration $j = 0$, set $\lambda_j = \lambda_s$, $q_{1_j} = q_{1_s}$, $q_{2_j} = q_{2_s}$, $p_{1_j} = p_{1_s}$, and $p_{2_j} = p_{2_s}$ and choose $F_j = \lambda_j$ as an initial guess. Then solve the equinoctial form of Kepler's equation for Vinti theory

$$\lambda_j = F_j - e'' q_{1_j} \sin F_j + e'' q_{2_j} \cos F_j \tag{5.86}$$

where

$$e'' = \frac{a}{a_0} = \frac{a}{a + b_1} \leq 1 \tag{5.87}$$

using a desired root-solving routine. The author recommends employing Laguerre's method to solve Eq. (5.86). Once converged on a value for F_j, obtain L_j by first computing the sine and cosine as

$$\sin L_j = \frac{\left(1 - q_{1_j}^2 b_j\right) \sin F_j + q_{1_j} q_{2_j} b_j \cos F_j - q_{2_j}}{1 - q_{1_j} \cos F_j - q_{2_j} \sin F_j} \tag{5.88}$$

$$\cos L_j = \frac{\left(1 - q_{2_j}^2 b_j\right) \cos F_j + q_{1_j} q_{2_j} b_j \sin F_j - q_{1_j}}{1 - q_{1_j} \cos F_j - q_{2_j} \sin F_j} \tag{5.89}$$

where

$$b_j = \frac{1}{1 + \sqrt{1 - q_{1_j}^2 - q_{2_j}^2}} \tag{5.90}$$

and then use the arctangent to compute L_j as

$$L_j = \text{atan2}\left(\sin L_j, \cos L_j\right) \tag{5.91}$$

Next, it is necessary to perform an update step to incorporate the periodic terms that were neglected earlier. These periodic components are ω'_{p_j}, Ω'_{p_j},

185

and λ_{p_j}, and they are calculable from the available quantities, which consist of some variables but mostly constants. First, compute $l_j + \omega'_j + K\Omega'_j$ as

$$
\begin{aligned}
l_j + \omega'_j + K\Omega'_j = 2\pi\nu_1 \Bigg\{ & (-2\alpha_1)^{-1/2} \Bigg[b_1 F_j \\
& + a \left(F_j - q_{1_j} \sin F_j + q_{2_j} \cos F_j \right) \\
& + A_1 L_j + \sum_{k=1}^{2} \tilde{A}_{1k} \tilde{q}_k \left(q_{1_j}, q_{2_j}, L_j \right) \Bigg] \\
& + c^2 \frac{u^{1/2}}{\alpha_2} \Bigg[B'_1 L_j + \sum_{k=1}^{2} \tilde{B}_{1(2k)} \tilde{p}_{2k} \left(p_{1_j}, p_{2_j}, L_j \right) \Bigg] \\
& + \frac{c^2 B'_1}{B_2 \left(-2\alpha_1 \right)^{1/2}} \Bigg[A_2 L_j + \sum_{k=1}^{4} \tilde{A}_{2k} \tilde{q}_k \left(q_{1_j}, q_{2_j}, L_j \right) \Bigg] \\
& - c^2 B'_1 B_2^{-1} \frac{u^{1/2}}{\alpha_2} \Bigg[B_2 L_j + \sum_{k=1}^{2} \tilde{B}_{2(2k)} \tilde{p}_{2k} \left(p_{1_j}, p_{2_j}, L_j \right) \Bigg] \Bigg\}
\end{aligned}
\tag{5.92}
$$

which is analogous to Eq. (5.76), and then compute $l_j + g_j + K\Omega'_j$ as

$$
\begin{aligned}
l_j + g_j + K\Omega'_j = 2\pi\nu_2 \Bigg\{ & (-2\alpha_1)^{-1/2} \Bigg[b_1 F_j \\
& + a \left(F_j - q_{1_j} \sin F_j + q_{2_j} \cos F_j \right) \\
& + A_1 L_j + \sum_{k=1}^{2} \tilde{A}_{1k} \tilde{q}_k \left(q_{1_j}, q_{2_j}, L_j \right) \Bigg] \\
& + c^2 \frac{u^{1/2}}{\alpha_2} \Bigg[B'_1 L_j + \sum_{k=1}^{2} \tilde{B}_{1(2k)} \tilde{p}_{2k} \left(p_{1_j}, p_{2_j}, L_j \right) \Bigg] \\
& - \frac{(a + b_1 + A_1)}{A_2 \left(-2\alpha_1 \right)^{1/2}} \Bigg[A_2 L_j + \sum_{k=1}^{4} \tilde{A}_{2k} \tilde{q}_k \left(q_{1_j}, q_{2_j}, L_j \right) \Bigg] \\
& + \frac{u^{1/2} (a + b_1 + A_1)}{\alpha_2 A_2} \\
& \times \Bigg[B_2 L_j + \sum_{k=1}^{2} \tilde{B}_{2(2k)} \tilde{p}_{2k} \left(p_{1_j}, p_{2_j}, L_j \right) \Bigg] \Bigg\}
\end{aligned}
\tag{5.93}
$$

which is analogous to Eq. (5.77). It follows that ω'_{p_j} can be determined as

$$\omega'_{p_j} = \left(l_j + \omega'_j + K\Omega'_j\right) - \left(l_j + g_j + K\Omega'_j\right) \tag{5.94}$$

Ω'_{p_j} as

$$\begin{aligned}
\Omega'_{p_j} = &- c^2\alpha_3\left(-2\alpha_1\right)^{-1/2}\left[A_3 L_j + \sum_{k=1}^{4}\tilde{A}_{3k}\tilde{q}_k\left(q_{1_j}, q_{2_j}, L_j\right)\right] \\
&+ \alpha_3\alpha_2^{-1}u^{1/2}\left[B_3 L_j + \sum_{k=1}^{1}\tilde{B}_{3(2k)}\tilde{p}_{2k}\left(p_{1_j}, p_{2_j}, L_j\right)\right] \\
&+ c^2\alpha_3\left(-2\alpha_1\right)^{-1/2}A_3\left(l_j + \omega'_j + K\Omega'_j\right) \\
&- \alpha_3\alpha_2^{-1}u^{1/2}B_3\left(l_j + g_j + K\Omega'_j\right)
\end{aligned} \tag{5.95}$$

and λ_{p_j} as

$$\begin{aligned}
\lambda_{p_j} = &\frac{a + b_1 + A_1}{a + b_1}\left(\omega'_{p_j} + K\Omega'_{p_j}\right) + c^2\frac{\left(-2\alpha_1\right)^{1/2}u^{1/2}}{\alpha_2\left(a + b_1\right)}B'_1 K\Omega'_{p_j} \\
&- \frac{1}{a + b_1}\left[A_1\left(L_j - \lambda_s\right) + \sum_{k=1}^{2}\tilde{A}_{1k}\tilde{q}_k\left(q_{1_j}, q_{2_j}, L_j\right)\right] \\
&- c^2\frac{\left(-2\alpha_1\right)^{1/2}u^{1/2}}{\alpha_2\left(a + b_1\right)}\left[B'_1\left(L_j - \lambda_s\right) + \sum_{k=1}^{2}\tilde{B}_{1(2k)}\tilde{p}_{2k}\left(p_{1_j}, p_{2_j}, L_j\right)\right]
\end{aligned} \tag{5.96}$$

Then q_{1_j} and q_{2_j} can be updated with the inverse of Eq. (5.56) and p_{1_j} and p_{2_j} can be updated with the inverse of Eq. (5.57). The whole process is then repeated until converged by returning to Eq. (5.86), setting $j = j + 1$, $\lambda_j = \lambda_s + \lambda_{p_j}$, and choosing $F_j = \lambda_j$ as an initial guess. The algorithm concludes when convergence is achieved to a desired tolerance.

5.6   Examples

Figure 5.1 shows how the equinoctial elements evolve over approximately 18 orbits for a nominally circular equatorial LEO case with an initial

187

periapsis radius of $r_p = 7,000$ km. To better spotlight the disparity between the spheroidal and spherical elements, oblateness is exaggerated an order of

(a) Complete spheroidal elements   (b) Osculating spherical elements
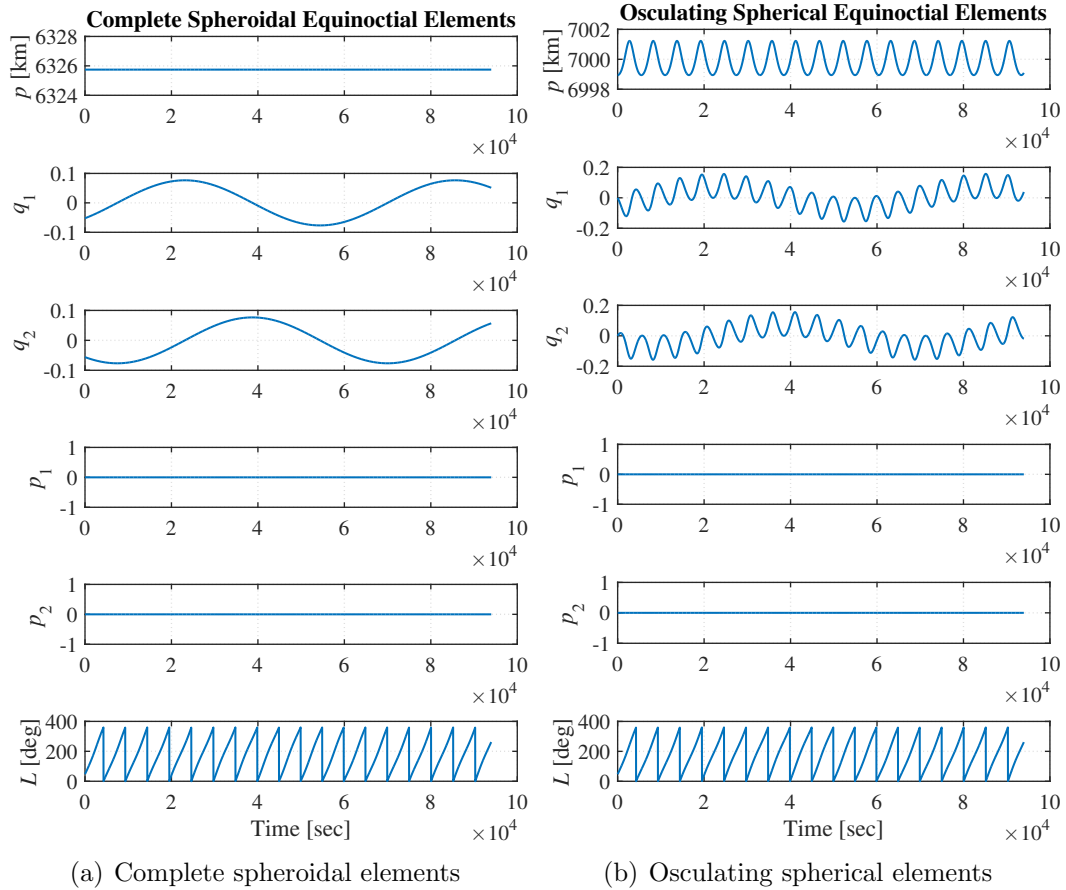
Figure 5.1: Side-by-side comparison of spheroidal and spherical equinoctial elements for a nominally circular equatorial Vinti problem evolving over roughly 18 orbits with $J_2 = 5.08 \times 10^{-2}$.

magnitude above Earth's by setting $J_2 = 5.08 \times 10^{-2}$. Figure 5.1(a) shows the spheroidal elements and Figure 5.1(b) the spherical elements. These plots are overlaid in Fig. 5.2 to emphasize the short-periodic averaging effect. The spherical elements are obtained by numerically integrating the equations of

motion under the Vinti potential and transforming from ECI coordinates to osculating spherical elements. Thus, with this comparison, it is possible to

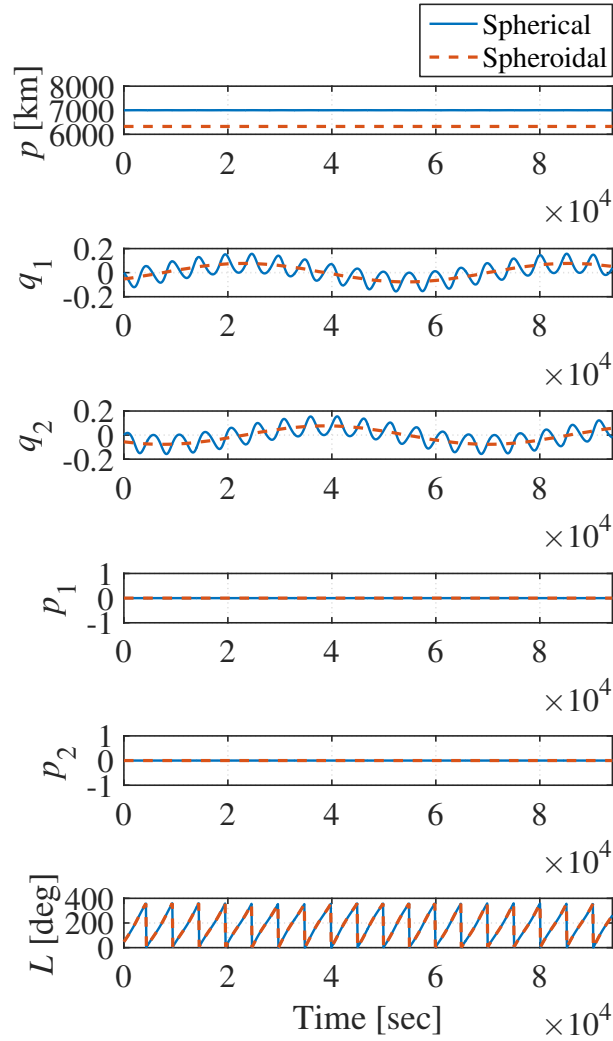Figure 5.2: Complete spheroidal equinoctial elements overlaid on the osculating spherical elements for the scenario in Fig. 5.1.

interpret a geometric relationship between spheroidal and spherical elements. The last three elements appear almost indistinguishable from each other, but the first three are remarkably different. While the spherical p has variations

189

centered around 7,000 km, the spheroidal p is strictly a constant of the motion and notably almost 700 km smaller. Note the long-periodic effects evident in the spheroidal q_1 and q_2 agree with those of their spherical counterparts. The short-periodic effects in the spherical q's are a consequence of the short-periodic variations in spherical eccentricity. These short-periodic effects do not appear in the spheroidal q's because, like the spheroidal semi-latus rectum, the spheroidal eccentricity is a constant of the motion. The spheroidal q's appear to track the short-periodic average of the spherical q's, but this is an artifact of the spheroidal coordinate transformation. Solving the Vinti problem does not invoke any averaging techniques, as the spheroidal p is clearly not an average of the spherical p. The effective averaging of short-periodic variations generally applies to p_1, p_2, and L as well, but the effects are not visible for the particular example in Figure 5.1. Even if the orbit were inclined in this example, the amplitude of the short-periodic variations would be on a much smaller scale than the amplitude of the long-periodic variations for these three elements; the averaging effect would still not be apparent in a comparison similar to Figure 5.1. Figure 5.3 illustrates the associated Vinti trajectory in the ECI frame.

The next example looks at Saturn orbit insertion using the Vinti potential, where Figure 5.4 illustrates the associated Vinti trajectory in the Saturn-centered inertial frame. Gravity field data is taken from Jacobson et al. [89], where $J_2 \approx 1.6291 \times 10^{-2}$ and $J_4 \approx 9.36 \times 10^{-4}$. Recall that the Vinti potential captures approximately 72% of J_4 for the Earth. At Saturn, the Vinti potential captures roughly 28% of J_4. Other parameter values used are
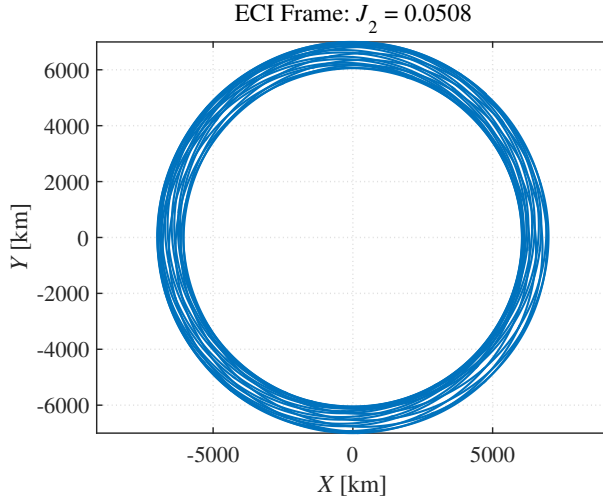
Figure 5.3: Vinti trajectory in the ECI frame for a nominally circular equatorial orbit.

$\mu = 3.7931 \times 10^7$ km^3/s^2 and $R_e = 60,330$ km. Initial osculating spherical orbit parameters are chosen as $r_p = 61,330$ km, $e_K = 0.99$, $I_K = 10°$, $\Omega_K = 30°$, $\omega_K = 11°$, $f_K = 6°$. The subscript "K" denotes Keplerian as opposed to spheroidal orbital elements. The simulation is carried out for a little over a year (≈ 10 revolutions) to visualize the long-term effects on the orbit. A comparison of spheroidal and spherical elements is shown in Figure 5.5. While the short-periodic averaging effects still exist, at this scale, they are not apparent and the last five spheroidal and spherical elements have similar values. Again, the semi-latus rectum is seen to be distinctly different between the spheroidal and spherical elements. Note that after one year, the effect of neglecting 72% of J_4 will manifest itself as a sizable phase error. For the much shorter duration of orbit insertion, however, the phase error will not accumulate significantly and the Vinti trajectory would offer a good approximation.
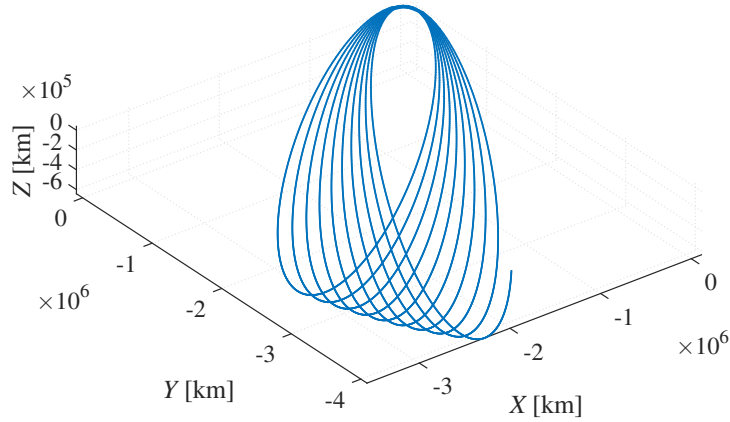
Figure 5.4: Vinti trajectory in the Saturn-centered inertial frame for a Saturn orbit insertion scenario.

5.7 Final Remarks

A nonsingular analytical solution to the unperturbed Vinti problem is presented for bounded orbits. The method avoids the angle ambiguities of classical orbital elements by solving the problem in oblate spheroidal equinoctial orbital elements, the generalization of traditional equinoctial elements to an oblate spheroidal geometry. The analytical solution does not invoke any formal averaging, but, innate to the geometrical description in these coordinates, five of the oblate spheroidal equinoctial elements appear to naturally track the singly averaged value of the spherical equinoctial elements. The constant element is the spheroidal semilatus rectum, which in general is not the average of its spherical counterpart. Such an analytical solution may be useful in preliminary orbit design as a more accurate starting point relative to a two-body-based solution, offering increased accuracy for bounded orbits, including in the vicinity of the critical inclination. This solution also enables

192

future work on the study of perturbations through the variational equations, and, being nonsingular for bounded orbits, prescribes an analytical state transition matrix that is nonsingular in regimes where the analytical ECI state transition matrix in Chapter 3 is singular.
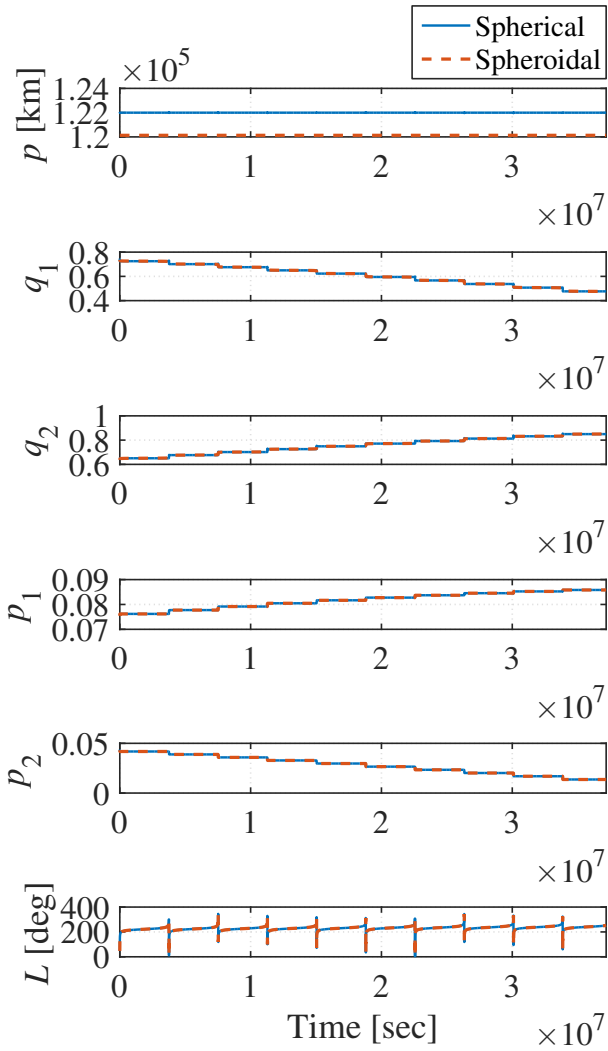
Figure 5.5: Comparison of spheroidal and spherical equinoctial elements for a Saturn orbit insertion scenario, propagated over roughly 10 revolutions.

Chapter 6

Conclusions

The innovations to Vinti theory introduced in this dissertation are a springboard for many intriguing and potentially impactful research directions. In this chapter, the broader context and main contributions are reviewed and avenues of further study are proposed.

6.1 Vinti Theory Context and Overview

Vinti theory, and, by association, intermediaries in general, are seen to be many things. They are analytical solutions to integrable dynamical problems, and analytical solutions are the low-level, tier-one mainstays that enable the attainment of various high-level mission goals, but that does not preclude their application to numerical methods. In fact, as mentioned in Chapter 1, intermediaries hold promise for improving numerical methods that disconnect certain analytical solutions from their inherent limitations in accuracy.

While these benefits are attractive, it is known that analytical theories exceeding the accuracy of the Kepler problem are notoriously complex, which is a deterrent for widespread use. The development of complex models is prone to human error, making validation expensive. The incorporation of Brouwer theory into critical operational processes may have sealed its fate,

but it cannot be denied that Brouwer theory has benefited tremendously from the public release of open-source code in the form of SGP4. In contrast, Vinti orbit propagators remained closely guarded until the release of a handful of implementations in 1998 (roughly 35 years after publication). Indeed, open-source software is a good way to combat the apprehensions and misgivings that arise when practitioners are confronted with complex analytical models, where the release of validated code effectively creates lower risk for end-users.

As pointed out in Chapter 1, the state of Vinti theory up to now was pinned in the awkward position of simultaneously failing to gain traction, at least operationally, and having the presence of many singularities in popular orbital regimes. One can imagine a sort of feedback loop, where the multitude of singularities may have encouraged the lack of use, in turn discouraging the investment of work required to resolve the singularities, especially considering these singularities are avoided in other theories. The contributions of this dissertation address both concerns.

The application in Chapter 3 of the classical element formulation of Vinti's solution to the relative motion problem serves several important purposes. In addition to contributing a handful of fundamental advances to Vinti theory collected in Chapter 2, including the removal of some singularities in Vinti's solution, the new linear, analytical relative motion model is shown to be competitive with a benchmark model, engendering confidence that Vinti theory may be competitive elsewhere. Some particularly resilient singularities in the partial derivatives are also removed in the process by various careful changes of variables, leading to a piecewise differentiable solution to the Vinti

problem with J_3 that did not previously exist. The new analytical STM also has applications to optimization and orbit determination, enabling the development of an analytical or numerical second-order STM that may be required in a quadratic model.

Considering the abundance of singularities, the elimination of all removable singularities in Vinti theory for the first time with the introduction of spheroidal equinoctial elements in Chapter 4 and other enhancements in Chapter 2 represents a true milestone. These singularities have greatly hampered Vinti theory's applicability to different areas, and so their removal can open many doors. That Vinti theory remains invalid for nearly rectilinear orbits should not greatly limit its practical use, as all other singularities are mitigated. The transformation of Vinti's classical solution to an equinoctial solution in Chapter 5 enables the future development of an analytical STM that is also nonsingular in rectangular coordinates. In the process of developing the solution, the removal of short-periodic effects due to oblateness is revealed and clearly identified as a convenient artifact of oblate spheroidal geometry, implying faster numerical integration of GVEs as compared to the basic Keplerian GVEs.

As a generalization of two-body dynamics, Vinti theory is accordingly more complex. Indeed, Vinti theory is no stranger to the inescapable paradigm of complexity increasing with model fidelity, but a number of steps have been taken to counter this disincentive. First, code is provided online to stimulate interest in the Vinti method for both direct application and further research. Secondly, the delineation between coordinate transformation and solution is

197

revisited and scrutinized. The coordinate transformations of Vinti theory are historically entangled in a particular solution method, especially with respect to orbital elements. A different perspective is presented in Chapters 4 and 5 that encourages distinct divisions between the coordinate transformations and the desired solution process. Alongside offering clearer insight to Vinti theory, the overall complexity is distilled while simultaneously creating versatility, where the new equinoctial elements may conceivably be applied to analytical or numerical solutions to the Vinti problem.

6.2   Future Work

With the preceding ideas in mind, some potential research directions are discussed next. First, the following covers a variety of possible short-term efforts:

- The new equinoctial element set can replace the set used in the Vinti-based relative motion model, mitigating singularities in the Jacobians that map to rectangular coordinates. This effort entails deriving new analytical partial derivatives. To facilitate the addition of perturbations, the STM can be developed in terms of the elements tied to the natural Delaunay elements and the bookend Jacobians can be applied if desired.

- The piecewise nonsingular element set establishes a nonsingular Vinti theory, but the corresponding analytical solution for the nearly parabolic and hyperbolic orbit regimes has not been investigated. It is anticipated that the methodology for that regime will be similar to material in Chap-

ter 5 but with some modifications that utilize the element set described in Section 2.5.4. The work should include and test algorithms for obtaining a good initial guess in universal variables. Analytical partials may then also be obtained for these orbit regimes.

- Gauss' variational equations for Vinti theory can be derived for the new equinoctial elements, either the complete elements or the secular ones. These equations stand in contrast to the existing GVEs for Vinti theory, which were developed for the secular classical elements to leverage canonical transformations. Follow-on work can compare timings of numerically integrating Keplerian GVEs versus Vinti-based GVEs and explore the sensitivity of results to J_2. So-called secular GVEs may be preferred as they would be closely tied to mean GVEs should perturbations be added in this manner. These equations are directly applicable to Monte Carlo analyses.

- As sun-synchronous, repeat ground track, and other specialized orbits are common, it would be useful to have algorithms for designing such orbits with Vinti theory. These techniques can be developed with further study.

- With the development of partial derivatives and application to relative motion, a logical next step is to use the natural Delaunay variables to devise linear constraints for invariant orbits under the Vinti potential. When using perturbation methods, notions of osculating elements are often adopted, but they represent a choice of zero gauge velocity, where

in general the gauge velocity can take on different values. This choice constrains the mean element design space. Viewing the Vinti problem as an unperturbed problem, notions of "gauge freedom" do not come into play, so that resulting invariant orbits must necessarily span the entire design space. In contrast, invariant orbits designed with Brouwer's mean elements, for example, span a subset of the design space [68].

A number of more ambitious goals can also be identified:

- Very little work has looked at the boundary value problem for Vinti theory and it would be worthwhile to revisit and test Lavrik's algorithm. Any deficiencies should be identified and improved upon. The successful development of such an algorithm would enable the application of Vinti theory to a variety of mission design problems, such as the optimal debris clean-up problem of GTOC9 that considered oblateness[1]. The concept of "patched Vinti trajectories" may prove useful for certain interplanetary work, particularly near Jupiter and Saturn, where including insertion requires the universal approach described in the short-term goals. Together, the ability and suitability of Vinti theory to replace Keplerian dynamics in preliminary mission design can be assessed.

- The general incorporation of other perturbations can be further investigated, either with Vinti theory or other intermediaries. One option is to push the limits of how many perturbations can be incorporated

---

[1]GTOC9 refers to the 9th Global Trajectory Optimization Competition.

without perturbation methods. The question of how to fit the free parameter of Vinti theory to a gravitational potential should be revisited. One interesting option is to make the free parameter a function of orbit inclination to increase the accuracy of a Vinti trajectory, but other formulations may be devised. There may be various ways to determine the functional relationship, but one option involves a least squares fit process. Fitting directly to J_2 as Vinti did may not be ideal. The effect is dominant, but it seems a least squares fit could better capture some of the qualitative details induced by a gravitational potential that result from the interaction of different harmonics. The procedure can be viewed as a type of pre-fit process. Note that the partials of the nonsingular solution enable this work. The utility of some of the other coordinate systems merit further investigation as well, and follow-on work can look at the triaxial ellipsoidal coordinates, where the larger number of free parameters implies the ability to fit the coordinate system to different perturbations simultaneously.

- Because Vinti theory can be viewed as a general perturbations method, Vinti's solution and the associated STM can also be augmented with other perturbations using the same techniques, such as Lie transforms or von Zeipel's method. Drag perturbations have been given the most attention in the literature, but differential drag has not been investigated. The incorporation of low-order sectoral and tesseral terms along with other zonal harmonics are also of interest.

- The space object catalog was mentioned earlier as a temporary GP application for Vinti theory. Vinti theory may find a more permanent role in initial orbit determination, which is presently performed with Keplerian dynamics. Vinti-based admissible region concepts can be explored, with a goal of generally assessing the utility of Vinti theory for initial orbit determination.

- Revisiting the potential of Aksenov et al. [1] may prove promising. One issue encountered in this dissertation is that Vinti's potential with J_3 is not amenable to the definition of equinoctial elements due to the shift of the origin. It is unfortunate because the solution process with or without J_3 is nearly identical, so that the effects of J_3 are almost obtained for free relative to the lower-fidelity Vinti potential. By using complex masses, the potential of Aksenov et al. [1] can capture J_3 without shifting the origin, implying that it should be possible to use similar techniques to those introduced in Chapter 4 to define equinoctial elements with respect to this potential. The development of an associated analytical solution should follow.

6.3 Concluding Remarks

The development of an analytical, Vinti-based STM and the elimination of singularities in Vinti theory is seen to enable a variety of research directions that can have direct impacts in several important areas of astrodynamics in practice. The common thread is that, despite consistent hardware advances,

these applications continue to leverage analytical solutions while managing to push the boundaries of hardware, typically using Keplerian dynamics. Since these dynamics can be viewed as a special case contained exactly within Vinti theory, it is a small step to consider an upgrade to Vinti dynamics. Ultimately, timing analyses need to be performed on both the results of this dissertation and any future modifications. Nonetheless, the fundamental work in Vinti theory presented in this dissertation has established a firm, broad platform for future work. The absence of singularities and availability of a convenient, familiar nonsingular orbital element set may inspire a renewed interest in Vinti theory, and even intermediaries in general. Intermediaries may be able to fulfill the continued need for analytical solutions in modern astrodynamics applications while injecting a boost in accuracy or speed into existing high-level software tools.

Appendices

Appendix A

Analytical Matrix Inverse for Obtaining the Vinti-based STM in the Spheroidal Element Space

Equation (3.6) establishes the structure of the Jacobian mapping VOEs to the time-varying elements. The analytical inverse transformation is defined in this Appendix. The first three rows of $^ST^V$ are equal to the first three rows of $(^ST^V)^{-1}$ and the sixth column of $^ST^V$ is equal to the sixth column of $(^ST^V)^{-1}$. Thus, similar to Eq. (3.6), the inverse transformation can be expressed as

$$(^ST^V)^{-1} = \begin{bmatrix} 1 & 0 & 0 & 0 & 0 & 0 \\ 0 & 1 & 0 & 0 & 0 & 0 \\ 0 & 0 & 1 & 0 & 0 & 0 \\ T_{41}^{-1} & T_{42}^{-1} & T_{43}^{-1} & T_{44}^{-1} & T_{45}^{-1} & 0 \\ T_{51}^{-1} & T_{52}^{-1} & T_{53}^{-1} & T_{54}^{-1} & T_{55}^{-1} & 0 \\ T_{61}^{-1} & T_{62}^{-1} & T_{63}^{-1} & T_{64}^{-1} & T_{65}^{-1} & 1 \end{bmatrix} \tag{A.1}$$

The 15 elements of the remaining three rows of $(^ST^V)^{-1}$ are determined as follows. First, define the common denominator D used in the elements of the inverse as

$$D = T_{55}T_{44} - T_{45}T_{54}$$

Then, the elements of the matrix inverse can be expressed as

$$T_{41}^{-1} = \frac{T_{45}T_{51} - T_{41}T_{55}}{D}; \quad T_{42}^{-1} = \frac{T_{45}T_{52} - T_{42}T_{55}}{D}; \quad T_{43}^{-1} = \frac{T_{45}T_{53} - T_{43}T_{55}}{D};$$

$$T_{44}^{-1} = \frac{T_{55}}{D}; \quad T_{45}^{-1} = -\frac{T_{45}}{D};$$

$$T_{51}^{-1} = \frac{T_{54}T_{41} - T_{44}T_{51}}{D}; \quad T_{52}^{-1} = \frac{T_{54}T_{42} - T_{44}T_{52}}{D}; \quad T_{53}^{-1} = \frac{T_{54}T_{43} - T_{44}T_{53}}{D};$$

$$T_{54}^{-1} = -\frac{T_{54}}{D}; \quad T_{55}^{-1} = \frac{T_{44}}{D};$$

$$T_{61}^{-1} = \frac{(T_{41}T_{55} - T_{45}T_{51})T_{64} - (T_{54}T_{41} - T_{44}T_{51})T_{65}}{D} - T_{61};$$

$$T_{62}^{-1} = \frac{(T_{42}T_{55} - T_{45}T_{52})T_{64} - (T_{54}T_{42} - T_{44}T_{52})T_{65}}{D} - T_{62};$$

$$T_{63}^{-1} = \frac{(T_{43}T_{55} - T_{45}T_{53})T_{64} - (T_{54}T_{43} - T_{44}T_{53})T_{65}}{D} - T_{63};$$

$$T_{64}^{-1} = \frac{T_{54}T_{65} - T_{55}T_{64}}{D}; \quad T_{65}^{-1} = -\frac{T_{44}T_{65} - T_{45}T_{64}}{D}$$

Appendix B

Basis Vectors and Coordinates

This Appendix is intended to provide supplementary background material on topics related to Vinti theory. Some of the concepts are not found elsewhere, such as pertain to oblate spheroidal coordinates. Additionally, a review of coordinate transformations is presented to facilitate drawing analogies between Vinti theory and the two-body problem. Readers can easily compare and contrast various spherical and oblate spheroidal orbital elements, including classical, quasi-nonsingular, and equinoctial elements. Delaunay variables are presented as well. The reader is referred to Vinti's papers for comprehensive details of the essentials of Vinti theory and Vinti's analytical solution.

B.1 Properties of Oblate Spheroidal Coordinates with Descriptions of Position and Velocity

The oblate spheroidal coordinates implicitly define a unique rotating reference frame analogous to how spherical coordinates are associated with a different rotating reference frame. In orbital mechanics applications, these frames essentially track the spacecraft position, i.e. the frame's rotation is connected to the spacecraft motion. For a right-handed coordinate system, the order of the orthogonal OS basis vectors is $\{\hat{\boldsymbol{\rho}}, \hat{\boldsymbol{\phi}}, \hat{\boldsymbol{\eta}}\}$, where $\hat{\boldsymbol{\rho}}$ is the normal to

the tangent spheroid's surface at the tangent point, $\hat{\boldsymbol{\phi}}$ is tangent to the tangent spheroid's surface at the tangent point and parallel to the XY or equatorial plane, and $\hat{\boldsymbol{\eta}} = \hat{\boldsymbol{\rho}} \times \hat{\boldsymbol{\phi}}$ completes the triad. Note that $\hat{\boldsymbol{\eta}}$ is also tangent to the tangent spheroid's surface, pointing in a slightly different direction from the latitudinal unit vector. The $\hat{\boldsymbol{\phi}}$ vector is identical to the longitudinal unit vector.

B.1.1 OS Basis Vectors

The unit vectors of the OS reference frame are defined in terms of those of the inertial frame as

$$\hat{\boldsymbol{\rho}} = \frac{\rho\sqrt{1-\eta^2}\cos\phi}{\sqrt{\rho^2+c^2\eta^2}}\hat{\mathbf{X}} + \frac{\rho\sqrt{1-\eta^2}\sin\phi}{\sqrt{\rho^2+c^2\eta^2}}\hat{\mathbf{Y}} + \frac{\eta\sqrt{\rho^2+c^2}}{\sqrt{\rho^2+c^2\eta^2}}\hat{\mathbf{Z}} \tag{B.1}$$

$$\hat{\boldsymbol{\phi}} = -\sin\phi\,\hat{\mathbf{X}} + \cos\phi\,\hat{\mathbf{Y}} \tag{B.2}$$

$$\hat{\boldsymbol{\eta}} = -\frac{\eta\sqrt{\rho^2+c^2}\cos\phi}{\sqrt{\rho^2+c^2\eta^2}}\hat{\mathbf{X}} - \frac{\eta\sqrt{\rho^2+c^2}\sin\phi}{\sqrt{\rho^2+c^2\eta^2}}\hat{\mathbf{Y}} + \frac{\rho\sqrt{1-\eta^2}}{\sqrt{\rho^2+c^2\eta^2}}\hat{\mathbf{Z}} \tag{B.3}$$

The definition can be written compactly in matrix form as

$$\begin{bmatrix} \hat{\boldsymbol{\rho}} \\ \hat{\boldsymbol{\phi}} \\ \hat{\boldsymbol{\eta}} \end{bmatrix} = \begin{bmatrix} \dfrac{\rho\sqrt{1-\eta^2}\cos\phi}{\sqrt{\rho^2+c^2\eta^2}} & \dfrac{\rho\sqrt{1-\eta^2}\sin\phi}{\sqrt{\rho^2+c^2\eta^2}} & \dfrac{\eta\sqrt{\rho^2+c^2}}{\sqrt{\rho^2+c^2\eta^2}} \\ -\sin\phi & \cos\phi & 0 \\ -\dfrac{\eta\sqrt{\rho^2+c^2}\cos\phi}{\sqrt{\rho^2+c^2\eta^2}} & -\dfrac{\eta\sqrt{\rho^2+c^2}\sin\phi}{\sqrt{\rho^2+c^2\eta^2}} & \dfrac{\rho\sqrt{1-\eta^2}}{\sqrt{\rho^2+c^2\eta^2}} \end{bmatrix} \begin{bmatrix} \hat{\mathbf{X}} \\ \hat{\mathbf{Y}} \\ \hat{\mathbf{Z}} \end{bmatrix}$$

B.1.2 Time Derivatives of the OS Basis Vectors

Naturally, the time derivatives of the OS basis vectors possess singularities at the poles. Nevertheless, they are presented for completeness.

$$\dot{\hat{\boldsymbol{\rho}}} = \frac{\rho\dot{\phi}\sqrt{1-\eta^2}}{\sqrt{\rho^2+c^2\eta^2}}\hat{\boldsymbol{\phi}} + \frac{1}{\rho^2+c^2\eta^2}\left(\frac{\rho\dot{\eta}\sqrt{\rho^2+c^2}}{\sqrt{1-\eta^2}} - \frac{c^2\eta\dot{\rho}\sqrt{1-\eta^2}}{\sqrt{\rho^2+c^2}}\right)\hat{\boldsymbol{\eta}} \qquad \text{(B.4)}$$

$$\dot{\hat{\boldsymbol{\phi}}} = -\frac{\rho\dot{\phi}\sqrt{1-\eta^2}}{\sqrt{\rho^2+c^2\eta^2}}\hat{\boldsymbol{\rho}} + \frac{\eta\dot{\phi}\sqrt{\rho^2+c^2}}{\sqrt{\rho^2+c^2\eta^2}}\hat{\boldsymbol{\eta}} \qquad \text{(B.5)}$$

$$\dot{\hat{\boldsymbol{\eta}}} = -\frac{1}{\rho^2+c^2\eta^2}\left(\frac{\rho\dot{\eta}\sqrt{\rho^2+c^2}}{\sqrt{1-\eta^2}} - \frac{c^2\eta\dot{\rho}\sqrt{1-\eta^2}}{\sqrt{\rho^2+c^2}}\right)\hat{\boldsymbol{\rho}} - \frac{\rho\dot{\phi}\sqrt{1-\eta^2}}{\sqrt{\rho^2+c^2\eta^2}}\hat{\boldsymbol{\phi}} \qquad \text{(B.6)}$$

The author is not aware of existing literature containing these equations.

B.1.3 Spacecraft Position and Velocity

The expressions for spacecraft position and body-fixed velocity in terms of OS coordinates are presented here for the first time, along with a new derivation of the inertial velocity in OS coordinates. With the above definitions, the position and velocity can be described entirely in terms of the OS basis vectors, where the shift z_δ is now relevant if $J_3 \neq 0$. The spacecraft position in the rotating OS frame can be expressed as

$$\mathbf{r}_{OS} = {}^{OS}\begin{bmatrix} \dfrac{(\rho - \eta z_\delta)\sqrt{\rho^2+c^2}}{\sqrt{\rho^2+c^2\eta^2}} \\ 0 \\ -\dfrac{(c^2\eta - \rho z_\delta)\sqrt{1-\eta^2}}{\sqrt{\rho^2+c^2\eta^2}} \end{bmatrix} \qquad \text{(B.7)}$$

which has no singularities. The position magnitude or radial distance can be obtained as

$$\|\mathbf{r}_{OS}\| = \sqrt{\rho^2 + c^2\left(1 - \eta^2\right) + z_\delta\left(z_\delta - 2\rho\eta\right)} \tag{B.8}$$

The expressions for velocity have singularities on the poles, but are nonetheless defined as follows. The body-fixed velocity (in the rotating OS frame) is given by

$$
{}^R\mathbf{v}_{OS} =
\begin{bmatrix}
\dfrac{\left(\dot{\rho} - \dot{\eta}z_\delta\right)\left(\rho^2 + c^2\right)^{1/2}}{\left(\rho^2 + c^2\eta^2\right)^{1/2}} \\[2ex]
-\dfrac{c^2\left(\rho - \eta z_\delta\right)\left[\rho\dot{\rho}\left(1 - \eta^2\right) + \eta\dot{\eta}\left(\rho^2 + c^2\right)\right]}{\left(\rho^2 + c^2\right)^{1/2}\left(\rho^2 + c^2\eta^2\right)^{3/2}} \\[2ex]
0 \\[2ex]
-\dfrac{\left(c^2\dot{\eta} - \dot{\rho}z_\delta\right)\left(1 - \eta^2\right)^{1/2}}{\left(\rho^2 + c^2\eta^2\right)^{1/2}} \\[2ex]
+\dfrac{\left(c^2\eta - \rho z_\delta\right)\left[\rho\dot{\rho}\left(1 - \eta^2\right) + \eta\dot{\eta}\left(\rho^2 + c^2\right)\right]}{\left(1 - \eta^2\right)^{1/2}\left(\rho^2 + c^2\eta^2\right)^{3/2}}
\end{bmatrix}^{OS} \tag{B.9}
$$

The inertial velocity represented in the OS basis vectors can be derived from the product rule

$$
{}^N\mathbf{v}_{OS} = {}^R\mathbf{v}_{OS} + r_\rho\dot{\hat{\boldsymbol{\rho}}} + r_\eta\dot{\hat{\boldsymbol{\eta}}} \tag{B.10}
$$

and is given by

$$
{}^N\mathbf{v}_{OS} = {}^N\dot{\mathbf{r}}_{OS} =
\begin{bmatrix}
\dfrac{\dot{\rho}\sqrt{\rho^2 + c^2\eta^2}}{\sqrt{\rho^2 + c^2}} \\[2ex]
\dot{\phi}\sqrt{\left(\rho^2 + c^2\right)\left(1 - \eta^2\right)} \\[2ex]
\dfrac{\dot{\eta}\sqrt{\rho^2 + c^2\eta^2}}{\sqrt{1 - \eta^2}}
\end{bmatrix}^{OS} \tag{B.11}
$$

Notice that the inertial velocity is independent of z_δ, the translation of the origin of the OS frame along the Z axis.

B.2 Coordinate Transformations

A number of coordinate transformations used in or relevant to this dissertation are presented in this section for convenience. The focus is on mappings between ECI coordinates and various spherical orbital element sets. The element sets considered include the equinoctial set and spherical Delaunay variables.

B.2.1 Converting ECI Coordinates to Spherical Equinoctial Orbital Elements

The algorithms in the next two sections mostly follow those presented by Danielson et al. [42], but with extra commentary that compares these processes to the oblate spheroidal elements. The six modified spherical equinoctial orbital elements are described as follows using the notation of Gim and Alfriend [65] for the vector components:

$$
\begin{aligned}
&\text{œ}_{K_1} = p_K && \text{spherical semi-latus rectum} \\
&\text{œ}_{K_2} = q_{K_1} \\
&\text{œ}_{K_3} = q_{K_2} && \left.\vphantom{\begin{matrix}a\\a\end{matrix}}\right\} \text{ components of the spherical eccentricity vector} \\
&\text{œ}_{K_4} = p_{K_1} && \left.\vphantom{\begin{matrix}a\\a\end{matrix}}\right\} \text{ components of the spherical ascending} \\
&\text{œ}_{K_5} = p_{K_2} && \text{node vector} \\
&\text{œ}_{K_6} = L_K && \text{spherical true longitude}
\end{aligned}
\tag{B.12}
$$

The spherical equinoctial elements are defined in terms of the spherical classical elements as

$$p_K = p_K$$

$$q_{K_1} = e_K \cos\left(\omega_K + K\Omega_K\right)$$

$$q_{K_2} = e_K \sin\left(\omega_K + K\Omega_K\right)$$

$$p_{K_1} = \left[\tan\left(\frac{I_K}{2}\right)\right]^K \cos\Omega_K \tag{B.13}$$

$$p_{K_2} = \left[\tan\left(\frac{I_K}{2}\right)\right]^K \sin\Omega_K$$

$$L_K = f_K + \omega_K + K\Omega_K$$

where K is a retrograde factor defined as

$$K = \begin{cases} +1 & \text{direct spherical equinoctial elements} \\ -1 & \text{retrograde spherical equinoctial elements} \end{cases} \tag{B.14}$$

As before, and throughout the dissertation, when K is used as a subscript, it denotes Keplerian or spherical orbital elements of any variety.

Suppose now that ECI coordinates are given as position vector $\mathbf{r}$ and velocity vector $\mathbf{v}$. The first step in the conversion process is to compute the angular momentum $\mathbf{h}$ as

$$\mathbf{h} = \mathbf{r} \times \mathbf{v} \tag{B.15}$$

With $h = \|\mathbf{h}\|$, the semi-latus rectum is computed as

$$p_K = \frac{h^2}{\mu} \tag{B.16}$$

The semimajor axis could be computed instead as

$$a_K = \frac{1}{\dfrac{2}{r} - \dfrac{v^2}{\mu}} \tag{B.17}$$

212

where $r = \|\mathbf{r}\|$ and $v = \|\mathbf{v}\|$, but a_K is not well-behaved for all orbits, tending to infinity for parabolic orbits when the energy, or half the denominator in Eq. (B.17), goes to zero.

Next, compute the basis vectors $\{\hat{\mathbf{f}}_K, \hat{\mathbf{g}}_K, \hat{\mathbf{w}}_K\}$ of the spherical equinoctial reference frame. The $\hat{\mathbf{w}}_K$ vector points along the direction of the angular momentum vector and is obtained simply by normalizing $\mathbf{h}$ as

$$\hat{\mathbf{w}}_K = \frac{\mathbf{h}}{h} \tag{B.18}$$

The elements p_{K_1} and p_{K_2} are determined from the components of $\hat{\mathbf{w}}_K$ as

$$
\begin{aligned}
p_{K_1} &= -\frac{w_{K_y}}{1 + K w_{K_z}} \\
p_{K_2} &= +\frac{w_{K_x}}{1 + K w_{K_z}}
\end{aligned}
\tag{B.19}
$$

The components of the ascending node vector are now obtained, but the other basis vectors, $\hat{\mathbf{f}}_K$ and $\hat{\mathbf{g}}_K$, are required for computing the true longitude and the components of the eccentricity vector. Those basis vectors are given by

$$
\begin{aligned}
\hat{\mathbf{f}}_K &= \frac{1}{1 + p_{K_1}^2 + p_{K_2}^2} \begin{bmatrix} 1 + p_{K_1}^2 - p_{K_2}^2 \\ 2 p_{K_1} p_{K_2} \\ -2 K p_{K_2} \end{bmatrix} \\
\hat{\mathbf{g}}_K &= \frac{1}{1 + p_{K_1}^2 + p_{K_2}^2} \begin{bmatrix} 2 K p_{K_1} p_{K_2} \\ \left(1 - p_{K_1}^2 + p_{K_2}^2\right) K \\ -2 p_{K_1} \end{bmatrix}
\end{aligned}
\tag{B.20}
$$

The third step is to compute the components of the eccentricity vector. First obtain the eccentricity vector as

$$\mathbf{e}_K = \frac{\mathbf{v} \times \mathbf{h}}{\mu} - \frac{\mathbf{r}}{r} \tag{B.21}$$

Its components are then computed from a simple dot product as

$$q_{K_1} = \mathbf{e}_K \cdot \hat{\mathbf{f}}_K$$
$$q_{K_2} = \mathbf{e}_K \cdot \hat{\mathbf{g}}_K$$
(B.22)

The fourth and final step is to compute the spherical true longitude L_K. An instructive and simplifying interpretation of the spherical equinoctial elements is that the position coordinates of a spacecraft in the equinoctial reference frame are given by

$$X_K = \mathbf{r} \cdot \hat{\mathbf{f}}_K$$
$$Y_K = \mathbf{r} \cdot \hat{\mathbf{g}}_K$$
(B.23)

where Z_K is obviously zero because all motion occurs in an invariant plane. The true longitude is then determined as

$$L_K = \arctan\left(\frac{Y_K}{X_K}\right)$$
(B.24)

The coordinate transformation is now complete, and this particular set is free from singularities for any conic. If desired or required, additional steps can be taken to compute the eccentric longitude F_K and the mean longitude λ_K, but these quantities are not well-defined for nearly parabolic orbits. For closed orbits, compute the eccentric longitude from

$$\cos F_K = q_{K_1} + \frac{\left(1 - q_{K_1}^2 b_K\right) Y_K - q_{K_1} q_{K_2} b_K X_K}{a_K \sqrt{1 - e_K^2}}$$
$$\sin F_K = q_{K_2} + \frac{\left(1 - q_{K_2}^2 b_K\right) X_K - q_{K_1} q_{K_2} b_K Y_K}{a_K \sqrt{1 - e_K^2}}$$
(B.25)

where $e_K = \|\mathbf{e}_K\|$ is the Keplerian eccentricity and

$$b_K = \frac{1}{1 + \sqrt{1 - e_K^2}}$$
(B.26)

The mean longitude is then determined from the equinoctial form of Kepler's equation as

$$\lambda_K = F_K - q_{K_1} \sin F_K + q_{K_2} \cos F_K \tag{B.27}$$

B.2.2 Converting Spherical Equinoctial Orbital Elements to ECI Coordinates

The first step is to apply Eq. (B.20) to compute $\hat{\mathbf{f}}_K$ and $\hat{\mathbf{g}}_K$ from p_{K_1} and p_{K_2}. If mean longitude is given, the next step is to iteratively solve the equinoctial form of Kepler's equation, given earlier as Eq. (B.27), by any desired method. Examples include the Newton-Raphson method, Laguerre's method, and Halley's method. Once the eccentric longitude is obtained, the true longitude can be computed from

$$
\begin{aligned}
\cos L_K &= \frac{\left(1 - q_{K_2}^2 b_K\right) \cos F_K + q_{K_1} q_{K_2} b_K \sin F_K - q_{K_1}}{1 - q_{K_1} \cos F_K - q_{K_2} \sin F_K} \\
\sin L_K &= \frac{\left(1 - q_{K_1}^2 b_K\right) \sin F_K + q_{K_1} q_{K_2} b_K \cos F_K - q_{K_2}}{1 - q_{K_1} \cos F_K - q_{K_2} \sin F_K}
\end{aligned}
\tag{B.28}
$$

The third step is to determine the spacecraft's position and velocity coordinates in the spherical equinoctial reference frame. Compute the spacecraft's radial distance as

$$r = \frac{p_K}{1 + q_{K_1} \cos L_K + q_{K_2} \sin L_K} = a_K \left(1 - q_{K_1} \cos F_K - q_{K_2} \sin F_K\right) \tag{B.29}$$

Then obtain the position coordinates as

$$
\begin{aligned}
X_K &= r \cos L_K = a_K \left[\left(1 - q_{K_2}^2 b_K\right) \cos F_K + q_{K_1} q_{K_2} b_K \sin F_K - q_{K_1}\right] \\
Y_K &= r \sin L_K = a_K \left[\left(1 - q_{K_1}^2 b_K\right) \sin F_K + q_{K_1} q_{K_2} b_K \cos F_K - q_{K_2}\right]
\end{aligned}
\tag{B.30}
$$

and the velocity coordinates as

$$
\begin{aligned}
\dot{X}_K &= -\sqrt{\frac{\mu}{p_K}}\left(q_{K_2} + \sin L_K\right) \\
&= \frac{n_K a_K^2}{r}\left[-\left(1 - q_{K_2}^2 b_K\right)\sin F_K + q_{K_1} q_{K_2} b_K \cos F_K\right] \\
\dot{Y}_K &= +\sqrt{\frac{\mu}{p_K}}\left(q_{K_1} + \cos L_K\right) \\
&= \frac{n_K a_K^2}{r}\left[\left(1 - q_{K_1}^2 b_K\right)\cos F_K - q_{K_1} q_{K_2} b_K \sin F_K\right]
\end{aligned}
\tag{B.31}
$$

where

$$
n_K = \sqrt{\frac{\mu}{a_K^3}}
\tag{B.32}
$$

is the Keplerian mean motion. Again, the components in the Z_K direction are clearly zero.

The fourth and final step is to determine the position and velocity vectors. Compared to oblate spheroidal equinoctial elements, the equations for this step are especially simple:

$$
\begin{aligned}
\mathbf{r} &= X_K \hat{\mathbf{f}}_K + Y_K \hat{\mathbf{g}}_K \\
\mathbf{v} &= \dot{X}_K \hat{\mathbf{f}}_K + \dot{Y}_K \hat{\mathbf{g}}_K
\end{aligned}
\tag{B.33}
$$

B.2.3   Spherical Delaunay Variables

The derivation and transformation presented in this section mostly follows the approach taken by Der and Bonavito [50], but with some extra commentary that compares these processes to those required for oblate spheroidal elements. The spherical Delaunay variables result from a particular canonical transformation applied to the Jacobi constants (α's and β's) of the two-body problem. As such, it is not necessary to have conversion algorithms that

map between rectangular coordinates and Delaunay variables. The canonical transformation itself is of primary interest along with the mapping between spherical Delaunay variables and the classical spherical orbital elements. For a Keplerian reference, it is not necessary to derive them from action and angle variables as Vinti did for the spheroidal method.

Beginning with generalized coordinates $\mathbf{q}$ and conjugate (generalized) momenta $\mathbf{p}$ in Cartesian or spherical coordinates, an application of Hamilton-Jacobi theory to a Keplerian reference Hamiltonian yields new canonical variables $\mathbf{P} = \boldsymbol{\alpha}$ as the new momenta and $\mathbf{Q} = \boldsymbol{\beta}$ as the new coordinates. If the α's and β's are adopted as the canonical variables on which a perturbation theory is constructed, then nonphysical Poisson terms appear in the solution. Nonphysical terms do not appear if Delaunay variables are adopted instead, hence their common use. Let the Hamiltonian of the perturbed problem be expressed as

$$\mathcal{H} = \mathcal{H}_0 + \mathcal{H}_1 \tag{B.34}$$

where $\mathcal{H}_0 = \mathcal{H}_0\left(\mathbf{Q}, \mathbf{P}\right)$ is the reference, unperturbed Hamiltonian and $\mathcal{H}_1 = \mathcal{H}_1\left(\mathbf{Q}, \mathbf{P}, t\right)$ is the perturbing Hamiltonian. Since $\mathcal{H}_0$ is independent of time, $\mathcal{H}_0 = \alpha_1$. The α's and β's are canonical with respect to the new Hamiltonian $\mathcal{K} = 0$ for the unperturbed problem or

$$\mathcal{K} = \mathcal{H}_1 \tag{B.35}$$

for the perturbed problem. Alternatively, with a sign reversal,

$$\mathcal{F} = -\mathcal{K} = -\mathcal{H}_1 = \mathcal{F}_1 \tag{B.36}$$

217

and the equations of motion reduce to the following simple form:

$$\dot{\boldsymbol{\alpha}}^\top = -\frac{\partial \mathcal{K}}{\partial \boldsymbol{\beta}} = -\frac{\partial \mathcal{H}_1}{\partial \boldsymbol{\beta}} = +\frac{\partial \mathcal{F}_1}{\partial \boldsymbol{\beta}} \tag{B.37}$$

$$\dot{\boldsymbol{\beta}}^\top = +\frac{\partial \mathcal{K}}{\partial \boldsymbol{\alpha}} = +\frac{\partial \mathcal{H}_1}{\partial \boldsymbol{\alpha}} = -\frac{\partial \mathcal{F}_1}{\partial \boldsymbol{\alpha}} \tag{B.38}$$

Note the adoption of Delaunay's convention

$$\mathcal{F} = -\mathcal{K} \tag{B.39}$$

that reverses the sign of the new Hamiltonian. The only real effect of the sign reversal is that the mathematical interpretation of the α's and β's are swapped. While the α's and β's are now mathematically "coordinates" and "momenta", respectively, they are physically still momenta and coordinates.

The generating function has the particular form $S' = S'(\mathbf{Q}, \mathbf{P}', t) = S'(\boldsymbol{\alpha}, \boldsymbol{\beta}', t)$, noting the mathematical swapping between coordinates and momenta, and is given by

$$S' = -\alpha_1 t + \mu \left(-2\alpha_1\right)^{-1/2} \beta_1' + \alpha_2 \beta_2' + \alpha_3 \beta_3' \tag{B.40}$$

where, in general, $\mu = G\left(m_1 + m_2\right)$ and G is the universal constant of gravitation. Equation (B.40) can be found in many references [156]. The canonical transformation associated with this generating function is given by the mapping

$$\mathbf{P}^\top = \boldsymbol{\beta}^\top = \frac{\partial S'}{\partial \boldsymbol{\alpha}} = \frac{\partial S'}{\partial \mathbf{Q}} \tag{B.41}$$

$$\mathbf{Q}'^\top = \boldsymbol{\alpha}'^\top = \frac{\partial S'}{\partial \boldsymbol{\beta}'} = \frac{\partial S'}{\partial \mathbf{P}'} \tag{B.42}$$

218

where $\mathbf{Q}'$ and $\mathbf{P}'$ are canonical with respect to the new Hamiltonian $\mathcal{K}' = \alpha_1$ for the unperturbed problem or

$$\mathcal{K}' = \mathcal{K} - \frac{\partial S'}{\partial t} = \mathcal{H}_1 + \alpha_1 \tag{B.43}$$

for the perturbed problem, so that

$$\mathcal{F}' = -\mathcal{K}' = -\mathcal{K} + \frac{\partial S'}{\partial t} = \mathcal{F} + \frac{\partial S'}{\partial t} = \mathcal{F}_1 + \frac{\partial S'}{\partial t} = \mathcal{F}_1 - \alpha_1 \tag{B.44}$$

The Delaunay Hamiltonian for the perturbed problem is

$$\mathcal{F}' = \mathcal{F}_1 + \frac{\partial S'}{\partial t} = \mathcal{F}_1 - \alpha_1 \tag{B.45}$$

The new α's and β's (with prime symbols) have the following relationships to the old α's and β's:

$$\begin{array}{ll} \beta_1 = -t + \mu \left(-2\alpha_1\right)^{-3/2} \beta_1' & \alpha_1' = \mu \left(-2\alpha_1\right)^{-1/2} \\ \beta_2 = \beta_2' & \alpha_2' = \alpha_2 \\ \beta_3 = \beta_3' & \alpha_3' = \alpha_3 \end{array} \tag{B.46}$$

Equation (B.46) can be rewritten in Delaunay's notation as

$$\begin{array}{ll} L_K = \alpha_1' = \sqrt{\mu a_K} & \ell_K = \beta_1' = n_K \left(t + \beta_1\right) \\ G_K = \alpha_2' = \sqrt{\mu a_K \left(1 - e_K^2\right)} & g_K = \beta_2' = \omega_K \\ H_K = \alpha_3' = \sqrt{\mu a_K \left(1 - e_K^2\right)} \cos I_K & h_K = \beta_3' = \Omega_K \end{array} \tag{B.47}$$

where

$$n_K = \sqrt{\frac{\mu}{a_K^3}} \tag{B.48}$$

is the Keplerian mean motion. The K subscripts are added to distinguish these elements from the spheroidal elements employed throughout the dissertation. The Delaunay Hamiltonian becomes

$$\mathcal{F}' = \frac{\mu^2}{2L_K^2} + \mathcal{F}_1 \tag{B.49}$$

Appendix C

New Nonsingular Partial Derivatives

This Appendix gives explicit expressions for all new nonsingular partial derivatives of Vinti's solution to the Vinti problem. The partials are based on the 1966 potential, which shifts the origin of the OS reference frame to capture J_3 effects.

C.1 Nonsingular Partials Related to the Constant b_2

The following relation for $b_2 \cdot \partial b_2 / \partial \sigma_j$ should be used in all partial derivative expressions where it appears:

$$b_2 \frac{\partial b_2}{\partial \sigma_j} = \frac{1}{2a} \left[(ap - c^2) \left(\frac{b_1}{a} \delta_{1j} - \frac{\partial b_1}{\partial \sigma_j} \right) - b_1 \left(p \delta_{1j} + a \frac{\partial p}{\partial \sigma_j} \right) \right] \qquad \text{(C.1)}$$

The term appears in equations for partials of p_0, L_m, A_{jk}, $\dot{\rho}$, and $\dot{f}$. The expressions containing $\partial / \partial \sigma_j (b_2/p)$ and $\partial / \partial \sigma_j (b_1/b_2)$ in the equations for $\partial A_k / \partial \sigma_j$ are replaced with the following. First, define

$$L_m \equiv \left(\frac{b_2}{p} \right)^m P_m \left(\frac{b_1}{b_2} \right) = \frac{1}{(2p)^m} \sum_{k=0}^{[m/2]} \frac{(-1)^k (2m - 2k)!}{k!(m-k)!(m-2k)!} b_1^{m-2k} b_2^{2k} \qquad \text{(C.2)}$$

where

$$[m/2] = \begin{cases} m/2, & \text{if } m \text{ even} \\ (m-1)/2, & \text{if } m \text{ odd} \end{cases}$$

220

For $j = 1, 2, 3$, the partials of L_m can be expressed as

$$\frac{\partial L_m}{\partial \sigma_j} = -\frac{m L_m}{p} \frac{\partial p}{\partial \sigma_j} + \frac{1}{(2p)^m} \sum_{k=0}^{[m/2]} \frac{(-1)^k (2m - 2k)!}{k!(m-k)!(m-2k)!}$$

$$\times \left[(m - 2k) b_1^{m-2k-1} b_2^{2k} \frac{\partial b_1}{\partial \sigma_j} + (2k) b_1^{m-2k} b_2^{2k-1} \frac{\partial b_2}{\partial \sigma_j} \right] \qquad \text{(C.3)}$$

Then, for $m > 0$, define

$$\hat{L}_m \equiv \frac{1}{(2p)^m} \sum_{k=0}^{[m/2]} \frac{(-1)^k (2m - 2k)!}{k!(m-k)!(m-2k-1)!} b_1^{m-2k-1} b_2^{2k} \qquad \text{(C.4)}$$

With this definition, it can be shown that the recursive relationship

$$\frac{\partial L_m}{\partial \sigma_j} = -\frac{m L_m}{p} \frac{\partial p}{\partial \sigma_j} + \hat{L}_m \frac{\partial b_1}{\partial \sigma_j} - \hat{L}_{m-1} b_2 \frac{\partial b_2}{\partial \sigma_j} \qquad \text{(C.5)}$$

is equivalent to Eq. (C.3), with $\hat{L}_0 = 0$. Accordingly, the new expressions for $\partial A_k / \partial \sigma_j$ are now presented. For $j = 1, 2, 3$,

$$\frac{\partial A_1}{\partial \sigma_j} = \frac{A_1}{p} \frac{\partial p}{\partial \sigma_j} - \delta_{2j} A_1 \frac{e}{1 - e^2} + p(1 - e^2)^{\frac{1}{2}} \sum_{n=2}^{\infty} \frac{\partial L_n}{\partial \sigma_j} R_{n-2} \left[(1 - e^2)^{\frac{1}{2}} \right]$$

$$+ \delta_{2j} pe \left\{ (1 - e^2)^{-1} \sum_{n=3}^{\infty} \left[(1 - e^2)^{\frac{1}{2}} \right]^{n-2} L_n P'_{n-2} \left[(1 - e^2)^{-\frac{1}{2}} \right] \right. \qquad \text{(C.6)}$$

$$\left. - (1 - e^2)^{-\frac{1}{2}} \sum_{n=3}^{\infty} (n - 2) L_n R_{n-2} \left[(1 - e^2)^{-\frac{1}{2}} \right] \right\}$$

$$\frac{\partial A_2}{\partial \sigma_j} = -\frac{A_2}{p} \frac{\partial p}{\partial \sigma_j} - \delta_{2j} A_2 \frac{e}{1 - e^2} + \frac{(1 - e^2)^{\frac{1}{2}}}{p} \sum_{n=1}^{\infty} \frac{\partial L_n}{\partial \sigma_j} R_n \left[(1 - e^2)^{\frac{1}{2}} \right]$$

$$+ \delta_{2j} \frac{e}{p} \left\{ (1 - e^2)^{-1} \sum_{n=1}^{\infty} \left[(1 - e^2)^{\frac{1}{2}} \right]^n L_n P'_n \left[(1 - e^2)^{-\frac{1}{2}} \right] \right. \qquad \text{(C.7)}$$

$$\left. - (1 - e^2)^{-\frac{1}{2}} \sum_{n=1}^{\infty} n L_n R_n \left[(1 - e^2)^{-\frac{1}{2}} \right] \right\}$$

221

$$\frac{\partial A_3}{\partial \sigma_j} = -\frac{3A_3}{p}\frac{\partial p}{\partial \sigma_j} - \delta_{2j}A_3\frac{e}{1-e^2}$$
$$+ \frac{(1-e^2)^{\frac{1}{2}}}{p^3}\sum_{n=1}^{\infty}\frac{\partial D_n}{\partial \sigma_j}R_{n+2}\left[(1-e^2)^{\frac{1}{2}}\right]$$
$$+ \delta_{2j}\frac{e}{p^3}\left\{(1-e^2)^{-1}\sum_{n=0}^{\infty}\left[(1-e^2)^{\frac{1}{2}}\right]^{n+2}D_nP'_{n+2}\left[(1-e^2)^{-\frac{1}{2}}\right]\right.$$
$$\left. - (1-e^2)^{-\frac{1}{2}}\sum_{n=0}^{\infty}(n+2)D_nR_{n+2}\left[(1-e^2)^{-\frac{1}{2}}\right]\right\} \tag{C.8}$$

where $P'_m(x)$ is the derivative of the Legendre polynomial with respect to the argument and

$$D_n = \begin{cases} D_{2k} = \sum_{m=0}^{k}(-1)^{k-m}\left(\frac{c}{p}\right)^{2(k-m)}L_{2m} & \text{if } m \text{ even} \\ D_{2k+1} = \sum_{m=0}^{k}(-1)^{k-m}\left(\frac{c}{p}\right)^{2(k-m)}L_{2m+1} & \text{if } m \text{ odd} \end{cases} \tag{C.9}$$

A recursive option for computing the derivative of $P'_{m+1}(x)$ is given by

$$P'_{m+1}(x) = (m+1)P_m(x) + xP'_m(x) \tag{C.10}$$

Notice that in the third line of each of Eqs. (C.6), (C.7), and (C.8), the expression has been simplified from its original form through the use of the $R_m(x)$ function. The new partials of D_n, for $j = 1, 2, 3$, become

$$\frac{\partial D_n}{\partial \sigma_j} = \frac{\partial D_{2k}}{\partial \sigma_j} = -2\left[\frac{1}{p}\sum_{m=0}^{k}(-1)^{k-m}(k-m)\left(\frac{c}{p}\right)^{2(k-m)}L_{2m}\right]$$
$$\times \frac{\partial p}{\partial \sigma_j} + \sum_{m=0}^{k}(-1)^{k-m}\left(\frac{c}{p}\right)^{2(k-m)}\frac{\partial L_{2m}}{\partial \sigma_j} \tag{C.11}$$

for even n and

$$\frac{\partial D_n}{\partial \sigma_j} = \frac{\partial D_{2k+1}}{\partial \sigma_j} = -2\left[\frac{1}{p}\sum_{m=0}^{k}(-1)^{k-m}(k-m)\left(\frac{c}{p}\right)^{2(k-m)}L_{2m+1}\right]$$
$$\times \frac{\partial p}{\partial \sigma_j} + \sum_{m=0}^{k}(-1)^{k-m}\left(\frac{c}{p}\right)^{2(k-m)}\frac{\partial L_{2m+1}}{\partial \sigma_j} \tag{C.12}$$

for odd n.

C.2 Removing Artificial Singularities in the Partials of True Anomaly

The partial derivatives that Walden and Watson [164] derived for the periodic terms of the true anomaly, f_0, f_1, and f_2, contain singularities when the associated true anomaly, f', f'', or f, is 0 or π. New partial derivatives are presented here that avoid the singularity of dividing the sine of eccentric anomaly by the sine of true anomaly.

The partials of the zeroth order term, for $j = 1, 2, 3$, are determined as

$$\frac{\partial f_0}{\partial \sigma_j} = \frac{\sqrt{1 - e^2}}{1 - e \cos E'} \frac{\partial E'}{\partial \sigma_j} + \delta_{2j} \frac{\sin f'}{1 - e^2} - \frac{\partial M_s}{\partial \sigma_j} \tag{C.13}$$

and for $j = 1, 2$,

$$\frac{\partial f_0}{\partial \lambda_j} = \frac{\sqrt{1 - e^2}}{1 - e \cos E'} \frac{\partial E'}{\partial \lambda_j} - \frac{\partial M_s}{\partial \lambda_j} \tag{C.14}$$

where

$$E' = M_s + E_0 \tag{C.15}$$

Next, the partials of the first order term, for $j = 1, 2, 3$, are computed as

$$\frac{\partial f_1}{\partial \sigma_j} = \frac{\sqrt{1 - e^2}}{1 - e \cos E''} \frac{\partial E''}{\partial \sigma_j} + \delta_{2j} \frac{\sin f''}{1 - e^2} - \frac{\partial f'}{\partial \sigma_j} \tag{C.16}$$

and for $j = 1, 2$,

$$\frac{\partial f_1}{\partial \lambda_j} = \frac{\sqrt{1 - e^2}}{1 - e \cos E''} \frac{\partial E''}{\partial \lambda_j} - \frac{\partial f'}{\partial \lambda_j} \tag{C.17}$$

where

$$E'' = M_s + E_0 + E_1 \tag{C.18}$$

Finally, the partials of the second order term, for $j = 1, 2, 3$, are determined as

$$\frac{\partial f_2}{\partial \sigma_j} = \frac{\sqrt{1 - e^2}}{1 - e \cos E} \frac{\partial E}{\partial \sigma_j} + \delta_{2j} \frac{\sin f}{1 - e^2} - \left(\frac{\partial f'}{\partial \sigma_j} + \frac{\partial f_1}{\partial \sigma_j} \right) \tag{C.19}$$

and for $j = 1, 2$,

$$\frac{\partial f_2}{\partial \lambda_j} = \frac{\sqrt{1 - e^2}}{1 - e \cos E} \frac{\partial E}{\partial \lambda_j} - \left(\frac{\partial f'}{\partial \lambda_j} + \frac{\partial f_1}{\partial \lambda_j} \right) \tag{C.20}$$

where

$$E = M_s + E_0 + E_1 + E_2 \tag{C.21}$$

The partials of f_0, f_1, and f_2 with respect to β_3 vanish.

C.3 Other Partials Required for the Spheroidal Element Solution

Walden and Watson developed partial derivatives using the singular oblate spheroidal coordinates [164, 163] They took partials of equations that suffer from singularities for polar orbits. Vinti [160] developed a new transformation from oblate spheroidal orbital elements to Cartesian coordinates that avoids the singularities associated with polar orbits by introducing a slowly-varying element, Ω'.

If the STM is desired in the spheroidal element space, then the only additional partials required to propagate a relative Vinti trajectory are those of Ω'. The partials of Ω' are obtained from Eq. (51d) in Vinti [160] as follows.

For $j = 1, 2, 3$,

$$
\frac{\partial \Omega'}{\partial \sigma_j} = -c^2 \left[(-2\alpha_1)^{-\frac{1}{2}} \frac{\partial \alpha_3}{\partial \sigma_j} + \alpha_3 (-2\alpha_1)^{-\frac{3}{2}} \frac{\partial \alpha_1}{\partial \sigma_j} \right]
$$

$$
\times \left(A_3 f + \sum_{k=1}^{4} A_{3k} \sin kf \right) - c^2 \alpha_3 (-2\alpha_1)^{-\frac{1}{2}} \left[f \frac{\partial A_3}{\partial \sigma_j} \right.
$$

$$
+ \sum_{k=1}^{4} \sin kf \frac{\partial A_{3k}}{\partial \sigma_j} + \left(A_3 + \sum_{k=1}^{4} k A_{3k} \cos kf \right) \frac{\partial v}{\partial \sigma_j} \right]
$$

$$
+ \frac{u^{\frac{1}{2}}}{\alpha_2} \left(\frac{\partial \alpha_3}{\partial \sigma_j} - \frac{\alpha_3}{\alpha_2} \frac{\partial \alpha_2}{\partial \sigma_j} + \frac{\alpha_3}{2u} \frac{\partial u}{\partial \sigma_j} \right)
$$

$$
\times \left(B_3 \psi - \frac{3}{4} C_1 C_2 Q \cos \psi + \frac{3}{32} C_2^2 Q^2 \sin 2\psi \right)
$$

$$
+ \frac{\alpha_3 u^{\frac{1}{2}}}{\alpha_2} \left[\psi \frac{\partial B_3}{\partial \sigma_j} - \frac{3}{4} \left(C_2 Q \frac{\partial C_1}{\partial \sigma_j} + C_1 Q \frac{\partial C_2}{\partial \sigma_j} + C_1 C_2 \frac{\partial Q}{\partial \sigma_j} \right) \cos \psi \right.
$$

$$
+ \frac{3}{16} C_2 Q \left(Q \frac{\partial C_2}{\partial \sigma_j} + C_2 \frac{\partial Q}{\partial \sigma_j} \right) \sin 2\psi
$$

$$
\left. + \left(B_3 + \frac{3}{4} C_1 C_2 Q \sin \psi + \frac{3}{16} C_2^2 Q^2 \cos 2\psi \right) \frac{\partial \psi}{\partial \sigma_j} \right]
$$

(C.22)

Then, for $j = 1, 2$,

$$
\frac{\partial \Omega'}{\partial \lambda_j} = -c^2 \alpha_3 (-2\alpha_1)^{-\frac{1}{2}} \left(A_3 + \sum_{k=1}^{4} k A_{3k} \cos kf \right) \frac{\partial v}{\partial \lambda_j}
$$

$$
+ \frac{\alpha_3 u^{\frac{1}{2}}}{\alpha_2} \left(B_3 + \frac{3}{4} C_1 C_2 Q \sin \psi + \frac{3}{16} C_2^2 Q^2 \cos 2\psi \right) \frac{\partial \psi}{\partial \lambda_j}
$$

(C.23)

and

$$
\frac{\partial \Omega'}{\partial \beta_3} = 1
$$

(C.24)

However, in the current investigation, the partial derivatives of three other quantities are also modified. First, the partials of the polar component of angular momentum, α_3, are modified to remove singularities. Next, the partials of M_s and ψ_s are modified to convert all the partials to be with respect to the spheroidal Delaunay elements, λ_j, instead of the Jacobi constants β_j.

Beginning with the partials of α_3, if near the equatorial singularity such that the element set containing Q is used, then the only changes are that Eqs. (3.27) and (3.28) must be applied to the existing partials with respect to q_j from Walden and Watson [164]. Recall that q_j is defined differently in this paper, where $q_1 = a$, $q_2 = e$, and $q_3 = Q$. To avoid the polar orbit singularity, the partials of α_3 with respect to σ_j must be completely rederived from Eq. (3.16) and taken with respect to $\tilde{\sigma}_j$, where $\tilde{\sigma}_1 = a$, $\tilde{\sigma}_2 = e$, $\tilde{\sigma}_3 = \tilde{S}$. The partials are determined as

$$\frac{\partial \alpha_3}{\partial \tilde{\sigma}_j} = \operatorname{sgn} \alpha_3 \left(\tilde{S} u_\alpha \frac{\partial \alpha_2}{\partial \tilde{\sigma}_j} - \delta_{3j} \alpha_2 u_\alpha + \frac{1}{2} \frac{\alpha_2 \tilde{S}}{u_\alpha} \frac{\partial u_\alpha}{\partial \tilde{\sigma}_j} \right) \qquad \text{(C.25)}$$

where

$$u_\alpha \equiv \left\{ 1 - \frac{c^2}{a_0 p_0} S - \frac{\left(\frac{2z_\delta}{p_0}\right)^2 \left(1 - \frac{c^2}{a_0 p_0} S\right)}{\left[1 + \frac{c^2}{a_0 p_0}(1 - 2S)\right]^2} S \right\}^{\frac{1}{2}} \qquad \text{(C.26)}$$

from Eq. (3.16) and, for $j = 1, 2$,

$$\frac{\partial u_\alpha}{\partial \tilde{\sigma}_j} = S \left\{ -c^2 \frac{\partial}{\partial \tilde{\sigma}_j} (a_0 p_0)^{-1} \right.$$

$$+ \frac{\left(\frac{2z_\delta}{p_0}\right)^2 \left[\frac{2}{p_0}\left(1 - \frac{c^2}{a_0 p_0} S\right) \frac{\partial p_0}{\partial \tilde{\sigma}_j} + c^2 S \frac{\partial}{\partial \tilde{\sigma}_j}(a_0 p_0)^{-1}\right]}{\left[1 + \frac{c^2}{a_0 p_0}(1 - 2S)\right]^2} \qquad \text{(C.27)}$$

$$\left. + \frac{2c^2 \left(\frac{2z_\delta}{p_0}\right)^2 (1 - 2S)\left(1 - \frac{c^2}{a_0 p_0} S\right)}{\left[1 + \frac{c^2}{a_0 p_0}(1 - 2S)\right]^3} \frac{\partial}{\partial \tilde{\sigma}_j}(a_0 p_0)^{-1} \right\}$$

226

For $j = 3$ (with respect to $\tilde{S}$),

$$
\begin{aligned}
\frac{\partial u_\alpha}{\partial \tilde{S}} = \Bigg\{ &-c^2 \left(S \frac{\partial}{\partial S} (a_0 p_0)^{-1} + \frac{1}{a_0 p_0} \right) + \left(\frac{2z_\delta}{p_0} \right)^2 \\
&\times \frac{\left(1 - \frac{c^2}{a_0 p_0} S \right) \left(-1 + \frac{2S}{p_0} \frac{\partial p_0}{\partial S} \right) + c^2 S \left(S \frac{\partial}{\partial S} (a_0 p_0)^{-1} + \frac{1}{a_0 p_0} \right)}{\left[1 + \frac{c^2}{a_0 p_0} (1 - 2S) \right]^2} \\
&+ \frac{2c^2 \left(\frac{2z_\delta}{p_0} \right)^2 S \left(1 - \frac{c^2}{a_0 p_0} S \right) \left[(1 - 2S) \frac{\partial}{\partial S} (a_0 p_0)^{-1} - \frac{2}{a_0 p_0} \right]}{\left[1 + \frac{c^2}{a_0 p_0} (1 - 2S) \right]^3} \Bigg\} \frac{\partial S}{\partial \tilde{S}}
\end{aligned}
\tag{C.28}
$$

Notice the strong similarities between these partials of u_α and those of u located in Walden and Watson [164].

Next, all the partial derivatives can be converted to be with respect to the spheroidal Delaunay elements. The partials of Walden and Watson [164] with respect to β_j can be decomposed as

$$
\frac{\partial (\cdot)}{\partial \beta_j} = \frac{\partial (\cdot)}{\partial \lambda_j} \frac{\partial \lambda_j}{\partial \beta_j}
\tag{C.29}
$$

By inspection, β_1 and β_2 only appear explicitly in the expressions for l_0 and $l_0 + g_0$. Therefore, to obtain the desired partial $\partial(\cdot)/\partial \lambda_j$ for an arbitrary quantity, one option is to simply not perform the final step of the chain rule in the existing partials. In other words, the partial derivative $\partial \lambda_j / \partial \beta_j$ should not be computed. This goal is accomplished by simply computing $\partial M_s / \partial \lambda_j$ and $\partial \psi_s / \partial \lambda_j$ and otherwise building up the partials in the same way as in Walden and Watson [164], except that $\partial \beta_j$ is replaced by $\partial \lambda_j$ in all the equations. None of the other partial derivatives need to be modified when changing the independent variables to spheroidal Delaunay elements. The specific partials

to be modified are as follows. For $j = 1, 2, 3$, the new partials of M_s are determined as

$$\frac{\partial M_s}{\partial \lambda_j} = \delta_{1j} \tag{C.30}$$

and those of ψ_s are given by

$$\frac{\partial \psi_s}{\partial l_0} = \frac{\partial \psi_s}{\partial g_0} = 1; \quad \frac{\partial \psi_s}{\partial \beta_3} = 0 \tag{C.31}$$

The simple partials of M_s and ψ_s given in Eqs. (C.30) and (C.31) replace the complicated expressions for their partials with respect to the Jacobi constants.

C.4 Partials of Vinti's Nonsingular Transformation to ECI Coordinates

When the linear transformation from oblate spheroidal orbital elements to ECI coordinates is desired, the partials of Vinti's nonsingular transformation must be computed. These partials have not been published previously and are given here.

The partials of position and velocity require the partials of several constants associated with the nonsingular transformation. Beginning with constant quantities, the nonsingular equation for ζ is used, given by

$$\zeta = \frac{C_1}{2(1 - C_2)} \tag{C.32}$$

where $C_2 \ll 1$. The equation for ζ given in Eq. (C.32) is Eq. (154) in Vinti [158], but Walden and Watson [164] used the singular form $\zeta = P/(1 - S)$. The nonsingular partial derivatives of ζ, for $j = 1, 2, 3$, are determined as

$$\frac{\partial \zeta}{\partial \sigma_j} = \frac{1}{2(1 - C_2)} \left(\frac{\partial C_1}{\partial \sigma_j} + 2\zeta \frac{\partial C_2}{\partial \sigma_j} \right) \tag{C.33}$$

The remaining constants are unique to the nonsingular transformation. First, note from Vinti [160] the constants H_k and C_3 determined as

$$H_1 = \sqrt{\frac{1 + S + (1 - S)\sqrt{1 - C_3^2 z_\delta^2}}{2}} \tag{C.34a}$$

$$H_2 = \frac{1}{2}Q\left[\sqrt{1 - C_3 z_\delta} - \sqrt{1 + C_3 z_\delta}\right] \tag{C.34b}$$

$$H_3 = \frac{1}{2}\left[(1 + P)\sqrt{1 - C_3 z_\delta} + (1 - P)\sqrt{1 + C_3 z_\delta}\right] \tag{C.34c}$$

and

$$C_3 = \frac{2u}{p_0(1 - C_2 S)} = \frac{2\zeta}{z_\delta} \tag{C.35}$$

Vinti [160] denoted C_3 as r, but r is avoided here to alleviate confusion between this quantity and the magnitude of a position vector. From Eq. (C.35), the partials of C_3 are determined as

$$\frac{\partial C_3}{\partial \sigma_j} = \frac{2}{p_0^2(1 - C_2 S)^2}\left\{p_0(1 - C_2 S)\frac{\partial u}{\partial \sigma_j}\right.$$
$$\left. - u\left[(1 - C_2 S)\frac{\partial p_0}{\partial \sigma_j} - p_0\left(\delta_{3j}C_2 + S\frac{\partial C_2}{\partial \sigma_j}\right)\right]\right\} \tag{C.36}$$

for $j = 1, 2, 3$, or more simply as

$$\frac{\partial C_3}{\partial \sigma_j} = \frac{2}{z_\delta}\frac{\partial \zeta}{\partial \sigma_j} \tag{C.37}$$

For $j = 1, 2, 3$, the partials of H_k are obtained from Eq. (C.34) as

$$\frac{\partial H_1}{\partial \sigma_j} = \frac{1}{4H_1}\left\{\delta_{3j}\left[1 - (1 - 4\zeta^2)^{\frac{1}{2}}\right] - \frac{(1 - S)4\zeta}{(1 - 4\zeta^2)^{\frac{1}{2}}}\frac{\partial \zeta}{\partial \sigma_j}\right\} \tag{C.38}$$

$$\frac{\partial H_2}{\partial \sigma_j} = \frac{1}{2}\left[(1 - 2\zeta)^{\frac{1}{2}} - (1 + 2\zeta)^{\frac{1}{2}}\right]\frac{\partial Q}{\partial \sigma_j}$$
$$- \frac{1}{2}Q\left[(1 - 2\zeta)^{-\frac{1}{2}} + (1 + 2\zeta)^{-\frac{1}{2}}\right]\frac{\partial \zeta}{\partial \sigma_j} \tag{C.39}$$

229

$$\frac{\partial H_3}{\partial \sigma_j} = \frac{1}{2} \left[(1 - 2\zeta)^{\frac{1}{2}} - (1 + 2\zeta)^{\frac{1}{2}} \right] \frac{\partial P}{\partial \sigma_j}$$

$$- \frac{1}{2} \left[\frac{1 + P}{(1 - 2\zeta)^{\frac{1}{2}}} - \frac{1 - P}{(1 + 2\zeta)^{\frac{1}{2}}} \right] \frac{\partial \zeta}{\partial \sigma_j} \tag{C.40}$$

To propagate a relative Vinti trajectory in ECI coordinates using an STM, the partials for $\dot{\Omega}'$, $\dot{\psi}$, and $\dot{f}$ are required in addition to those of position and velocity. From Eq. (55) for $\dot{\Omega}'$ in Vinti [160], for $j = 1, 2, 3$,

$$\begin{aligned}
\frac{\partial \dot{\Omega}'}{\partial \sigma_j} = &-c^2 \left[\frac{\partial \alpha_3}{\partial \sigma_j} (-2\alpha_1)^{-\frac{1}{2}} + \alpha_3 (-2\alpha_1)^{-\frac{3}{2}} \frac{\partial \alpha_1}{\partial \sigma_j} \right] \\
&\times \left(A_3 + \sum_{k=1}^{4} k A_{3k} \cos kf \right) \dot{f} - \frac{c^2 \alpha_3}{(-2\alpha_1)^{\frac{1}{2}}} \left\{ \left[\frac{\partial A_3}{\partial \sigma_j} \right. \right. \\
&+ \sum_{k=1}^{4} k \cos kf \frac{\partial A_{3k}}{\partial \sigma_j} - \left(\sum_{k=1}^{4} k^2 A_{3k} \sin kf \right) \frac{\partial v}{\partial \sigma_j} \left. \right] \dot{f} \\
&+ \left(A_3 + \sum_{k=1}^{4} k A_{3k} \cos kf \right) \frac{\partial \dot{f}}{\partial \sigma_j} \right\} + \frac{u^{\frac{1}{2}}}{\alpha_2} \left(\frac{\partial \alpha_3}{\partial \sigma_j} - \frac{\alpha_3}{\alpha_2} \frac{\partial \alpha_2}{\partial \sigma_j} \right. \\
&+ \frac{\alpha_3}{2u} \frac{\partial u}{\partial \sigma_j} \right) \left(B_3 + \frac{3}{4} C_1 C_2 Q \sin \psi + \frac{3}{16} C_2^2 Q^2 \cos 2\psi \right) \dot{\psi} \\
&+ \frac{\alpha_3 u^{\frac{1}{2}}}{\alpha_2} \left\{ \left[\frac{\partial B_3}{\partial \sigma_j} + \frac{3}{4} \left(C_2 Q \frac{\partial C_1}{\partial \sigma_j} + C_1 Q \frac{\partial C_2}{\partial \sigma_j} + C_1 C_2 \frac{\partial Q}{\partial \sigma_j} \right) \sin \psi \right. \right. \\
&+ \frac{3}{8} C_2 Q \left(Q \frac{\partial C_2}{\partial \sigma_j} + C_2 \frac{\partial Q}{\partial \sigma_j} \right) \cos 2\psi \\
&+ \left(\frac{3}{4} C_1 C_2 Q \cos \psi - \frac{3}{8} C_2^2 Q^2 \sin 2\psi \right) \frac{\partial \psi}{\partial \sigma_j} \left. \right] \dot{\psi} \\
&+ \left(B_3 + \frac{3}{4} C_1 C_2 Q \sin \psi + \frac{3}{16} C_2^2 Q^2 \cos 2\psi \right) \frac{\partial \dot{\psi}}{\partial \sigma_j} \right\}
\end{aligned} \tag{C.41}$$

Also, for $j = 1, 2$,

$$\frac{\partial \dot{\Omega}'}{\partial \lambda_j} = -\frac{c^2 \alpha_3}{(-2\alpha_1)^{\frac{1}{2}}} \left[-\left(\sum_{k=1}^{4} k^2 A_{3k} \sin kf \right) \frac{\partial v}{\partial \lambda_j} \dot{f} \right.$$
$$+ \left(A_3 + \sum_{k=1}^{4} k A_{3k} \cos kf \right) \frac{\partial \dot{f}}{\partial \lambda_j} \right]$$
$$+ \frac{\alpha_3 u^{\frac{1}{2}}}{\alpha_2} \left[\left(\frac{3}{4} C_1 C_2 Q \cos \psi - \frac{3}{8} C_2^2 Q^2 \sin 2\psi \right) \dot{\psi} \frac{\partial \psi}{\partial \lambda_j} \right.$$
$$+ \left(B_3 + \frac{3}{4} C_1 C_2 Q \sin \psi + \frac{3}{16} C_2^2 Q^2 \cos 2\psi \right) \frac{\partial \dot{\psi}}{\partial \lambda_j} \right] \quad (C.42)$$

From Eq. (23) for $\dot{f}$ in Vinti [160] with $-2\alpha_1 = \mu/a_0$, for $j = 1, 2, 3$,

$$\frac{\partial \dot{f}}{\partial \sigma_j} = \frac{[(-2\alpha_1)(\rho^2 - 2b_1\rho + b_2^2)]^{\frac{1}{2}}}{\rho(\rho^2 + c^2\eta^2)} \left[\delta_{1j}(1 - e^2)^{\frac{1}{2}} - \delta_{2j} \frac{ae}{(1 - e^2)^{\frac{1}{2}}} \right]$$
$$+ \dot{f} \left[-\frac{1}{\rho} \frac{\partial \rho}{\partial \sigma_j} + \frac{1}{2\alpha_1} \frac{\partial \alpha_1}{\partial \sigma_j} - 2 \left(\rho \frac{\partial \rho}{\partial \sigma_j} + c^2\eta \frac{\partial \eta}{\partial \sigma_j} \right) (\rho^2 + c^2\eta^2)^{-1} \right]$$
$$- \frac{2a\alpha_1(1 - e^2)^{\frac{1}{2}}}{\rho(\rho^2 + c^2\eta^2)[(-2\alpha_1)(\rho^2 - 2b_1\rho + b_2^2)]^{\frac{1}{2}}}$$
$$\times \left[(\rho - b_1) \frac{\partial \rho}{\partial \sigma_j} - \rho \frac{\partial b_1}{\partial \sigma_j} + b_2 \frac{\partial b_2}{\partial \sigma_j} \right] \quad (C.43)$$

Also, for $j = 1, 2$,

$$\frac{\partial \dot{f}}{\partial \lambda_j} = \dot{f} \left[-\frac{1}{\rho} \frac{\partial \rho}{\partial \lambda_j} + \frac{1}{2\alpha_1} \frac{\partial \alpha_1}{\partial \lambda_j} - 2 \left(\rho \frac{\partial \rho}{\partial \lambda_j} + c^2\eta \frac{\partial \eta}{\partial \lambda_j} \right) (\rho^2 + c^2\eta^2)^{-1} \right]$$
$$- \frac{2a\alpha_1(1 - e^2)^{\frac{1}{2}}}{\rho(\rho^2 + c^2\eta^2)[(-2\alpha_1)(\rho^2 - 2b_1\rho + b_2^2)]^{\frac{1}{2}}} (\rho - b_1) \frac{\partial \rho}{\partial \lambda_j} \quad (C.44)$$

231

From Eq. (57) for $\dot{\psi}$ in Vinti [160] with $\alpha_2 = \sqrt{\mu p_0}$, for $j = 1, 2, 3$,

$$
\begin{aligned}
\frac{\partial \dot{\psi}}{\partial \sigma_j} &= \left\{ (1 + C_1\eta - C_2\eta^2)^{\frac{1}{2}} \frac{\partial \alpha_2}{\partial \sigma_j} + \frac{\alpha_2}{2} \left[(C_1 - 2C_2\eta) \frac{\partial \eta}{\partial \sigma_j} \right.\right. \\
&\quad \left.\left. + \eta \frac{\partial C_1}{\partial \sigma_j} - \eta^2 \frac{\partial C_2}{\partial \sigma_j} \right] (1 + C_1\eta - C_2\eta^2)^{-\frac{1}{2}} \right\} [u^{\frac{1}{2}}(\rho^2 + c^2\eta^2)]^{-1} \\
&\quad - \frac{\alpha_2(1 + C_1\eta - C_2\eta^2)^{\frac{1}{2}}}{\rho^2 + c^2\eta^2} \left[\frac{1}{2u^{\frac{3}{2}}} \frac{\partial u}{\partial \sigma_j} \right. \\
&\quad \left. + \frac{2}{u^{\frac{1}{2}}(\rho^2 + c^2\eta^2)} \left(\rho \frac{\partial \rho}{\partial \sigma_j} + c^2\eta \frac{\partial \eta}{\partial \sigma_j} \right) \right]
\end{aligned}
\tag{C.45}
$$

which simplifies to

$$
\begin{aligned}
\frac{\partial \dot{\psi}}{\partial \sigma_j} &= \dot{\psi} \left\{ \frac{1}{\alpha_2} \frac{\partial \alpha_2}{\partial \sigma_j} + \frac{1}{2(1 + C_1\eta - C_2\eta^2)} \left[(C_1 - 2C_2\eta) \frac{\partial \eta}{\partial \sigma_j} \right.\right. \\
&\quad \left.\left. + \eta \frac{\partial C_1}{\partial \sigma_j} - \eta^2 \frac{\partial C_2}{\partial \sigma_j} \right] - \frac{1}{2u} \frac{\partial u}{\partial \sigma_j} - \frac{2}{(\rho^2 + c^2\eta^2)} \left(\rho \frac{\partial \rho}{\partial \sigma_j} + c^2\eta \frac{\partial \eta}{\partial \sigma_j} \right) \right\}
\end{aligned}
\tag{C.46}
$$

Also, for $j = 1, 2$,

$$
\begin{aligned}
\frac{\partial \dot{\psi}}{\partial \lambda_j} &= \frac{\alpha_2 (C_1 - 2C_2\eta)}{2u^{\frac{1}{2}}(\rho^2 + c^2\eta^2)(1 + C_1\eta - C_2\eta^2)^{\frac{1}{2}}} \frac{\partial \eta}{\partial \lambda_j} \\
&\quad - \frac{2\alpha_2(1 + C_1\eta - C_2\eta^2)^{\frac{1}{2}}}{u^{\frac{1}{2}}(\rho^2 + c^2\eta^2)^2} \left(\rho \frac{\partial \rho}{\partial \lambda_j} + c^2\eta \frac{\partial \eta}{\partial \lambda_j} \right)
\end{aligned}
\tag{C.47}
$$

The partials of $\dot{\Omega}'$, $\dot{\psi}$, and $\dot{f}$ with respect to β_3 vanish. Now, the new partials of the ECI state can be obtained in terms of the preceding partials and those of Walden and Watson [164] and Walden [163]. Note that Eqs. (C.50), (C.53), (C.56), and (C.60) each contain a Kronecker delta, δ_{3j}, in one of the terms. These small terms are slightly different depending on whether the partials are taken with respect to $\tilde{S}$ or Q. Each of these four equations expresses the partials with respect to $\tilde{S}$. To obtain the partials with respect to Q, simply make the following changes:

$$
\frac{\delta_{3j}}{H_1} \longrightarrow -\frac{\delta_{3j}}{2H_1\tilde{S}} \frac{\partial S}{\partial Q}
\tag{C.48}
$$

232

and

$$\frac{\partial(\cdot)}{\partial\tilde{\sigma}_j} \longrightarrow \frac{\partial(\cdot)}{\partial q_j} \tag{C.49}$$

Now, beginning with positions, for $j = 1, 2, 3$,

$$\begin{aligned}
\frac{\partial X}{\partial\tilde{\sigma}_j} &= \frac{X\rho}{\rho^2 + c^2}\frac{\partial\rho}{\partial\tilde{\sigma}_j} + (\rho^2 + c^2)^{\frac{1}{2}}\left\langle \cos\Omega'\cos\psi\frac{\partial H_1}{\partial\tilde{\sigma}_j}\right. \\
&\quad - H_1\left(\sin\Omega'\cos\psi\frac{\partial\Omega'}{\partial\tilde{\sigma}_j} + \cos\Omega'\sin\psi\frac{\partial\psi}{\partial\tilde{\sigma}_j}\right) \\
&\quad + \mathrm{sgn}\,\alpha_3\left\{\left(-\frac{\delta_{3j}}{H_1} + \frac{\tilde{S}}{H_1^2}\frac{\partial H_1}{\partial\tilde{\sigma}_j}\right)\sin\Omega'(H_2 + H_3\sin\psi)\right. \\
&\quad - \frac{\tilde{S}}{H_1}\left[\cos\Omega'(H_2 + H_3\sin\psi)\frac{\partial\Omega'}{\partial\tilde{\sigma}_j}\right. \\
&\quad \left.\left.\left. + \sin\Omega'\left(\frac{\partial H_2}{\partial\tilde{\sigma}_j} + \sin\psi\frac{\partial H_3}{\partial\tilde{\sigma}_j} + H_3\cos\psi\frac{\partial\psi}{\partial\tilde{\sigma}_j}\right)\right]\right\}\right\rangle
\end{aligned} \tag{C.50}$$

Also, for $j = 1, 2$,

$$\begin{aligned}
\frac{\partial X}{\partial\lambda_j} &= \frac{X\rho}{\rho^2 + c^2}\frac{\partial\rho}{\partial\lambda_j} \\
&\quad + (\rho^2 + c^2)^{\frac{1}{2}}\left\{-H_1\left(\sin\Omega'\cos\psi\frac{\partial\Omega'}{\partial\lambda_j} + \cos\Omega'\sin\psi\frac{\partial\psi}{\partial\lambda_j}\right)\right. \\
&\quad \left. - \mathrm{sgn}\,\alpha_3\frac{\tilde{S}}{H_1}\left[\cos\Omega'(H_2 + H_3\sin\psi)\frac{\partial\Omega'}{\partial\lambda_j} + H_3\sin\Omega'\cos\psi\frac{\partial\psi}{\partial\lambda_j}\right]\right\}
\end{aligned} \tag{C.51}$$

and

$$\begin{aligned}
\frac{\partial X}{\partial\beta_3} &= (\rho^2 + c^2)^{\frac{1}{2}}\left[-H_1\sin\Omega'\cos\psi\right. \\
&\quad \left. - \mathrm{sgn}\,\alpha_3\frac{\tilde{S}}{H_1}\cos\Omega'(H_2 + H_3\sin\psi)\right]
\end{aligned} \tag{C.52}$$

233

Next, for $j = 1, 2, 3$,

$$
\begin{aligned}
\frac{\partial Y}{\partial \tilde{\sigma}_j} &= \frac{Y \rho}{\rho^2 + c^2} \frac{\partial \rho}{\partial \tilde{\sigma}_j} + (\rho^2 + c^2)^{\frac{1}{2}} \bigg\langle \sin \Omega' \cos \psi \frac{\partial H_1}{\partial \tilde{\sigma}_j} \\
&\quad + H_1 \left(\cos \Omega' \cos \psi \frac{\partial \Omega'}{\partial \tilde{\sigma}_j} - \sin \Omega' \sin \psi \frac{\partial \psi}{\partial \tilde{\sigma}_j} \right) \\
&\quad + \operatorname{sgn} \alpha_3 \bigg\{ \left(\frac{\delta_{3j}}{H_1} - \frac{\tilde{S}}{H_1^2} \frac{\partial H_1}{\partial \tilde{\sigma}_j} \right) \cos \Omega'(H_2 + H_3 \sin \psi) \\
&\quad + \frac{\tilde{S}}{H_1} \bigg[- \sin \Omega'(H_2 + H_3 \sin \psi) \frac{\partial \Omega'}{\partial \tilde{\sigma}_j} \\
&\quad + \cos \Omega' \left(\frac{\partial H_2}{\partial \tilde{\sigma}_j} + \sin \psi \frac{\partial H_3}{\partial \tilde{\sigma}_j} + H_3 \cos \psi \frac{\partial \psi}{\partial \tilde{\sigma}_j} \right) \bigg] \bigg\} \bigg\rangle
\end{aligned}
\tag{C.53}
$$

Also, for $j = 1, 2$,

$$
\begin{aligned}
\frac{\partial Y}{\partial \lambda_j} &= \frac{Y \rho}{\rho^2 + c^2} \frac{\partial \rho}{\partial \lambda_j} \\
&\quad + (\rho^2 + c^2)^{\frac{1}{2}} \bigg\{ H_1 \left(\cos \Omega' \cos \psi \frac{\partial \Omega'}{\partial \lambda_j} - \sin \Omega' \sin \psi \frac{\partial \psi}{\partial \lambda_j} \right) \\
&\quad - \operatorname{sgn} \alpha_3 \frac{\tilde{S}}{H_1} \bigg[\sin \Omega'(H_2 + H_3 \sin \psi) \frac{\partial \Omega'}{\partial \lambda_j} - H_3 \cos \Omega' \cos \psi \frac{\partial \psi}{\partial \lambda_j} \bigg] \bigg\}
\end{aligned}
\tag{C.54}
$$

and

$$
\begin{aligned}
\frac{\partial Y}{\partial \beta_3} &= (\rho^2 + c^2)^{\frac{1}{2}} \bigg[H_1 \cos \Omega' \cos \psi \\
&\quad - \operatorname{sgn} \alpha_3 \frac{\tilde{S}}{H_1} \sin \Omega'(H_2 + H_3 \sin \psi) \bigg]
\end{aligned}
\tag{C.55}
$$

Considering the velocities, for $j = 1, 2, 3$,

$$
\begin{aligned}
\frac{\partial \dot{X}}{\partial \tilde{\sigma}_j} &= \frac{\rho}{\rho^2 + c^2} \left(\dot{\rho} \frac{\partial X}{\partial \tilde{\sigma}_j} + X \frac{\partial \dot{\rho}}{\partial \tilde{\sigma}_j} \right) + \frac{\dot{\rho} X}{\rho^2 + c^2} \left(1 - \frac{2\rho^2}{\rho^2 + c^2} \right) \frac{\partial \rho}{\partial \tilde{\sigma}_j} \\
&\quad - \dot{\Omega}' \frac{\partial Y}{\partial \tilde{\sigma}_j} - Y \frac{\partial \dot{\Omega}'}{\partial \tilde{\sigma}_j} + \frac{\rho G_X}{(\rho^2 + c^2)^{\frac{1}{2}}} \dot{\psi} \frac{\partial \rho}{\partial \tilde{\sigma}_j} \\
&\quad + (\rho^2 + c^2)^{\frac{1}{2}} \Bigg\langle - \cos \Omega' \sin \psi \frac{\partial H_1}{\partial \tilde{\sigma}_j} \\
&\quad + H_1 \left(\sin \Omega' \sin \psi \frac{\partial \Omega'}{\partial \tilde{\sigma}_j} - \cos \Omega' \cos \psi \frac{\partial \psi}{\partial \tilde{\sigma}_j} \right) + \operatorname{sgn} \alpha_3 \\
&\quad \times \Bigg\{ \left(-\frac{\delta_{3j}}{H_1} + \frac{\tilde{S}}{H_1^2} \frac{\partial H_1}{\partial \tilde{\sigma}_j} \right) H_3 \sin \Omega' \cos \psi - \frac{\tilde{S}}{H_1} \left[\sin \Omega' \cos \psi \frac{\partial H_3}{\partial \tilde{\sigma}_j} \right. \\
&\quad + H_3 \left(\cos \Omega' \cos \psi \frac{\partial \Omega'}{\partial \tilde{\sigma}_j} - \sin \Omega' \sin \psi \frac{\partial \psi}{\partial \tilde{\sigma}_j} \right) \Bigg] \Bigg\} \Bigg\rangle \dot{\psi} \\
&\quad + (\rho^2 + c^2)^{\frac{1}{2}} G_X \frac{\partial \dot{\psi}}{\partial \tilde{\sigma}_j}
\end{aligned}
\tag{C.56}
$$

where

$$
G_X \equiv -H_1 \cos \Omega' \sin \psi - \operatorname{sgn} \alpha_3 \frac{\tilde{S}}{H_1} H_3 \sin \Omega' \cos \psi \tag{C.57}
$$

Also, for $j = 1, 2$,

$$
\begin{aligned}
\frac{\partial \dot{X}}{\partial \lambda_j} &= \frac{\rho}{\rho^2 + c^2} \left(\dot{\rho} \frac{\partial X}{\partial \lambda_j} + X \frac{\partial \dot{\rho}}{\partial \lambda_j} \right) + \frac{\dot{\rho} X}{\rho^2 + c^2} \left(1 - \frac{2\rho^2}{\rho^2 + c^2} \right) \frac{\partial \rho}{\partial \lambda_j} \\
&\quad - \dot{\Omega}' \frac{\partial Y}{\partial \lambda_j} - Y \frac{\partial \dot{\Omega}'}{\partial \lambda_j} + \frac{\rho G_X}{(\rho^2 + c^2)^{\frac{1}{2}}} \dot{\psi} \frac{\partial \rho}{\partial \lambda_j} + (\rho^2 + c^2)^{\frac{1}{2}} \\
&\quad \times \Bigg[H_1 \left(\sin \Omega' \sin \psi \frac{\partial \Omega'}{\partial \lambda_j} - \cos \Omega' \cos \psi \frac{\partial \psi}{\partial \lambda_j} \right) - \operatorname{sgn} \alpha_3 \frac{\tilde{S}}{H_1} \\
&\quad \times H_3 \left(\cos \Omega' \cos \psi \frac{\partial \Omega'}{\partial \lambda_j} - \sin \Omega' \sin \psi \frac{\partial \psi}{\partial \lambda_j} \right) \Bigg] \dot{\psi} \\
&\quad + (\rho^2 + c^2)^{\frac{1}{2}} G_X \frac{\partial \dot{\psi}}{\partial \lambda_j}
\end{aligned}
\tag{C.58}
$$

and

$$\frac{\partial \dot{X}}{\partial \beta_3} = \frac{\rho \dot{\rho}}{\rho^2 + c^2}\frac{\partial X}{\partial \beta_3} - \dot{\Omega}'\frac{\partial Y}{\partial \beta_3} + (\rho^2 + c^2)^{\frac{1}{2}}\left[H_1 \sin \Omega' \sin \psi \right.$$
$$\left. - \operatorname{sgn}\alpha_3 \frac{\tilde{S}}{H_1} H_3 \cos \Omega' \cos \psi \right]\dot{\psi} \tag{C.59}$$

Next, for $j = 1, 2, 3$,

$$\frac{\partial \dot{Y}}{\partial \tilde{\sigma}_j} = \frac{\rho}{\rho^2 + c^2}\left(\dot{\rho}\frac{\partial Y}{\partial \tilde{\sigma}_j} + Y\frac{\partial \dot{\rho}}{\partial \tilde{\sigma}_j} \right) + \frac{\dot{\rho}Y}{\rho^2 + c^2}\left(1 - \frac{2\rho^2}{\rho^2 + c^2} \right)\frac{\partial \rho}{\partial \tilde{\sigma}_j}$$
$$+ \dot{\Omega}'\frac{\partial X}{\partial \tilde{\sigma}_j} + X\frac{\partial \dot{\Omega}'}{\partial \tilde{\sigma}_j} + \frac{\rho G_Y}{(\rho^2 + c^2)^{\frac{1}{2}}}\dot{\psi}\frac{\partial \rho}{\partial \tilde{\sigma}_j}$$
$$+ (\rho^2 + c^2)^{\frac{1}{2}}\left\langle -\sin \Omega' \sin \psi \frac{\partial H_1}{\partial \tilde{\sigma}_j} \right.$$
$$- H_1\left(\cos \Omega' \sin \psi \frac{\partial \Omega'}{\partial \tilde{\sigma}_j} + \sin \Omega' \cos \psi \frac{\partial \psi}{\partial \tilde{\sigma}_j} \right) + \operatorname{sgn}\alpha_3 \tag{C.60}$$
$$\times \left\{ \left(\frac{\delta_{3j}}{H_1} - \frac{\tilde{S}}{H_1^2}\frac{\partial H_1}{\partial \tilde{\sigma}_j} \right) H_3 \cos \Omega' \cos \psi + \frac{\tilde{S}}{H_1}\left[\cos \Omega' \cos \psi \frac{\partial H_3}{\partial \tilde{\sigma}_j} \right.\right.$$
$$\left.\left.\left. - H_3\left(\sin \Omega' \cos \psi \frac{\partial \Omega'}{\partial \tilde{\sigma}_j} + \cos \Omega' \sin \psi \frac{\partial \psi}{\partial \tilde{\sigma}_j} \right) \right] \right\} \right\rangle \dot{\psi}$$
$$+ (\rho^2 + c^2)^{\frac{1}{2}}G_Y\frac{\partial \dot{\psi}}{\partial \tilde{\sigma}_j}$$

where

$$G_Y \equiv -H_1 \sin \Omega' \sin \psi + \operatorname{sgn}\alpha_3 \frac{\tilde{S}}{H_1} H_3 \cos \Omega' \cos \psi \tag{C.61}$$

Also, for $j = 1, 2$,

$$
\frac{\partial \dot{Y}}{\partial \lambda_j} = \frac{\rho}{\rho^2 + c^2} \left(\dot{\rho} \frac{\partial Y}{\partial \lambda_j} + Y \frac{\partial \dot{\rho}}{\partial \lambda_j} \right) + \frac{\dot{\rho} Y}{\rho^2 + c^2} \left(1 - \frac{2\rho^2}{\rho^2 + c^2} \right) \frac{\partial \rho}{\partial \lambda_j}
$$

$$
+ \dot{\Omega}' \frac{\partial X}{\partial \lambda_j} + X \frac{\partial \dot{\Omega}'}{\partial \lambda_j} + \frac{\rho G_Y}{(\rho^2 + c^2)^{\frac{1}{2}}} \dot{\psi} \frac{\partial \rho}{\partial \lambda_j} + (\rho^2 + c^2)^{\frac{1}{2}}
$$

$$
\times \left[-H_1 \left(\cos \Omega' \sin \psi \frac{\partial \Omega'}{\partial \lambda_j} + \sin \Omega' \cos \psi \frac{\partial \psi}{\partial \lambda_j} \right) - \operatorname{sgn} \alpha_3 \frac{\tilde{S}}{H_1} \right. \qquad \text{(C.62)}
$$

$$
\times \left. H_3 \left(\sin \Omega' \cos \psi \frac{\partial \Omega'}{\partial \lambda_j} + \cos \Omega' \sin \psi \frac{\partial \psi}{\partial \lambda_j} \right) \right] \dot{\psi}
$$

$$
+ (\rho^2 + c^2)^{\frac{1}{2}} G_Y \frac{\partial \dot{\psi}}{\partial \lambda_j}
$$

and

$$
\frac{\partial \dot{Y}}{\partial \beta_3} = \frac{\rho \dot{\rho}}{\rho^2 + c^2} \frac{\partial Y}{\partial \beta_3} + \dot{\Omega}' \frac{\partial X}{\partial \beta_3} + (\rho^2 + c^2)^{\frac{1}{2}} \left[-H_1 \cos \Omega' \sin \psi \right.
$$

$$
\left. - \operatorname{sgn} \alpha_3 \frac{\tilde{S}}{H_1} H_3 \sin \Omega' \cos \psi \right] \dot{\psi} \qquad \text{(C.63)}
$$

237

Bibliography

[1] E. P. Aksenov, Evgenii A. Grebenikov, and Vladimir Grigor'evich Demin. The generalized problem of motion about two fixed centers and its application to the theory of artificial Earth satellites. *Soviet Astronomy*, 7(2):276–282, September–October 1963. Translated to English from *Astronomicheskii Zhurnal*, Vol. 40, No. 2, March–April 1963, pp. 363–372, `http://adsabs.harvard.edu/abs/1963SvA.....7..276A`, accessed May 28, 2017.

[2] Ye. (E.) P. Aksenov, Yevgeny (Evgenii) A. Grebenikov, and Vladimir Grigor'evich Demin. General solution of the problem of the motion of an artificial satellite in the normal field of the Earth's attraction. *Planetary and Space Science*, 9(8):491–498, August 1962. Translated by R. E. Daisley to English from *Iskusstvennye Sputniki Zemli (Artificial Earth Satellites)*, No. 8, 1961, pp. 64–72, doi:10.1016/0032-0633(62)90052-1.

[3] Ye. (E.) P. Aksenov, Yevgeny (Evgenii) A. Grebenikov, and Vladimir Grigor'evich Demin. Qualitative analysis of the forms of motion in the problem of the motion of an artificial satellite in the normal field of the Earth's attraction. *Planetary and Space Science*, 12(4):289–315, April 1964. Translated by H. S. H. Massey to English from *Iskusstven-*

nye Sputniki Zemli (Artificial Earth Satellites), No. 16, 1963, p. 173, doi:10.1016/0032-0633(64)90153-9.

[4] Kaare Aksnes. On the dynamical theory of a near-Earth satellite, I. *Astrophysica Norvegica*, 10(4):69–77, August 1965.

[5] Kaare Aksnes. On the dynamical theory of a near-Earth satellite II. *Astrophysica Norvegica*, 10(8):149–169, February 1967.

[6] Kaare Aksnes. *A Second-Order Solution for the Motion of an Artificial Earth Satellite Based on an Intermediate Orbit.* PhD thesis, Supervisor: Dr. Boris Garfinkel, Yale University, New Haven, CT, 1969.

[7] Kyle Terry Alfriend and Shannon L. Coffey. The elimination of the parallax in satellite theory. *Celestial Mechanics*, 32(2):163–172, February 1984. doi:10.1007/BF01231123.

[8] Kyle Terry Alfriend, Robert R. Dasenbrock, Henry M. Pickard, and André Deprit. The extended phase space formulation of the Vinti problem. *Celestial Mechanics*, 16(4):441–458, December 1977. doi:10.1007/BF01229287.

[9] William A. Allen. Differential corrections applied to an Izsak-Borchers ballistic trajectory. *AIAA Journal*, 7(5):890–895, May 1969. doi:10.2514/3.5241.

[10] William A. Allen and Werner E. Knolle. Corrections applied to the Izsak equations of artificial satellite motion. *The Astronomical Journal*, 69(6): 393–401, August 1964. doi:10.1086/109290.

[11] William A. Allen and Werner E. Knolle. Perturbations applied to the Izsak-Borchers relations. *The Astronomical Journal*, 70(2):152–154, March 1965. doi:10.1086/109705.

[12] J. L. Arsenault, K. C. Ford, and Paul E. Koskela. Orbit determination using analytic partial derivatives of perturbed motion. *AIAA Journal*, 8 (1):4–12, January 1970. doi:10.2514/3.5597.

[13] Roger R. Bate, Donald D. Mueller, and Jerry E. White. *Fundamentals of Astrodynamics*. Dover Publications, Inc., New York, NY, 1971.

[14] Richard Horace Battin. *An Introduction to the Mathematics and Methods of Astrodynamics*. AIAA Education Series. American Institute of Aeronautics and Astronautics, Inc., Reston, VA, revised edition, 1999.

[15] Vladimir Vasilyevich Beletsky. *Essays on the Motion of Celestial Bodies*. Birkhäuser Verlag, Basel, Switzerland, 2001. Translated by Andrei Iacob to English from *Ocherki o Dvizhenii Kosmicheskikh Tel*, Nauka Press, Moscow, 1972; author's name alternatively spelled Vladimir Vasil'evich Beletskiĭ.

[16] Ashley Darius Biria and Ryan Paul Russell. Periodic orbits in the elliptical relative motion problem with space surveillance applications. *Journal of Guidance, Control, and Dynamics*, 38(8):1452–1467, August 2015. doi:10.2514/1.G000622.

[17] Ashley Darius Biria and Ryan Paul Russell. A satellite relative motion

model including J_2 and J_3 via Vinti's intermediary. *Celestial Mechanics and Dynamical Astronomy*, 2016. submitted December 2016.

[18] Ashley Darius Biria and Ryan Paul Russell. A satellite relative motion model including J_2 and J_3 via Vinti's intermediary. In *AAS/AIAA Space Flight Mechanics Meeting*, Vol. 158 of *Advances in the Astronautical Sciences*, pp. 3475–3494, San Diego, CA, February 2016. Univelt, Inc. Paper AAS 16-537.

[19] Francesco Biscani and Dario Izzo. The Stark problem in the Weierstrassian formalism. *Monthly Notices of the Royal Astronomical Society*, 439(1):810–822, March 2014. doi:10.1093/mnras/stt2501.

[20] Francesco Biscani and Dario Izzo. A complete and explicit solution to the three-dimensional problem of two fixed centres. *Monthly Notices of the Royal Astronomical Society*, 455(4):3480–3493, February 2016. doi:10.1093/mnras/stv2512.

[21] Nino L. Bonavito. Computational procedure for Vinti's accurate reference orbit with inclusion of the third zonal harmonic. Technical Report TN D-3562, National Aeronautics and Space Administration, Washington, DC, August 1966.

[22] Nino L. Bonavito, Stan Watson, and Harvey Walden. An accuracy and speed comparison of the Vinti and Brouwer orbit prediction methods. Technical Report TN D-5203, National Aeronautics and Space Administration, Washington, DC, May 1969.

[23] Raymond V. Borchers. A satellite orbit computation program for Izsak's second-order solution of Vinti's dynamical problem. Technical Report TN D-1539, National Aeronautics and Space Administration, Washington, DC, February 1963.

[24] George H. Born and James C. Kirkpatrick. Application of Brouwer's artificial-satellite theory to computation of the state transition matrix. Technical Report TN D-5934, National Aeronautics and Space Administration, Washington, DC, August 1970.

[25] Roger A. Broucke. Solution of the elliptic rendezvous problem with the time as independent variable. *Journal of Guidance, Control, and Dynamics*, 26(4):615–621, July–August 2003. doi:10.2514/2.5089.

[26] Roger A. Broucke and Paul J. Cefola. On the equinoctial orbit elements. *Celestial Mechanics*, 5(3):303–310, May 1972. doi:10.1007/BF01228432.

[27] Dirk Brouwer. Solution of the problem of artificial satellite theory without drag. *The Astronomical Journal*, 64(9):378–397, November 1959. doi:10.1086/107958.

[28] Dirk Brouwer and Gerald M. Clemence. *Methods of Celestial Mechanics*. Academic Press, Inc., New York, NY, January 1 1961. `https://www.elsevier.com/books/methods-of-celestial-mechanics/brouwer/978-1-4832-0075-0`, accessed May 28, 2017.

[29] Dirk Brouwer and Gen-Ichiro Hori. Theoretical evaluation of atmo-

spheric drag effects in the motion of an artificial satellite. *The Astronomical Journal*, 66(5):193–225, June 1961. doi:10.1086/108399.

[30] Ernest William Brown. *An Introductory Treatise on the Lunar Theory.* Cambridge University Press, London, 1896.

[31] Thomas E. Carter. State transition matrices for terminal rendezvous studies: Brief survey and new example. *Journal of Guidance, Control, and Dynamics*, 21(1):148–155, January–February 1998. doi:10.2514/2.4211.

[32] Paul J. Cefola. Equinoctial orbit elements - Application to artificial satellite orbits. In *AIAA/AAS Astrodynamics Conference*, pp. 1–13, Reston, VA, 1972. American Institute of Aeronautics and Astronautics, Inc. AIAA Paper 72-937, doi:10.2514/6.1972-937.

[33] Paul J. Cefola, Anne C. Long, and G. Holloway Jr. The long-term prediction of artificial satellite orbits. In *Proceedings of the AIAA 12th Aerospace Sciences Meeting*, pp. 1–32, Reston, VA, 1974. American Institute of Aeronautics and Astronautics, Inc. AIAA Paper 74-170, doi:10.2514/6.1974-170.

[34] Paul J. Cefola, Chris Sabol, Keric Hill, and Daron Nishimoto. Demonstration of the DSST state transition matrix time-update properties using the linux GTDS program. In *Advanced Maui Optical and Space Surveillance Technologies (AMOS) Conference*, Maui, HI, September 2011.

[35] Rafael Cid and José F. Lahulla. Perturbaciones de corto período en el movimiento de un satélite artificial, en función de las variables de Hill. *Publicaciones de la Revista de la Academia de Ciencias de Zaragoza*, 24:159–165, 1969. `https://zaguan.unizar.es/record/4423`, accessed May 28, 2017.

[36] Rafael Cid and José F. Lahulla. Perturbaciones de segundo orden y corto período, para el movimiento de un satélite artificial, en las variables de Hill. *Publicaciones de la Revista de la Academia de Ciencias de Zaragoza*, 26:333–343, 1969. `https://zaguan.unizar.es/record/4426`, accessed May 28, 2017.

[37] W. H. Clohessy and R. S. Wiltshire. Terminal guidance system for satellite rendezvous. *Journal of the Aerospace Sciences*, 27(9):653–658, 674, September 1960. doi:10.2514/8.8704.

[38] Bruce A. Conway. An improved algorithm due to Laguerre for the solution of Kepler's equation. *Celestial Mechanics*, 39(2):199–211, June 1986. doi:10.1007/BF01230852.

[39] A. H. Cook. Exact solutions in the theory of orbits. *Monthly Notices of the Royal Astronomical Society*, 134(3):253–268, December 1966. doi:10.1093/mnras/134.3.253.

[40] Simone D'Amico and Oliver Montenbruck. Proximity operations of formation-flying spacecraft using an eccentricity/inclination vector sep-

aration. *Journal of Guidance, Control, and Dynamics*, 29(3):554–563, May–June 2006. doi:10.2514/1.15114.

[41] Donald A. Danielson, Beny Neta, and Leo W. Early. Seminanalytic satellite theory (SST): Mathematical algorithms. Technical Report NPS Report NPS-MA-94-001, Naval Postgraduate School Department of Mathematics, Monterey, CA, January 1994.

[42] Donald A. Danielson, Christopher Patrick Sagovac, Beny Neta, and Leo W. Early. Seminanalytic satellite theory. Technical Report NPS Report NPS-MA-95-002, Naval Postgraduate School Department of Mathematics, Monterey, CA, July 1995.

[43] Gaston Darboux. Sur un problème de mécanique. *Archives Néerlandaises des Sciences Exactes et Naturelles*, 2(6):371–376, 1901. In French: Série II, Tome VI.

[44] J. Pieter de Vries. Elliptic elements in terms of small increments of position and velocity components. *AIAA Journal*, 1(11):2626–2629, November 1963. doi:10.2514/3.2124.

[45] André Deprit. The elimination of the parallax in satellite theory. *Celestial Mechanics*, 24(2):111–153, June 1981. doi:10.1007/BF01229192.

[46] André Deprit and Sebastián Ferrer. Note on Cid's radial intermediary and the method of averaging. *Celestial Mechanics*, 40(3):335–343, September 1987. doi:10.1007/BF01235851.

[47] André Deprit and David L. Richardson. Comments on Aksnes' intermediary. *Celestial Mechanics*, 28(3):253–273, November 1982. doi:10.1007/BF01243737.

[48] Gim Jew Der. An elegant state transition matrix. *The Journal of the Astronautical Sciences*, 45(4):371–390, October–December 1997.

[49] Gim Jew Der. The superior Lambert algorithm. In *Advanced Maui Optical and Space Surveillance Technologies (AMOS) Conference*, Maui, HI, September 2011.

[50] Gim Jew Der and Nino L. Bonavito, editors. *Orbital and Celestial Mechanics*, Vol. 177 of *Progress in Astronautics and Aeronautics*. American Institute of Aeronautics and Astronautics, Inc., Reston, VA, 1998.

[51] Gim Jew Der and Roy Danchick. Analytic and numerical error covariance matrix propagation (for spacecraft in Earth orbital environments). In *AIAA/AAS Astrodynamics Conference*, pp. 854–878, Reston, VA, July 1996. American Institute of Aeronautics and Astronautics, Inc. AIAA Paper 96-3661, doi:10.2514/6.1996-3661.

[52] Gim Jew Der and Roy Danchick. Trajectory propagation over very short time spans. In *Proceedings of the AAS/AIAA Astrodynamics Specialist Conference*, Vol. 97 of *Advances in the Astronautical Sciences*, pp. 1331–1347, San Diego, CA, 1998. Univelt, Inc. Paper AAS 97-686.

[53] Alan Edelman and H. Murakami. Polynomial roots from companion ma-

trix eigenvalues. *Mathematics of Computation*, 64(210):763–776, April 1995. doi:10.1090/S0025-5718-1995-1262279-2.

[54] Todd A. Ely. Mean element propagations using numerical averaging. In *Proceedings of the AAS/AIAA Astrodynamics Specialist Conference*, Vol. 135 of *Advances in the Astronautical Sciences*, pp. 2287–2305, San Diego, CA, 2010. Univelt, Inc. Paper AAS 09-440.

[55] Todd A. Ely. Mean element propagations using numerical averaging. *The Journal of the Astronautical Sciences*, 61(3):275–304, September 2014. doi:10.1007/s40295-014-0020-2.

[56] Boris Garfinkel. On the motion of a satellite of an oblate planet. *The Astronomical Journal*, 63(3):88–96, March 1958. doi:10.1086/107697.

[57] Boris Garfinkel. The orbit of a satellite of an oblate planet. *The Astronomical Journal*, 64(9):353–367, November 1959. doi:10.1086/107956.

[58] Boris Garfinkel. An improved theory of motion of an artificial satellite. *The Astronomical Journal*, 69(3):223–229, April 1964. doi:10.1086/109260.

[59] Boris Garfinkel and Kaare Aksnes. Spherical coordinate intermediaries for an artificial satellite. *The Astronomical Journal*, 75(1):85–91, February 1970. doi:10.1086/110946.

[60] Boris Garfinkel, Gen-Ichiro Hori, and Kaare Aksnes. On the mixed-secular terms in perturbed intermediaries. *The Astronomical Journal*, 75(5):651–656, June 1970. doi:10.1086/111000.

[61] James L. Garrison, Thomas G. Gardner, and Penina Axelrad. Relative motion in highly elliptical orbits. In *Proceedings of the AAS/AIAA Space Flight Mechanics Meeting*, Vol. 89 of *Advances in the Astronautical Sciences*, pp. 1359–1376, San Diego, CA, February 1995. Univelt, Inc. Paper AAS 95-194.

[62] Bassford C. Getchell. Orbit computation with the Vinti potential and universal variables. *Journal of Spacecraft and Rockets*, 7(4):405–408, April 1970. doi:10.2514/3.29954.

[63] Franz Thomas Geyling and Howard Robert Westerman. *Introduction to Orbital Mechanics.* Addison-Wesley Publishing Company, Reading, MA, 1971.

[64] Dong-Woo Gim and Kyle Terry Alfriend. State transition matrix of relative motion for the perturbed noncircular reference orbit. *Journal of Guidance, Control, and Dynamics*, 26(6):956–971, November–December 2003. doi:10.2514/2.6924.

[65] Dong-Woo Gim and Kyle Terry Alfriend. Satellite relative motion using differential equinoctial elements. *Celestial Mechanics and Dynamical Astronomy*, 92(4):295–336, August 2005. doi:10.1007/s10569-004-1799-0.

[66] Robert A. Gordon, George D. Mistretta, and John S. Watson. A comparison of classical analytic theories for the motion of artificial satel-

lites. *Journal of Guidance and Control*, 2(3):184–189, May–June 1979.
doi:10.2514/3.55859.

[67] Evgenii A. Grebenikov. On the stability of the Lagrangian triangle solutions of the restricted elliptic three-body problem. *Soviet Astronomy*, 8(3):451–459, November–December 1964. Translated to English from *Astronomicheskii Zhurnal*, Vol. 41, No. 3, May–June 1964, pp. 567–578.

[68] Pini Gurfil. Generalized solutions for relative spacecraft orbits under arbitrary perturbations. *Acta Astronautica*, 60(2):61–78, January 2007. doi:10.1016/j.actaastro.2006.07.013.

[69] Pini Gurfil and Martin Lara. Satellite onboard orbit propagation using Deprit's radial intermediary. *Celestial Mechanics and Dynamical Astronomy*, 120(2):217–232, October 2014. doi:10.1007/s10569-014-9576-1.

[70] Hugo Gyldén. Die intermediäre Bahn des Mondes. *Acta Mathematica*, 7(1):125–172, December 1885. doi:10.1007/BF02402199.

[71] Noble Hatten and Ryan Paul Russell. Comparison of three Stark problem solution techniques for the bounded case. *Celestial Mechanics and Dynamical Astronomy*, 121(1):39–60, January 2015. doi:10.1007/s10569-014-9586-z.

[72] Liam M. Healy and C. Glen Henshaw. Trajectory guidance using periodic relative orbital motion. *Journal of Guidance, Control, and Dynamics*, 38(9):1714–1724, September 2015. doi:10.2514/1.G000945.

[73] George William Hill. Researches in the lunar theory. *American Journal of Mathematics*, 1(1):5–26, 1878. doi:10.2307/2369430.

[74] George William Hill. Motion of a system of material points under the action of gravitation. *The Astronomical Journal*, 27(22–23):171–182, April 1913. doi:10.1086/103991.

[75] Keric Hill, Chris Sabol, Craig A. McLaughlin, K. Kim Luu, and Michael Murai. Relative orbit determination of geosynchronous satellites using the COWPOKE equations. In *Proceedings of the AAS/AIAA Space Flight Mechanics Meeting*, Vol. 119 of *Advances in the Astronautical Sciences*, pp. 1507–1518, San Diego, CA, 2005. Univelt, Inc. Paper AAS 04-195.

[76] Gerald R. Hintz. Survey of orbit element sets. *Journal of Guidance, Control, and Dynamics*, 31(3):785–790, May–June 2008. doi:10.2514/1.32237.

[77] Felix R. Hoots. A nonsingular reformulation of the Brouwer geopotential theory. In *Proceedings of the AAS/AIAA Astrodynamics Specialist Conference*, Vol. 32 of *AAS Microfiche Series, supplement to Vol. 40 of Advances in the Astronautical Sciences*, p. 618, San Diego, CA, 1979. Univelt, Inc. Paper AAS 79-137.

[78] Felix R. Hoots. Reformulation of the brouwer geopotential theory for improved computational efficiency. *Celestial Mechanics*, 24(4):367–375, August 1981. doi:10.1007/BF01230396.

[79] Felix R. Hoots and Richard G. France. An analytic satellite theory using gravity and a dynamic atmosphere. *Celestial Mechanics*, 40(1): 1–18, March 1987. doi:10.1007/BF01232321.

[80] Felix R. Hoots and Ronald L. Roehrich. Models for propagation of NORAD element sets. Technical report, Project Spacetrack Report No. 3, U.S. Air Force Aerospace Defense Command, Colorado Springs, CO, December 1980.

[81] Felix R. Hoots, Paul W. Schumacher Jr., and Robert A. Glover. History of analytical orbit modeling in the U.S. space surveillance system. *Journal of Guidance, Control, and Dynamics*, 27(2):174–185, March–April 2004. doi:10.2514/1.9161.

[82] Gen-Ichiro Hori. Theory of general perturbations with unspecified canonical variables. *Publications of the Astronomical Society of Japan*, 18(4): 287–296, 1966.

[83] Richard S. Hujsak. A restricted four body solution for resonating satellite with an oblate Earth. In *Proceedings of the AAS/AIAA Astrodynamics Specialist Conference*, Vol. 32 of *AAS Microfiche Series, supplement to Vol. 40 of Advances in the Astronautical Sciences*, p. 617, San Diego, CA, 1979. Univelt, Inc. Paper AAS 79-136.

[84] Richard S. Hujsak. A restricted four body solution for resonating satellites without drag. Technical report, Project Spacetrack Report No. 1,

U.S. Air Force Aerospace Defense Command, Colorado Springs, CO, November 1979.

[85] Imre Gyula Izsak. A theory of satellite motion about an oblate planet—I. A second-order solution of Vinti's dynamical problem. Technical report, Smithsonian Institution Astrophysical Observatory, November 1960. Special Report No. 52.

[86] Imre Gyula Izsak. On the critical inclination in satellite theory. Technical report, Smithsonian Institution Astrophysical Observatory, March 1962. Special Report No. 90.

[87] Imre Gyula Izsak. A second-order solution of Vinti's dynamical problem. *Smithsonian Contributions to Astrophysics*, 6:81–107, 1963.

[88] L. G. Jacchia. New static models of the thermosphere and exosphere with empirical temperature profiles. Technical report, Smithsonian Institution Astrophysical Observatory, May 1970. Special Report No. 313.

[89] R. A. Jacobson, P. G. Antreasian, J. J. Bordi, K. E. Criddle, R. Ionasescu, J. B. Jones, R. A. Mackenzie, M. C. Meek, D. Parcher, F. J. Pelletier, Jr. W. M. Owen, D. C. Roth, I. M. Roundhill, and J. R. Stauch. The gravity field of the Saturnian system from satellite observations and spacecraft tracking data. *The Astronomical Journal*, 132(6):2520–2526, December 2006. doi:10.1086/508812.

[90] Donald J. Jezewski. An analytic solution for the J_2 perturbed

equatorial orbit. *Celestial Mechanics*, 30(4):363–371, August 1983. doi:10.1007/BF01375506.

[91] Paul W. Schumacher Jr. and Robert A. Glover. Analytical orbit model for U.S. naval space surveillance: An overview. In *Proceedings of the AAS/AIAA Astrodynamics Specialist Conference*, Vol. 90 of *Advances in the Astronautical Sciences*, pp. 1893–1912, San Diego, CA, 1995. Univelt, Inc. Paper AAS 95-427, the Univelt version contains only 20 out of 40 pages.

[92] Stephen J. Madden Jr. A separable potential in triaxially ellipsoidal coordinates satisfying the Laplace equation. *Celestial Mechanics*, 2(2): 217–227, June 1970. doi:10.1007/BF01229496.

[93] John L. Junkins, Maruthi R. Akella, and Kyle Terry Alfriend. Non-Gaussian error propagation in orbital mechanics. *The Journal of the Astronautical Sciences*, 44(4):541–563, October–December 1996.

[94] Hans K. Karrenberg. Comments on "Elliptic elements in terms of small increments of position and velocity components" and generalization of the solutions for an arbitrary initial point. *AIAA Journal*, 3(2):381, February 1965. doi:10.2514/3.55138.

[95] N. Jeremy Kasdin, Pini Gurfil, and Egemen Kolemen. Canonical modelling of relative spacecraft motion via epicyclic orbital elements. *Celestial Mechanics and Dynamical Astronomy*, 92(4):337–370, August 2005. doi:10.1007/s10569-004-6441-7.

[96] Bernard Kaufman, Kyle Terry Alfriend, and Robert R. Dasenbrock. Luni-solar perturbations in the extended phase space representation of the Vinti problem. *Acta Astronautica*, 5(10):727–744, October 1978. doi:10.1016/0094-5765(78)90065-6.

[97] Jean Albert Kechichian. Motion in general elliptic orbit with respect to a dragging and precessing coordinate frame. *The Journal of the Astronautical Sciences*, 46(1):25–45, January–March 1998.

[98] Thomas J. Kelly. An analytical approach to the two-impulse optimal rendezvous problem. In *Proceedings of the AAS/AIAA Space Flight Mechanics Meeting*, Vol. 87 of *Advances in the Astronautical Sciences*, pp. 337–347, San Diego, CA, 1994. Univelt, Inc. Paper AAS 94-156.

[99] Urs Kirchgraber. A problem of orbital dynamics, which is separable in KS-variables. *Celestial Mechanics*, 4(3):340–347, December 1971. doi:10.1007/BF01231396.

[100] M. D. Kislik. The path of an artificial Earth satellite in the normal gravitational field of the Earth. *Planetary and Space Science*, 8(2):86–96, November 1961. Translated by R. Matthews to English from *Iskusstvennye Sputniki Zemli (Artificial Earth Satellites)*, No. 4, 1960, pp. 3–17 [English version: "The Motion of an Artificial Satellite in the Normal Gravitational Field of the Earth", 1961, pp. 183-201], doi:10.1016/0032-0633(61)90161-1.

[101] Yoshihide Kozai. The motion of a close Earth satellite. *The Astronomical Journal*, 64(9):367–377, November 1959. doi:10.1086/107957.

[102] Yoshihide Kozai. Second-order solution of artificial satellite theory without air drag. *The Astronomical Journal*, 67(7):446–461, September 1962. doi:10.1086/108753.

[103] Max H. Lane and K. H. Cranford. An improved analytical drag theory for the artificial satellite problem. In *AIAA/AAS Astrodynamics Conference*, pp. 1–11, Reston, VA, 1969. American Institute of Aeronautics and Astronautics, Inc. AIAA Paper 69-925, doi:10.2514/6.1969-925.

[104] Thomas Joseph Lang. Spheroidal solution for unbounded orbits about an oblate planet. Master's thesis, Supervisor: Dr. John P. Vinti, Massachusetts Institute of Technology, Cambridge, MA, June 1969.

[105] Gregory Lantoine and Ryan Paul Russell. Complete closed-form solutions of the Stark problem. *Celestial Mechanics and Dynamical Astronomy*, 109(4):333–366, April 2011. doi:10.1007/s10569-010-9331-1.

[106] Martin Lara and Pini Gurfil. Integrable approximation of J_2-perturbed relative orbits. *Celestial Mechanics and Dynamical Astronomy*, 114(3): 229–254, November 2012. doi:10.1007/s10569-012-9437-8.

[107] V. N. Lavrik. Method for determining the osculating transfer orbit of an artificial Earth satellite. *Cosmic Research*, 5(2):168–172, March 1967. Translated to English from *Kosmicheskie Issledovaniya*, Vol. 5, No. 2, March–April 1967, pp. 194–199.

[108] Derek Frank Lawden. Fundamentals of space navigation. *Journal of the British Interplanetary Society*, 13(2):87–101, 1954.

[109] Joseph J. F. Liu. Satellite motion about an oblate Earth. *AIAA Journal*, 12(11):1511–1516, November 1974. doi:10.2514/3.49537.

[110] Thomas Alan Lovell and David A. Spencer. Relative orbital elements formulation based upon the Clohessy-Wiltshire equations. *The Journal of the Astronautical Sciences*, 61(4):341–366, December 2014. doi:10.1007/s40295-014-0029-6.

[111] Thomas Alan Lovell, Steven G. Tragesser, and Mark V. Tollefson. A practical guidance methodology for relative motion of leo spacecraft based on the Clohessy-Wiltshire equations. In *AAS/AIAA Space Flight Mechanics Meeting*, Vol. 119 of *Advances in the Astronautical Sciences*, pp. 2355–2369, San Diego, CA, 2004. Univelt, Inc. Paper AAS 04-252.

[112] Robert H. Lyddane. Small eccentricities or inclinations in the Brouwer theory of the artificial satellite. *The Astronomical Journal*, 68(8):555–558, October 1963. doi:10.1086/109179.

[113] Diarmuid Ó. Mathúna. The Vinti dynamical problem and the geopotential. Technical Report TR R-307, National Aeronautics and Space Administration, Washington, DC, April 1969.

[114] Diarmuid Ó. Mathúna. Satellite prediction formulae for Vinti's model. *Celestial Mechanics*, 1(3):467–478, June 1970. doi:10.1007/BF01231144.

[115] Diarmuid Ó. Mathúna. *Integrable Systems in Celestial Mechanics*. Birkhäuser Boston, 2008. doi:10.1007/978-0-8176-4595-3.

[116] Wayne D. McClain. A recursively formulated first-order semianalytic artificial satellite theory based on the generalized method of averaging; Volume 2: The explicit development of the first-order averaged equations of motion for the nonspherical gravitational and nonresonant third-body perturbations. Technical Report CSC/TR-78/6001, Computer Sciences Corporation, May 1978.

[117] Wayne D. McClain. A seminanalytic artificial satellite theory; Volume 1: Application of the generalized method of averaging to the artificial satellite problem. Technical report, The Charles Stark Draper Laboratory, Inc., July 1992. Updated/Corrected version of Computer Sciences Corporation CSC/TR-77/6010, November 1977.

[118] Albert T. Monuki. Vinti potential. Technical report, Unpublished TRW Internal Report, 1974.

[119] Philip McCord Morse and Herman Feshbach. *Methods of Theoretical Physics*. McGraw-Hill, New York, 1953. pp. 492–523.

[120] Ali Hasan Nayfeh. *Perturbation Methods*. Wiley-VCH Verlag GmbH & Co. KGaA, Weinheim, Germany, 2004. Chapter 5.

[121] Beny Neta. Partial list of orbit propagators. Technical report, Naval Postgraduate School, Monterey, CA, 2005. `https://calhoun.nps.edu/handle/10945/39471`, accessed May 28, 2017.

[122] Brett Newman and Thomas Alan Lovell. Second order nonlinear boundary value solution for relative motion using Volterra theory. In *AAS/AIAA Space Flight Mechanics Meeting*, Vol. 148 of *Advances in the Astronautical Sciences*, pp. 2151–2172, San Diego, CA, 2013. Univelt, Inc. Paper AAS 13-470.

[123] Ashraf Omran and Brett Newman. Nonlinear analytical solution of relative motion subject to J_2 perturbation using Volterra kernels. In *AAS/AIAA Astrodynamics Specialist Conference*, Vol. 142 of *Advances in the Astronautical Sciences*, pp. 987–1006, San Diego, CA, 2012. Univelt, Inc. Paper AAS 11-467.

[124] Etienne Pellegrini, Ryan Paul Russell, and Vivek Vittaldev. F and G Taylor series solutions to the Stark and Kepler problems with Sundman transformations. *Celestial Mechanics and Dynamical Astronomy*, 118 (4):355–378, April 2014. doi:10.1007/s10569-014-9538-7.

[125] Edward T. Pitkin. A regularized approach to universal orbit variables. *AIAA Journal*, 3(8):1508–1511, August 1965. doi:10.2514/3.3176.

[126] Daniel Rufer. Trajectory optimization by making use of the closed solution of constant thrust-acceleration motion. *Celestial Mechanics*, 14(1): 91–103, March 1976. doi:10.1007/BF01247135.

[127] Ryan Paul Russell and Gregory Lantoine. Optimal control of relative motion in arbitrary fields: Application at Deimos. *The Journal of the*

Astronautical Sciences, 59(1 and 2):197–219, 2012. doi:10.1007/s40295-013-0013-6.

[128] Chris Sabol, Rich Burns, and Craig A. McLaughlin. Satellite formation flying design and evolution. *Journal of Spacecraft and Rockets*, 38(2): 270–278, March–April 2001. doi:10.2514/2.3681.

[129] Chris Sabol, Craig A. McLaughlin, and K. Kim Luu. Meet the cluster orbits with perturbations of Keplerian elements (COWPOKE) equations. In *Proceedings of the AAS/AIAA Space Flight Mechanics Meeting*, Vol. 114 of *Advances in the Astronautical Sciences*, pp. 573–594, San Diego, CA, 2003. Univelt, Inc. Paper AAS 03-138.

[130] Hanspeter Schaub and Kyle Terry Alfriend. J_2 invariant relative orbits for spacecraft formations. *Celestial Mechanics and Dynamical Astronomy*, 79(2):77–95, February 2001. doi:10.1023/A:1011161811472.

[131] Samuel A. Schweighart and Raymond J. Sedwick. High-fidelity linearized J_2 model for satellite formation flight. *Journal of Guidance, Control, and Dynamics*, 25(6):1073–1080, November–December 2002. doi:10.2514/2.4986.

[132] Prasenjit Sengupta, Srinivas Rao Vadali, and Kyle Terry Alfriend. Second-order state transition for relative motion near perturbed, elliptic orbits. *Celestial Mechanics and Dynamical Astronomy*, 97(2):101–129, February 2007. doi:10.1007/s10569-006-9054-5.

[133] Thomas Joseph Sherrill. *Development of a Satellite Drag Theory Based on the Vinti Formulation*. PhD thesis, Supervisor: Dr. Leland E. Cunningham, University of California, Berkeley, Berkeley, CA, 1966.

[134] Andrew J. Sinclair, Ryan E. Sherrill, and Thomas Alan Lovell. Calibration of linearized solutions for satellite relative motion. *Journal of Guidance, Control, and Dynamics*, 37(4):1362–1367, July 2014. doi:10.2514/1.G000037.

[135] Andrew J. Sinclair, Brett Newman, and Thomas Alan Lovell. Decalibration of linearized solutions for satellite relative motion. In *Proceedings of the AAS/AIAA Space Flight Mechanics Meeting*, Vol. 155 of *Advances in the Astronautical Sciences*, pp. 2067–2076, San Diego, CA, 2015. Univelt, Inc. Paper AAS 15-331.

[136] William Marshall Smart. *Celestial Mechanics*. Longmans, Green and Co, London, 1953.

[137] Otto R. Spies. Two notes in orbit theory. In *Proceedings of the XIIth International Astronautical Congress*, pp. 121–130, New York, 1963. Academic Press, Inc. Held in Washington, D. C. in 1961.

[138] Johannes Stark. Beobachtungen über den Effekt des elektrischen Feldes auf Spektrallinien. I. Quereffekt. *Annalen der Physik*, 43(7):965–982, 1914.

[139] Theodore E. Sterne. The gravitational orbit of a satellite of an oblate

planet. *The Astronomical Journal*, 63(1255):28–40, January 1970. doi:10.1086/107673.

[140] Nathan J. Strange. *Analytical Methods for Gravity-Assist Tour Design.* PhD thesis, Supervisor: Dr. James M. Longuski, Purdue University, West Lafayette, IN, August 2016.

[141] Mary T. Stringer, Brett Newman, Thomas Alan Lovell, and Ashraf Omran. Analysis of a new nonlinear solution of relative orbital motion. In *International Symposium on Space Flight Dynamics*, 2012.

[142] Mary T. Stringer, Brett Newman, Thomas Alan Lovell, and Ashraf Omran. Second order nonlinear initial value solution for relative motion using Volterra theory. In *AAS/AIAA Space Flight Mechanics Meeting*, Vol. 148 of *Advances in the Astronautical Sciences*, pp. 2133–2149, San Diego, CA, 2013. Univelt, Inc. Paper AAS 13-469.

[143] Joshua Sullivan, Sebastian Grimberg, and Simone D'Amico. Comprehensive survey and assessment of spacecraft relative motion dynamics models. *Journal of Guidance, Control, and Dynamics*, 40(8):1837–1859, August 2017. doi:10.2514/1.G002309.

[144] Fu Tong and Zhen Chen. Second-order solution of Lindstedt's equation with constant coefficients. *Chinese Astronomy and Astrophysics*, 6(1):5–12, March 1982. Translated to English from *Acta Astronomica Sinica*, Vol. 22, No. 3, September 1981, pp. 214–222, doi:10.1016/0275-1062(82)90056-X.

[145] Fu Tong and Lian-da Wu. Perturbation equations of the elements of Vinti's intermediate orbit. *Chinese Astronomy and Astrophysics*, 5(3): 282–294, September 1981. Translated to English from *Acta Astronomica Sinica*, Vol. 22, No. 1, March 1981, pp. 1–14, doi:10.1016/0275-1062(81)90048-5.

[146] Fu Tong and Lian-da Wu. The third-order theory of artificial satellites of the Earth: A first exploration. *Chinese Astronomy and Astrophysics*, 6(4):288–292, December 1982. Translated to English from *Acta Astronomica Sinica*, Vol. 22, No. 2, June 1981, pp. 138–144, doi:10.1016/0275-1062(82)90003-0.

[147] Johann F. A. Tschauner and Peter R. Hempel. Rendezvous zu einem in elliptischer Bahn umlaufenden Ziel. *Astronautica Acta*, 11(2):104–109, 1965.

[148] Srinivas Rao Vadali. An analytical solution for relative motion of satellites. In *5th Cranfield Dynamics and Control of Systems and Structures in Space (DCSSS) Conference*, Cranfield, UK, July 2002. Cranfield University. Held at King's College, Cambridge, July 14–18, 2002, `http://naca.central.cranfield.ac.uk/dcsss/`, accessed May 28, 2017.

[149] David A. Vallado. *Fundamentals of Astrodynamics and Applications*. Space Technology Library. Microcosm Press, Hawthorne, CA, third edition, 2007.

[150] David A. Vallado, Paul Crawford, Richard S. Hujsak, and T. S. Kelso.

Revisiting spacetrack report #3. In *AIAA/AAS Astrodynamics Specialist Conference and Exhibit*, Reston, VA, 2006. American Institute of Aeronautics and Astronautics, Inc. AIAA Paper 2006-6753, Revision 2, November 2007, doi:10.2514/6.2006-6753.

[151] John Pascal Vinti. New approach in the theory of satellite orbits. *Physical Review Letters*, 3(1):8, July 1959. doi:10.1103/PhysRevLett.3.8.

[152] John Pascal Vinti. New method of solution for unretarded satellite orbits. *Journal of Research of the National Bureau of Standards*, 63B(2): 105–116, October–December 1959. doi:10.6028/jres.063B.012.

[153] John Pascal Vinti. Mean motions in conditionally periodic separable systems. *Journal of Research of the National Bureau of Standards*, 65B (2):131–135, April–June 1961. doi:10.6028/jres.065B.013.

[154] John Pascal Vinti. Theory of an accurate intermediary orbit for satellite astronomy. *Journal of Research of the National Bureau of Standards*, 65B(3):169–201, July–September 1961. doi:10.6028/jres.065B.017.

[155] John Pascal Vinti. Intermediary equatorial orbits of an artificial satellite. *Journal of Research of the National Bureau of Standards*, 66B(1):5–13, January–March 1962. doi:10.6028/jres.066B.002.

[156] John Pascal Vinti. Zonal harmonic perturbations of an accurate reference orbit of an artificial satellite. *Journal of Research of the National Bureau of Standards*, 67B(4):191–222, October–December 1963. doi:10.6028/jres.067B.016.

[157] John Pascal Vinti. Effects of a constant force on a Keplerian orbit. In Georgios Ioannou Kontopoulos, editor, *The Theory of Orbits in the Solar System and in Stellar Systems*, Proceedings of the International Astronomical Union Symposium no. 25, pp. 355–362, London, 1966. Academic Press. Held in Thessaloniki, August 17-22, 1964.

[158] John Pascal Vinti. Inclusion of the third zonal harmonic in an accurate reference orbit of an artificial satellite. *Journal of Research of the National Bureau of Standards*, 70B(1):17–46, January–March 1966. doi:10.6028/jres.070B.003.

[159] John Pascal Vinti. Invariant properties of the spheroidal potential of an oblate planet. *Journal of Research of the National Bureau of Standards*, 70B(1):1–16, January–March 1966. doi:10.6028/jres.070B.002.

[160] John Pascal Vinti. Improvement of the spheroidal method for artificial satellites. *The Astronomical Journal*, 74(1):25–34, February 1969. doi:10.1086/110770.

[161] John Pascal Vinti. Representation of the Earth's gravitational potential. *Celestial Mechanics*, 4(3):348–367, December 1971. doi:10.1007/BF01231397.

[162] John Pascal Vinti. Gaussian variational equations for osculating elements of an arbitrary separable reference orbit. *Celestial Mechanics*, 7 (3):367–375, April 1973. doi:10.1007/BF01227856.

[163] Harvey Walden. Improvement of mean orbital elements for Vinti's spheroidal satellite theory. *AIAA Journal*, 6(7):1305–1308, July 1968. doi:10.2514/3.4739.

[164] Harvey Walden and Stan Watson. Differential corrections applied to Vinti's accurate reference satellite orbit with inclusion of the third zonal harmonic. Technical Report TN D-4088, National Aeronautics and Space Administration, Washington, DC, August 1967.

[165] John S. Watson, George D. Mistretta, and Nino L. Bonavito. An analytic method to account for drag in the Vinti satellite theory. *Celestial Mechanics*, 11(2):145–177, March 1975. doi:10.1007/BF01230543.

[166] William E. Wiesel. Numerical solution to Vinti's problem. *Journal of Guidance, Control, and Dynamics*, 38(9):1757–1764, September 2015. doi:10.2514/1.G000661.

[167] James Woodburn and Sergei Tanygin. Efficient numerical integration of coupled orbit and attitude trajectories using an Encke type correction algorithm. In *AAS/AIAA Astrodynamics Specialist Conference*, Vol. 109 of *Advances in the Astronautical Sciences*, pp. 1837–1848, San Diego, CA, 2002. Univelt, Inc. Paper AAS 01-428.

[168] Steven P. Wright. *Orbit Determination Using Vinti's Solution*. PhD thesis, Supervisor: Dr. William E. Wiesel, Air Force Institute of Technology, Wright-Patterson Air Force Base, OH, September 2016.

[169] Lian-da Wu and Fu Tong. A third-order solution of Vinti's problem with explicit expressions for the Poisson brackets. *Chinese Astronomy and Astrophysics*, 5(2):192–201, June 1981. Translated to English from *Acta Astronomica Sinica*, Vol. 21, No. 4, December 1980, pp. 389–398, doi:10.1016/0275-1062(81)90031-X.

[170] Koji Yamanaka and Finn Ankersen. New state transition matrix for relative motion on an arbitrary elliptical orbit. *Journal of Guidance, Control, and Dynamics*, 25(1):60–66, January–February 2002. doi:10.2514/2.4875.

[171] Hui Yan. *Dynamics and Real-Time Optimal Control of Aerospace Systems.* PhD thesis, Supervisor: Dr. Kyle T. Alfriend, Texas A&M University, College Station, TX, June 2006.

[172] Hui Yan, Prasenjit Sengupta, Srinivas Rao Vadali, and Kyle Terry Alfriend. Development of a state transition matrix for relative motion using the unit sphere approach. In *AAS/AIAA Space Flight Mechanics Meeting*, Vol. 119 of *Advances in the Astronautical Sciences*, pp. 935–946, San Diego, CA, February 2005. Univelt, Inc. Paper AAS 04-163.

[173] Hui Yan, Kyle Terry Alfriend, Srinivas Rao Vadali, and Prasenjit Sengupta. Optimal design of satellite formation relative motion orbits using least-squares methods. *Journal of Guidance, Control, and Dynamics*, 32 (2):599–604, March–April 2009. doi:10.2514/1.35044.

[174] Hui Yan, Srinivas Rao Vadali, and Kyle Terry Alfriend. State transition

matrix for relative motion including higher-order gravity perturbations. In *Proceedings of the AAS/AIAA Space Flight Mechanics Meeting*, Vol. 150 of *Advances in the Astronautical Sciences*, pp. 1317–1336, San Diego, CA, August 2013. Univelt, Inc. Paper AAS 13-793.

Vita

Ashley Darius Biria was born in Seattle, Washington. He received the Bachelor of Science degree in Mechanical Engineering from Cornell University in May 2009. In August 2009, he entered graduate school in the Department of Aerospace Engineering and Engineering Mechanics at the University of Texas at Austin, receiving the Master of Science in Engineering degree in December 2011. He continued his graduate studies in Austin, but his doctoral research took a different direction.

Permanent address: biria@utexas.edu

This dissertation was typeset with LaTeX[†] by the author.

[†]LaTeX is a document preparation system developed by Leslie Lamport as a special version of Donald Knuth's TeX Program.